# Development of a biologically derived acellular construct for small intestine replacement

**A thesis submitted for the degree of**

**Doctor of Philosophy (Ph.D.)**

**By**

**Anna K. Nowocin M.Sc. (Hons)**

University College London

Division of Surgery and Interventional Sciences

**2011**

# Abstract

**Introduction:** Short bowel syndrome is characterised by a severe reduction in the amount of functional intestine available as an absorptive surface. Attempts to lengthen the intestine by interposition of artificial tubular scaffolds juxtaposed between healthy tissues have shown limited success. Transplantation is limited due to organ shortage. The most promising solution may be implantation of tissue-engineered small intestine using natural scaffold.

**Materials and Results:** Using a completely novel approach, up to 30cm lengths of ileum with the attached vasculature were harvested from porcine donors. Separate intestinal and vascular loops were identified and de-cellularised using individually tailored detergent-enzymatic protocols. The resulting scaffold was compared to native tissue in terms of retention of cellular and nuclear remnants, as well as structural and functional proteins. Its biocompatibility was assessed by subcutaneous implantation of $1cm^2$ pieces into rat recipients. The remodeling fate of grafts was determined by time related changes in the ratio of sub-populations of residual macrophages. Its mechanical strength and ease of handling was evaluated by performing a left-sided nephrectomy in an unrelated pig model, followed by end-to-end anastomosis of the de-cellularised scaffolds' mesenteric vasculature to the appropriate renal artery and vein. In the last stage, porcine organoid units were isolated and their yield estimated for future *in vitro* studies.

**Conclusions:** It is possible to simultaneously de-cellularise two different tissues of varying cellular configuration and composition effectively and efficiently over a relatively short period of time. The two key features of the de-cellularised scaffold are that 1) the scaffold has in place the necessary architectural topography of small intestine (including mucosal villi) and molecular cues for optimum re-cellularisation and 2) the attached vascular tree provides an ideal conduit for re-cellularisation using either vascular committed endothelial or progenitor cells. Ultimately, this scaffold can be used for constructing long segments of bio-engineered intestine with the possibility of immediate blood supply and re-vascularisation.

# Table of Contents

# List of Figures

## Chapter 1: General introduction



## Chapter 2: Small intestine tissue engineering using biological/ synthetic hybrid scaffold in rat model



## Chapter 3: De-cellularisation of a segment of porcine small intestine with its attached vasculature as a single entity

## Chapter 4: Biocompatibility tests in rodent model

## Chapter 5: Stereological analysis of scaffold performance *in vivo*



## Chapter 6: *In vivo* evaluation of scaffold biomechanics

## Chapter 7: Isolation and characterisation of porcine organoid units and endothelial cells

# List of Tables

## Chapter 1: General introduction



## Chapter 2: Small intestine tissue engineering using biological/ synthetic hybrid scaffold in rat model



## Chapter 3: De-cellularisation of a segment of porcine small intestine with its attached vasculature as a single entity



## Chapter 4: Biocompatibility tests in rodent model.

## Chapter 5: Stereological analysis of scaffold performance *in vivo*



## Chapter 6: *In vivo* evaluation of scaffold biomechanics



## Chapter 7: Isolation and characterisation of porcine organoid units and endothelial cells

# International Presentations

- June 2010: TERMIS, Galaway, Ireland – International Tissue Engineering Conference: Preparation of surgically viable scaffold-constructs for small intestine tissue engineering

- October 2009: World Conference on Regenerative Medicine, Leipzig, Germany: The preparation of pre-vascularised scaffold for small intestine tissue engineering

- June 2008: TERMIS, Porto, Portugal – International Tissue Engineering Conference: Tissue engineered bowel using biologically derived de-cellularised scaffold

# List of Abbreviations

**α-Gal** - Alpha Gal
**αSMA** - Alpha Smooth Muscle Actin
**ABC** - Avidin-Biotin-Complex
**AD** - Absorbance
**ANOVA -** Analysis Of Variance
**APTS** - 3-aminopropyltriethoxysilane
**BSA** - Bovine serum albumin
**CCR7** - Chemokine Receptor 7
**CE** - Coefficient of Error
**CHAPS** - 3- ((3-Cholamidopropyl) dimethylammonio)-1-Propanesulfonic Acid
**CK8** - Cytokeratin 8
**Col I** - Collagen I
**Col III** - Collagen III
**Ctr** - Control
**DAB** - 3', 3-diaminobenzidine
**DAPI** - 4',6-diamidino-2-phenylindole
**DCAMKL-1** - Doublecortin and CaM Kinase-like-1
**D-PBS** - Dulbecco's Phosphate Buffer Saline
**DPX** - Di-N-Butyle Phthalate in Xylene
**DMEM** - Dulbecco's Modified Eagle's Medium
**DNA** - Deoxyribonucleic Acid
**DNaseI** - Deoxyrybonuclease I
**EDTA** - Ethylenediaminetetraacetic Acid
**EGTA -** Ethyleneglycotetraacetic Acid
**ECM** - Extracellular Matrix
**EGF** - Epithelial Growth Factor
**ESC** - Embryonic Stem Cells
**EtOH** - Ethanol
**FBS** - Fetal Bovine Serum
**FGF** - Fibroblast Growth Factor
**FVIII** - Factor VIII
**GAGs** - Glycosaminoglycans
**GFP** - Green Fluorescent Protein
**GH** - Growth Hormone
**GLP-2** - Glucagon-like-peptide-2
**GMP** - Good Manufacturing Practice
**HBSS** - Hank's Balanced Salt Solution
**HCl** - Hydrochloric Acid
**H&E** - Haematoxylin and Eosin
**HGF** - Hepatocyte Growth Factor
**HMDI** - Hexamethylene Di-isocyanate
**$H_2O_2$** - Hydrogen Peroxide
**ICC** - Immunocytochemistry
**IFNγ** - Interferon Gamma

**IGF** - Insulin –like Growth Factor
**IgG** - Immunoglobulin
**IHC** - Immunohistochemistry
**IL-2** - Interleukin – 2
**IPA** - Isopropanol
**IV** - Intravenous
**LILT** - Longitudinal Intestinal Lengthening
**M**- molecular marker
**MeOH** - Methanol
**MSC** - Mesenchymal Stem Cells
**Msi-1** - Musashi-1
**M1** - Cytotoxic Macrophage Phenotype
**M2** - Anti-inflammatory Macrophage Phenotype
**NaCl** - Sodium Chloride
**$NaHCO_3$** - Sodium Carbonate
**OU** - Organoid Units
**PA** - Paracetic Acid
**PBS** - Phosphate Buffer Saline
**PGA** - Polyglycolic Acid
**PLA** - Poly-lactic Acid
**PLGA** - Poly (lactic-co-glycolic) Acid
**PLLA** - Poly(L-lactic) Acid
**PN** - Parenteral Nutrition
**P3HB** - Poly(3-hydroxy)butyrate
**SBS** - Short Bowel Syndrome
**SDS** - Sodium Dodecyl Sulphate
**SDX** - Sodium Deoxycholic Acid
**SDS/Trpx1-3** - one, two or three cycles of combined SDS-trypsin protocol
**$SDX2^{nd}$** - two cycles of Sodium Deoxycholic Acid
**SEM** - Standard Error of the Mean
**SGLT1** - Sodium-dependent Glucose Transporter
**SIS** - Small Intestinal Submucosa
**SMC** - Smooth Muscle Cells
**STDEV** – Standard Deviation
**STEP** - Serial Transverse Enteroplasty
**S-100** - Neural Markers
**TAE** - Tris-acetate Ethylendiaminetetraacetic Acid
**TBS-T** - Tris-Buffer Saline with Tween-20
**TGF** - Transforming Growth Factor
**TNFβ** - Tumour Necrosis Factor Beta
**Trp** - Trypsin Solution
**Tx100** - Triton X100
**Tx100/Nucl** - Triton X100 with nucleases
**UBM** - Urinary Bladder Matrix
**UV** - Ultraviolet
**VEGF** - Vascular Endothelial Growth Factor
**VEGF-R** - Vascular Endothelial Growth Factor Receptor
**VWF** - Von Willebrand Factor
**2D** - Two Dimensional
**3D** - Three Dimensional

# Glossary

**α-Gal** - epitope responsible for hyperacute rejection in xenotransplantation

**Absolute Cell Number** – stereological estimate of a total quantity of cells in the structure

**Absolute Volume** – stereologicaly estimated volume of an entire organ/structure

**Acellular** – not containing any intact cells

**Allograft** - the transplant of an organ or tissue from one individual to another of the same species with a different genotype

**Anastomosis** - reconnection of two luminal constructs such as blood vessels or intestine

**Anticoagulation** – prevention of a blood clot formation

**Autograft** - tissue transplanted from one part of the body to another in the same individual

**"Bench-to-bedside"** - translation of laboratory-based research into viable therapies

**Biodegradable Scaffold** - capable of being decomposed by the action of biological agents scaffold

**Bio-engineering** - is the application of concepts and methods of engineering to solve problems in life sciences, usually refers to scaffold-based tissue engineering

**Biomechanics** - the application of mechanical principles to biological systems

**Bioreactor** - manufactured or engineered device or system that supports a biologically active environment

**Blood Clot** - early product of the blood coagulation

**Cellular viability** - a determination of living or dead cells, based on a total cell sample

**Collagen** - the main component of ECM

**Cross-linking of ECM** - method of improving biological scaffolds' biodegradability by fixing its epitopes

**De-cellularisation** - cell removal from a tissue

**Dynamic Culture** - the maintenance or growth of cells/tissues/organs in non-static conditions, e.g. using perfusion or elecrostimulation

**Elastin** - a protein of ECM that is elastic and allows many tissues in the body to resume their shape after stretching or contracting

**Embryonic Stem Cell** - pluripotent stem cells derived from the inner cell mass of the blastocyst

**Endothelium** - the thin layer of endothelial cells that lines the interior surface of blood vessels, forming an interface between circulating blood in the lumen and the rest of the vessel wall

**Explant** – tissue or its part removed from the body

**Extracellular matrix** - is the extracellular part of animal tissue that usually provides structural support to the cells in addition to performing various other important functions

**Fibrosis** - the formation of excess fibrous connective tissue in an organ or tissue in a reparative or reactive process

**Foreign Body Reaction** - a granulomatous inflammatory response evoked by the presence of a foreign body in the tissues; a characteristic feature of this is the formation of foreign body giant cells

**Glycosaminoglycans** - long unbranched polysaccharides consisting of a repeating disaccharide unit, residual within the cells as well as ECM

**Heparin** - a highly-sulfated glycosaminoglycan, widely used as an anticoagulant

**Histology** - the study of the microscopic anatomy of cells and tissues

**Hybrid Scaffold** – in tissue engineering scaffold composed of biologic and synthetic elements

**Immune Reaction** - the reaction resulting from the recognition and binding of an antigen by its specific antibody or by a previously sensitized lymphocyte, also called immunoreaction

**Immunocytochemistry** - a common laboratory technique that uses antibodies that target specific peptides or protein antigens in the cell via specific epitopes

**Immunohistochemistry** - a common laboratory technique that uses antibodies that target specific peptides or protein antigens in the tissue via specific epitopes

**Immunosuppression** - the reduction or de-activation of efficacy of the immune system

**Implant** - a piece of tissue, prosthetic device, or other object implanted in the body
**Inflammation** – nonspecific, early stage immune response, manifest by increased blood supply and vascular permeability which, in technical terms, allows chemotactic peptides, neutrophils, and mononuclear cells to leave the intravascular compartment

**Intestinal adaptation** - process in which the small intestine increases in size so it has more surface area through which to absorb nutrients, often occurring after bowel resection surgery

**Intestinal epithelium** - simple columnar and conciliated epithelium that covers the small and large intestine

**Intestinal failure** - reduced intestinal absorption so that macronutrient and/or water and electrolyte supplements are needed to maintain health or growth

**In Vitro** - refers to studies in experimental biology that are conducted using components of an organism that have been isolated from their usual biological context in order to permit a more detailed or more convenient analysis than can be done with whole organisms

**In Vivo** - is experimentation using a whole, living organism as opposed to a partial or dead organism

**Macrophages** - white blood cells produced by the differentiation of monocytes in tissues

**Mesenteric Arcade** - a branch of blood vessels, nerves, and lymphatics within the mesentery to supply the intestine

**Mucosa** - the innermost layer of the gastrointestinal wall that is surrounding the lumen, or open space within the tube; this layer comes in direct contact with food called bolus, and is responsible for absorption, digestion and secretion

**Neomucosa** – tissue-engineered mucosa

**Neonatal** – new-born

**Number Density** – stereologicaly estimated numerical density of the objects

**Organoid Units** - multi cellular aggregates containing polarised epithelium including the epithelial and epithelial stem cells, surrounding a core of mesenchymal derived stromal cells (all of the cells of a full-thickness intestinal section)

**Organ Re-perfusion** – intraluminal introduction of fluid (usually blood) into a blood vessel in order to reach an organ or tissues, usually to supply nutrients and oxygen post-trans-/implantation

**Parental feeding** - intravenous bypassing the usual process of eating and digestion

**Progenitor Cells** - a biological cell that, like a stem cell, has a tendency to differentiate into a specific type of cell, but is already more specific than a stem cell and is pushed to differentiate into its "target" cell

**Regenerative medicine** - the process of creating living, functional tissues to repair or replace tissue or organ function lost due to damage, or congenital defects; synonym of tissue engineering involving stem cells use

**Scaffold** - structure capable of supporting three-dimensional tissue formation

**Seeding of a Scaffold** – introduction of cells into the scaffold

**Serosa** - serous coat of the small intestine; the peritoneal covering of the external surface of the small intestine

**Short Bowel Syndrome** - a malabsorption disorder caused by the surgical removal of the small intestine, or rarely due to the complete dysfunction of a large segment of bowel

**Stem Cell** - biological cells found in all multicellular organisms, that can divide through mitosis and differentiate into diverse specialized cell types and can self renew to produce more stem cells

**Stereology** - an interdisciplinary field that is largely concerned with the three-dimensional interpretation of planar sections of materials or tissues

**Subcutaneous** - just under the dermis

**Submucosa** - a dense irregular layer of connective tissue within the intestine with large blood vessels, lymphatics, and nerves branching into the mucosa and muscularis externa

**Surface Marker** - a molecule usually found on the plasma membrane of a specific cell type or a limited number of cell types

**Tissue Graft** - tissue surgically moved from one site to another on the body, or from another individual, without bringing its own blood supply with it

**Thrombogenicity** - tendency of a material in contact with the blood to produce a thrombus, or a blood clot

**Thrombus** - late product of the blood coagulation

**Tissue engineering** - use of a combination of cells, engineering and materials methods, and suitable biochemical and physio-chemical factors to improve or replace biological functions

**Tissue remodeling** - the reorganization or renovation of existing tissues

**Unbiased Counting Frame** – a tool used in stereology to assist in implementing the counting rules resulting in all particles having an equal probability of being selected, regardless of shape, size, orientation, and distribution.

**Warfarin** – anticoagulative drug

**Xenograft** - a surgical graft of tissue from one to another species

**Xylene** – organic solvent used in fixed tissue processing

# Statement of Originality

I, Anna K Nowocin, confirm that the work presented in this thesis is my own but had help with specific areas. All assistance was from other members of the NPIMR except where information has been derived from other sources, I confirm that this has been indicated in the thesis.

Surgical procedures were performed by: myself, Mrs Sandra Surey, Mr Aaron Southgate, and Dr Tahera Ansari, with the assistance of NPIMR-theatre staff.

# Acknowledgements

It would not have been possible to produce this doctoral thesis without the help and support of the kind people around me, only some of whom I am able to mention here.

I would also like to thank my supervisors, Professor Barry Fuller and Doctor Simon Gabe for their wide-ranged help, advice and the support they have shown to my scientific career during the last few years.

I would like to express my appreciation to Sandra Surey for her involvement in the animal experiments. Special Thanks go to Aaron Southgate for his valued input and opinion in the creation of this thesis and being a 'no-matter-what-time-it-is' friend.

Sincerest thanks go also to the NPIMR-staff, especially: Cathy, Lindsay, Dave, Mark and Farhana for all the help in the laboratory and creating a fantastic atmosphere at the department. This thesis would not have been possible without all their help and advice.

There are many others who have given me encouragement within the department. Special thanks go to Kajal, Ania, Jo, Andrey, and most particularly Murali. I am very grateful for the constant support but most of all for their friendship.

I would also like to thank St Mark's Foundation for the financial support of my PhD and Doctor Tahera Ansari for giving me the opportunity to carry out this project.

Thank you to my dearest parents, Lidia and Andrzej, for their patience, support, encouragement and understanding, especially when year after year I was the only Nowocin missing at the Christmas table. Thanks also to my sister, Agnieszka for keeping me entertained and up-to-date with the latest Polish gossip.

I cannot even begin to express my gratitude towards Clai, Amy, Marta and my other friends either here or in Poland. You have helped and supported me in so many ways.

Finally, I would like to thank Joseph Hill, who has been put through every high and low this Ph.D. has thrown at me and took time to read 'the brick'. I could have not made it without you.

*"…Mr artist,*

*Builds a world*

*Not from atoms*

*But from remnants…"*

Zbigniew Herbert
*The Collected Poems 1956-1998*

*This thesis is dedicated to my family and friends.*

# Chapter 1.

# General Introduction

In the 1990's tissue engineering moved from a concept to an approachable and viable clinical solution. Its branching into regenerative therapies provided an opportunity for exploration of alternative treatments for end-stage organ/tissue failures.

Chronic intestinal failures are often severe conditions requiring long-term management or/and intestinal transplantation which significantly decrease quality of life. They are also a source of considerable morbidity and mortality. Investigations into the possibility of using bio-engineered bowel as an alternative treatment option has been mostly performed using small animal models and artificial scaffolds. Early research within the field proved that even though intestine is an organ with the highest rate of proliferation, the source of cells needed to create "off-the-shelf" intestine is very limited. It also became obvious that the straight forward intestinal interposition of synthetic tubular scaffold is currently not viable to make a transition into the clinics (82, 83).

The aim of the present thesis is to investigate the possibility of creating a scaffold for small intestine tissue engineering that could be successfully used in a large animal model. As patients suffering from end-stage bowel failure require significant improvements in absorptive function, engineering biologically derived

grafts approximately 50cm in length could be considered clinically relevant. To avoid graft necrosis and rejection, large constructs need to be provided with immediate re-vascularisation post-implantation. The thesis will explore the method of obtaining lengths of de-cellularised porcine ileum together with its attached mesenteric vascular arcade as a single entity, which can be easily anastomosed to native tissue. The evaluation of the scaffold and sources of cells for seeding it will also be described.

Chapter 1 of the thesis describes the definition, possible outcomes and managements of intestinal failure focusing on patients suffering from short bowel syndrome. It also gives a general introduction into tissue engineering principles, and in particular the branch using de-cellularised organs and tissues. The achievements of tissue engineering in the field of bowel regeneration are also discussed.

Chapter 2 to 7 focus on experimental development of a model and bio-tools for the investigation into the small intestine tissue engineering. Chapter 2 investigates the use of a hybrid scaffold for intestinal regeneration in rodents. It also highlights the advantages of further use of a porcine model. Chapter 3 presents a novel method of de-cellularisation, which allows production of capillarised and ready-to-implant intestinal scaffold. Biocompatibility tests of the produced matrix are described in Chapter 4. Chapter 5 explains how short-term animal studies can give a good prediction of the type of immune response taking place within the scaffold and possibility of implant rejection or acceptance. Chapter 6 presents the results of bio-mechanical performance of acellular scaffold *in vivo*. The last part of experimental work (Chapter 7) shows possible sources of cells that could be used in future investigation of small intestine regeneration. It focuses on sources, methods of

isolation and characterization of cells that could be used for seeding acellular, intestinal lumen and acellular vascular conduits of the scaffold.

Finally the thesis concludes with a general discussion of the finding of the studies described previously. Chapter 8 presents final conclusions and contemplates the production of intestinal substitutes as an alternative to existing management of intestinal failure, shows the importance of using large animal models, as well as tools to reduce time and subsequently the number of animals needed to predict the outcome of the graft's implantation. Furthermore, the sources of cells that could possibly be used in further studies are discussed. Moreover, the chapter summarizes the limitation of the current trend in creating bio-engineered bowel as well as the limitations of the studies. It concludes with a discussion regarding the transition of the presented results into the clinical phase. Chapter finishes with the presentation of the aims of future investigations into studies presented in thesis.

## *1.1. Intestinal failure*

Intestinal failure (loss of absorptive function) most commonly occurs from a loss of intestinal length. It can also occur due to impaired intestinal motility, mucosal function or combination of all three (1). Resection is performed generally for disease, injury or dysfunction sometimes resulting in a short bowel syndrome (SBS) (subcategory of intestinal failure) followed by inadequate enteral caloric absorption, electrolyte, or micronutrient balance for maintenance in adults and growth in children (2). As prolonged malabsorption leads to deficiencies of micronutrients and growth retardations (3), SBS patients are known to require prolonged periods of parenteral nutrition (PN).

The normal small bowel length is estimated to be approximately 600cm. Short bowel was first defined by Rickham (4) as an intestinal remnant of 30% or less, which is a maximum of 75cm of normal small bowel length in neonates and 150 - 200 cm in adults. The incidence of SBS has been estimated to be between 3 and 24.5/100 000 births per year (5).

Extensive small intestinal resection in animals results in marked structural and functional change in the residual intestine, with a significant increase in intestinal mass over a period of weeks post-operatively, called intestinal adaptation (6). It can last up to two years but the ability to become independent from parenteral feeding as a result of intestinal adaptation is possible only in very few patients (7).

The goal of medical therapies is to improve the absorption of enteral calories in order to promote adaptation and weaning of PN. The management of intestinal failure can be achieved either via a surgical or non-surgical route, but favourable outcomes are achieved through the efforts of a multidisciplinary management approach (8).

PN is linked to many complications and the main goal of treating SBS-patients is weaning them off it. Some patients also achieve a plateau in enteral or parenteral nutrition and further intestinal failure management is the only option to facilitate advancement (9). Although PN revolutionized intestinal failure treatment it reduces quality of life as it may be responsible for various complications including growth failure, metabolic disorders and bone disease.

Pharmacological and hormonal adjuncts to promote increase in intestinal absorptive capacity are in the early stage of development. Although some studies show a positive effect of epithelial growth factor (EGF) glutamine, glucagon-like-peptide-2 (GLP-2) and growth hormone (GH) in the treatment of SBS (10).

Numerous surgical options have been pursued to attempt to improve absorption of nutrients from intestinal content. The main goal of these procedures is to slow intestinal transit, taper dilated bowel and promote intestinal adaptation. Experience of these techniques is limited in adults with the majority of surgeries being performed in infants and children.

In patients who are unable to wean off the PN small bowel transplantation is been used as a rescue procedure. Intestinal transplantation offers the possibility of small intestine replacement, albeit with the burden of long term immunosuppressive therapy. For the majority of patients, small intestinal transplantation is indicated only when irreversible small intestinal failure coexists with the failure of PN (loss of venous access due to venous thrombosis, PN related liver failure, and recurrent line related sepsis) (7). Even though performing earlier intestine transplantation could stop the development of irreversible liver failure, earlier transplantation may not improve the quality of life if renal failure, infection, malignancy and graft dysfunction lead to frequent hospitalization (11). Combined liver and small bowel transplantation offers a treatment option in cases where there is irreversible liver damage. There are a number of technical issues with such a procedure (12).

Chronic intestinal failure requiring long term nutritional support is a source of considerable morbidity and mortality. The overall related mortality in infants with SBS ranges from 15 to 25%, and in adults from 15 to 47%. Babies with a congenital SBS, with only 30-40 cm of remaining small intestine and severely disturbed motility represent a special subgroup, characterised by 80% mortality rate (9). Reported patient survival of 95% in group weaned from PN contrasts highly with those remaining PN dependant (52%) at 5 years (13).

The pre-transplant mortality remains higher than any other group awaiting solid-organ (kidney, liver, heart) transplantation (2). Little improvement in graft survival over the last 5 years suggests that a ceiling may have been reached. Almost all patients experience at least one infection following transplantation (12). Complications after intestinal transplantation occur frequently even after the first year and hospital readmission rates are higher than after other solid organ transplants (11).

There has been little improvement in the methods of management of intestinal failure. It can indicate that the plateau has been reached and alternative methods of treatment need to be considered. Taking all treatment options (including transplantation), only 20% SBS patients succeed to wean off PN (14). Only every fifth patient has a chance to be completely treated and it is crucial to develop a uniform in terms of outcome method of treatment that would increase this rate. Poor quality of life after development of intestinal failure and high costs of its management are additional reasons for investigating new solutions. At the moment each little step towards a successful outcome in SBS patients is difficult to achieve, and progress follows an exponential curve in regards to time and cost (9).

The last 20 years has brought a new solution to some end-stage organ failures. Tissue engineering allows constructing the failing organ/tissue using autologus cells, which can eliminate immunosuppression-related complications. Small intestine tissue engineering could create an opportunity to use *ex vivo* grown autografts to lengthen small intestine in SBS patients. This would not preclude more traditional lengthening but in fact could potentially increase the overall gain if both techniques could be used either sequentially or simultaneously making this strategy especially attractive. Tissue engineered grafts could have potential to become indications not only for life threatening complications, but also for improved quality of life. Moreover, bio-

engineered grafts could potentially be grown appropriately early, and implanted while resecting the diseased bowel. This would eliminate the need for multiple procedures and lower the risk of surgical complications. The rate of adaptation of the remaining bowel following resection is highest within the first few weeks after the operation. Therefore grafts implanted at resection time would have a grater chance to undergo adaptation at the same rate as the remnant bowel. *In vitro* manipulation and pre-conditioning (e.g. with GLP-2 or GH) of grafts could also benefit the adaptation process.

## *1.2. Tissue engineering: general introduction*

Scientists in the field of regenerative medicine and tissue engineering are now applying the principles of cell transplantation, material science, and bio-engineering to construct biological substitutes that will restore and maintain normal function in diseased and injured tissues (15). Application of tissue engineering technology may offer novel therapies for patients with injuries, end-stage organ failures, or other clinical problems (15).

New techniques of cell harvesting, *in vitro* culturing and extracellular matrix (ECM) analysis led the way to more advanced understanding of the tissues' functionality, proliferation and differentiation. This was the beginning of an era, when scientists started combining the devices and materials with a cell biology concept, creating a new field called tissue engineering (16).

Tissue engineering was brought into the public eye with the airing of a BBC broadcast on the potential of tissue-engineering cartilage using images of the now infamous 'mouse with the human ear', later called *auriculosaurus*. Since then science-fiction dogma started to form a more realistic shape, and the new field underwent

drastic development. In the last few decades scientists have attempted to grow native and stem cells, engineer tissue and design treatment method using regenerative medicine techniques for virtually every tissue of the human body (17).

Engineering new tissues, ideally from the patient's own body cells to prevent rejection by the immune system, has got to be seen as the way forward also when alternative SBS management is considered. Tissue engineering rests on three pillars: cells, supporting structures (scaffold) and stimulating biomolecules.

It entails the *in vitro* generation of biological tissue from individual cells with the aid of support structures and growth factors. This approach differs from *in vivo* guided tissue regeneration which is based on implanting matrices that are populated with the patient's cells to support the regenerative abilities of the body. A widely used basic strategy has been to harvest cells from a patient, expand them in cell culture, and seed them onto a scaffold that provides a biomechanical environment that drives formation of the required tissue until the cells produce their own ECM. After implantation, the tissue engineered construct must be able to survive, restore normal function, and integrate with the surrounding tissues (18). Success in tissue engineering will only be achievable if issues at these three different levels: cell technology, construct technology and integration into the living system can be addressed.

### 1.2.1. Scaffolds in tissue engineering

The design and choice of biomaterials is critical in the development of engineered tissues. The biomaterial must be capable of controlling the structure and function of the engineered tissue in a predesigned manner by interacting with transplanted cells and/or the host cells. Generally, the ideal scaffold should be

biocompatible, promote cellular interaction and tissue development, and possess proper mechanical and physical properties. If the selected biomaterial is biodegradable, the degradation products should not provoke inflammation or toxicity and must be removed from the body via metabolic pathways. The degradation rate and the concentration of degradation products in the tissue surrounding the implant must be at a tolerable level (19). The biomaterial should provide an appropriate regulation of cell behaviour, such as adhesion, proliferation, migration and differentiation in order to promote the development of functional new tissue. Most mammalian cells will die if no cell-adhesion substrate is available, therefore scaffolds should provide a cell-adhesion substrate that can deliver cells to specific sites in the body with high loading efficiency. Cell behaviour in engineered tissues is regulated by multiple interactions with microenvironment, including interactions with cell ligands and growth factors (20). The biomaterials should possess appropriate mechanical properties to regenerate tissue with predefined sizes and shapes. The composition, structure, and therefore the mechanical properties of the ECM can be specific to each organ or tissue. Therefore, scaffolds for certain applications should provide temporary mechanical support sufficient to withstand *in vivo* forces put on them by the surrounding tissue and to maintain space for potential tissue development. The scaffolds should also be maintained until neotissue has sufficient mechanical integrity and strength to support itself. It must also allow cells to be supplied with nutrients during vascularisation (21).

The scaffolds used in tissue engineering can be biologically derived or synthetic. As the field evolved it became obvious that engineering soft tissues mostly needs the involvement of the biological materials whereas regeneration of bones and cartilages usually requires use of artificial, mechanically stronger scaffolds. The third

group are hybrid scaffolds, which are fabricated from naturally derived (collagen) and synthetic (polymers) ingredients. They express characteristics of both subgroups depending on the ratio of biologic/artificial elements.

### 1.2.2. Sources of cells in tissue engineering

Something very important for the success of tissue engineering is the ability to generate sufficient numbers of cells that maintain the appropriate phenotype and perform the required biological functions. For example cells need to produce the ECM in the correct organisation, secret cytokines and other signalling molecules, and interact with neighbouring cells/tissue. This immediately rises a number of potential problems, not least of which is obtaining appropriate cell numbers to promote repair. Cells used in tissue engineering could be primary cells or stem cells (including embryonic, fetal and adult stem cells). They can come from three sources: the patient him/herself (autologus cells), another donor of the same species (allogeneic cells) or another species (xenogeneic cells) (22). Deriving cells from the patient by biopsy is advantageous as it avoids an immune reaction and has a low risk of infection. However, the availability might be limited, depending on the cells that are needed.

Therapeutic cloning, cellular reprogramming and gene therapy may one day provide a potentially limitless sources of cells for tissue engineering applications, but currently none of them are widely investigated in tissue engineered constructs (15).

The fundamental biophysical constrain of mass transfer of living tissue needs to be understood and dealt with on an individual basis as tissue engineering moves towards human applications. Large masses of cells for tissue engineering need to be kept alive, not only *in vitro* but also *in vivo*. The design of systems to accomplish this,

including *in vitro* bioreactors and *in vivo* strategies for maintenance of cell mass, presents an enormous challenge, in which significant advances have been made.

### 1.2.3. *In vitro* and *in vivo* development of tissue engineered constructs

Once a scaffold and the cells that are to be employed have been selected, there are other issues to address. A critical one is what will be the environment that will foster the appropriate growth and/or conditioning of the tissue substitute.

*In vitro* tissue engineering involves manipulation of the cells in the culture, before implanting into the *in vivo* environment. Controlled incubation conditions play an important role in the construction and use of modern *in vitro* systems for tissue engineering (23).

An overall comparison of different culture methods shows clearly the advantage of bioreactor culture. The most common approach in culturing specimens for organ or tissue replacement is to immobilize appropriate cells in the scaffold and use a bioreactor that confers a dynamic *in vitro* environment for tissue growth (24).

The design of bioreactors intended for tissue engineering is focused upon influencing cell behaviour, and incorporates such features as the controlled and steady flow of cell media, pulsatile fluid flow, or culture vessel rotation to influence tissue development (25). These attributes are pivotal not only for controlled, reproducible investigations but also for routine manufacturing of tissues for clinical applications (26).

Fluid dynamic stress, or ‘shear stress’, induced by the fluid flowing across the construct surface and into the porous space, is believed to be the most important mechanical stimulus in activating the mechano-transduction signalling. Consequently,

fluid flow induces mechanical stimuli. Pulsatile fluid flow has been used to develop tissue engineered heart valves and blood vessels, which makes them better adapted and pre-conditioned for *in vivo* placement tissue (27). The cyclic stress increases tissue organization and expression of elastin by smooth muscle cells (SMC) as well as stimulates glycosaminoglycans (GAGs) synthesis (28). Controlled flow of cell media has also been used for the dynamic seeding, which in the cases of many organs is more efficient than a static one (29). Currently most of the bioreactors used *in vitro* fail to provide all the necessary stimuli, but it is very encouraging that most of the studies move from static to dynamic culturing (20).

Like most areas involving biologicals, the translational lag from experimental work to clinical applications has varied depending on the complexity involved. Preclinical studies are another step in decreasing this lag and they usually follow the *in vitro* stage of developing tissue engineering therapy. Elegant methods of *in vitro* tissue engineering are very often difficult to transfer to the patient and that is where *in vivo* studies become essential precursors to clinical applications. The choices of *in vivo* remodelling systems are many, including rodent animal models, large anima models and eventually nonhuman primates. The choice of the system depends on the type of the construct being tested, the variable we want to asses (e.g. biocompatibility tests, survival rate of seeded cells, neo-vascularisation), time of the planned experiments, similarities of the pathophysiology, physiology and structural components and last but not least the costs and availability of the animal facilities (30).

The final analysis of tissue engineered products need to be performed *in vivo* in order to evaluate mammalian response to the implant. Tests of *in vitro* constructs implanted *in vivo* focus on maximizing cell survival and differentiation after grafting

and assessment of their biocompatibility and toxicity (31). The most important is the potential immune response that the graft could induce. The bioengineered materials tested in pre-clinical studies are of various biocompatibilities and therefore acute or chronic immune responses towards the end products should be evaluated *in vivo*. This usually involves the use of rodent model (in instance of this thesis: rat) to check for immediate toxicity and distinguish between acute and chronic reactions. It is important to be aware of the species differences (especially considering rat vice human ones) but as a general it is very likely that if a material elicits chronic inflammation and is rejected in rodents it will do so when implanted in humans. At the same time the reverse assumption is more difficult to certify. Even with primate systems (the most sophisticated and costly tests) there still remains a question of the eventual outcome in humans, thus the necessity for phased human clinical trials (30).

*In vivo* methods in tissue engineering can be used as testing systems for constructs developed *in vitro* or they can be an integral part of the actual remodelling process. *In vivo* remodelling processes rely on the body's natural ability to regenerate over non-cell-seeded biomaterials. In many situations, remodelling may facilitate or be necessary for successful integration of the tissue-engineered construct. Host remodelling is viewed as an inevitable and often beneficial stage of the tissue-engineering process (32).

Recently scientists recognized the importance of two key issues when they started to use animal models: vascularisation and innervation (33). Moreover, an importance of achieving 'ready-to-anastomosed' constructs has been discussed (34). In addition, there is a significant need for development of methods to evaluate quantitatively the performance of an implant (35).

### 1.2.4. Biomechanical properties of tissue engineered constructs

The *in vivo* and *in vitro* systems presented above play a key role in the advancement of the tissue-engineered products. Tissue culture systems provide dynamic media fluids flow around or within the tissue-engineered construct to not only enhance nutrient and waste exchange but also improve mass transport delivering flow-mediated sheer-stress to the specimen. Exposure to these load-bearing situations requires the consideration of biomechanical aspects for their integrity and function. Almost every scaffold developed for load-bearing situations must obviously sustain the stress it will be exposed to (36). Thus, in the design of a scaffold, the biomechanics is very crucial to insure its functional and structural integrity.

At first, the mechanical properties of the tissue should be well defined. For intestine, it includes all its morphological and functional aspects, and most importantly its peristalsis, which is directly affected by functionality of *Muscularis Externa* and luminal content flow. Biomechanics highlight many challenges when considering replacing tissues like small bowel that function within complex and demanding mechanical environment *in vivo*. Therefore material properties of the scaffold used for intestinal regeneration need to be taken into account when designing intestinal scaffolds. The particular loading conditions need to be evaluated in relevant *in vivo* and/or *in vitro* tests linked to the clinical application target (as lack of motility and peristalsis is second to surgical resection cause of SBS). Most common estimation of soft, contractible constructs (blood vessels, intestine, bladder) includes values of burst pressure, which state of their elasticity to expanding volumes.

Moreover, the success of the given scaffold is only complete when the decreasing mechanical properties during its biodegradation will be compensated by appropriately organised new-formed tissue (36), and ease of handling by surgeons (37).

Biomechanical properties are also very important in directing tissue-engineered construct maturation stimulating (by e.g. cyclic distension, stretching, compression, elecrostimulation) specific cell lines (e.g. endothelial, smooth muscle), which differentiation is modulated by varying the stiffness of the underlying matrix (38). Local stresses and strains play a ubiquitous role in modulating cell behaviour and thus the tissues they create and maintain.

Testing and optimization of the biomechanical properties of constructs fall outside the scope of the present thesis. It should however be noted that such biomechanical properties are likely to have a significant bearing on the viability of the construct post-implantation. Thus, the biomechanical evaluation needs to precede further *in vitro* and *in vivo* studies, especially when designing a bioreactor that will use the optimal mechanical conditioning strategies to grow functional tissue.

## *1.3. Engineering of tissues/organs using de-cellularised matrices*

Scaffolds that provide a favourable environment for normal cellular growth, differentiation and angiogenesis are important components for tissue engineered grafts because rapid integration with the host tissue is essential for long term graft viability. Biologically derived scaffold materials upon implantation elicit such response and therefore contribute considerably to restoration of structure and function specific to the grafted site.

### 1.3.1. The concept of ECM scaffolds

Removal of cells from a tissue or organ leaves behind a complex mixture of structural and functional proteins that constitute the ECM and provide cell-to-cell, and cell-to-matrix contact creating an ideal environment for the growth of new tissue. It provides a source for allogeneic and xenogeneic whole-organ grafts (32). Crucial for the use of ECM as a scaffold for tissue engineering is that growth factors, cytokines and other small molecules, released from cells during the de-cellularisation process stay within the ECM, survive tissue processing and sterilization, and maintain their functionality (39). The therapeutic approach where growth factors and cytokines are loaded onto the synthetic or biologically derived scaffolds has struggled in determining the optimal dose, sustained and localized release at the desired site, and the inability to turn the factors 'on' and 'off' as needed during the course of tissue repair.

There are two main approaches to using these biologically occurring matrices in repair and regeneration of the tissues. In the first approach tissues, that have been denuded of cellular and nuclear content are implanted as intact acellular grafts, which act as the scaffold for ingrown of the host cells. This approach places high priority on the native structure and composition of ECM and its inherent ability to interact with the host tissue. The other approach focuses less on the bioactive molecules and more on the scaffolds macrostructure. This approach first requires for the scaffold to support *in vitro* cell growth. Autologus cells are grown to confluence or are sculptured into bioartificial organs that are then returned to the patient as a 'living' tissue (40). Most of the preclinical and clinical work uses the first approach or uses acellular matrices, which are seeded with cells, but not cultured *in vitro* for a long time, prior to implantation into the recipient.

Components of the ECM are generally conserved among species and are tolerated well even by xenogeneic recipients (41). Those matrixes, though harvested from different body systems, all share similarities when processed into a graft material. Acellular matrices keep their natural, 3D structure almost identical to their native tissue, which can significantly influence proliferation and differentiation of host-derived cells seeded onto the scaffold (42). The internal geometry of a tissue engineered scaffold specific to a particular tissue or organ will not only direct new tissue formation unique to that particular topography but also allow for mass transport properties sufficient for the exchange of biological nutrients and waste.

The composition of ECM is a polymeric network consisting of macromolecules encapsulating smaller molecules, ions and water. The macromolecules are a complex mixture of polymer forming proteins, glycosaminoglycans, glycoproteins and micromolecules in a unique, tissue specific 3D architecture (43). Whilst all ECM share these basic components, the organisation and mechanical properties of ECM are influenced by the chemical composition and 3D configurations of its components and can vary widely in different tissue. Thus, the ability of the ECM harvested from one tissue to function as a biological scaffold material for different tissue may vary (44).

Use of ECM prevents many of the complications associated with foreign materials as they are known to induce less of adverse responses due to removal of most of the cell-related epitopes from the tissue, preserving naturally existing proteins in specific body locations (40).

The foremost features of ECM include recruitment of host cells followed by smart remodelling which when not cross-linked causes degradation of the ECM, and replacement of the scaffold by the new host-derived matrix (45). This smart, ECM-

induced remodelling response is a distinctly different phenomenon from that of scar tissue formation. These features are highly advantageous making de-cellularised tissues and organs ideal scaffolds. The mechanical behaviour of ECM scaffolds changes during the process of *in vivo* remodelling, and these changes are dependant on factors such as local tissue microenvironment, the rate of scaffold degradation, forces present within the mechanical environment, and the rate and extent to which the infiltrating cells deposit new ECM and interact with it (46). Structural changes that occur during *in vivo* remodelling of ECM scaffolds are associated with marked changes in scaffold strength. Shortly after implantation, ECM scaffolds typically show a decrease in strength that is temporally associated with the rapid *in vivo* degradation of the scaffold (47). However, once the infiltrating cells have established residence and begin producing site-specific new ECM, rapid scaffold remodelling occurs, with an increase in the strength and site-appropriate mechanical behaviour (48). Furthermore, active loading of a remodelled ECM scaffold accelerates the formation of robust site-specific tissue by facilitating normal ratio of different types of collagen and distribution of collagen fibril diameters (49).

Angiogenesis is another common event during the remodelling of ECM scaffolds. Peptides that modulate angiogenesis and the recruitment of endothelial cells facilitate the development of a rich blood supply to the remodelling tissue for as long as 6-8 weeks (50).

The tissue from which the ECM is harvested, the species of origin, the de-cellularisation method and the method of terminal manipulations of the scaffold vary widely, and they all affect the composition and ultrastructure of the ECM and accordingly, following implantation affect the host response to the matrix.

### 1.3.2. Methods of de-cellularisation

The goal of de-cellularisation is to remove all cellular and nuclear material while minimizing any adverse effect on biological composition, ECM activity, and mechanical integrity of the remaining structure. The process itself affects the biochemical composition of ECM, tissue ultrastructure and to some extent the mechanical behaviour of ECM. Essential during the removal of cellular components of the tissue is disruption of the ECM to allow adequate exposure of all cells to the lyses-inducing agents and to provide a path for cellular material to be removed from the tissue (51). The efficiency of de-cellularisation depends upon the origin of the tissue, method of cell removal, and the technique used for terminal sterilization of the ECM. As studies advance towards tissue with more complex geometries, the de-cellularisation process has evolved to meet stricter standards needed for allo- and xenograft studies. While a de-cellularisation treatment may efficiently remove cellular material in some tissues, denser, thicker tissues and organs may need improved penetration into the tissue (51). All methods of de-cellularisation will alter the native 3D architecture of the ECM and the most commonly used methods aim to restrict this drawback to a minimum. After determining methods of de-cellularisation, optimization of de-cellularisation reagent incubation times, temperature, concentration or number of solvent cycles have to be optimized (52). Agents most commonly used in de-cellularisation of specific organs and tissues have been summarised in **Table 1 (Appendix 1)**.

### 1.3.3. Manipulation of de-cellularised tissues/organs

Cross-linking and terminal sterilization are two most commonly used modifications of ECM scaffolds. ECM scaffolds can also be dehydrated to minimize

changes in the tissue architecture (collapse of collagen fibres upon each other, formation of physical bonds between ECM molecules) caused by disinfection and sterilization. Cross linking may be necessary when using scaffolds for mechano-skeletal applications in order to increase ECM strength and allow neo-tissue formation over longer period of time than when using a non-modified scaffold. Sterilization processes are always necessary prior to *in vivo* evaluation.

Generally, *in vivo* and *in vitro* performance of non-modified scaffolds is better than the modified ones, and the optimal configuration and method of processing ECM scaffolds should be determined for each scaffold and application (bearing in mind clinical use).

### 1.3.4. Immune response to ECM scaffolds

Variables that affect the host response include manufacturing process, the rate of scaffold degradation, and the presence of cross species antigens. In spite of extensive measures taken to de-cellularise tissues in the preparation of ECM scaffolds, the complete elimination of all cell membrane and nuclear material is very difficult and perhaps impossible.

The long term immune response in the host of implanted ECM scaffold has yet to be fully elucidated, but includes chronic inflammation, fibrosis, scarring and encapsulation or acute inflammation and immune response followed by site appropriate tissue remodelling (53). An immune reaction to biomaterials starts with the immediate recruitment of protein adsorption onto the biomaterial surface, this in turn attract neutrophils followed closely by macrophages resulting in a fibrotic encapsulation or smart remodeling (54).

A host immune reaction to a biological ECM scaffold is both acquired and innate and is material specific (initial source of the ECM and the methods used to manufacture it). This device specificity was highlighted in a recent study investigating host immune response to five commercially available ECM based devices (53) and concluded that scaffolds composed of ECM differ noticeably in the elicited host immune response. This made also clear that traditional histological methods of evaluating the host response are not necessarily predictive of the long term remodelling outcome (55). Use of ECM scaffolds that are completely de-cellularised and not cross-linked has been proven in most cases not to induce fibrosis or results in noticeable voiding dysfunction (56).

Immediately following implantation of the ECM scaffolds *in vivo*, there is an intense cellular infiltrate consisting of equal numbers of polymorph nuclear leukocytes and mononuclear cells. After 72 h post implantation, the infiltrate is almost entirely mononuclear cell in appearance with early evidence for neovascularisation (57). Between days 3 and 14, the number of mononuclear cells increases, vascularisation becomes intense, and there is a progressive degradation of the non-cross-linked scaffold with associated deposition of host derived neomatrix. Post 14 days, the mononuclear cell infiltrate diminishes and there is the appearance of site specific parenchymal cells that orient along lines of stress (56).

#### *1.3.4.1. DNA-induced response*

As mentioned earlier it is highly unlikely that all cellular or nuclear material will be effectively removed from biological scaffolds, especially from relatively dense tissues (e.g. dermis). DNA residual in bioscaffolds has been suggested to be responsible in some cases for the inflammatory reaction after implanting in patients or animals (53). Remnant DNA found in most commercially available ECM is short

strand DNA of less than 300 base pairs. (58). The quantity of remaining DNA after reaching a certain threshold may influence the process of ECM remodelling or induce an inflammatory response (53).

#### *1.3.4.3. Th1 and Th2 lymphocyte response*

Several studies have examined the role of Th1 and Th2 lymphocytes in cell mediated immune response to ECM grafts. Activation of the Th1 pathway produces interleukin – 2 (IL-2), interferon gamma (IFNγ) and tumour necrosis factor beta (TNFβ) leading to macrophage activation, stimulation of complement fixing immunoglobulin (IgG) isotypes (2a and 2b) and differentiation of CD8+ cells to a cytotoxic phenotype. Activation of this pathway is associated with both allogeneic and xenogeneic transplant rejections. The Th2 lymphocyte response produces IL-4, IL-5, IL-6 and IL-10, cytokines that do not activate cytotoxic macrophages and lead to the production of non-complement fixing antibody isotypes (IgG1). The Th2 pathway is associated with transplant acceptance. In summary, the immune response to ECM scaffolds that are acellular and non-cross-linked has been partially characterized and suggests a Th2 restricted type of response. The pathophysiology of this response is unknown, but the lack of cellular component within the grafts is likely to be an important mediator of the host tissue response of Th2 character (53).

#### *1.3.4.4. M1 and M2 macrophage response*

Phenotypic and functional polarization of the mononuclear macrophages has recently been described (59). It is similar in its polarization to Th1 and Th2 host response pattern. The pro-inflammatory, cytotoxic macrophage phenotype (M1) is characterised by pathogen killing cells and cells associated with classic signs of

inflammation (especially chronic one). The anti-inflammatory macrophage phenotype (M2), promotes immunoregulation, tissue repair and constructive remodelling. These two phenotypes are only distinguishable by analysis of their surface markers, and cytokine and gene expression profiles (60). M1 macrophages are CD68+, CCR7+ and CD80+ in terms of surface markers (there are some species differences though). They secrete large amounts of nitric oxide and other reactive oxygen intermediates, and copious amounts of inflammatory cytokines such as IL-12 and TNFα. M2 type produce high levels of IL-10 and TGF-β and arginase, and they also inhibit release of pro-inflammatory cytokines, scavenge debris, promote angiogenesis, and recruit cells involved in constructive tissue modelling. They express CD163 as their surface marker and no CD80 or CCR7, but again species differences exist.

### 1.3.5. Application of de-cellularised tissues in preclinical and clinical studies

Today more than 500,000 human patients have been implanted with de-cellularised scaffolds (61). The ECM scaffolds have been mostly used to repair or restore the tissues, but the first implantation of a bio-engineered trachea can be considered as an application towards regeneration of an organ (62). Examples of use of the ECM scaffolds for repair of tissues and organs in preclinical and human studies have been presented in **Table 2 (Appendix 2)**.

## 1.4. Tissue engineering of the small intestine: current status

The native small intestine composed of duodenum, jejunum, and ileum, is the most critical portion of the gastrointestinal tract. It is a complex and unique organ due to its digestion and gradient transport (absorption and secretion) capabilities. The digestion and absorption capacity of the small intestine is facilitated by its highly specialised columnar epithelium, which features microscopic, finger-like projections, known as villi, which help to increase total surface area. Brush border enzymes facilitate the digestion of carbohydrates as they are absorbed. In addition, each villus contains a lacteal and capillaries. The lacteal absorb the digested fat into the lymphatic system, whereas the capillaries absorb all other digested nutrients. By the time the remaining products have reached the end of the small intestine, almost all nutrients and 90% of the water have been absorbed. The smooth muscle layers of the small intestine are well organised and consist of an inner circular layer and an outer longitudinal layer. Intestinal smooth muscle helps to initiate peristalsis. Both muscle layers are innervated intrinsically by autonomic nerve fibres and extrinsically by vagal and sympathetic nerve fibres. The celiac and superior mesenteric arteries provide essential arterial blood flow to the entire small intestine. The organ is a rich source of regulatory peptides, including secretin, cholecystokinin, and somatostatin, which are important for the control of various aspects of gut function. The mucosal immune system within the small intestine is critically important for defence against toxic and pathogenic threats from the lumenal content (63). Such structural and functional complexity is partly a cause of the fact that tissue engineering of the small intestine is still in its infancy.

### 1.4.1. Approaches to tissue engineering of the small intestine

Conceptually, there are two possible approaches to tissue engineering of the small intestine. The first approach is to try to replicate the anatomical structure of the small intestine with the assumption that this will produce functional replacement tissue. But recapturing such complexity is almost impossible. The second approach is to concentrate primarily on producing a functional absorptive surface without necessarily reproducing the exact anatomical structure of the small intestine. While ultimately this is likely to be inferior to the production of functional replica tissue, which would be considered to be the gold standard of tissue engineering, it is likely to yield greater therapeutic possibilities in the short to medium term.

The majority of studies to date have concentrated on the production of a tissue engineered layer of small intestinal mucosa, often referred to as neomucosa. Generation of an intact neomucosal layer is understandably considered to be vital for the manufacture of a functional replacement intestinal tissue (neointestine). However, it must be remembered that the function of the small intestine is also dependent on an adequate vascular supply and lymphatic drainage as well as coordinated peristalsis dependent on correctly innervated muscular layers.

### 1.4.2. Possible source of intestinal regeneration

Native intestinal mucosa has an impressive capacity for replication and regeneration both under normal physiological conditions and following injury. This regenerative capacity is dependent on the activity of intestinal epithelial stem cells. Advances in the ability to identify and culture intestinal stem cell populations have made it possible to transplant stem cells onto artificial scaffolds in order to create neointestine.

### *1.4.2.1. Epithelial cell lineages of the small intestine*

The epithelium of the intestine is a confluent cell layer consisting of a number of cell subtypes each with specialized functions that help it to perform its two major physiological functions: providing an effective barrier between the lumenal contents of the intestinal tract and underlying sterile mucosa, and efficiently absorbing nutrients and water from ingested food (64). The epithelial lining of the intestine is folded into invaginations called crypts, which vary in size, depending on their location, species, age and their function. In addition, the surface area is further increased by the formation of lumenal prominences called villi.

Intestinal epithelium consists of five cell lineages. Enterocytes also called columnar or absorptive cells, are the most abundant cell type. They are responsible for membrane digestion and absorption of nutrients within the lumen of gut. They are facilitated by the presence of microvilli at their apical surface that increase the absorptive surface area. Goblet cells are found scattered between enterocytes and can be easily identified by the large mucin filled vacuole in their cytoplasm **(Fig.1)**. Enteroendocrine cells secrete peptide hormones and are found scattered throughout the epithelium. M (membranous or microfold) cells are antigen-sampling cells and are found near lymphoid follicles. Paneth cells are found at the base of crypts and are packed with strongly eosinophilic granules, which contain lysozyme and antibacterial defensins. Enterocytes, goblet cells and enteroendocrine cells become more differentiated as they mature and migrate upward from the base of the crypt towards the villous tip. Paneth cells differ and migrate down towards the crypt base (65). Once the epithelial cells reach the tip of the villi they undergo spontaneous apoptosis and are shed into the lumen or phagocytosed. In the healthy gut the net amount of

apoptosis equals the influx of epithelial cells migrating onto the villi per day, maintaining homeostasis of the epithelial cell population (66).

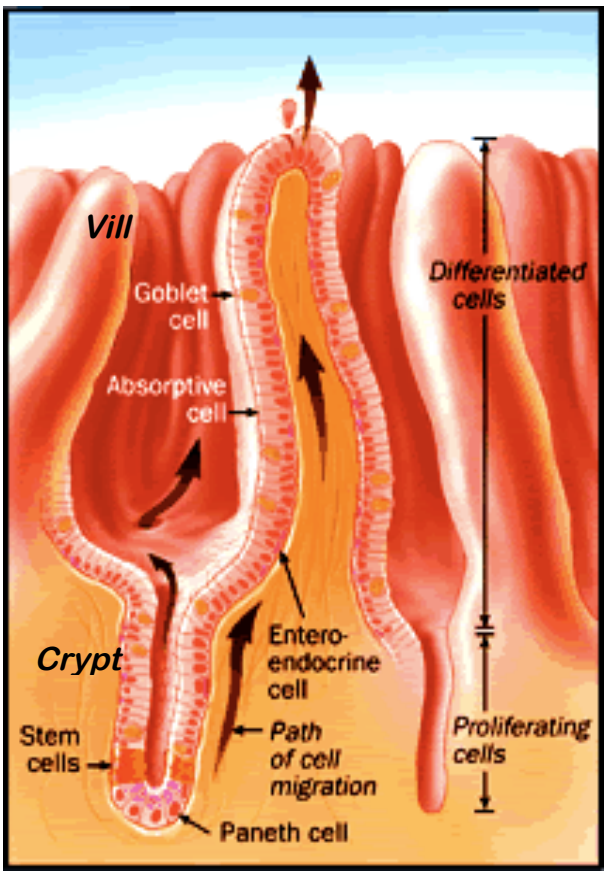


**Fig. 1**. Epithelial cell lineages of the small intestine; the arrows indicate the direction of proliferating and moving towards tip of the villi enterocytes, goblet and enteroendocrine cells. http://medicine.emory.edu/divisions/gi/research/yang_lab.cfm

### *1.4.2.2. Epithelial stem cells of small intestine*

The intestinal mucosa has an amazing regenerative capacity, enabling rapid restoration of its physiological functions following injury. Mucosal epithelium undergoes a continuous rapid turnover throughout life, with the entire epithelial lining being replaced every 3-5 days. However the potential capacity of this mechanism is only demonstrated during pathological conditions when major damage has occurred to the intestine, for example following trauma or disease, resulting in increased epithelial regeneration. The ability to do this resides with the epithelial stem cells (64). This

ability is now recognised as a potential therapeutic strategy for conditions where the absorptive and/or barrier function of the intestine are insufficient, and that recognition is especially strong in the new field of tissue engineering.

Intestinal epithelial stem cells reside in specific niches within crypts, on the mucosal surface also known as the 'stem cell niche' (67) **(Fig. 1)**. This niche comprises the intestinal epithelial stem cell, neighbouring proliferating cells, and adjacent mesenchymal cells such as the pericryptal fibroblasts and intestinal subepithelial myofibroblasts. These mesenchymal cells are believed to play an important role in the maintenance of the stem cell population and the control and regulation of proliferation via the secretion of various peptides including hepatocyte growth factor, keratinocyte growth factor and tissue growth factor-β (67). There are complex signalling pathways between the different components of the stem cell niche, including the Wnt, hedgehog and notch pathways and understanding of this signalling is increasing rapidly (67) Despite the lack of well-characterised molecular stem cell markers, the likely location and identity of the intestinal stem cells has been determined using both cell morphological and functional criteria. Morphologically, stem cells appear undifferentiated and may exhibit embryonic cell-like features (68). Functional characteristics include the ability to proliferate to replicate and to regenerate the lineage precursors that differentiate and produce mature cell populations that migrate upwards from the crypt base. The regenerative capacity of intestinal stem cells following pathological damage has for the first time been demonstrated by microcolony assays after cytotoxic radiation of intestine (69).

Small intestinal stem cells are located in the base of the crypts (70). These stem cells are interspersed with Paneth cells and daughter cells, which move up the crypt, where they make up a population of transit cells. The transit cells in turn supply

mature enterocytes for the surrounding villi and replace those enterocytes that are lost at the villus tip (71).

The number of stem cells per crypt has not been established and estimates vary between few to few tens per crypt. This variation depends on differences of opinion regarding what defines a stem cell, species and stage of development (72). More and more authors accept the fact that 4-6 intestinal stem cells may residing in one crypt (64).

Unitarian hypothesis, that a single intestinal stem cell can give rise to all intestinal epithelial cell lines is supported by a significant body of evidence and, appears to apply to both rodents and humans (67). Stem cells, daughter cells, and initial transit cells retain their clonogenicity and are able to revert back to stem cells if the crypt is damaged and existing stem cells are lost. However, as the transit cells divide further they lose their capacity for clonal expansion. Furthermore, it is well proven that villi are derived from stem cells of more than one crypt and intestinal crypts are monoclonal and derived from a single multipotential stem cell (20).

#### *1.4.2.3. Organoid units*

A major advancement for small intestine tissue engineering resulted from the development of a reproducible method suitable for isolating and growing small intestinal epithelium in primary cultures. One of the most commonly used techniques involves the gentle enzymatic digestion (using cocktail of collagenase and dispase) of tissue fragments of neonatal intestine into multi cellular aggregates, named organoid units (OU) that contain polarised epithelium including the epithelial and epithelial stem cells, surrounding a core of mesenchymal derived stromal cells (all of the cells of a full-thickness intestinal section). Interestingly, more extensive dissociation by

prolonged enzymatic action to yield single cell suspensions appeared to inhibit cell proliferation (73). This would appear to support the importance of maintaining the stem cell niche.

Approximately 50 000 organoid units, each measuring 100-200 microns in diameter, could be isolated per neonatal rat intestine. *In vitro* culture of these organoids was demonstrated for up to 14 days (73). The majority of researchers have adopted this method as a primary technique in isolating intestinal stem cells. There is even a report presenting continuous *in vivo* observation using an optical tissue window for engrafted organoid units promoting intestinal regeneration (74).

Weiser described his method where he alternatively dissociated cells using a citrate buffer and obtained sequential fractions of epithelial cells in a villus-to-crypt gradient by a series of incubations and washing of gut loops avoiding overmanipulation (75). Subsequent experiments demonstrated that suspensions of intestinal organoids transplanted into subcutaneous pockets in adult rodents could develop into small, short, tubular structures which consisted of a central mucin filled lumen surrounded by a epithelial layer (76). At the same time implantation of single cell suspensions did not result in the formation of cysts containing neomucosa (77). This neomucosa was shown to contain all epithelial cell lineages including Paneth cells which were not identified in six day old neonatal small intestine (76). This is of particular relevance as it suggests development of these cells from pluripotent stem cells in the transplanted intestinal organoids rather than simply from multiplication of more differentiated cells already in the transplanted tissue. Lactase, sucrase, aminopeptidase and alkaline phosphatase activity was also demonstrated in the neomucosa as was sodium-dependent glucose transport (78) suggesting that the neointestine had functional potential. In addition to the neomucosal components,

smooth muscle-like cells were identified adjacent to the neomucosa although they had not developed into discrete muscle layers (76).

Sattar *et al.* demonstrated that intestinal organoids produced from human fetal small intestine could be successfully implanted subcutaneously into immuno-deficient mice to produce cysts of neomucosa similar to that described in rat models (79).

Recently it was reported that the organoid units could also be isolated and promote intestinal regeneration in juvenile pigs (80) and dogs (81).

### 1.4.3. Animal studies in regeneration of the small intestine

Although the study of intestinal regeneration and the attempt to tissue engineer neointestine is a relatively novel field of study, investigators have developed some creative animal models in this pursuit.

Scaffold materials used in tissue engineering of the small intestine are either synthetic or natural. Natural materials have been used principally as scaffolds for intestinal lengthening procedures, where experiments attempting to create neointestine by transplanting stem cell cultures have employed synthetic scaffolds. In the field of small intestine tissue engineering, most studies have used synthetic polymers, (82) and some naturally derived SIS, acellular dermis, and collagen sponges (83).

All studies investigating small intestine tissue engineering have used *in vivo* implantation of cell-scaffold constructs or acellular scaffolds only. This is due to the poor understanding of *ex vivo* behaviour of the intestinal epithelium and intestinal stem cells.

### *1.4.3.1. Intestinal lengthening using artificial tubular scaffolds*

Joseph Vacanti and his colleagues (82) in Boston have been pioneers in tissue engineering neointestine using an absorbable synthetic material. Their methodology consisted of seeding intestinal organoid units onto a tubular scaffold made of PGA and PLLA. Each tube (1 cm long) was highly porous and had a mean pore size of 250 microns to accommodate the size of the organoid units (84). The constructs were implanted into syngeneic rat omentum where within two to eight weeks they developed into vascularised cystic structures lined with intestinal neomucosa (this was also confirmed by other investigators) (85). Moreover, the scaffold wascompletely absorbed and immunohistochemical (IHC) staining for alpha smooth muscle actin (αSMA) was positive in the stroma adjacent to the neomucosa, suggesting of the appropriate reconstitution of an intestinal smooth muscle layer. S-100 stained neuronal cells have also been detected in these constructs. Histologically, the neomucosa was characterised by columnar epithelium containing goblet and Paneth cells. Crypt-like invaginations that resembled crypt-villus structures were also evident. The neointestine had the histological appearance of small bowel and severe biochemical features of digestive enterocyte function, mucus secretion and polarity have been demonstrated in these cysts. Electrophysiology studies of the neomucosa revealed similar transepithelial resistance values to adult rat ileum mucosa, but decreased active transepithelial ion-transport. The brush border enzyme sucrase and basement membrane protein laminin also had a similar distribution to that found in adult rat ileum (86). As a continuum of this prior work, the mature, vascularised cysts were placed in continuity with the gastrointestinal tract following an 85% enterectomy in rats. Most compelling was the rapid return to preoperative weight in the animal implanted with tissue engineered cysts when compared with the animals undergoing

small bowel resection alone. Again the histology of the harvested anastomosed cysts was similar to that of normal adjacent intestine. Anastomosis to the native small bowel resulted in the exposure of the neomucosa to lumenal content including bacteria, gastrointestinal secretions and nutrients, which coincided with the development of a mucosal of a mucosal immune system that contained a similar population of immune cells to that of native jejunum (87). The lumens of these engineered intestinal grafts has been maintained open for up to 36 weeks, where non-anastomosed grafts could survive only up to ten weeks (88). The short survival time of similarly prepared constructs was confirmed by different group (89). Lymphoid aggregates similar to Peyer's patches or isolated lymphoid follicles were identified in the tissue engineered cysts, but the phenotype of the follicle associated epithelium overlying the gut associated lymphoid tissue or presence of M cells were not reported. Furthermore, the neointestine was shown to have preserved expression of green fluorescent protein (GFP) that had been introduced into the organoid units prior to implantation. The inclusion of this marker strongly suggests that the neointestine was derived primarily from the neonatal-derived organoid units, as opposed to ingrowth of the adjacent recipient intestine (90). It also was demonstrated that massive small bowel resection contributes significantly to regenerative stimuli for the heterotropically transplanted tissue engineered intestine (91). Additionally, it has been shown that anastomosis between the tissue engineered small intestine and native small bowel contributes significant trophic effects on neomucosal morphogenesis. Anastomosis of intestinal cysts to native intestine enhanced expression of the sodium-dependent glucose transporter (SGLT1) (92). Mucosal growth and SGLT1 expression could also be augmented in this model if rats were given GLP-2 (93). This study

emphasizes also the importance of the growth factors (EGF,HGF and VEGF) which need to be considered after implantation of tissue engineered small intestine (82).

All this data suggests that tissue engineered intestinal cysts measuring as little as 10% of the length of native small intestine may be enough to provide adequate absorptive function in a rat model. In light of these promising results, large animal studies using the same approach have been initiated and have since demonstrated successful generation of tissue engineered small intestine from autologus tissue in a juvenile porcine model (80). The resulting neointestine was composed of all anatomic layers of the native intestine, including a mucosa, with all of the epithelial cell types adjacent to an innervated muscularis. In addition, the presence of intestinal stem cells and the corresponding mesenchymal supporting cells, intestinal subepithelial myofibroblasts that are thought to sustain the intestinal stem cell niche through mesenchyme-epithelium cross-talk was proved.

An intriguing variation to the Boston group approach was the implantation of a tubular PGLA foam scaffold subcutaneously into rats (94). The PLGA had a thickness of two millimetres and was supported by inner silicone tubing. After five weeks, the silicone tubing was removed, and the lumen was filled with intestinal organoid units suspended in ECM gel. All constructs examined four weeks later revealed spheroid cysts with evidence of intestinal mucosa within the lumen. A potential benefit of this approach is the efficiency by which neomucosa can be generated from a given sample of donor tissue. It was possible to populate nine scaffolds, each with an internal surface area of 0.6cm$^2$, with organoid units extracted from a single neonatal rat intestine, which was a four-fold improvement in yield compared to the technique used by Vacanti's group. It was also shown that neointestinal mucosa could be maintained for at least 12 weeks on a subcutaneous

PLGA scaffold, and the presence of actively proliferating cells at that point suggest potential for further development beyond 12 weeks (95).

A perfusion bioreactor, fabricated using specific parameters was successfully designed and manufactured to keep organoid units seeded onto polymer scaffold viable and in differentiated state for up to two days (96).

#### *1.4.3.2. Intestinal lengthening using biological scaffolds*

As far as cell attachment and natural cues of ECM for cellular re-population are concerned acellular matrices have an obvious advantage over the polymers in small intestine tissue engineering. The most commonly ECM scaffold used in the field is SIS. The use of SIS as a scaffold for intestinal engineering makes intuitive sense because it is an acellular matrix harvested from a gastrointestinal source. Unfortunately the results using SIS have generally been more mixed than when applying Vacanti's method. Chen and Badylak have repaired partial and circumferential defects in the small intestine using either single layer or multilayered SIS in canine models (97). None of these scaffolds were seeded with cells or organoid units prior to implantation. Evaluation of the partial circumferential repairs showed no lumenal narrowing when followed up one year postoperatively. Histology at later time points demonstrated layers of remodelled wall containing a mucosal epithelium as well as varying amounts of smooth muscle and collagen that resembled native small intestine. Unfortunately, all dogs that received a tubular segment of SIS placed as interposition graft had significant problems, including obstruction and anastomotic leakage and subsequently died. The authors concluded that SIS patches can be used for small bowel regeneration but tubular segment replacement is not feasible.

The use of rat derived-SIS as an interposition graft in an ileal loop in rodent model has also been reported (98). A four-ply layer of two centimetres tubular SIS without any cell seeding was interposed into isolated ileal loop and the authors experienced no complications with this material. However, up to 40% graft shrinkage was observed when rats were followed for 24 weeks post-operatively. Histologically, the neointestine wall showed three layers of mucosa, smooth muscle and serosa, although no neuronal cells could be demonstrated within the grafts, but re-innervation usually takes much longer than that (99). The pathologic finding in this study showed one feature of SIS graft involving early capillary growth into the graft tissue. The rich and rapid blood supply to the grafts is probably the responsible for graft viability and infection resistance.

Similar studies performed in a rat model using Surgisis (porcine SIS) were able to prove innervation of three centimetres long tubular graft within 24 weeks post-implantation (100).

Contradicting results were reported by Lee et al. using the same rat model. Here a significant shrinkage was observed and none of the implanted scaffolds supported significant amount of intestinal regeneration up to eight weeks post-implantation (101).

De Ugarte et al. reported experience with SIS after duodenostomy in a rodent model and observed complete epithelialisation of a 6-mm-diameter defect by four weeks post-operatively (102). Nevertheless, the muscularis layer was notably absent in all examined species.

SIS showed effectiveness in intestinal patching in a rabbit model (103). Elliptical SIS grafts measuring six centimetres long and two centimetres wide were sutured to the jejunal defects as a patch graft. The grafts were covered with a

complete intestinal mucosa as soon as six weeks post-implantation, nevertheless the mortality of the study was very high due to anastomotic leakage. Significant graft contractions were also observed.

Efficacy of acellular dermal matrix for intestinal elongation in a rabbit model was also investigated (104). The animals survived the interposition of three centimetres long graft, however severe adhesions were found between the graft and surrounding intestine. Almost all of the grafts were completely absorbed within two to three months, and histological observation showed inflammation in the grafts with fibrinoid necroses, infiltration of a large amount of neutrophils and leukomonocytes. The neointestine with well-formed structures was not observed in the study. Therefore, it was concluded that acellular dermal matrix is not suitable as a scaffold material for intestinal elongation. Pahari et al. used the acellular human dermis in the form of tubular scaffold for intestinal patching, and showed intact mucosa with well-formed crypts evident at six months post-implantation (105). However when the same scaffold was used in elongation studies using tubular ECM all animals developed peritonitis and were sacrificed within one week postoperatively.

Parnigotto et al. (106) used homologous, two centimetres long, tubular, acellular matrix obtained from the gastric wall to increase the small bowel surface by interposition into an isolated loop of rat intestine. They proved that this method can support cell migration and the reconstructions of the intestinal wall without inducing any adverse symptoms.

Collagen sponge is another natural scaffold that has been used in small intestine tissue engineering (107). In a canine model, a portion of jejunum (5 cm) has been resected and reconstructed using an acellular collagen sponge, enzymatically processed from porcine skin, supported by a silicon stent. The stent was removed

endoscopically at one month. By four months, the collagen sponge was resorbed and the small intestine epithelium was present overlying these grafts at harvest. However, no muscle layer, essential for peristalsis was present. In follow up studies, cell seeding of the collagen sponge with gastric smooth muscle cells, but not bone marrow-derived mesenchymal stem cells, seem to induce long-term formation of smooth muscle layer beneath the intestinal epithelium in a canine patching model (108). Also nerve and endocrine cells regeneration was reported by this group (109).

None of the naturally-derived scaffold straight forward interposition studies included use of organoid units. Nevertheless, one group developed a method to transplant intestinal stem cells to rats that underwent resection of the distal 25% of their small intestine (ileum). Organoid units were harvested from neonatal donors, the mucosa from a segment of proximal intestine (jejunum) was removed, and organoid units were implanted into the debrided segment of jejunum. After four weeks, the animals had developed a functional neomucosa, and neointestine segment was inserted into continuity as a substitute ileum. Postoperative measurements of faecal bile acid excretion showed that it was possible to reverse the malabsorption syndrome in this model (85). Even though this model is not suitable to help patients with malabsorption caused by SBS, as they need generation of intestine *de novo*, it shows the possibility of transplanting intestinal stem cells on acellular, 'off-the-shelf' scaffolds.

### 1.4.4. Limitations of current approaches and clinical viability of tissue engineered small intestine

Despite the first pioneering investigations in the field of intestinal bioengineering date back to the 1990's, the initial excitement has been blunted by the considerable limitations encountered in the course of experimental investigations. The main reason for this is the complexity of intestinal anatomy and the various functions of the intestine.

The technology using organoid units and synthetic scaffolds is not efficient, as the whole intestine of a neonatal rat is necessary to produce organoid units sufficient for regeneration of only few centimetres of intestine. Moreover, organoid units at this point can not be cultured and grown *in vitro*. In clinical application use of organoid units is hardly feasible as there is no access to fetal tissue that can be easily obtained, and even if it was, the problem of immunosuppression would still be valid. Harvesting a sufficient amount of intestinal stem cells from SBS patients is almost impossible, unless the organoid units could be isolated from the patients at the time of resection and cultured in the bioreactor to grow a sufficient amount of tissue. At this point it is crucial to fill the gap in the knowledge of OU behaviour in the appropriate bioreactor systems. At the same time humans would require a much greater absorptive area to overcome SBS.

Secondly, apart from absorption the intestine exhibits peristalsis. However, tissue engineered intestinal constructs lack proper motility based on both morphological and functional criteria, which is the reason why many of the intestinal constructs exhibit intestinal obstruction, become dilated and result in faecal stasis and bacterial overgrowth due to aperistalsis. Generation of smooth muscles has been already reported but growing innervated tissue is very difficult and time consuming.

It's important to understand that at this stage of development within the field of intestinal regeneration the attempts are exclusively focused on delivering new absorptive surface. The difficulty in re-creating peristalsis will be as big obstacle as regeneration of mucosal layer. Non-innervated and non-muscular bowel ould become obstructed within hours after intestinal interposition. It is possible that neo-mucosal segments will have to primarily be isolated or form a digestive pouch, and only when generation of *Muscularis Externa* is achieved the graft could be incorporated in-between the native motile intestine. The aim of the thesis presented here was to prepare scaffold and cellular ingredients for regeneration of mucosal layer only. However, it should be highlighted that this would not provide complete intestinal function in all its complexity. As a matter of fact, in many studies it has been suggested that the weight gain and reduced malabsorption in animal models of intestinal regeneration is caused by the construct slowing down the transit time due to amotility of the tissue engineered construct rather than increasing functional absorptive surface (110).

Most of the studies using synthetic scaffolds seeded with organoid units are limited to rodent models with only one exception of a juvenile porcine model. This indicates how difficult it is to obtain sufficient amount of neointestine to perform interposition in animals with a bigger diameter of small intestine. Furthermore, in studies where biologically-derived acellular materials were used none of the scaffolds were shown to be seeded with organoid units. The possibility of incorporating the two most successful components used in both artificial and natural scaffold studies (easily vascularised scaffold containing natural cues for ingrowth of intestinal neomucosa and organoid units respectively) is exciting and is a main aim at filling this gap in the knowledge of intestinal regeneration. It is likely to improve the yield of intestinal

tissue engineering by modulating the scaffold properties in order to accelerate and augment neointestinal growth and development. As mentioned above, intestinal organoids grafted onto denuded bowel appear more successful than engraftment onto synthetic scaffolds as suggested by the lower number of intestinal organoids required.

## *1.5. Aim of thesis*

The aim of the present thesis is the development of an acellular biological scaffold which can be used to investigate small intestine tissue engineering as a new approach in the treatment of chronic intestinal failure.

Crucially, the new biological scaffold needs (i) to allow the creation of sufficient lengths of neo-mucosa for SBS patients, (ii) to be fully biocompatible and (iii) to promote the survival of seeded and/or cultured cells.

The fulfilment of these three criteria requires culture of the intestinal constructs in complex bioreactors, and the present thesis is focused on the design and manufacturing of such a system. In terms of validation of the acellular intestinal scaffolds produced by the novel bioreactor, the present thesis goes as far as to fully characterise the biocompatibility of the construct following implantation in vivo and to test the function of isolated porcine organoid units that could be used to seed the implant.

Assessment of the functionality of the construct in enabling the regeneration of porcine neo-mucosa and of its biomechanical properties both before and after implantation fall outside the scope of the present thesis and are proposed as future work.

# Hypothesis

Intestinal tissue can be subjected to enzymatic removal of living cells whilst still retaining the 3D structure and matrix properties, necessary to allow its use in tissue engineering.

Successfully de-cellularised porcine ileum with attached mesentery provides a highly biocompatible matrix that can provide immediate blood supply post-implantation to all parts of the scaffold.

# Chapter 2.

# Small intestine tissue engineering using biological/synthetic hybrid scaffold in rat model

## *2.1. Background and aims*

As stated previously the biggest and most significant finding in the field of small intestine tissue engineering was the use of organoid units to grow the neomucosa when seeded onto the polymeric scaffold and implanted into the rats omentum (84) or subcutaneously (94). These intestinal organoids are believed to contain intestinal epithelial stem cells maintained in the stem cell niche which supports ongoing replication and regeneration of the intestinal mucosa.

When biologically derived scaffolds were used for intestinal elongation or patching smart remodelling caused immediate neovascularisation, and in most cases grafts were rapidly infiltrated with host cells. Moreover, all three layers of intestine regenerated over the patch (97;103). However, the acellular, biological scaffolds were never combined with organoid units in order to create intestinal tissue *de novo*. This is despite the finding that coating of the synthetic scaffolds with type I collagen improved intestinal organoid engraftment (111). It is also noteworthy that no attempt has been made to combine intestinal organoid transplantation with intestinal lengthening procedures as part of a combined small intestinal tissue engineering technique.

Previously conducted studies in this department highlighted the possibility of incorporating acellular rat intestine into neomucosa regeneration. Acellular intestine provides the natural architecture of the intestine and ideal conditions for *in vivo* neovascularisation and therefore repopulation and survival of seeded organoid units. However, cell removal impaired the physical properties of the de-cellularised tissue so when prepared scaffolds seeded with organoid units were subcutaneously implanted into rat recipients most of them did not keep their lumens open over the period of study and failed to regenerate the neomucosa.

One of the methods previously used to strengthen ECM resulting from the de-cellularisation process was creating matrix/polymer hybrid scaffolds for tissue engineering of the heart and aortic valves in rabbit and sheep models (112).

The aim of the experiments presented below was to generate a graft composed of acellular intestine seeded with organoid units, which lumen could be kept open over a certain amount of time in subcutaneous position *in vivo*. To address the issue of poor mechanical properties of de-cellularised rat intestine, ECM/polymer composite based on acellular tissue that is coated with biodegradable, porous polymer was developed. The hybrid scaffold (a de-cellularised rat small intestine, coated with porous layer of polymer) was created to make the de-cellularised rat intestine stronger to withstand the *in vivo* loading. The behaviour of the construct *in vivo* was tested when they were seeded with intestinal organoid units derived from a neonatal rat and subcutaneously implanted into adult rat recipients. This behaviour was compared to a performance of control scaffolds (de-cellularised rat intestine, not coated with the polymer) seeded with organoid units and implanted in a similar way.

## *2.2. Methodology*

### 2.2.1. Materials

The list of materials and equipment used in experiments described in this chapter is presented in **Appendix 4**.

### 2.2.2. Solutions

Solutions used in experiments presented in this chapter are described in **Appendix 10**.

### 2.2.3. Animal husbandry

All animals were maintained and handled in accordance with the Animals (Scientific Procedures) Act 1986 and the study performed following guidelines stipulated by the UK Home Office. Experiments were performed using inbred male Sprague-Dawley rats (Harlan UK Ltd). All animals were kept under standard laboratory conditions and fed a commercial pelleted diet.

Surgery on live rats was performed after general anaesthesia using 0.25ml intramuscular Hypnorm (0.315mg/ml Fentanyl Citrate and 10mg/ml Fluanisone) and 1mg intraperitoneal Diazepam. Prior to incision, the skin was cleaned with Chlorhexidine solution and aseptic techniques were used subsequently. Post-operatively, all rats received analgesia using subcutaneous Carpofen; 8mg/kg intramuscular Gentamicin was given to all animals as prophylaxis against sepsis. Rats were encouraged to resume an oral pelleted diet post-operatively. Those rats that did not appear to be maintaining sufficient fluid intake were given supplemental boluses of 0.9% sodium chloride solution subcutaneously as required. Tissue was harvested

from animals after termination either by cervical dislocation (neonatal rats) or by lethal injection of sodium pentobarbitone (adult rats).

## 2.2.4. Preparation of organoid units from neonatal rats

Intestinal organoid units were isolated as described by Evans et al. (73). A six-days old Sprague-Dawley rat was sacrificed by cervical dislocation, and the entire neonatal small bowel was resected. The harvested intestine was opened longitudinally and cut into two millimetres-long segments. These intestinal pieces were washed six times in 50 ml of HBSS solution, and minced into pieces smaller than $1mm^3$, transferred into 20 ml of enzyme solution and incubated at room temperature on a roller for 25 minutes. Subsequently the suspension was shaken vigorously and allowed to sediment for about one minute. The supernatant was carefully transferred to a new tube and pellet discarded. This process was repeated three times, clearing the suspension of larger debris. The cleared solution was then mixed with equal amount of DMEM solution and centrifuged for three minutes at 300rpm at room temperature. Supernatant was discarded and pellet was washed with DMEM solution three times more, centrifuging in between the washes. 100µl of the suspension was used for yield analysis and the rest was resuspended in growth medium. Yield of isolation procedure was measured by counting (using hemocytometer) organoid units in one millilitre of solution after adding 0.4% trypan blue.

Each 200µl of the organoid units suspension was supplemented with one volume of ice cold ECM and used for the seeding of one scaffold.

## 2.2.5. Preparation of biological/synthetic hybrid scaffold

The whole length of small intestine and colon was harvested from adult Sprague-Dawley rats and washed thoroughly in 0.9% saline solution. This intestinal tissue was transferred to Tissue Science Laboratories-TSL (UK) for further processing. There the specimens underwent a patented process of de-cellularisation and cross-linking in order to preserve the tissue architecture and prevent biodegradation. In summary, the intestinal tissue was chemically defatted in acetone for 37 hours. It was then rinsed in 0.9% saline for 3 hours and underwent de-cellularisation in a trypsin solution for a further 24 hours. The tissue was then rinsed in acetone for 3 hours and cross-linked for 20 hours (with hexamethylene di-isocyanate: HMDI). Finally it was rinsed in acetone for 3 hours, 0.9% saline for 3 hours, and finally sterilised and packed prior to return. The entire process was performed under sterile conditions. On return, the processed tissue was either fixed in 10% NBF overnight and used for H&E analysis or used for the preparation of hybrid scaffolds.

Biodegradable polymer solution was supplied by Professor Aldo Boccaccini from Imperial College London. Poly(3-hydroxy)butyrate (P3HB) was dissolved in chloroform to final concentration of 4%. Secondly polymer solution was thoroughly mixed with fine brown sugar (0.2g of sugar per 0.1g of polymer) in order to create pores. So prepared polymer solution was used for coating experiments.

Glass stents were inserted into the lumens of the two-centimetres-long segments of de-cellularised rat small intestine. Secondly the specimens were dehydrated in a gradient of ethanol (EtOH) and dipped in P3HB solution supplied with sugar (3x5min). Subsequently scaffolds were dried in vacuo for two weeks to allow solvent evaporation and rehydrated in the gradient of EtOH. Glass stents were

removed and segments of hybrid scaffold were sterilised by UV light and stored in sterile PBS until the day of implantation.

### 2.2.6. *In vivo* studies of hybrid scaffolds seeded with organoid units

To investigate the mechanical and biological properties of hybrid scaffolds, 400µl of the organoid units suspension (organoid units isolate mixed with ice cold ECM gel 1:1) was seeded onto each scaffold by injecting the suspension into the lumen of 1cm long segments of scaffolds (control and hybrid scaffolds) using a 5ml pipette tip. The edges of tubular segments of the scaffolds were closed with 4.0 Ethicon sutures and so prepared constructs were implanted bilaterally (one hybrid and one control-uncoated scaffold) into subcutaneous pockets formed in the inguinal folds of two male adults 210-260g Sprague-Dawley rats within two hours. The skin was closed with 3/0 Mersilk® sutures and the animals were allowed to recover. After one and two weeks sacrificed and the grafts were explanted and prepared for histology using xylene-free process.

### 2.2.7. Tissue preparation

Harvested tissue was fixed in 10% Natural Buffered Saline (NBF) for at least 48 hours. Due to the fact that used polymer dissolves when exposed to xylene, tissue was processed to wax using an automated xylene-free processor **(Table 9, Appendix 11)** and then embedded into wax blocks. Five microns sections were cut using a rotary microtome, mounted onto glass microscope slides using a 40-45ºC water bath, and left to dry at 60ºC for up to 72 hours. Prior to staining, slides with mounted tissue

were dewaxed and rehydrated using a xylene-free protocol**.** That included incubation in two changes of Soap Water (30 seconds each) followed by five seconds in distilled water (all warmed up to 90ºC). Secondly sections were rinsed in tap water two times for five seconds and histological staining of H&E was conducted accordingly to protocol presented in **Table 5 (Appendix 6)**.

### 2.2.8. Histology

#### *2.2.8.1. Haematoxylin and eosin staining*

Haematoxylin and Eosin (H&E) staining was performed in order to assess basic implant morphology **(Table 6, Appendix 7)**.

## *2.3. Results*

### 2.3.1. Preparation of the organoid units from neonatal rats

The intestinal organoids isolation was performed twice prior to the constructs implantation and the yield of these procedures was 34 000 organoid units /ml and 64 000 organoid units/ml (which equals 34 000 and 64 000 organoid units per isolation and per length of neonatal small intestine). The third batch, used for implantations had a yield of 52 000 organoid units/ml, which means around 10 400 organoid units were seeded per 1-1.5cm of the scaffold (either hybrid or uncoated).

The overall viability of the organoid units was ranging from 86-90% with only few peripheral cells dead within the clusters (that was indicated by the intake of trypan blue solution through the cell membrane).

### 2.3.2. Preparation of biological/synthetic hybrid scaffold

The de-cellularisation procedures removed all the intact cells of the rat intestine preserving the structure of ECM, with easily distinguishable collagen of villi,

submucosa and serosa **(Fig.2)**. There was some cellular debris within the scaffolds but as mentioned in Chapter 1 a complete de-cellularisation is almost impossible and small amounts of nuclear and cellular remnants (as long as they do not induce inflammation or rejection of an implant) are acceptable.

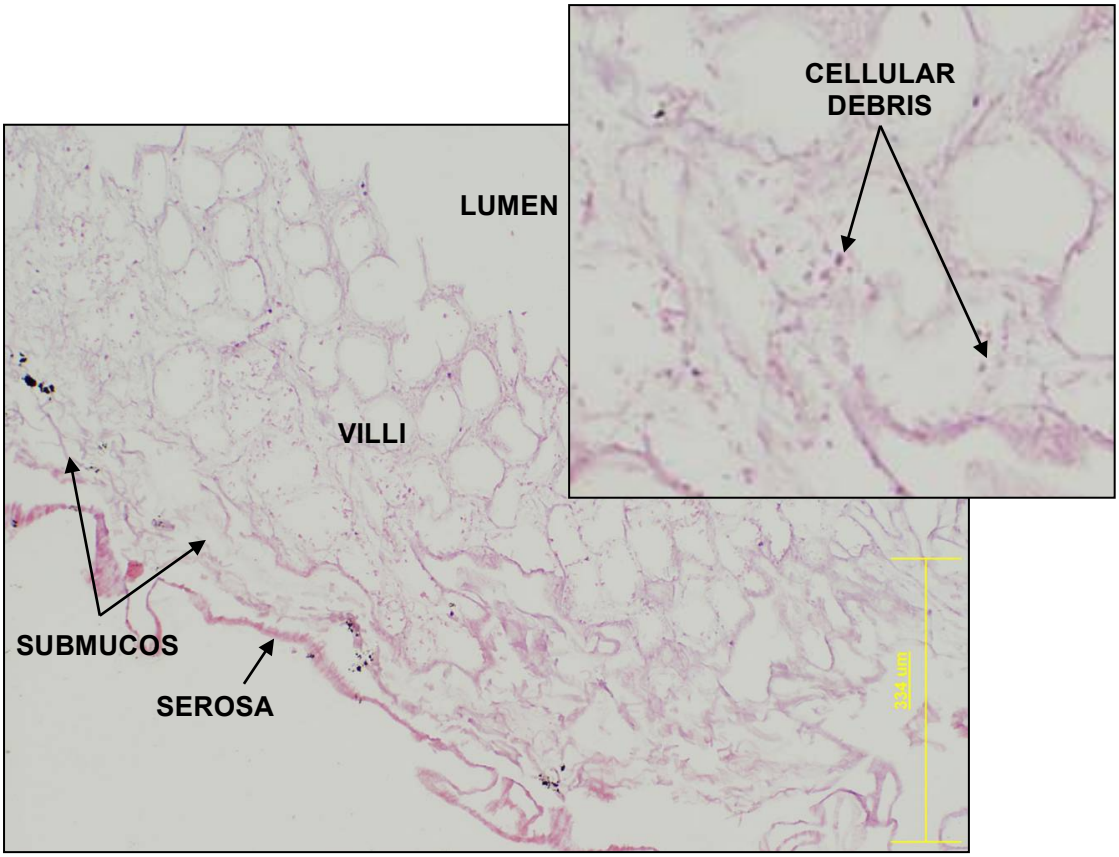


**Fig. 2** H&E of a cross section of a rat de-cellularised small intestine showing ECM layers of native tissue. Yellow bar indicates the scale of the image.

The surface of the tubular ECM scaffold was covered by a thin, polymer layer, which could be seen after separating it from the ECM scaffold using a dissecting microscope **(Fig.3)**.

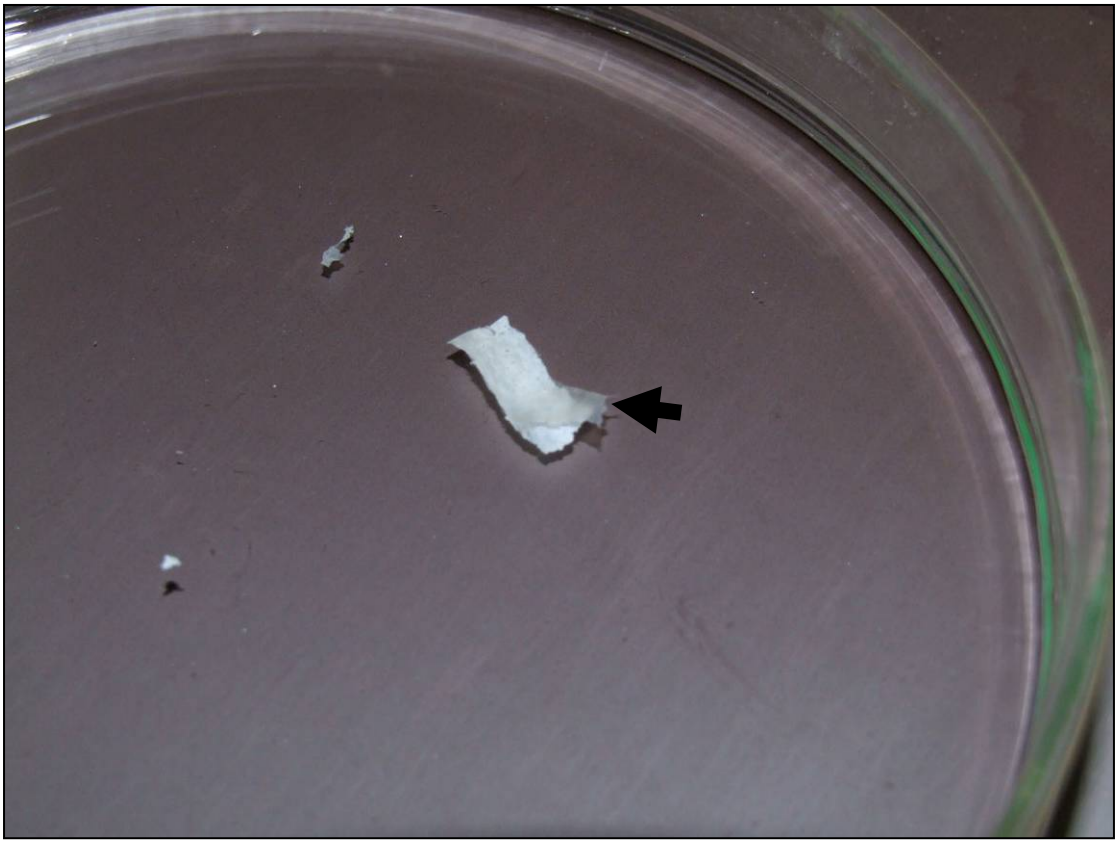

**Fig. 3** De-cellularised rat intestine coated with a thin layer of P3HB (arrow).

### 2.3.3. *In vivo* studies of seeded with organoid units hybrid scaffolds

All animals survived from the initial scaffold implantation to the final scaffold harvesting without any significant complications. The scaffolds were easily identifiable at harvesting as firm spheroid cyst-like structures measuring 12 mm to 17 mm in length and approximately 5mm in diameter **(Fig.4)**. There was slight size difference between test (hybrid) and ECM scaffold constructs (with hybrid grafts being smaller) at one week post-implantation. There was no noticeable difference in gross-appearance and the sizes between the two hybrid cysts.

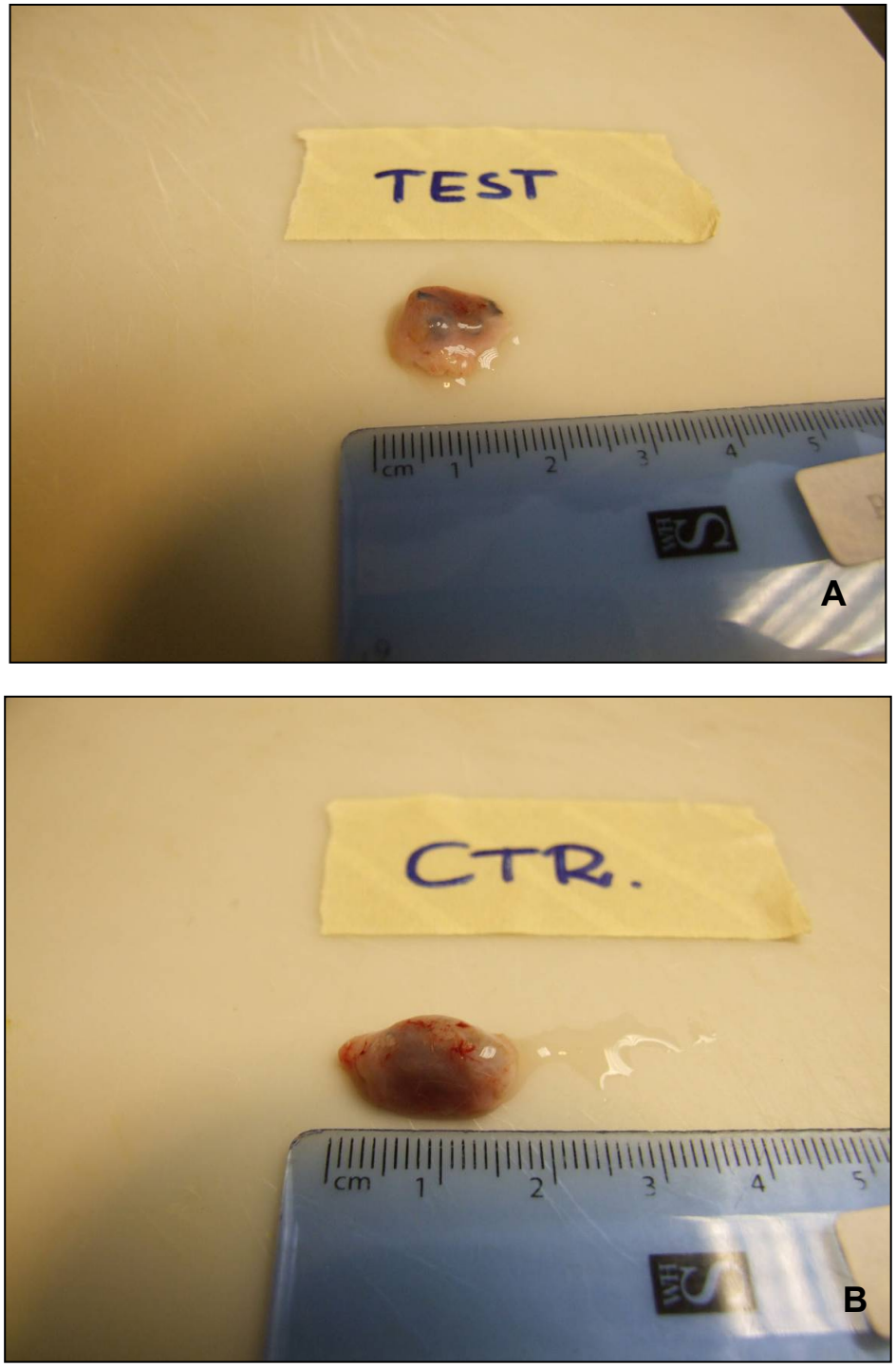


**Fig. 4** Cyst-like structures explanted from an adult rat one-week post-implantation. A-test-hybrid scaffold graft; B- graft of a control de-cellularised rat small intestine.

Histological findings showed that the lumen of the control graft (uncoated ECM scaffold) was open at the time of first harvesting (one week post-surgery), and not open at two weeks post-implantation. In the case of latter H&E sections it was difficult to distinguish the scaffold from the surrounding tissue.

The thickness of the polymer layer was estimated on H&E slides to be about 30-50µm. The hybrid graft harvested one week after implantation showed extensive inflammation taking place on the periphery of the scaffold. Wherever the wall of the hybrid construct was fractured or misplaced the inflammatory cells were penetrating the lumen of the cyst **(Fig. 5)**.

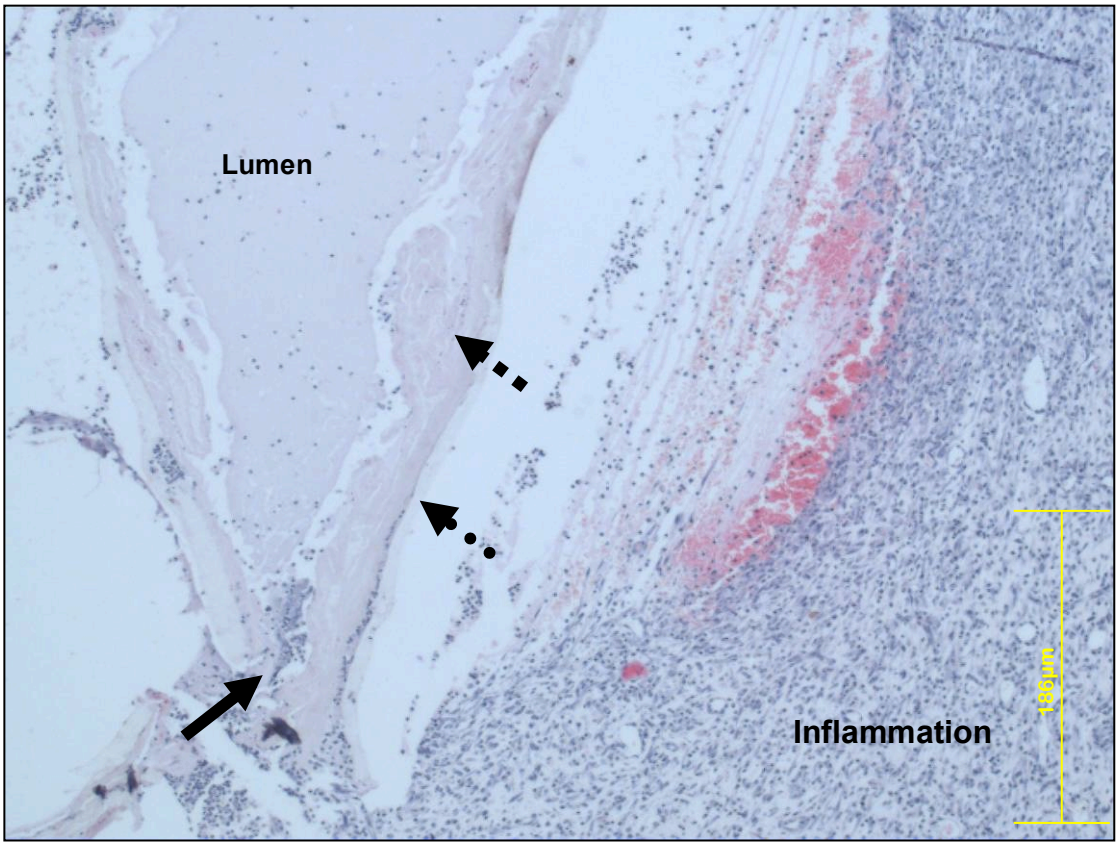


**Fig. 5** H&E cross section of the hybrid cyst harvested one week post-implantation. Extensive inflammation can be seen around the graft. De-cellularised scaffold (dashed arrow) was successfully coated with the thin layer of polymer (dotted arrow). The plain arrow indicates the place where inflammatory cells infiltrate the ECM-gel-filled lumen of the cyst in the place of scaffold's fracture. There is very few cells repopulating the hybrid lumen and most of the organoid units seeded into the lumen of the hybrid scaffold were not present anymore. Yellow bar indicates the scale of the image.

However, the histological analysis showed that the very few cells repopulating the hybrid scaffold were of inflammatory origin including neutrophils, lymphocytes and monocytes only without any characteristics of columnar epithelial lining.

At the same time the control scaffold kept the continuity of the wall and it's lumen stayed open. Moreover, it showed a much higher rate of cellular infiltration with some of the cells lining the lumen **(Fig. 6)**. However, abundant amounts of inflammatory cells were also present in the outer parts of the cyst. Also here no neomucosa formation could be identified.

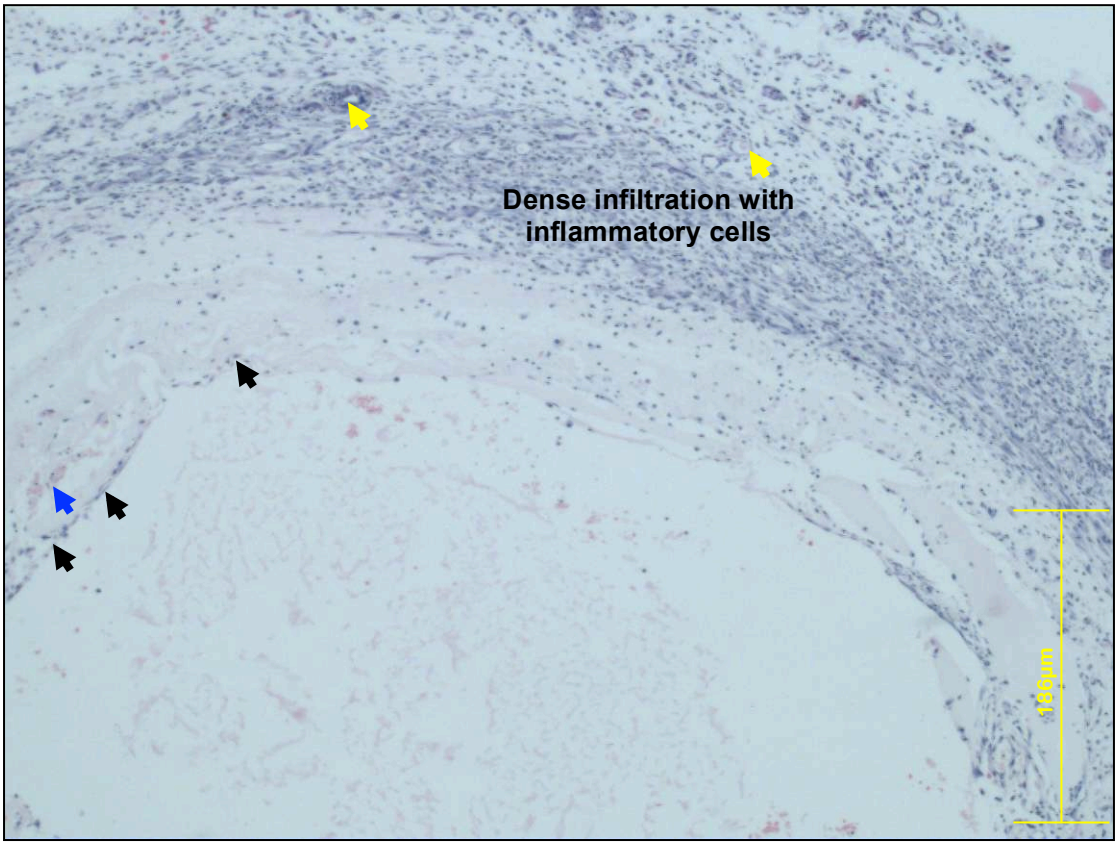


**Fig. 6** H&E cross section of the control cyst harvested one week post-implantation. Extensive inflammation and the beginning of fibroblasts deposition can be seen around the graft. ECM scaffold was repopulated with cells and some of them were lining the lumen of the scaffold (arrows). Neovascularisation could be seen within the scaffold (blue arrow) and within the surrounding tissue (yellow arrows). Yellow bar indicates the scale of the image.

In terms of histological findings there was very little difference in the appearance of the hybrid scaffold-grafts harvested at both of the time points. Still no cellular infiltration was present within the scaffold and there was evidence of inflammatory cells being replaced by fibroblasts. The scaffold's lumen did not stay open and part of it was discontinued and folded (under the weight of fibrotic capsule)

towards the half that managed to keep the lumen open **(Fig. 7)**. Some sections of the grafts showed large amounts of cellular remnants and apoptotic cells surrounded by macrophages in the centre of the lumen within the ECM gel.

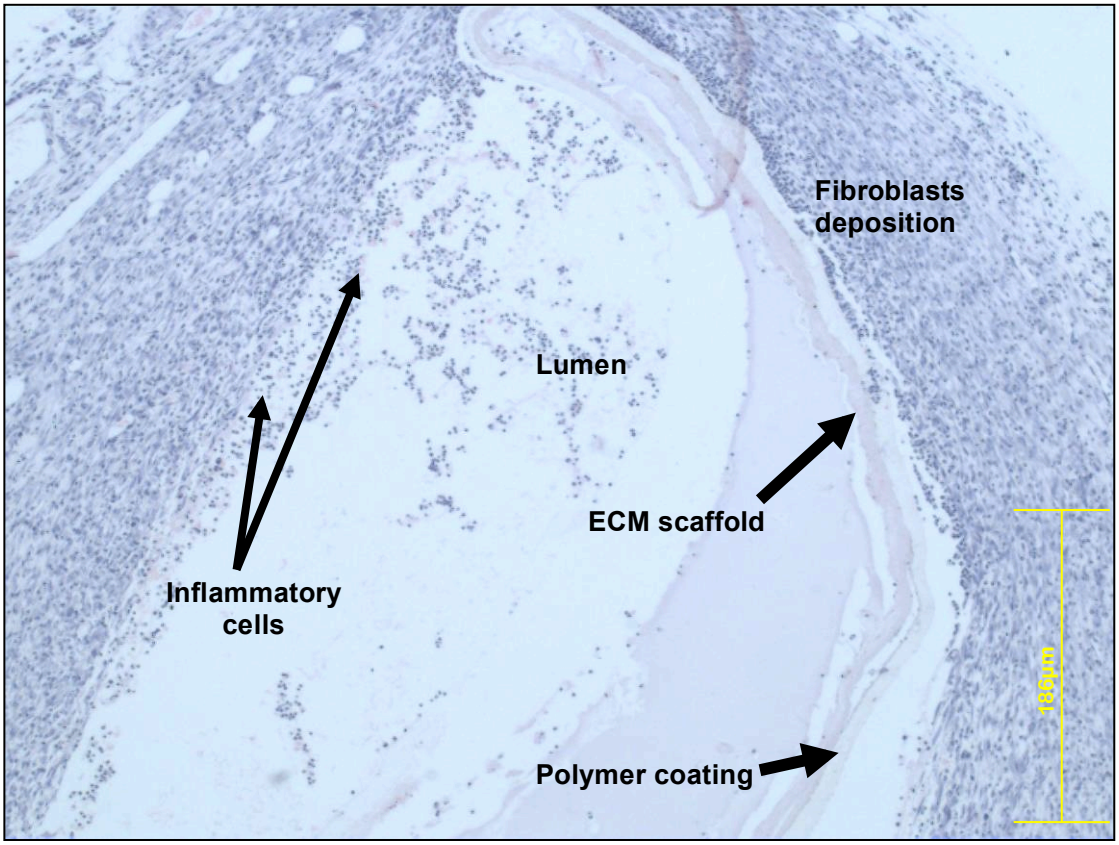


**Fig. 7** H&E cross section of the hybrid cyst harvested two weeks post-implantation indicating extensive inflammation around the graft. The scaffold was infiltrated with very few cells and no neomucosa formation could be seen in any part of it. The beginning of fibrotic capsule formation can be seen around the graft. Inflammatory cells penetrate the lumen where the wall of the tubular scaffold was discontinued Yellow bar indicates the scale of the image.

## *2.4. Discussion*

Previous studies proved that biologically-derived matrices can serve as scaffolds that promote growth of neomucosa. Nevertheless, the process of de-cellularisation inevitably weakened the structure of remaining ECM, which caused scaffolds to collapse when implanted subcutaneously into rat recipients. Therefore, it

was sought to combine the advantageous properties of the native ECM scaffold with those of an artificial polymer as it previously been done with heart and aortic valves in rabbit and sheep studies (112). Such solution would provide anatomically shaped readily implantable small intestine scaffold exhibiting physical strength, capable of bearing subcutaneous loads *in vivo*.

In order to check the biocompatibility of so prepared scaffolds, subcutaneous implantations in rat model were performed. The method of isolation of reliable amounts of organoid units was established by Evans et al. (73), and the yield studies described in this chapter had only a confirmatory character and were not an aim of the presented experiments. Nevertheless, it was important to establish the amount of organoid units that were used for seeding hybrid and control scaffolds in order to evaluate biological performance of the grafts and compare it to published data. The yield values, ranging between 30-60 000 organoid units per length of neonatal small intestine, were very similar to ones published in other reports (73). More thorough analysis of intestinal organoid units were not performed as much published data describing their morphology already exists. Furthermore, lack of reliable markers of intestinal stem cells makes it difficult to characterise stem cell populations. IHC staining of Musashi-1 (proposed intestinal stem cell marker) (113) has been attempted, but none of the antibodies currently available on the market gave reliable repeatable results when using control tissue (cortex and small intestine: data not shown), and therefore they could not be used for identification of organoid units. The amount seeded onto the scaffolds organoid units was calculated accordingly to suggested optimal seeding densities (10 000 organoid units per 1.5cm of a scaffold) in similar animal models (114).

The process of de-cellularisation was successful and removed most of the cellular content of the rat intestine, leaving only some cellular debris preserving the structure of native ECM **(Fig. 2)**. Even the fine collagen fibres of the villi were still visible in a H&E staining of a cross section of de-cellularised small intestine **(Fig. 2)**. Whether these villous remnants are maintained after implantation and whether they have a beneficial effect on the generation of neomucosa can only be postulated. It is certainly possible that they would aid the regeneration of crypt-villus architecture.

All the de-cellularised segments of rat intestine that were destined to become hybrid scaffolds were successfully coated with a thin layer of P3HB, which was shown on histology slides of harvested grafts **(Fig. 5)**. Nevertheless, both of the hybrid constructs failed to stay intact and open and H&E sections showed that the wall of the both scaffolds was fractured or missing. This could be caused by the dense, growing fibroblasts population gathering at the outside of the scaffold and the fact that P3HB has been reported rather brittle and shown decreased bending stiffness, which does not makes it very suitable for soft tissue applications (112). On the other hand, the lumen of the control scaffold was able to stay open but only as long as the surrounding tissue was composed of inflammatory cells and not densely packed fibroblasts. The coating thickness was deducted from H&E slides and was estimated at about 30-50μm. Such thickness is comparable to the coating of more dense ECM scaffolds (for example sheep heart valves) (112) and might have not been ideal for the fragile ECM of rat intestine. To incorporate more adequate coating or impregnating techniques (112) much more complex laboratory requirements would be necessary.

Interestingly the rate of cellular infiltration was much lower within the hybrid scaffolds than within the un-coated controls. The hybrid scaffolds were hardly infiltrated with any cells where control graft at one week post-implantation showed

even cellular repopulation with inflammatory cells **(Fig 5. vice 6. and 7.)**. At both time points all the scaffolds were surrounded by the layer of dense inflammatory cells but that layer seemed thicker and much more compact in the hybrid grafts. It was obvious that both kinds of the scaffolds induced a brisk extensive inflammatory reaction, which at one-week post implantation is a common outcome. However, the two-week old graft of the hybrid scaffold showed the beginning of a fibrotic capsule formation, which is a characteristic of foreign body reaction rather than constructive remodelling. It has been shown that P3HB can induce a prolonged acute and chronic inflammatory response (115) so the choice of polymer could have been wrong for that particular application. The extensive inflammation caused by the control graft could be a result of cross-linking, which as mentioned before can induce a foreign body reaction towards the implanted matrix. Moreover, attachment of organoid units to the scaffold is critical for survival and proliferation of seeded cell populations, and cross-linked acellular scaffolds were proven to have worse biocompatibility properties than non-cross-linked ones.

Seeded intestinal organoid units did not cause any mucosa regeneration. What is more, hardly any cells could grow within the scaffolds. It seems that the choice of the rat strain could cause the immune reaction towards the seeded organoid units. When inbred Lewis rats were used in previously conducted studies no host reaction towards organoid units derived from the neonatal donor rat was seen. In this study some sections of all the grafts showed extensive immune reaction towards remnants and apoptotic cells suspended in the ECM gel within the lumen of the cysts. It was speculated that ECM gel can exhibit growth of epithelial cells derived from organoid units (73), however similarly designed study to the presented one proved it wrong (116). Most of the cases of neomucosa regeneration state that the minimum time

needed for its generation is two to four weeks (20), but considering the fact that only a small amount of inflammatory cells could be seen at the lumen of the control scaffold at one week post-implantation, it is very unlikely that neomucosa would form within next couple of weeks.

In general the outcome of control implants was much better than the hybrid grafts. The application of synthetic/natural hybrid scaffold for subcutaneous implantations of organoid units and neomucosa regeneration was unsuccessful, but acellular matrix on its own could not survive physiological loading at the place of grafting. All the scaffolds within the presented rat model failed to provide an environment in which the organoid units could survive and generate neomucosa, and therefore the other aspects of intestinal regeneration were considered.

The de-cellularised porcine intestine is much stronger, and what is more, subcutaneous implantations are of very limited use in swine models. Therefore there is no need for mechanical strengthening of the porcine scaffold. If the methodological limitations of the study start to arise, and the 'proof-of-concept' using simple experimental model, the transition to more complicated, large animal model, is advisable. Therefore, it was quite obvious that transition into porcine model, which would not require a polymer coating, was the next step. The de-cellularised porcine intestine is much stronger, and what is more, subcutaneous implantations are of very limited use in swine models. Thus, a decision to move into animal porcine model that more closely resembles human anatomy and physiology was made. Promising results in simultaneous development of pig-derived scaffold for small intestine tissue engineering justified that decision even more.

# Chapter 3.

# De-cellularisation of a segment of porcine small intestine with its attached vasculature as a single entity

## *3.1. Background and aims*

In recent years bio-engineered products have become viable treatment option for the repair and regeneration of tissues and organs. Nevertheless, the principles of tissue engineering meet many limitations when applied to the restoration of the functionality of more complex organs such as the heart, liver or intestine (117). Tissue thicker than 0.8mm requires growth of blood vessels to supply all cellular components with oxygen and nutrients to inhibit graft degeneration and cell death after implantation (118). *De novo* creation of thick tissues consisting of a few layers, and their *in vivo* implantation require generation of vascularized bio-elements.

Complex structures require not only neo-vascularisation at a capillary level but they also need to be provided with a whole network of vessels, consisting of implantable, large, feeding pedicles dividing into smaller vessels and capillaries.

The small intestine is an organ that is not only very sophisticated in its morphology, but also its function is length dependant. SBS patients have 100-150 cm of functional bowel and another 50-100 cm could wean them off the PN (119). Therefore, creating a single construct smaller than 50 cm in length may not be regarded as a clinically viable treatment for SBS patients who have undergone multiple, surgical interventions. Unless the method to provide the appropriate vascular supply to the engineered intestine is established, its dimensions will be restricted by the diffusion distances (120). Solid organs such as intestine have an intricate vascular tree, which, through a series of branching vessels, forms a pervasive capillary network that ensures that all cells in the organ are no more than 1mm from nutrient and oxygen sources (121). Researchers have used various techniques in polymer biochemistry and scaffold design (122) to mimic the structure of this vascular network in engineered tissues. However, these efforts have fallen short of producing scaffolds that contain a vascular tree with centralized inlet and outlet vessels that are suitable for implantation and capable of nutrient and gas exchange.

The above problem was approached by the preparation of ready to re-vascularise scaffold-construct developed primarily for bio-engineering of long segments of small intestine. Using a completely novel approach, up to 30 cm segment of porcine ileum with attached vasculature was de-cellularised via perfusion. The preserved ECM of the intestine and mesenteric vessels could allow future culturing and growth of two different types of tissues (intestinal epithelium and endothelial cells) possible. Such a construct could provide absorptive function immediately after implantation.

The generated scaffold was evaluated using histological, IHC and molecular tools. The aims and methods for evaluation of the scaffold as well as the tests that

were not performed are gathered in **Table 10.** The aim of the scaffold analysis presented in this chapter was to show a completely de-cellularised construct that maintained its 3D integrity and functional elements post-treatment. The following chapters present biocompatibility of the scaffold upon implantation.

**Table 10.** Evaluation of acellular intestinal scaffold.

| Field of ECM scaffold evaluation | If tested | Method used |
|---|---|---|
| Quality of de-cellularisation | Yes | H&E, DAPI staining |
| Quality of collagen | Yes | Picro Sirius Red staining and polarised light microscopy |
| Quantity of collagen | No | - |
| Distribution of collagen | Yes | IHC: ColI and Col III staining |
| Quality of elastin | Yes | Miller's elastin staining |
| Quantity of elastin | No | - |
| Quantity of GAGs | Yes | BLYSCAN quantification of sulphated GAGs in fresh tissue |
| Residual DNA | Yes | DNA isolation and separation o agarose gel |
| Biomechanics | No | - |
| Biocompatibility | Yes | *In vivo* implantation into rat and porcine recipient; and histological and IHC analysis of the implants |

The results indicate the practicability of generating ready-to-implant scaffold for small intestine tissue engineering.

## *3.2. Methodology*

### 3.2.1. Materials

The list of materials and equipment used in experiments described in this chapter is presented in **Appendix 4**.

### 3.2.2. Solutions

Solutions used in experiments presented in this chapter are described in **Appendix 12**.

### 3.2.3. Animal husbandry

All animals were maintained and handled in accordance with the Animals (Scientific Procedures) Act 1986 and the study performed following guidelines stipulated by the UK Home Office. Experiments were performed using Large White Landrace crossbreed pigs. All animals were kept under standard laboratory conditions and fed a commercial pelleted diet.

Prior to surgery, pigs were given intramuscular injection of Ampicillin LA (25mg/kg) and a subcutaneous injection of Ivermectin (0.2mg/kg) to kill any internal or external parasites. On the day of surgery, the pig was given premedication of Ketamine (5mg/kg) and Xylazine (1mg/kg) intramuscularly. Anaesthesia was induced and maintained with Isofluorane over nitrous oxide and oxygen delivered by endotracheal intubation. Anaesthesia was monitored throughout the procedure by recording the pulse rate and core body temperature. Any adverse clinical signs were recorded. At the end of the harvesting procedure pigs were terminated by lethal injection of sodium pentobarbitone (100mg/kg).

### 3.2.4. Harvesting of porcine tissue

Following intravenous administration of heparin (7 000 U) in a 60-65kg Large White Landrace crossbreed pig a midline incision was created and segment of ileum was isolated together with its attached vascular supply approximately 20cm in length. Residual lymph nodes in the mesentery were dissected; keeping the whole specimen leak proof; the distal end of pedicle was tied off and isolated. The proximal end of the artery was cannulated with a 14G Radiopaque I.V. cannula and flushed with 0.9% sodium chloride (NaCl) containing heparin (2 000U) until there was no blood in the outflow at the proximal end of the vein. To maintain intralumenal pressure within the vasculature and maintain their lumen's open, a pulsatile pump perfusing heparinised (2000U/l) 0.9% NaCl through the pedicle was attached to the arterial cannula. All vessels not involved in supplying the section of the small intestine that was to be harvested were tied off, and the whole tissue segment was removed from the animal. At the end of the procedure, the animal was terminated by intravenous overdose of anaesthesia. The vascular circuit was checked for any leakage and the intestinal lumen was flushed with 1 litre of 0.9% NaCl. At both ends of the ileac segment, silicon tubes were attached with purse-string sutures, and this segment of small intestine was attached to the second perfusion circuit. The harvested specimen was then ready for de-cellularisation.

### 3.2.5. Development of a protocol for simultaneous de-cellularisation of porcine small intestine together with its vasculature

Immediately after harvesting, heparinised saline solution was flushed through the vasculature and de-cellularising solutions were introduced into the two separate circuits of the specimen. Circuit I was attached via a cannula into the main artery and exited via the main vein and circuit II was attached to the silicon tubes tied to each end of the explanted segment of ileum.

The optimization of the de-cellularisation protocol involved application of many different agents, such as 0.05-0.2% trypsin solution, Triton X-100 solution, Triton X-100 solution followed by nucleases (deoxyrybonuclease I: DNaseI) treatment, 0.075-1.5% SDS solution, SDX solution, one or two cycles, and combined SDS and trypsin treatment (1-3 cycles). The outcome of each process was evaluated using H&E and Picro Sirius red stainings as well as checking the amount of remaining DNA. The optimal de-cellularisation protocol is presented in **Table 11.**

**Table 11.** De-cellularisation of small intestine and its vascular pedicle.

| | *CIRCUIT I AND II* | | |
|---|---|---|---|
| | ***Solution*** | ***Time*** | ***Temperature*** |
| **1.** | 0.075% SDS solution | 90min | 25°C |
| **2.** | Antibiotics solution | 3 changes; 15 min each | 25°C |
| **3.** | 0.05% Trypsin solution | 90min | 37°C |
| **4.** | Antibiotics solution | 3 changes; 15 min each | 25°C |
| **5.** | DNase I solution | 120min | 37°C |
| **6.** | Antibiotics solution | Overnight | 4°C |
| **7.** | 0.075% SDS solution | 90min | 25°C |
| **8.** | Antibiotics solution | 3 changes; 15 min each | 25°C |
| **9.** | 0.05% Trypsin solution | 90min | 37°C |
| **10.** | Antibiotics solution | 3 changes; 15 min each | 25°C |
| | *Circuit I* | | |
| **11.** | Antibiotics solution | Till the end of process | 25-37°C |
| | *Circuit II* | | |
| **11.** | 0.075% SDS solution | 90min | 25°C |
| **12.** | Antibiotics solution | 3 changes; 15 min each | 25°C |
| **13.** | 0.05% Trypsin solution | 90min | 37°C |
| **14.** | Antibiotics solution | 3 changes; 15 min each | 25°C |

The specimen was submerged in the solutions used for perfusion through circuit I **(Fig 8).**


**Fig. 8** Perfusion system for de-cellularisation of porcine intestine

Perfusion was conducted with a pulsatile rate of 30-60rpm throughout the whole process, preserving physiological direction of the intraluminal flow (intestinal: proximal to distal; vascular arterial to venous). The cells, cytoplasmic components and finally deoxyribonucleic acids were broken down by subsequent perfusions of SDS, trypsin and DNase I solutions, washed between each step with PBS supplied with antibiotics. After the last stage of the de-cellularisation process the acellular scaffold was sterilized by perfusing a solution of paracetic acid (PA) in PBS for three hours at room temperature in the laminar flow cabinet. Subsequently, the specimen was washed in sterile PBS supplemented with antibiotics.

## 3.2.6. Analysis of de-cellularised tissue

### *3.2.6.1. Macroscopic*

Once the scaffold-construct was de-cellularised and detached from the perfusion circuits, care was taken to keep the vascular part of it filled with liquid in order to prevent fragile vessels and capillaries from collapsing. General macroscopic appearance of the scaffold was checked. To confirm that the scaffold could be easily perfused, and to visualize vessel's ability to perfuse 0.01% Evans Blue solution was injected via arterial cannula and its outflow was identified on the venous side of the pedicle.

#### *3.2.6.2. Histological*

Tissue for histological analysis was fixed in 10% Natural Buffered Saline (NBF) for at least 48 hours. Prior to sectioning, tissue was processed to wax using an automated processor **(Table 4, Appendix 5)** and then embedded into wax blocks. Five microns sections were cut using a rotary microtome, mounted onto glass microscope slides using a 40-45ºC water bath, and left to dry at 60ºC for up to 72 hours. Tissue that was to undergo IHC was mounted onto slides coated with 3-aminopropyltriethoxysilane (APTS) to improve adhesion. Prior to staining, slide mounted tissue was dewaxed and rehydrated using a standard protocol **(Table 5, Appendix 6).**

Histological analyses were conducted on scaffolds prepared using protocols undergoing optimisation (n=1 for each of the protocols) and on scaffolds prepared using the optimal one (n=3). A whole segment of the main vein and artery, as well as seven samples from the mesenteric vascular arcade and ileal segments of the acellular scaffold were selected for histological analysis **(Fig 9)**. The remaining part of the specimen was frozen in liquid nitrogen and stored at -20°C for molecular analysis. For

comparative studies samples of control intestinal tissue, harvested from animals at the same age and of the same weight were prepared.

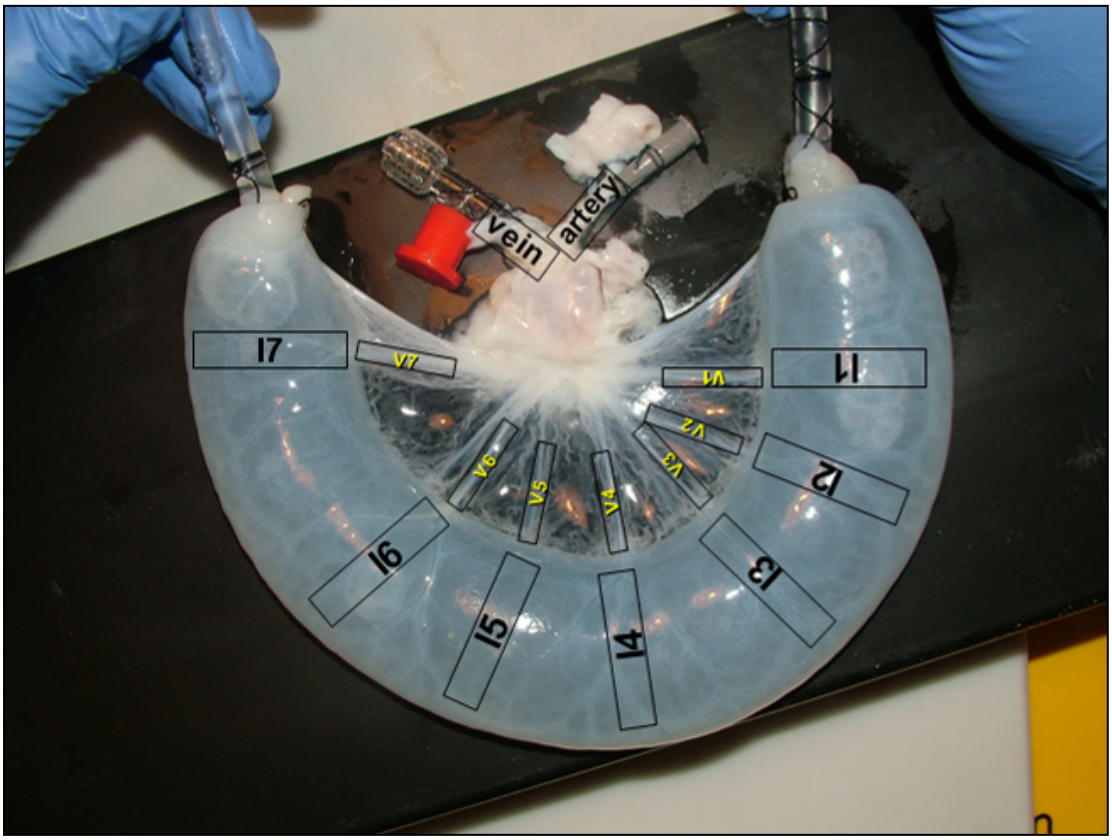


**Fig 9.** Layout of sampling sites for histological analysis in porcine acellular scaffold. I1-7: samples of ileum, V1-7: samples of vasculature.

Haematoxylin and Eosin (H&E) staining was performed in order to assess basic tissue morphology and as a control for the decellularization process **(Table 6, Appendix 7)**.

Picro-Sirius Red staining was employed in order to identify collagen in the tissue and acellular scaffolds and to asses its status using biofringed light under light microscope. Miller's elastin was used to visualize elastin within the vasculature of de-cellularised tissue **(Table 7, Appendix 8)**.

Sections of the scaffolds obtained using the optimised protocol also underwent 4',6-diamidino-2-phenylindole (DAPI) staining to visualise any remaining nuclear material. All histological sections of the specimen were compared with native tissue.

### *3.2.6.3. Immunohistochemical*

Indirect IHC was performed to visualise the expression of collagen I (Col I) and collagen III (Col III) and to track changes in the presence and layout of the two types of collagen abundant in small intestine before and after de-cellularisation.

Prior to IHC staining all sections were dewaxed and rehydrated in a gradient of alcohol solutions. Any necessary antigen retrieval was carried out at this point. All sections were treated with a solution of hydrogen peroxide ($H_2O_2$) in methanol (MeOH) to block endogenous peroxidase activity before being washed with adequate wash buffer 3x3min. Sections were then treated with non-specific block to prevent non-specific staining before being incubated with the primary antibody. The primary antibody was conjugated with a species-appropriate biotinylated secondary antibody and Avidin-Biotin-Complex (ABC), or with species-appropriate universal secondary antibody kit (ImmPress Kit). Following 3x3min wash immunoreactivity was visualized with a 3', 3-diaminobenzidine (DAB) substrate. Finally sections were washed for five minutes in distilled water and counterstained with Harris haematoxylin, dehydrated, cleared in xylene and mounted with cover slips. Specific IHC protocols are summarised in **Table 8 (Appendix 9)**.

### *3.2.6.4. Molecular*

Samples obtained from scaffolds produced while optimizing de-cellularisation process (n=1), using optimal protocol (n=3) and samples harvested from control native small intestine underwent DNA isolation and quantification. The amount of GAG's surviving the de-cellularisation process was checked in scaffolds produced using combined (optimal) protocol, and compared to the amounts found in native small intestine (n=3).

#### 3.2.6.4.1. DNA

Samples of the scaffolds and control tissue were defrosted and 0.025g of each was used for DNA isolation using GenElute Mammalian Genomic DNA Miniprep Kit according to manufacturer's instructions. Isolated DNA was stored at -20°C until further use.

Electrophoretic separation of DNA was conducted in order to show the presence of DNA in the samples of acellular bowel and to compare the amount of DNA remaining within the scaffold while optimizing de-cellularisation process. DNA was separated on 1% agarose gel in Tris-acetate ethylendiaminetetraacetic acid (TAE) buffer for 2h at 100V. Subsequently, the gel was stained with ethidium bromide solution for 15 min. The gel was viewed and photographed on a long wave A) transilluminator.

The amount of DNA residual in the vascular and intestinal part of the scaffold-construct as well as DNA isolated from native ileum and vessels were quantified using spectrophotometer (absorbance (AD)=260, AD260/280).

#### 3.2.6.4.2. GAG's isolation and quantification

The quantity of GAG's in acellular scaffold was tested using Blyscan Sulphated Glycosaminoglycan Assay according to the manufacturer's instructions. The assay was used to calculate the total sulphated glycan content according to spectrophotometric (656nm) absorbance values of sulphation level (dye-binding capability) as calculated using the supplied assay standards (range 2-50μg/ml) of GAG's. GAG's were isolated from 3 different batches of specimen, and the concentration was calculated using a standard curve. The results were presented as μg/g of wet weight. Values obtained for the acellular scaffold were compared to values for control porcine intestinal tissue.

### 3.2.7. Statistical analysis

All continuous data was expressed as the mean ± Standard Error of the Mean (SEM) and $p<0.05$ was taken as significant. $p$ Values were estimated using one-way Analysis Of Variance (ANOVA) with post hoc Tukey intergroup comparison, and all computations were performed using GraphPad Prism 4 software.

## *3.3. Results*

### 3.3.1. Development of a protocol for de-cellularisation of porcine small intestine together with its vasculature

A procedure was developed whereby segments of ileum together with an intact vasculature could be harvested. The de-cellularisation reagents were successfully applied via the organ's vasculature, and the perfusion of the whole segment of ileum could be maintained during the whole process. Few vessels within mesenteric arcade

that showed some leakage were tied off whilst undergoing de-cellularisation. The application of other solutions than the ones used in the final optimal protocol resulted in various amounts of cellular and nuclear content remaining within the tissue after the process. Briefly, high concentrations of trypsin damaged collagen and lower ones resulted in an abundant amount of DNA and cellular remnants in the de-cellularised tissue. Triton X-100 was successful in removing nuclear content only when combined with nucleases treatment, but even then the removal of the cellular debris from the tissue was incomplete. Nevertheless, it was the least disruptive protocol in terms of ECM structure. Application of single cycle of SDX was unsuccessful in removal of cellular and nuclear content. The outcome was better when two cycles were applied. Yet in comparison with SDS treatment it was unfavourable in terms of collagen degradation.

Joint enzymatic-chemical process allowed the continuity of the cell membrane to be broken and then digestion using proteases and nucleases of the cellular remnants. However, only the application of three cycles was successful in removing cells and DNA from the intestinal part of the scaffold. Such treatment was too harsh for the fragile ECM of the mesenteric arcade and intestinal capillaries. They were shown to be completely de-cellularised after only two cycles of combined protocol (trypsin and SDS). Thus, after the second cycle of de-cellularising reagents the two circuits (intestinal and vascular) were separated and the process followed as described previously **(Table 11)**.

## 3.3.1. Analysis of de-cellularised tissue

### *3.3.1.1. Macroscopic*

De-cellularised ileum and its vasculature maintained its overall shape and macroscopic structure **(Fig. 9)**. During the de-cellularisation process, the specimen continuously lost its natural colour until it became translucent beginning with the mesenteric arcade, and then the intestine. The de-cellularised bowel dilated showing 0.5-1.5 fold increase in length and ~0.5 fold increase in diameter. The measurements of the de-cellularised intestinal segment are presented in **Fig. 10**, which should be also treated as a scale reference for any following macroscopic photographs of the scaffold.

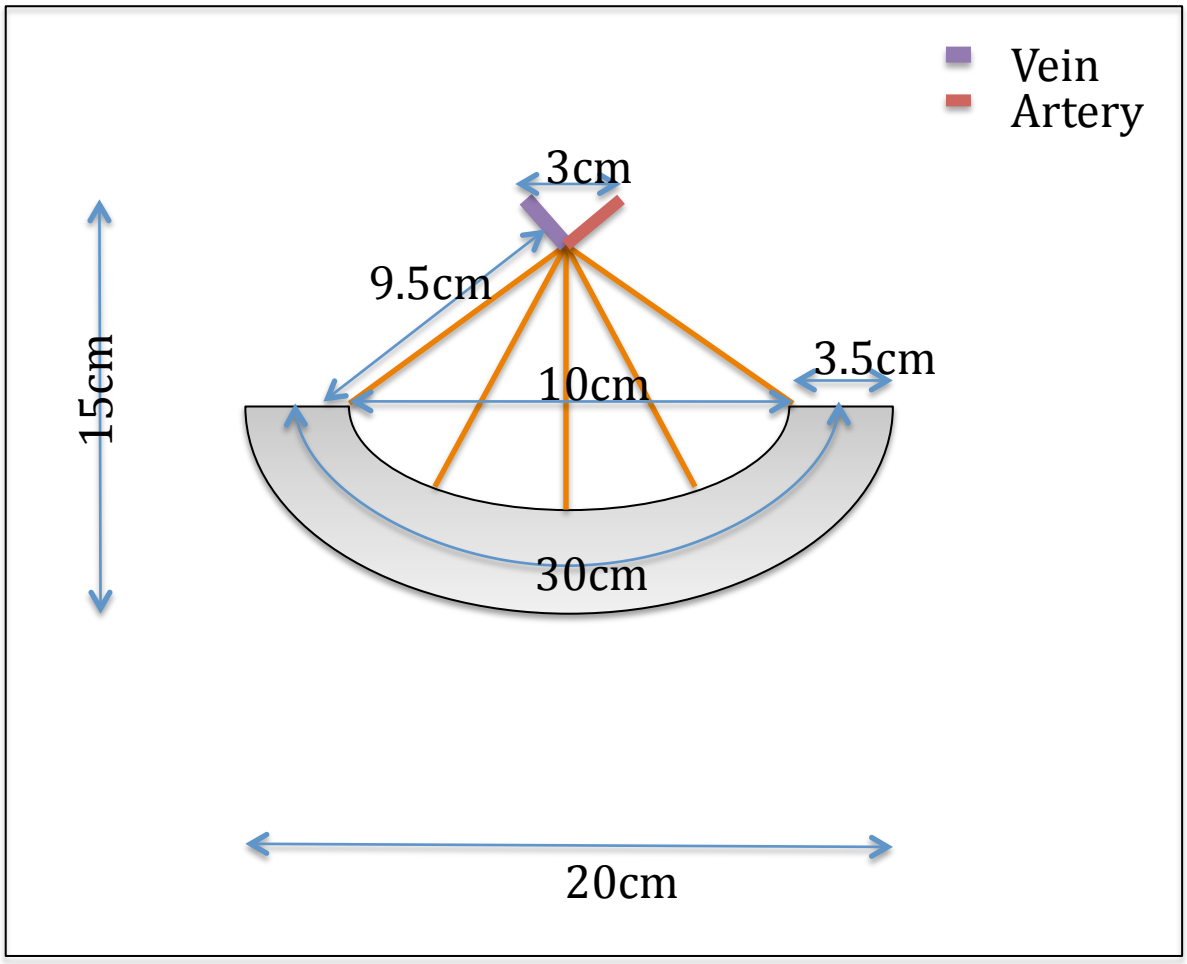


**Fig. 10** Average reference scale of the macroscopic view of the acellular segment of small intestine with intact mesenteric arcade.

Injection of 50ml of Evans Blue solution into the vascular pedicle, via the arterial cannula revealed that the perfusability of the capillaries within the de-cellularised ileum was preserved throughout the process and venous outflow of circuit I was viable at the end of de-cellularisation process **(Fig. 11)**.

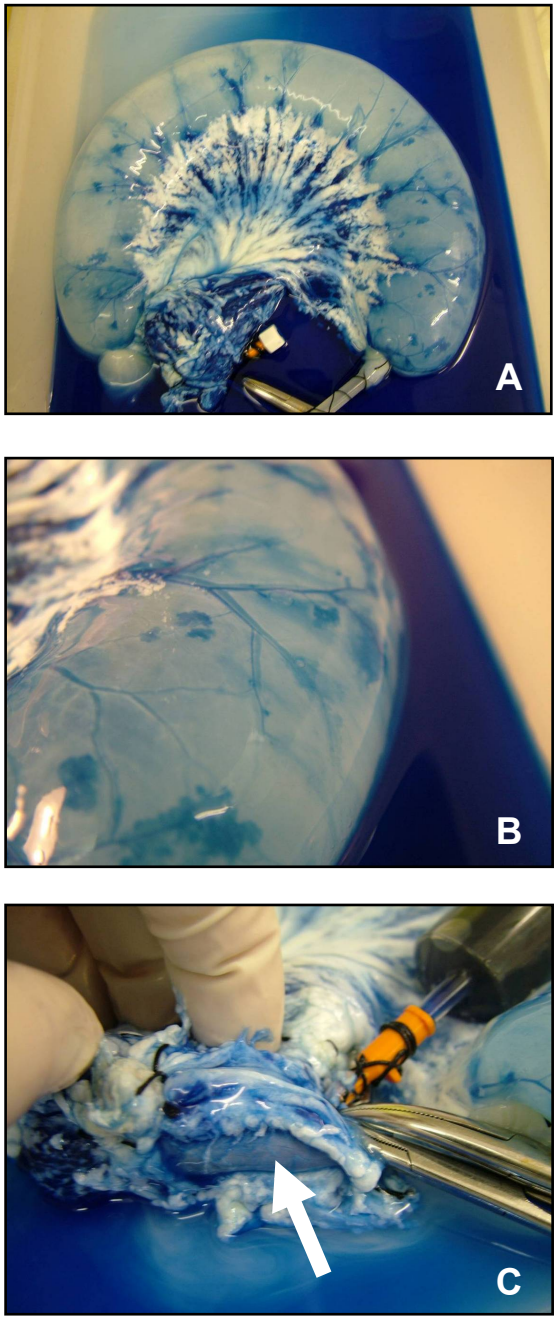


**Fig. 11** Vasculature of the scaffold visualized by the injection of 0.01% Evans Blue solution. Whole scaffold was perfused by the dye (A), including capillaries within the intestinal part (B). Following fluid injection the clamped main vessel expanded as shown (arrow) (C).

### *3.3.1.2. Histological*

H&E and DAPI stains were used as a first line of inspection to determine if remnant nuclear structures could be observed. Picro Sirius red and Miller's elastin stains revealed the state of the remaining ECM after de-cellularisation. Following Picro Sirius red staining the intensity of the biofringence increases proportionally to collagen fibres thickness. Therefore the comparison of control, native tissue with de-cellularised intestine could show the rate of the collagenous fibres destruction. When viewed using polarised light the thick fibres are usually yellowish-orange-to-red and thin fibres are green (112). If the native tissue would contain mostly orange and red fibres and the scaffold only green fibres it could be concluded that the de-cellularisation process visibly destructs the collagen structure.

#### 3.3.1.2.1. H&E and DAPI

H&E staining revealed that no remaining intact cells could be seen at the end of the process in any parts of the specimen. Throughout the preserved vascular arcade neither endothelial cells nor smooth muscle cells could be seen **(Fig. 12)**. The intestinal part of the scaffold was also cell-free, showing only the eosinophilic staining of the collagen. Furthermore, the histological structure of the intestinal layers was preserved, showing serosal, submucosal and ECM of intestinal crypts and villi **(Fig. 13)**.

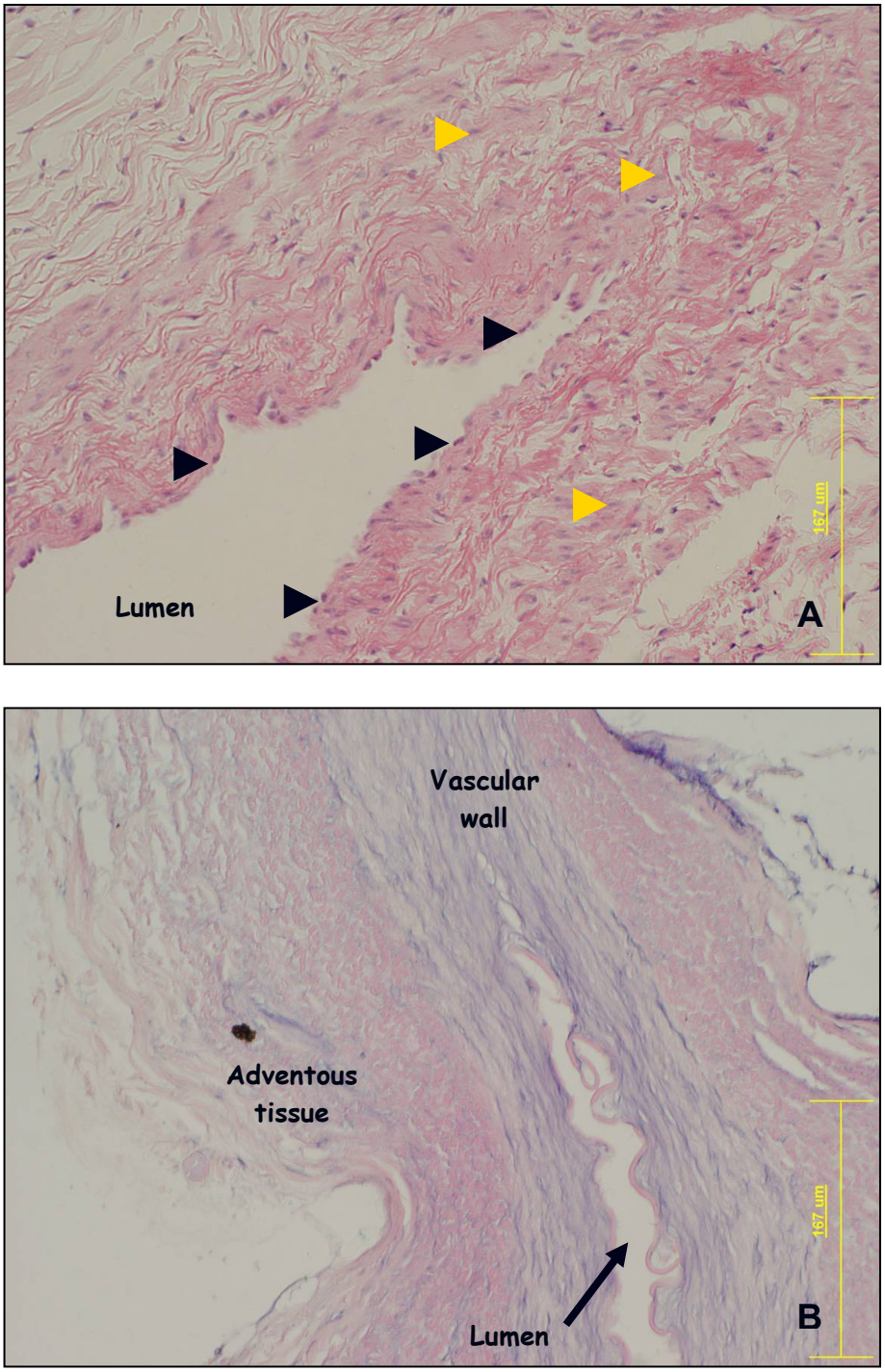


**Fig. 12** Representative H&E stained section of the main pedicle showing the absence of nuclear and cellular staining after de-cellularisation. A- native vessel supplying ileum; visible purple haematoxylin staining indicates nuclei of endothelial cells lining the lumen (black arrows) and smooth muscle cells within the vessel wall (yellow arrows); B- de-cellularised vessel supplying the ileum with no nuclei stained within the lumen or the vascular wall.

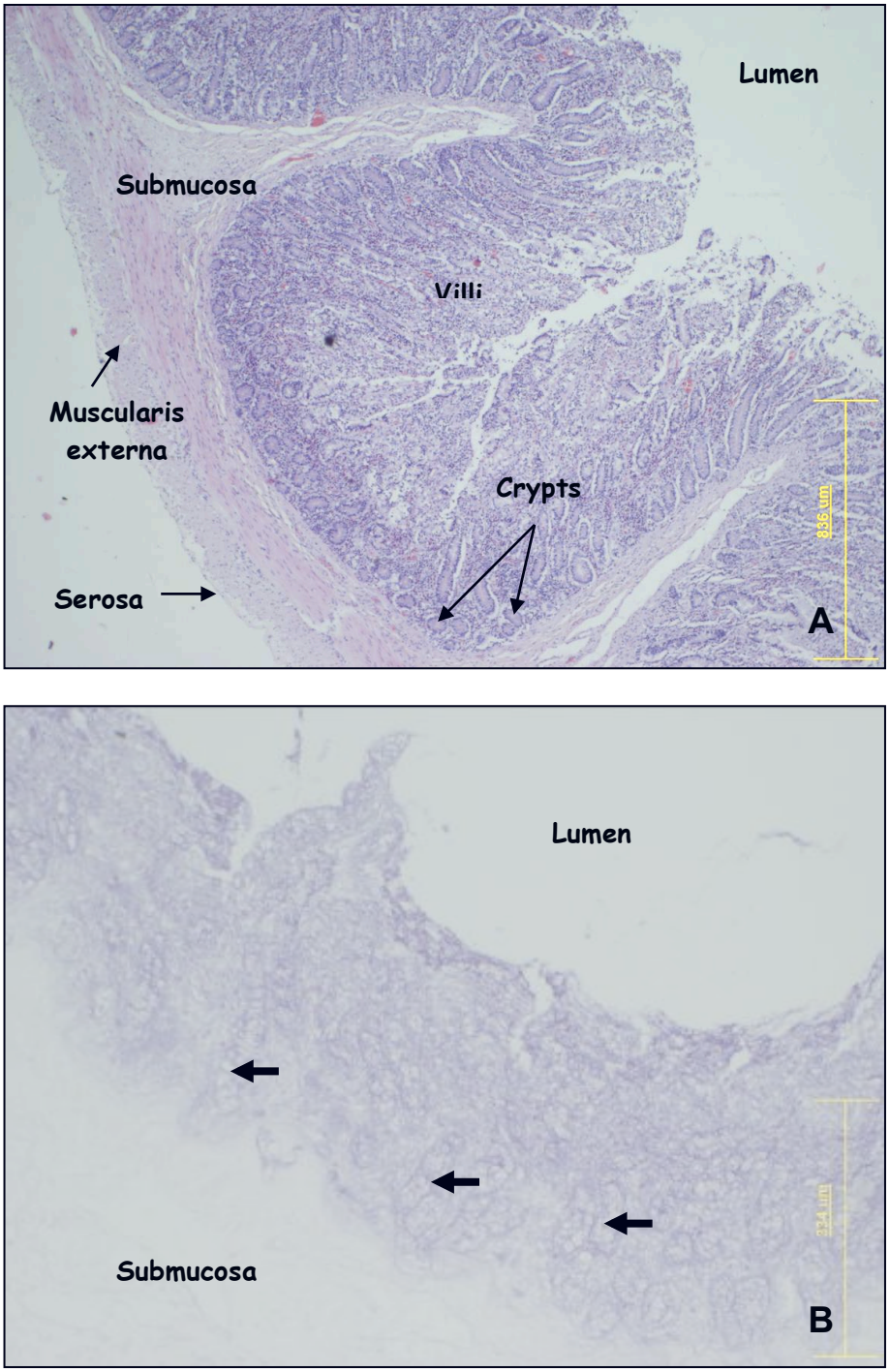


**Fig. 13** Representative H&E stained section of native and acellular ileum. A - cross section of the native ileum with visible haematoxylin-stained nuclei and eosin-stained cytoplasm of intact cells; B - de-cellularised ileum with no eosin staining of cytoplasm or haematoxylin-stained nuclei, and preserved histological layout of intestinal tissue, including organised ECM crypts and villi (arrows indicate obvious acellular crypts).

No nuclei were evident by DAPI staining in the vascular part **(Fig. 14)** and the intestinal part of the scaffold **(Fig. 15)**, confirming the success of the de-cellularisation.

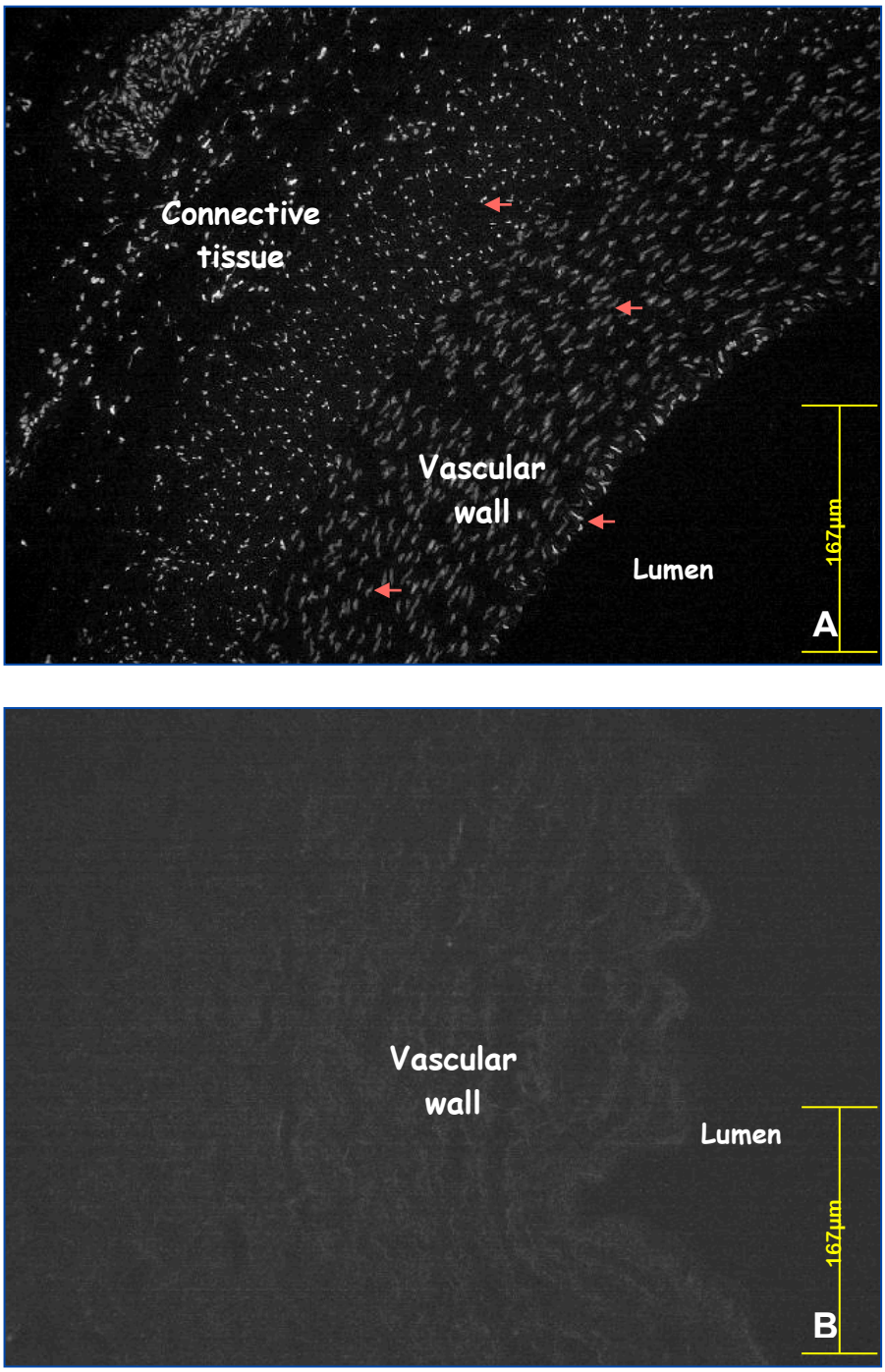


**Fig. 14** Representative DAPI stained section of the main pedicle. A- native vessel supplying the ileum with visible fluorescent staining of nuclei; B- de-cellularised vessel supplying the ileum with no fluorescent staining of nuclei. Red arrows indicate DAPI stained nuclei.

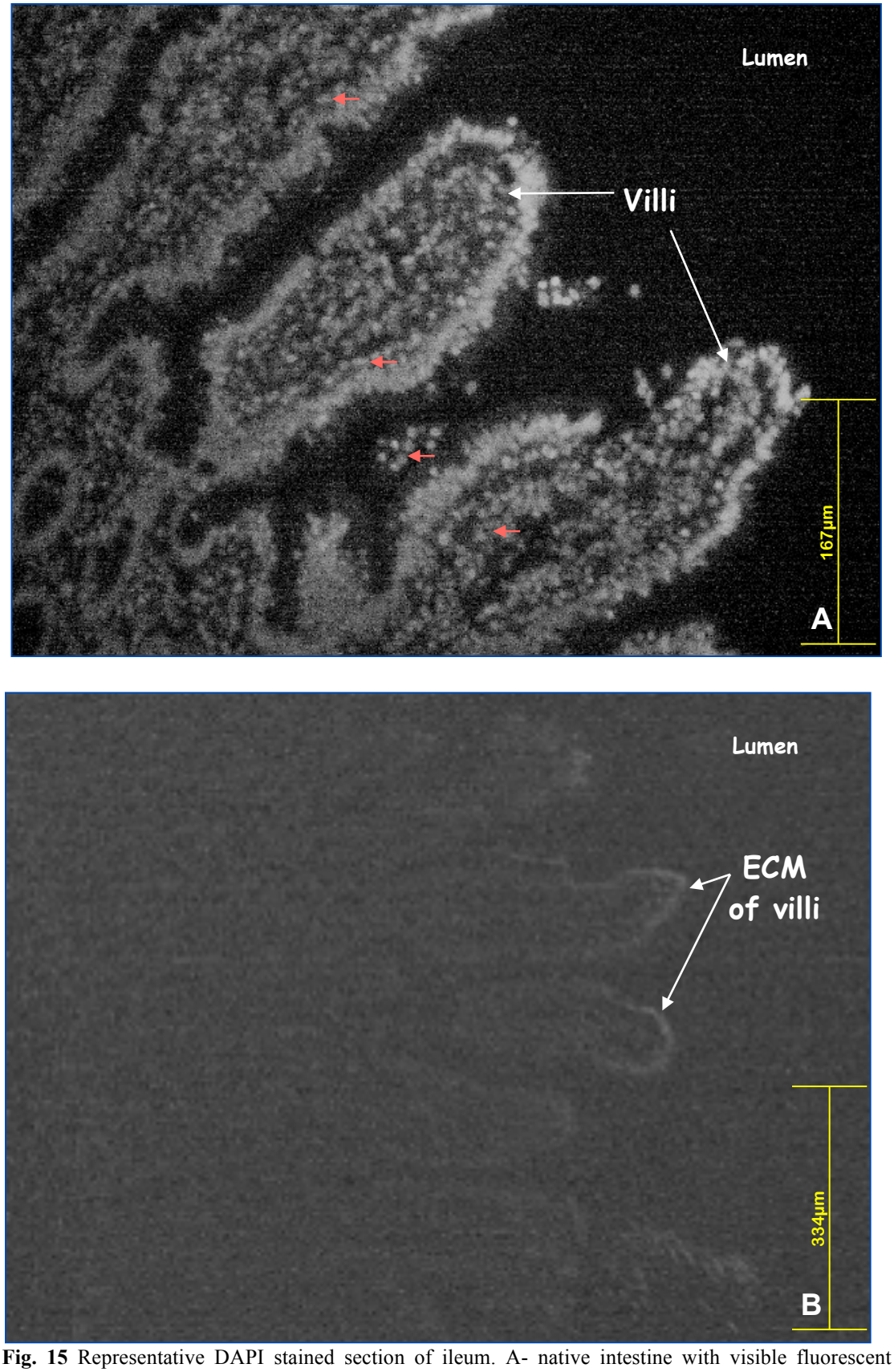


**Fig. 15** Representative DAPI stained section of ileum. A- native intestine with visible fluorescent staining of nuclei; B- de-cellularised ileum with no fluorescent staining of nuclei. Red arrows indicate DAPI stained nuclei. Yellow bar indicates the scale of the images.

#### 3.3.1.2.2. Picro Sirius red/Miller's elastin

Picro Sirius red staining showed that the organisation and status of collagen fibres of the arcade and main pedicle within the scaffold and native tissue remained similar (arterial collagen fibres are thicker - orange-to-red in colour, and venous collagen fibres are thinner – green-to-yellow).

Intestinal ECM of native tissue was mostly composed of yellow, orange and orange-to-red fibres. De-cellularised ileum predominantly contained thinner than tissue than native, green-to-yellow, yellow, yellow-to-orange and orange fibres **(Fig. 16)** but in general the collagen status and layout was similar in native and de-cellularised intestine. The histological layers of the ECM were well preserved and easily identifiable after the process. The removal of the cells caused a decrease in thickness of mucosal layer which even in native tissue is composed of very fine collagen fibres **(Fig. 17)**.

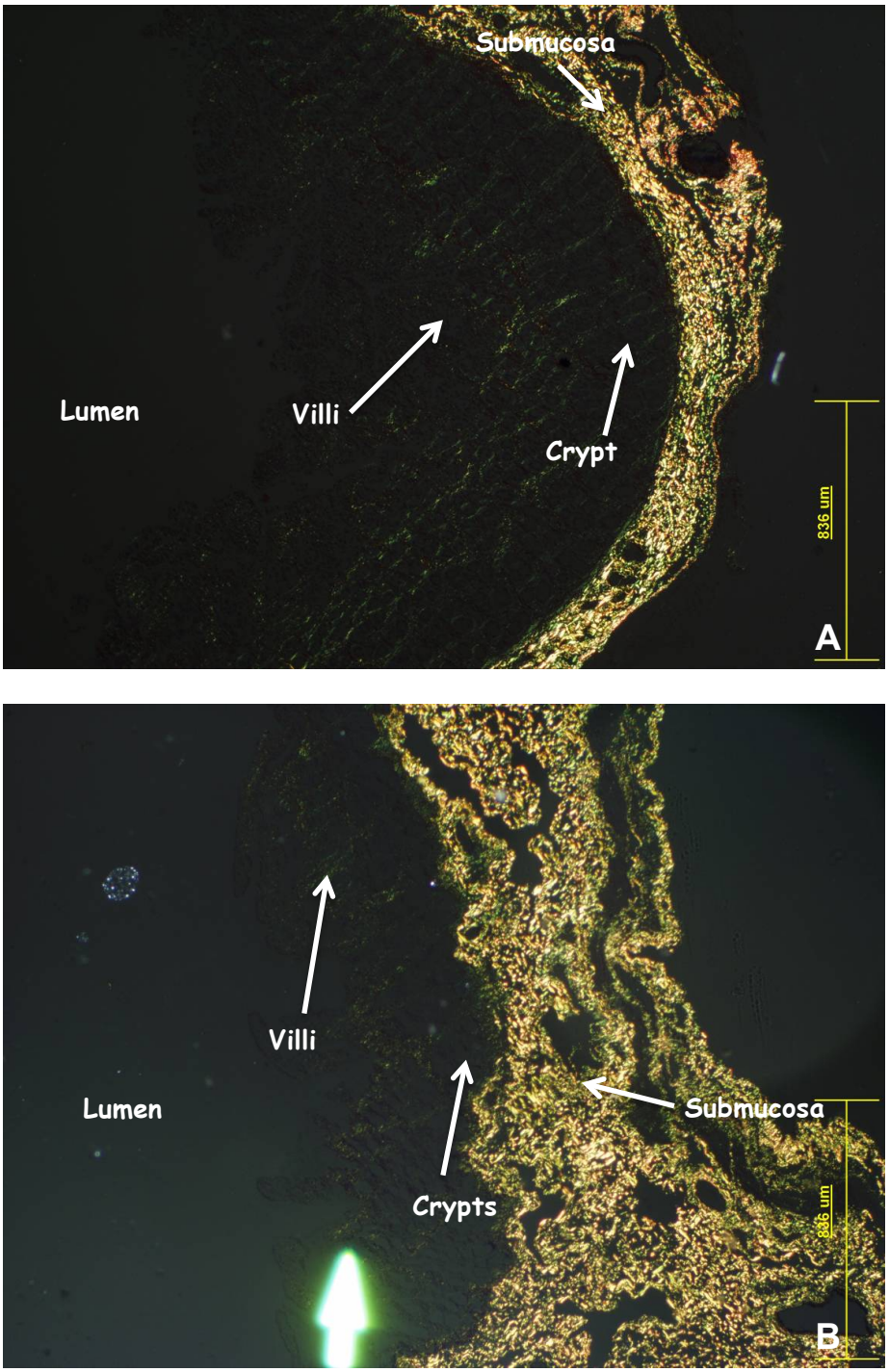


**Fig. 16** Representative Picro Sirius red stained section of ileum viewed under polarised light. A- native intestine composed of thick orange-to-red collagen fibres within the submucosa and thin green fibres of villi and crypts; B- de-cellularised ileum showing mainly yellow-to-orange collagen fibres of submucosa and thin, green fibres of mucosal layer.

Elastin was preserved in all the parts of de-cellularised specimen, including internal elastin within arteries and veins, as well as external elastin within the arteries.

What is more, the elastin of small vessels within the acellular ileum was also present **(Fig. 17)**.

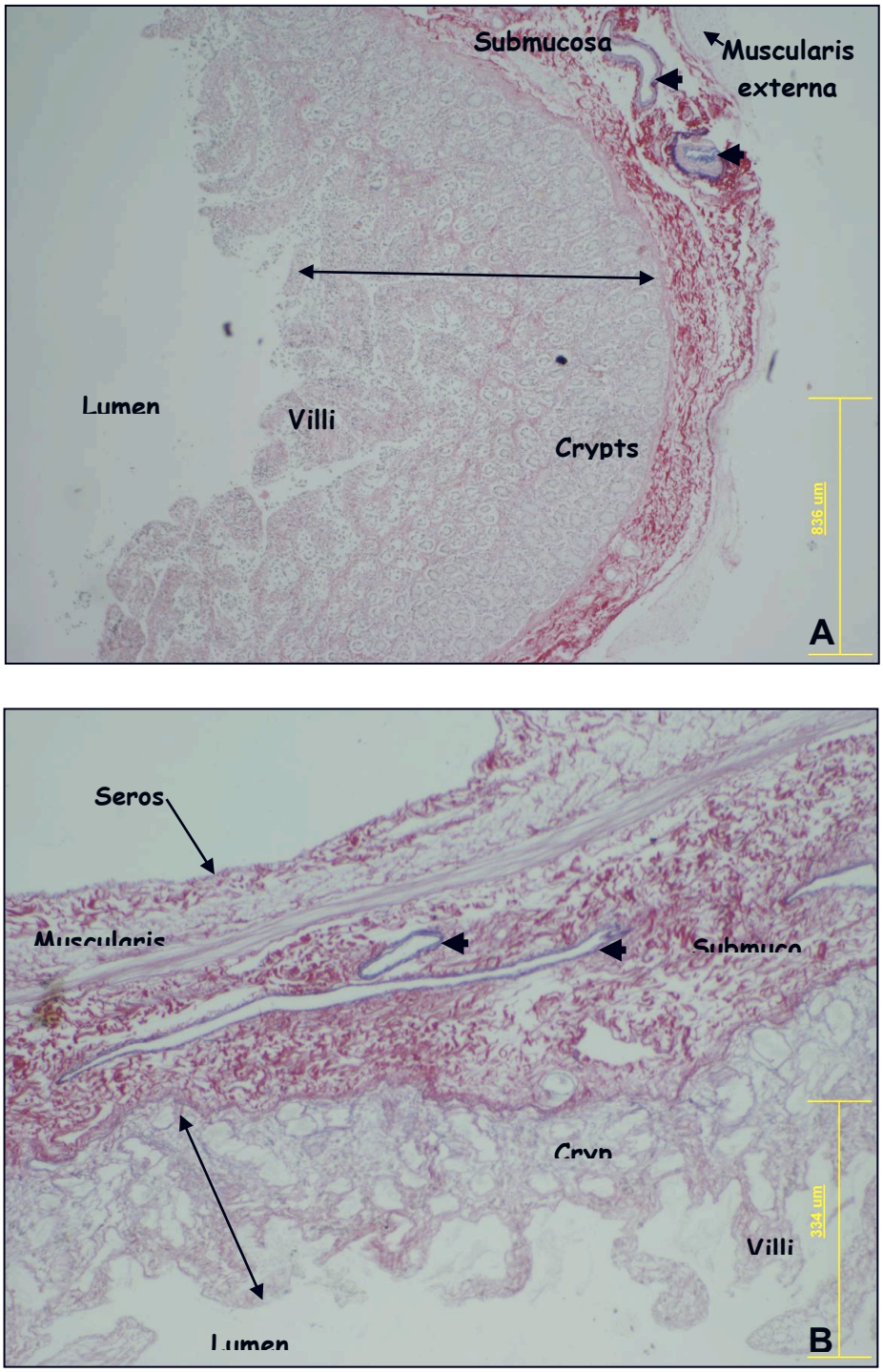


**Fig. 17** Representative Picro Sirius red/Miller's elastin stained section of ileum. A- native intestine with easily distinguishable histological layers, thick mucosal layer (double arrow) and blue-stained elastin of intestinal vessels within the submucosa (arrows); B- de-cellularised ileum showing all histological layers, thinner than in native tissue mucosal layer (double arrow) and blue-stained elastin of intestinal vessels within the submucosa (arrows).

### *3.3.1.3. Immunohistochemical*

IHC staining of Col I and Col III showed that both types of collagen are present in a de-cellularised specimen. There are no changes in the distribution of Col I **(Fig. 18)** and Col III **(Fig. 19)** between normal ileum and acellular scaffold.

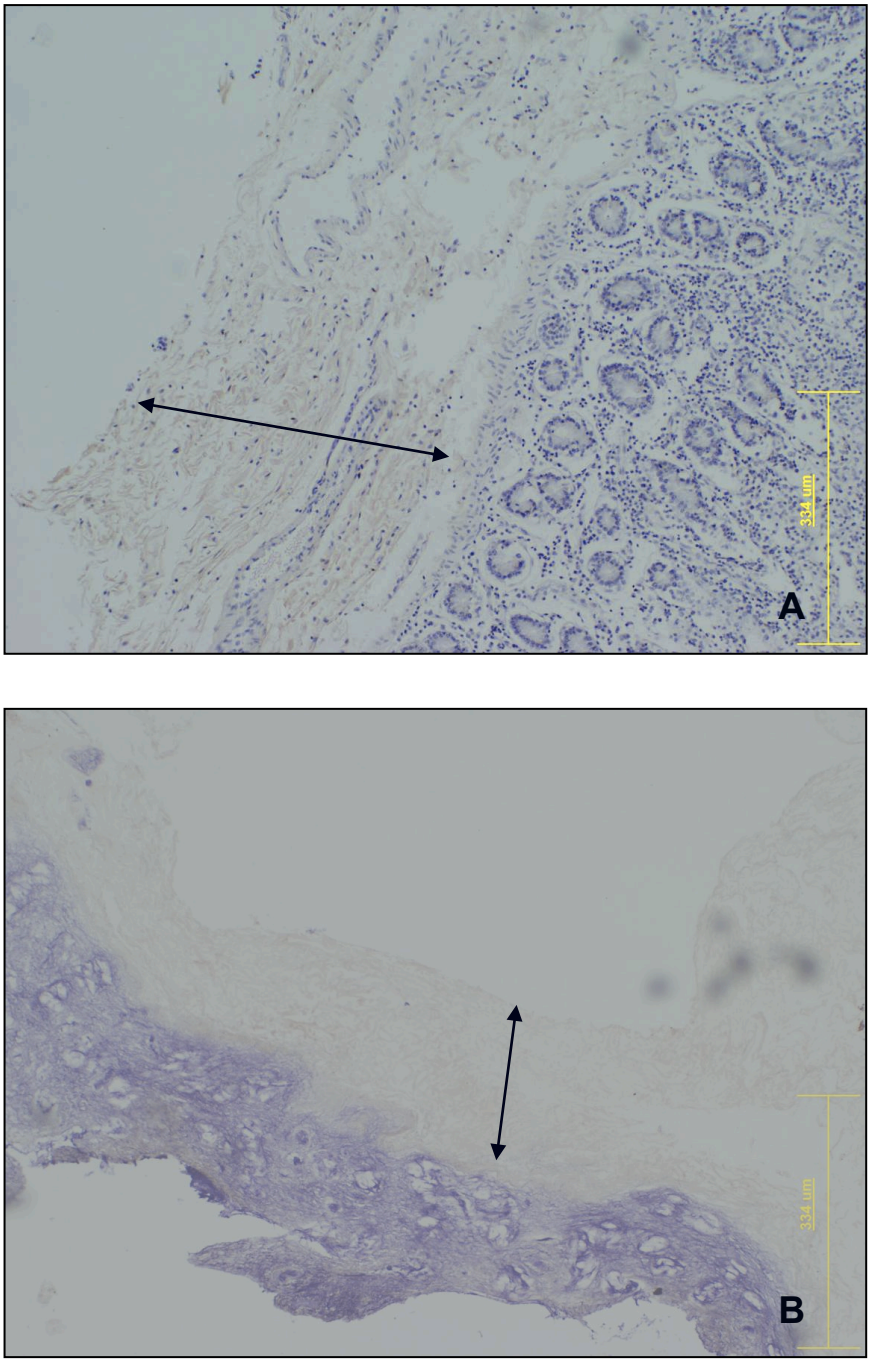


**Fig. 18** IHC staining (brown, double arrow) of Col I within control porcine intestinal tissue (A), and de-cellularised porcine ileum (B).

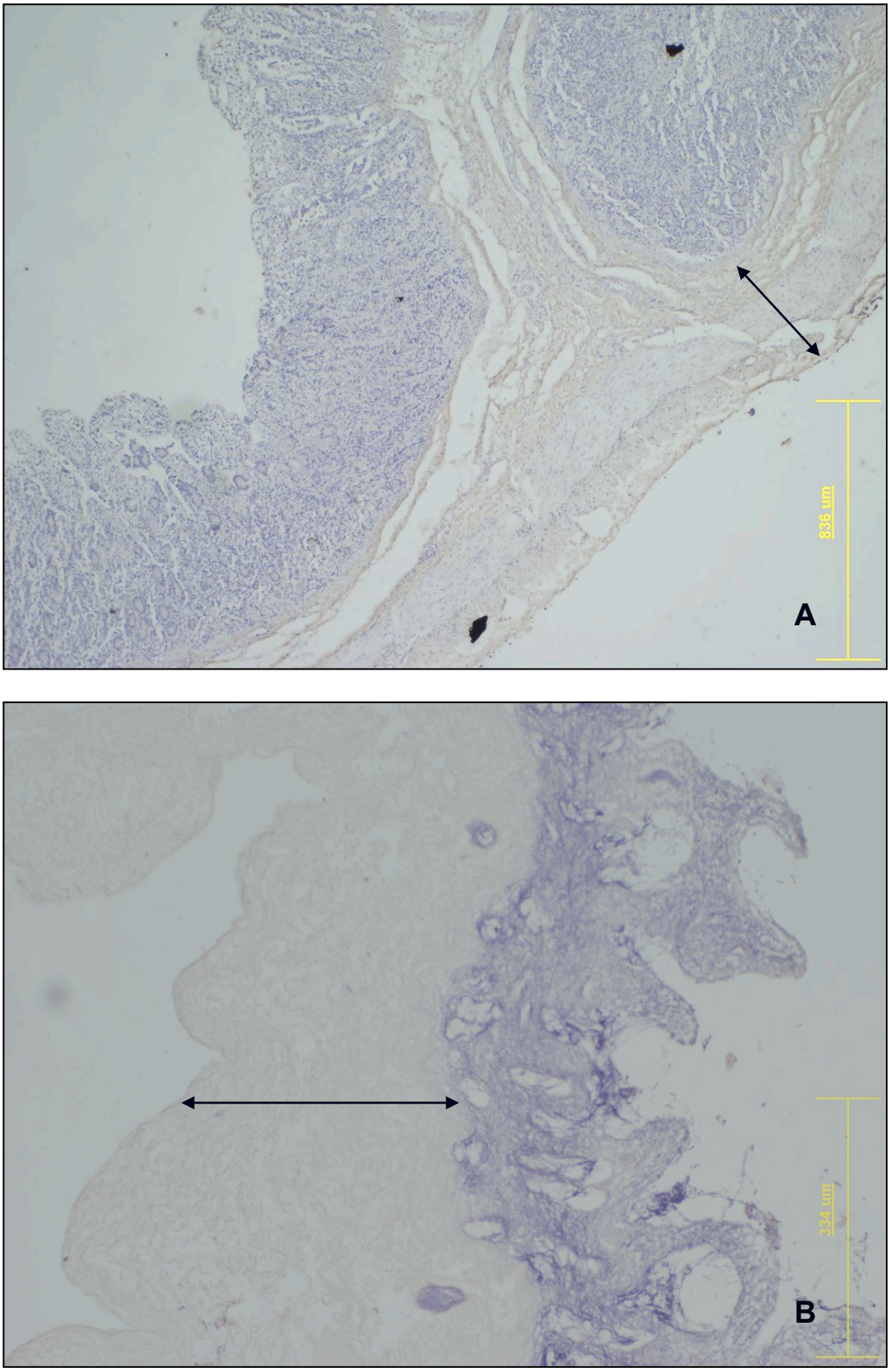


**Fig. 1**9IHC staining (brown, double arrow) of Col III within control porcine intestinal tissue (A), and de-cellularised porcine ileum (B). Yellow bar indicates the scale of the images.

### *3.3.1.4. Molecular*

### 3.3.1.4.1. DNA

While optimizing the de-cellularisation protocol the amount of residual DNA in the tissue after the process was checked with every change in the protocol. None of the protocols completely removed all DNA. However, based on histological and molecular findings the most successful protocol was chosen. Use of Triton X 100 or trypsin resulted in significantly larger amounts of remaining in the scaffold nuclear material, than when ionic detergents (SDS, SDX) or their combinations (SDS and trypsin) were applied **(Fig. 20)**.

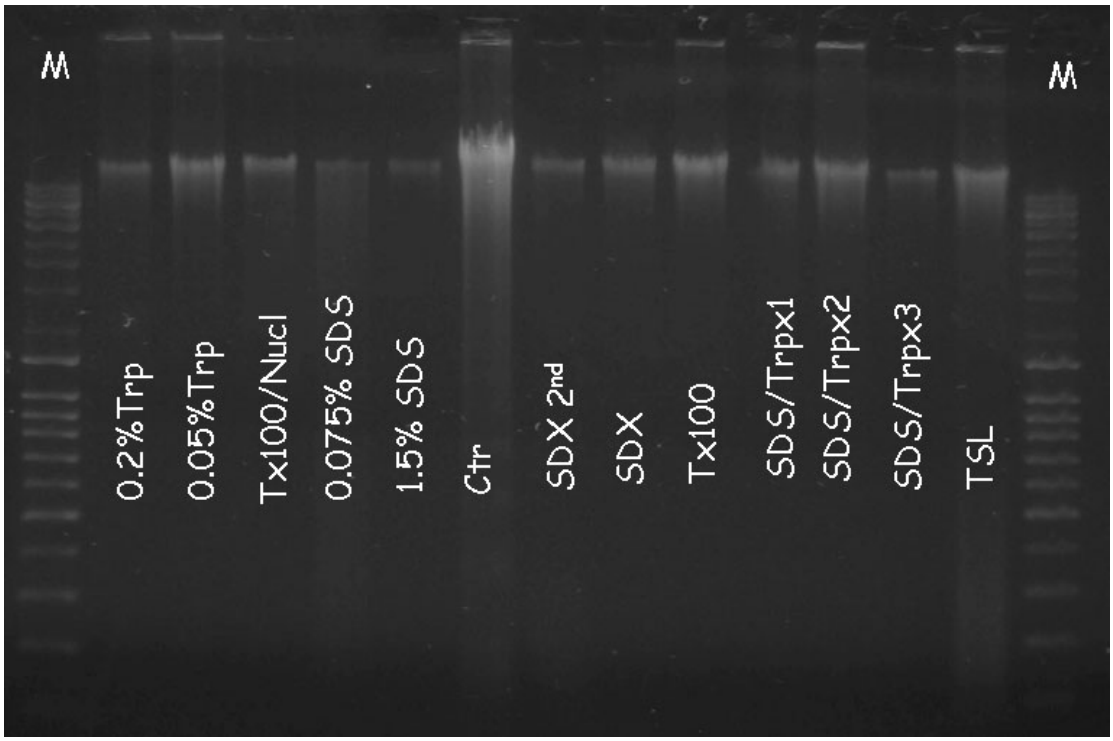


**Fig. 20** DNA quantities in control ileum and tissue de-cellularised using different protocols while optimizing the process; lanes contain DNA extracted from: scaffolds prepared using 0.2-0.05% trypsin solutions (Trp), Triton X100 with (Tx100/Nucl) or without nucleases (Tx100), 0.075-1.5% SDS, one (SDX) and two (SDX2$^{nd}$) cycles of SDX, one, two or three cycles of combined SDS-trypsin protocol (SDS/Trpx1-3), as well as control ileum (Ctr), and porcine ileum de-cellularised using commercial protocol (TSL). M- molecular marker.

Residual DNA was detected in both vascular and intestinal part of the scaffold prepared using the optimised protocol **(Fig. 20)**. Quantitative analysis of DNA content within the scaffold showed a significant decrease in the amount of detectable residual

DNA in the native tissue. The amount of DNA found in the intestinal part of the scaffold was 3.9 ± ng/mg of fresh weight, which constituted to only 0.75% of the DNA found in native tissue (0.74 ± 0.17µg DNA/mg tissue). The amount of DNA characterised in the de-cellularised vessels was also significantly lower (decrease of 99%) in comparison with the native specimen (3.7 ± 2.4ng DNA/mg fresh scaffold versus 0.36 ± 0.08µg DNA/mg of native tissue) **(Table 12)**.

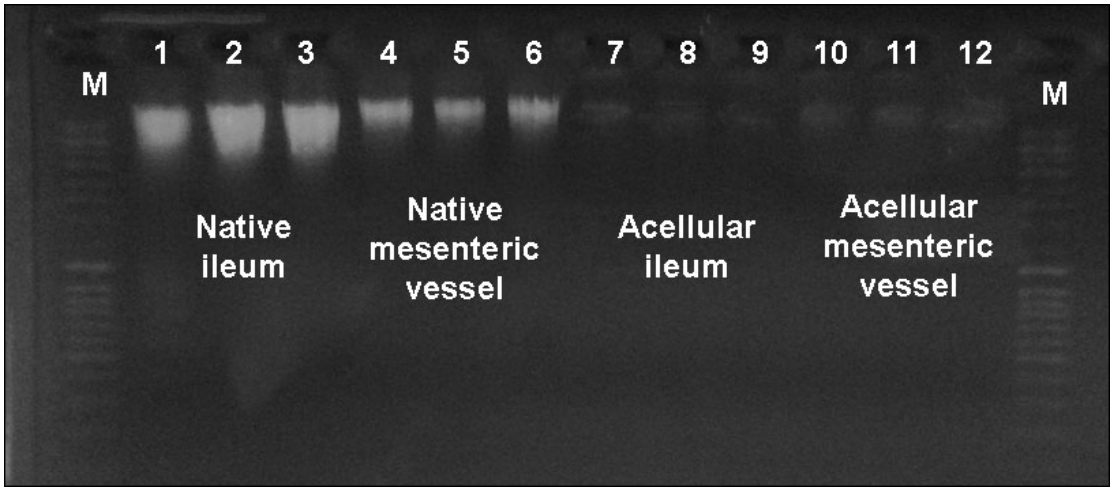


**Fig. 21** DNA quantities in control ileum and tissue de-cellularised using optimal protocol. Lanes 1-3: DNA in native ileum, 4-6: DNA in native mesenteric vessel, 7-9: DNA in de-cellularised ileum, 10-12: DNA in de-cellularised mesenteric vessel. M- molecular marker.

**Table 12** Quantification of residual in de-cellularised specimen DNA and GAG's in comparison to native tissues.

| **Specimen** | **DNA (STDEV*) [µg/mg]** | *GAG's (STDEV) [µg/g]* |
|---|---|---|
| Native ileum | 0.74 (0.17) | 3.1 (0.05) |
| Native blood vessel | 0.36 (0.08) | 2.9 (0.03) |
| De-cellularised ileum | 0.005 (0.002) | 1.1 (0.005) |
| De-cellularised blood vessel | 0.004 (0.002) | 0.9 (0.03) |

**STDEV – standard deviation*

### 3.3.1.4.2. GAG's

The amount of GAG's remaining after de-cellularisation and in control tissue was measured using spectrophotometric detection of sulphated GAG's fresh specimen, and expressed as µg of GAG's in a gram of fresh tissue **(Table 12)**. The

quantity of GAG's present in normal tissue ranged between 3 and 3.2 μg/g fresh weight (mean: 3.1 μg/g; ±SEM= 0.07 μg/g). Mean concentration of GAG's in the scaffolds produced in our laboratory came to 1.3 μg/g (with minimum of 1.2 μg/g, and maximum of 1.35 μg/g; ±SEM=0.06 μg/g). There was a significant drop in the quantity of GAG's remaining after the decellularisation. The GAG's remaining after the de-cellularisation constituted 42% of GAG's found in native tissue.

## *3.4. Discussion*

"Bench-to bedside" translation has been widely discussed since the first implantations of bioengineered organs and tissues (123). The creation of specific constructs for specific clinical settings which are not only non-immunogenic and bio-compatible, but also provide immediate functionality and contain internal vascular network, are believed to fulfil the patients' needs (124). There are few well-researched strategies to increase the rate of vascularisation. However, most of them rely on *in vivo* ingrowth of host vessels that can last few weeks (125), with the threat of ischemia and necrosis (126). At this stage of development of regenerative therapies and scaffold fabrication, only constructs which can be surgically or microsurgically connected into to the patient vasculature have chance for quick translation into clinics.

According to Rowkema el al. (125) there are four strategies to improve neo-vascularisation of tissue-engineered grafts: scaffold design, angiogenic factor delivery, *in vivo* pre-vascularisation and *in vitro* pre-vascularisation. The problems encountered when creating a model which would address the need for large, pre-vascularised constructs is one of the reasons why investigation into construction of an artificial ileum has been a long process. Our scaffold was obtained in a way that allows improvement in terms of its application via integrating all four strategies and

creating the opportunity to direct the creation of intestinal/vascular construct. The structure of the scaffold enables the incorporation of two different tissues, the use of ECM provides the necessary cellular cross-talk molecules and immediately after implantation all parts of the scaffold are supplied with blood.

Scaffolds with a preserved vascular network that have been de-cellularised via their vascular tree create a viable opportunity of obtaining off-the-shelf organs, which are ready to implant. This technique has been used to de-cellularise liver (127), kidney (128), pancreas (128), intestine (128), lungs (129), placenta (130), and heart (131). They all resulted in preserving perfusable vascular architecture and the organ geometry.

Our presented scaffold also resulted in the 3D structure and molecular composition bein preserved using individually tailored vascular and intestinal part de-cellularisation protocols, and at the same time removed cellular and nuclear content of the tissues. Although others have already reported the results of de-cellularisation of intestinal tissue, and use of vascular tree for delivery of de-cellularising agents, none of the existing protocols separated the process for the tissue of interest and its vasculature. What is more, none of the published results investigate in detail the state of the de-cellularised vascular tree of the scaffolds. The scaffold contains a perfusable acellular feeding artery, a draining vein and microvascular connections, which were analysed with the same emphasis as the ileum. The de-cellularisation of a more fragile vasculature was achieved quicker than the thicker and more complex ileum, that is why the process was divided into cycles and the amount of cycles applied to vessels was lower than the one introduced via a second, intestinal circuit. All segments of ileum and mesenteric arcade with the main pedicle were cell-free. The use of enzyme-detergent cycles and the perfusion was a major advantage over standard water bath

process, which failed to remove all cells (132). The final perfusion with Evans blue solution proved that all the conduits within the specimen were competent following the de-cellularisation. The dye-experiment demonstrated that the injected fluid was perfusing through the intact vascular network and slowly moved from larger vessels to smaller capillaries. The technique presented can be applied to segments of intestine long enough to create viable treatment for SBS patients.

The perfusion de-cellularisation system has several technical and practical advantages. It is compact in size (does not take much bench space), has a low perfusion volume (one litre of solution per change), little production costs, and is easy to handle. In comparison to other time-consuming processes this one is reasonably short (130). The scaffolds sterility could be achieved using simple incubation of the scaffold in 0.1% solution of PA and no expensive apparatuses for irradiation or ethylene oxide exposure are needed.

What is more, modifications of the model could easily be used in perfusion and de-cellularisation of other tissues and organs. Nonetheless, one of the biggest advantages of this scaffold is the fact that it can be used to culture two different cell lines, facilitating a new level of complexity for cellular interactions and organization. So far this has been an unmet need in bio-engineering of intestinal tissue.

The distinctive differences in using different de-cellularising agents emerged while optimising the process. Many combinations of the detergent solutions as well as enzymes were less successful in the removal of cells (trypsin, Triton X-100, SDX), nuclear content (trypsin, Triton X-100, SDX), or preserving ECM structure. Some of the applied methods were better in terms of preservation of the collagen and elastin; however, they failed to remove the nuclear or cellular components of the tissue (Triton X-100).

The use of SDS gave better results than any other detergent or trypsin digestion on its own. De-cellularising reagents used in the optimal protocol removed cellular components as well as the majority of DNA while preserving functional ECM proteins and structure. SDS or combined methods of SDS and enzymes have been reported to show excellent cell removal (133). However it was also shown that the treatment with SDS results in disintegration of the collagen (134) as well as fragmentation and swelling of the fibres (135). The influence on ECM state varies depending on detergent concentration, duration of treatment, presence of protease inhibitors and differences in tissue morphology or age (136). The separation of the two circuits within the scaffold was done to avoid overexposure of more fragile parts, and the resultant negative side effects of SDS.

Trypsin is a serine protease commonly used as an enzymatic de-cellularisation agent. However, ECM proteins such as collagen have limited resistance to trypsin cleavage (137). Removal of cells and ECM constituents by trypsin is time-dependant, and complete de-cellularisation of intestinal tissue by trypsin alone would take days. Thus, tissue exposure to trypsin was used with caution and other agents were added in order to shorten the time of tissue exposure to the enzyme. In comparison to SDS, trypsin is more disruptive to elastin and collagen and slower to remove cells but shows better preservation of GAGs (134).

Chelating agents such as EDTA aid in cell dissociation from ECM proteins by sequestering metal ions (138;139). EDTA alone is insufficient for cell removal, and is therefore typically used in combination with enzymes such as trypsin (140).

DNase I is a nuclease that cleaves nucleic acids sequences and can therefore aid in removal of nucleotides after cell lyses in tissue (141).

The de-cullarisation process may never reach the theoretically possible 100% (142), but a virtually complete de-cellularised intestinal/vascular matrix was shown by the analysis of DNA. The DNA remaining in the scaffold constituted less than 1% of native tissue (both ileum and blood vessels), which is comparable to the amounts of DNA found in commercially available ECM used in clinical applications (143), and often is much less than the nuclear content found in acellular scaffolds under pre-clinical investigation (144). Gilbert et al. (51) described the impossibility of any combination of de-cellularising agents to remove 100% of cellular and nuclear components. It was concluded that methods which remove most or all of the visible cellular material result in most of the cases in biologic scaffold materials that are safe for implantation. Crapo et al. (145) goes even further with this estimation and points out that the scaffolds containing less than 50ng of double stranded DNA per mg of dry weight of ECM, less than 200 base pairs-long DNA fragments, and no DAPI staining are safe to implant. DNA remaining in the presented scaffold ranged from 4-5ng/mg of ECM.

While optimizing the de-cellularisation protocol care was taken in order to maintain the 3D integrity of the functional and structural proteins. Vascular and lymphatic structures, nerves and the tissue specific cells should easily find the cues for ingrowth and differentiation within the preserved ECM. Collagen content, status and distribution within the scaffold was shown to be very similar to these of native tissue. The thickness of intestinal layers within the ECM scaffold was lower; however this is unavoidable while removing the cellular components of the tissue.

In this experimental model the existence of internal elastin within the de-cellularised vasculature was of high importance. It is not only crucial in the process of re-endothialisation (and secondary in preventing blood from interacting with the

highly thrombogenic collagen) but also provides the elasticity to the vessels which prevents them from breakage while stretching under the load, and it also prevents fibrocellular pathology (146).

GAG's are important attachment and information highway molecules within the ECM. They are highly functionalised, linear, and negatively charged polysaccharides present in animal tissue, which are covalently bound to a protein core in macromolecular assemblies known as proteoglycans (147). A reduction in sulphated GAG content is observed after any de-cellularisation procedure. A considerable removal of GAGs from the ECM can affect the bioactivity of the scaffold (148). Significant amount of GAG's (42%) was preserved, and this result is comparable to 15-60% range reported by others (149). What is more, the assay measured the sulphated GAG's, and the de-cellularisation process may have affected the amount of sulphated residues of ECM.

The host tissue response following *in vivo* implantation of ECM scaffolds is dependant upon efficacy of cells and their remnants removal, therefore adequate application of the appropriate de-cellularising agents, is critical. The balanced protocol provided little of the cellular and DNA components as possible, without huge compromises on the amount of functional proteins, structure of collagen and elastin within all parts of the scaffold.

The use of porcine intestine as a biologically-based scaffold offers several potential advantages. Tissue is easy to harvest even in large quantities, in size it is appropriate for transplant procedure, human and porcine intestine show anatomical and physiological similarities, and porcine ECM surface has strong cellular adhesive properties (150). Moreover, this 3D supporting matrix includes vasculature which would allow the survival of cells that thanks to important ECM proteins such as

collagen, elastin and GAGs migrate into and repopulate these scaffolds. All this is missed in polymeric materials, which have been previously used in small intestine tissue engineering.

# Chapter 4.

# Biocompatibility tests in the rodent model

## *4.1. Background and aims*

Since the immune response induced by bio-engineered products can decide their fate, it is extremely important to evaluate the implant's biocompatibility before incorporating it into further studies. Animal studies provide an understanding of how the body responds to the scaffold, its evaluation, as well how to estimate long-term outcomes. Since most of the products are designed to be surgically implanted for the patient's entire life, the duration of the study should extend the time when final clinical outcome is achieved (20). However, the biocompatibility tests should state the first line of reaction towards the device and therefore the time of the *in vivo* studies at this stage usually extend the transition period from the acute to chronic immune response. The model presented in this chapter was used to check if the acellular scaffold produces any immediate negative outcome in mammals, and thus it was used as a negative control rather than an immediately translatable into human or even porcine outcome. The aim was to show that the scaffold did not induce any adverse clinical reaction in rats, which would be linked with probability of positive outcome in other *in vivo* models. However, if the scaffold would appear to be toxic or reject acutely it could suggest that the same pattern could be expected in all other mammals.

It is clear that species differences exist in the structure and function of the immune system and that these differences need to be kept in mind when designing experiments with the goal of extrapolating the data to humans. Taking into account the experiments presented in this chapter it was also necessary to identify which differences would be relevant for the endpoint that was considered. Therefore the rat model was chosen, as it is the best described one across the field of tissue engineering, and has been used in many biocompatibility studies (166). The abundant data on the characteristics of the cell-mediated immunity in rodent models is readily available for comparison. The humoral immune response can be enhanced in rats in comparison to humans, however strain-differences exist (213). On the other hand, cellular responses and induction of foreign-body granulomatous inflammation (main concerns when considering tissue-engineered implants) have been proven to develop more severely in rats than in humans (213). Thus, this model makes it a good negative control for hyperacute and acute rejections and toxicity.

Pig model used in Chapter 6 is not very well characterised for the immune responses in tissue-engineering scenarios. However, pigs in contrast to rodents are proven to produce Pulmunary Intravascular Macrophages (213), which is an additional reason (except the fact that it was crucial to check scaffold performance under systemic perfusion using appropriately sized animal) for conducting vascular anastomosis in porcine model.

The differences between both (rat and pig) responses and human immunity exist, but it is important to check *in vivo* performance of a scaffold before incorporating it into further investigation. The use of animal model is sometimes more beneficial than use of *in vitro* human cultures, but one should not exclude the other during the scientific process.

To evaluate biocompatibility *in vivo*, the scaffolds described in the previous chapter were implanted subcutaneously into nine adult male Sprague Dawley rats (three rats per time point; two pieces of scaffold per animal resulting in six explants per time point) for two, four and eight weeks. After each time point a macroscopic, histological and IHC analysis was conducted in order to estimate long-term outcome of the grafts, and assess if the acellular matrix would result in scar tissue formation or smart remodelling.

These studies were designed in a way that allowed testing of the acellular scaffold for its toxicity and biocompatibility, based on promoting cellular ingrowth and neovascularisation, and not for its regenerative potencies.

## *4.2. Methodology*

### 4.2.1. Materials

The list of materials and equipment used in experiments described in this chapter is presented in **Appendix 4**.

### 4.2.2. Animal husbandry

All animals were maintained and handled similarly to the procedure presented in Chapter 2 (2.2.2).

### 4.2.3. Subcutaneous implantation into rat recipients

1cm$^2$ squares of porcine acellular scaffold (intestinal part) were implanted subcutaneously into adult male Sprague-Dawley rats. All rats were weighed prior to surgery and later on the termination day. Weight controls, were conducted every week

to monitor the animals' well-being and general health. Following a midline incision and creation of subcutaneous pouch, corners of two trimmed intestinal scaffolds were attached using 5-0 Prolene sutures to the abdominal muscle **(Fig. 22)**. Skin was closed with 3-0 Vicryl (horizontal mattress suture). At two, four and eight weeks post-surgery tissue was harvested from the animals after termination by lethal injection of sodium pentobarbitone**.**

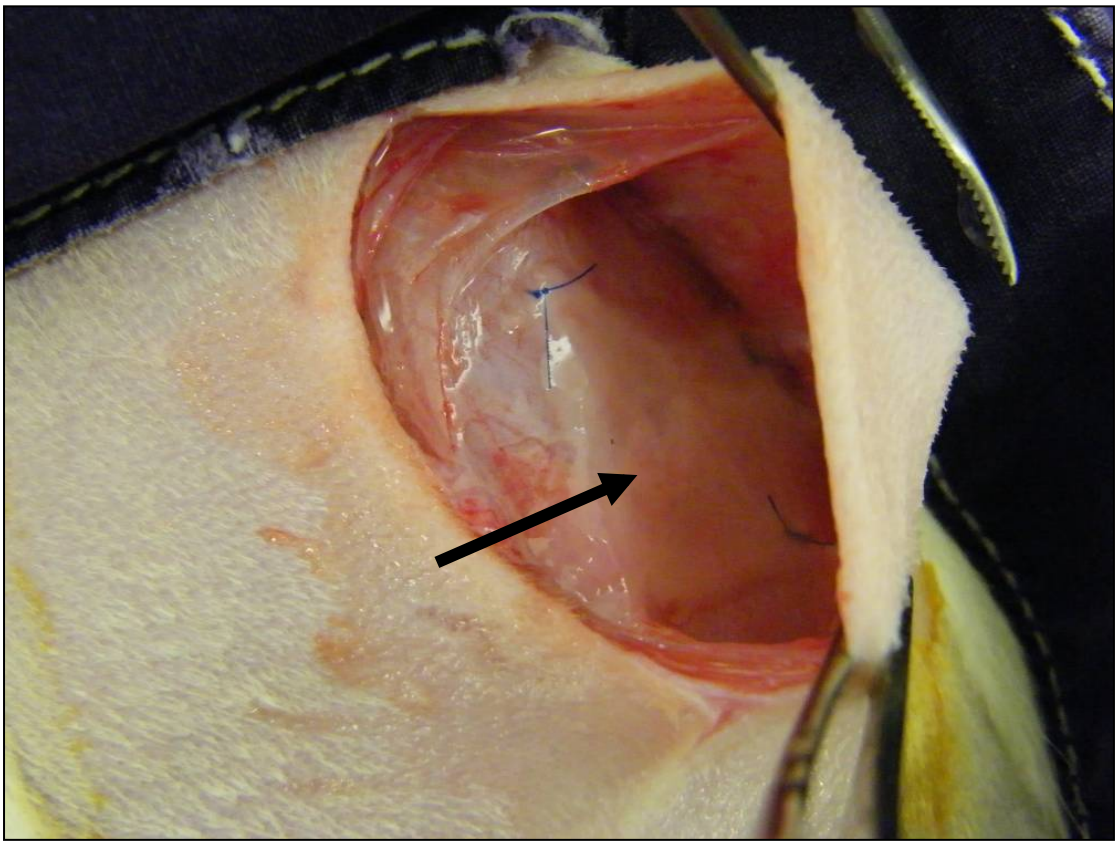

**Fig. 22** Subcutaneous implantation of the trimmed porcine scaffold (arrow) into a rat recipient (day 0).

## 4.2.4. Evaluation of the grafts

### *4.2.4.1. Macroscopic*

At the time of harvesting grafts were photographed, measured and their general appearance recorded **(Fig. 23)**. Moreover, the surrounding tissue was checked for any obvious macroscopic signs of inflammation (e.g. redness, extensive fibrosis).

### *4.2.4.2. Histological*

Tissue was processed and prepared for histological staining in the way described in sub-chapter 3.2.6.2.

Full thickness of the abdominal muscle together with the sutured scaffold was analysed. H&E staining was performed to assess basic tissue, cell morphology and cell distribution within the grafts. Picro Sirius red staining was used to visualise collagen fibres and comparatively estimate their thickness (the relation between collagen thickness and the colour of Picro Sirius red stained tissue viewed using biofringed light is described in methods of Chapter 3). The presence of aggregates of dense thick (red) collagen fibres could suggest the secretion of new ECM by re-populating cells. The implants were expected to contain green, thin fibres mostly in the periphery, which would mean that the ECM is undergoing biodegradation at the same time. Miller's elastin staining was incorporated to visualise the presence of neo-vessels within the grafts.

### *4.2.4.3. Immunohistochemical*

IHC was performed to visualise: epithelial cells (cytokeratin 8: CK8), proliferating cells (Ki67), neural progenitors (S-100), smooth muscle actin (αSMA), endothelium of the blood vessels (Factor VIII: FVIII), VEGF, and its receptors

(VEGF-R) in the grafts harvested at each time-point. Expression of VEGF was also checked in the scaffold prior-implantation. The staining was performed in a way described in sub-chapter 3.2.6.3. Specific IHC protocols are summarised in **Table 8 (Appendix 9)**.

## 4.3. Results

All rats survived the operation. The scaffolds could be easily sutured onto the abdominal muscle. Two scaffolds were implanted into one recipient (either sides of the midline opening).

Eight out of nine rats survived the planned study period. One animal had to be euthanised three days before (at day 25 post-surgery) the planned termination date due to problems not associated with implantation. Eight out of nine animals were feeding well, and gained weight post-surgery **(Table 13)**. Three rats were terminated two weeks after scaffold implantation, two four weeks post-surgery (and one after three weeks and four days) and three rats eight weeks after operation.

**Table 13** Weight changes of the rats with subcutaneous implants of porcine de-cellularised ileum.

| Animal Number | Time of explantation | Weight of the animal at the day of surgery [g] | Weight of the animal at the day of termination [g] | *Δ weight [g]* |
|---|---|---|---|---|
| ***1.*** | 2 weeks | 409 | 410 | +1 |
| ***2.*** | 2 weeks | 407 | 422 | +15 |
| ***3.*** | 2 weeks | 439 | 462 | +23 |
| ***4.*** | 3 weeks and 4 days | 517 | 407 | -110 |
| ***5.*** | 4 weeks | 480 | 513 | +33 |
| ***6.*** | 4 weeks | 572 | 579 | +7 |
| ***7.*** | 8 weeks | 515 | 630 | +115 |
| ***8.*** | 8 weeks | 502 | 557 | +55 |
| ***9.*** | 8 weeks | 538 | 598 | +60 |

## 4.3.1. Evaluation of the grafts

### *4.3.1.1. Macroscopic*

All the grafts could be easily identified post-mortem and were still attached to the abdominal muscle when harvested from the animals. Sutures at the corners of the grafts kept them in position throughout the duration of the experiment. Macroscopic examination showed no major adhesions to the skin or fibrotic encapsulation of the grafts at any time-point. Graft shrinkage was minimal and occurring only in the implants harvested eight weeks post-surgery **(Fig 23).**

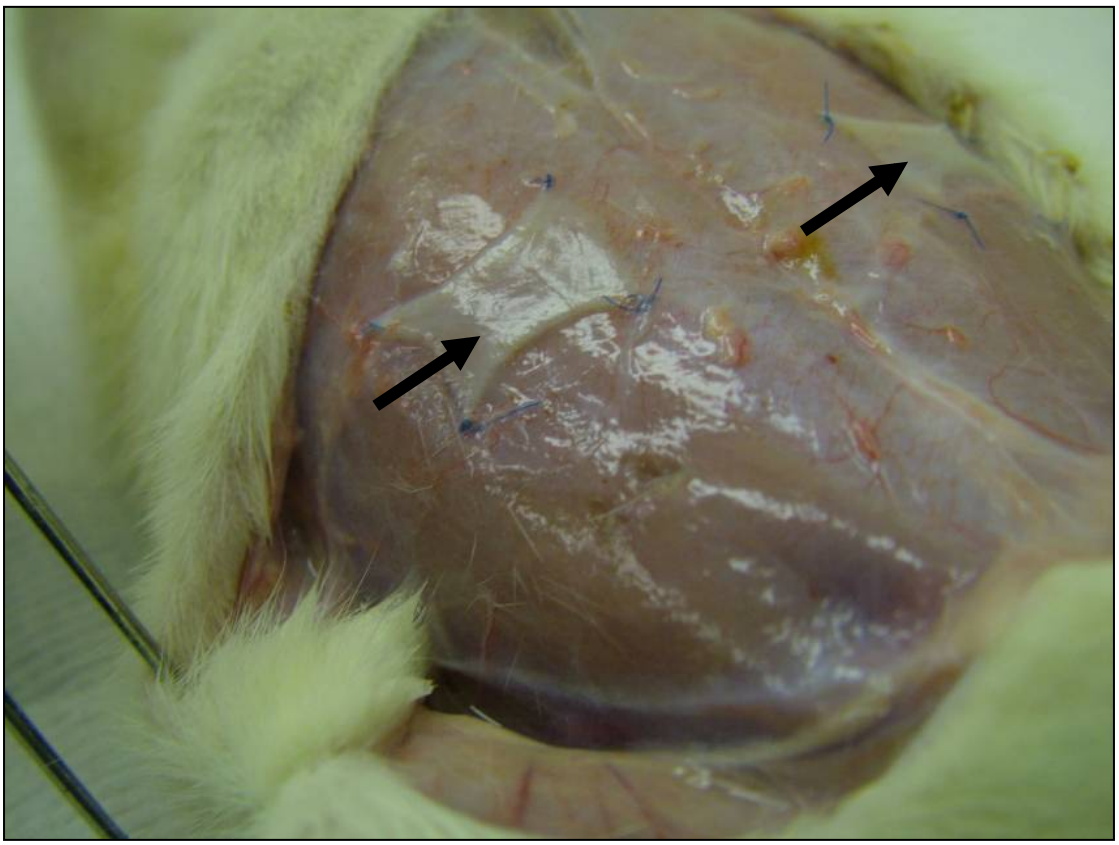

**Fig. 23** Gross appearance of the grafts (arrows) harvested eight weeks after subcutaneous implantation. The length of the implants was oscillating around one centimetre.

### *4.3.1.2. Histological*

#### 4.3.1.2.1. H&E staining

H&E staining showed that as early as two weeks post-implantation all the grafts were evenly infiltrated with cells (mostly polymorphic, inflammatory cells) **(Fig. 24)**. Signs of early neo-vascularisation were mostly visible in the parts of the scaffold adjoining the abdominal muscle.

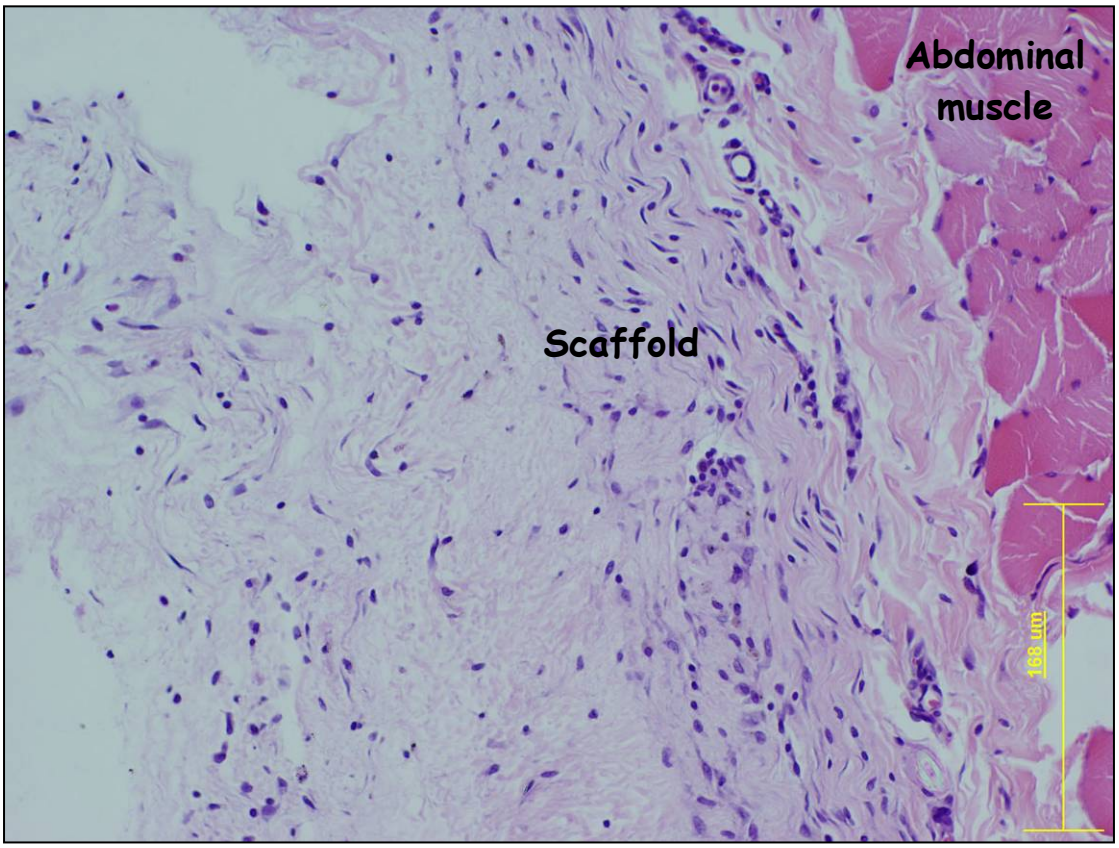


**Fig. 24** H&E staining of the scaffold harvested two weeks after implantation showing intense cellular infiltration. Yellow bar indicates the scale of the image.

H&E staining of the specimen harvested four weeks after implantation showed that the grafts remodelling continued, and no chronic inflammation could be seen within the scaffold or adjoining muscle. Cells were repopulating the whole volume of the grafts, and most of them no longer showed characteristics of inflammatory cells. Moreover, the neo-vessels could be seen in all parts of the grafts and throughout the

whole thickness **(Fig. 25)**. Nevertheless, most of the vasculature was still present in the muscle-adjoining part of the scaffold.

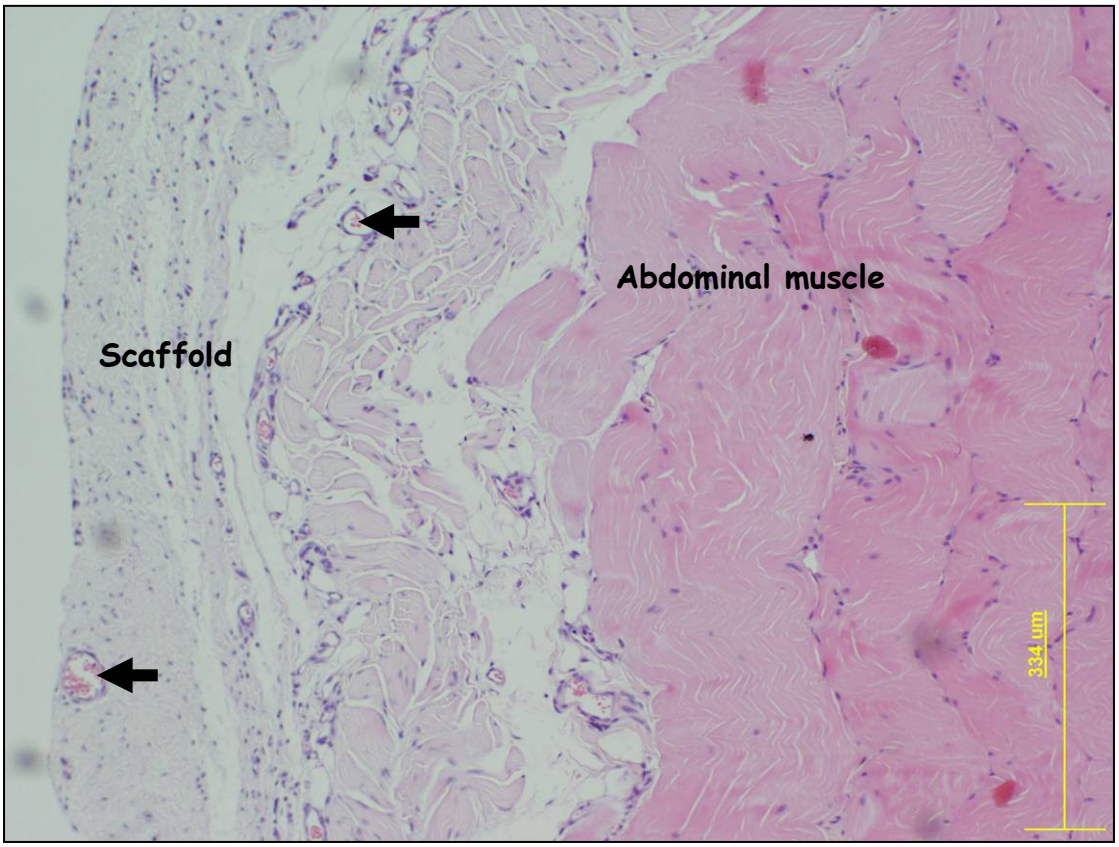


**Fig. 25** H&E staining of scaffold harvested four weeks after implantation. Black arrows indicate possible, newly-created blood vessels. Yellow bar indicates the scale of the image.

H&E staining of the grafts harvested from the rat that did not survive till the planned end-point showed no extensive inflammation or immune reaction. As in the case of all the other grafts harvested four weeks post-implantation the cellular infiltration was extensive and there were signs of rapid angiogenesis **(Fig. 26)**.

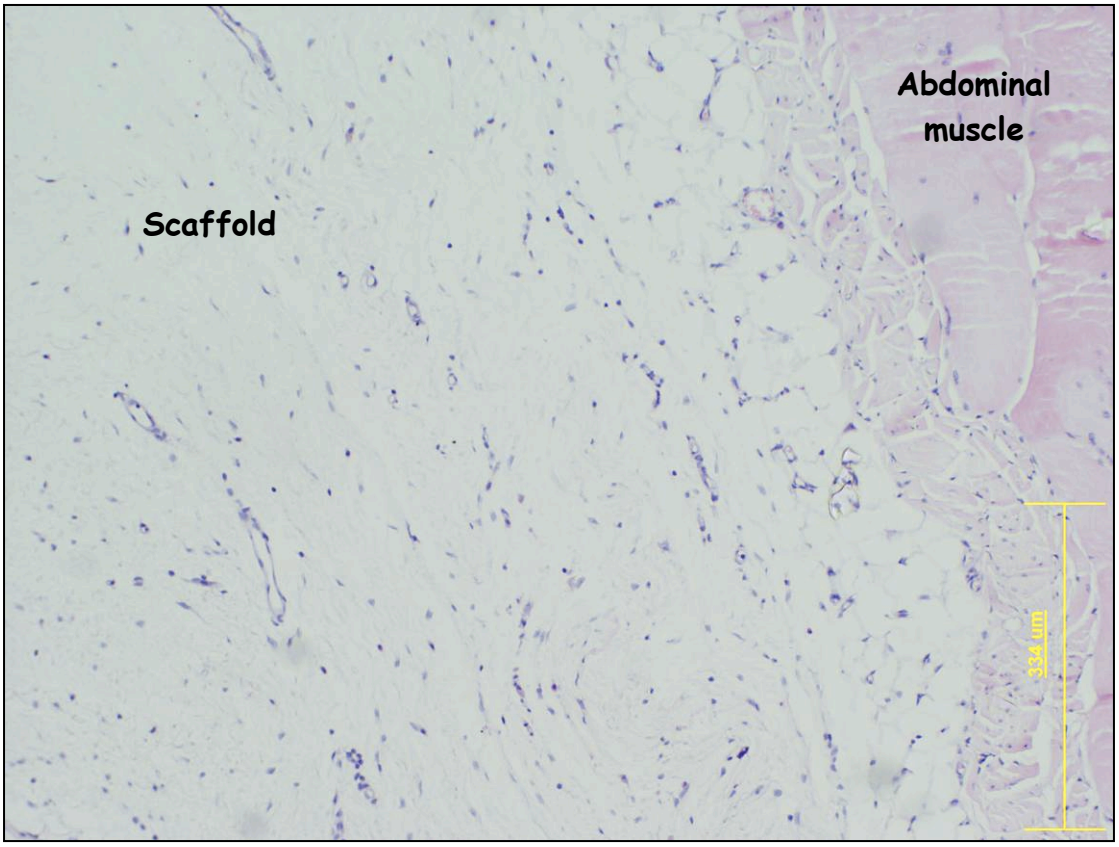


**Fig. 26** H&E staining of the scaffold harvested during the fourth week after the implantation, from a rat that had to be terminated prior to the planned time-point of four weeks, showing even cellular infiltration. Yellow bar indicates the scale of the image.

Eight weeks post-implantation the cells were also present within the grafts. No 'empty-spaces' could be seen in any part of the scaffolds. Even though the graft surface seemed to be smaller on macroscopic examination at the harvest time, no significant reduction in thickness of the scaffolds was visible. Inflammatory cells were mostly gathered around the big blood vessels or sutures. Intense neovascularisation occurred over two months, and from week four vessels developed full circumferential lining of lumen with endothelial cells surrounded with well distinguishable smooth muscles layers. What is more, acellular nerves within the scaffolds were re-populated with cells **(Fig. 27)**. No signs of fibrotic encapsulation, or scar tissue formation within the muscles or grafts were seen.

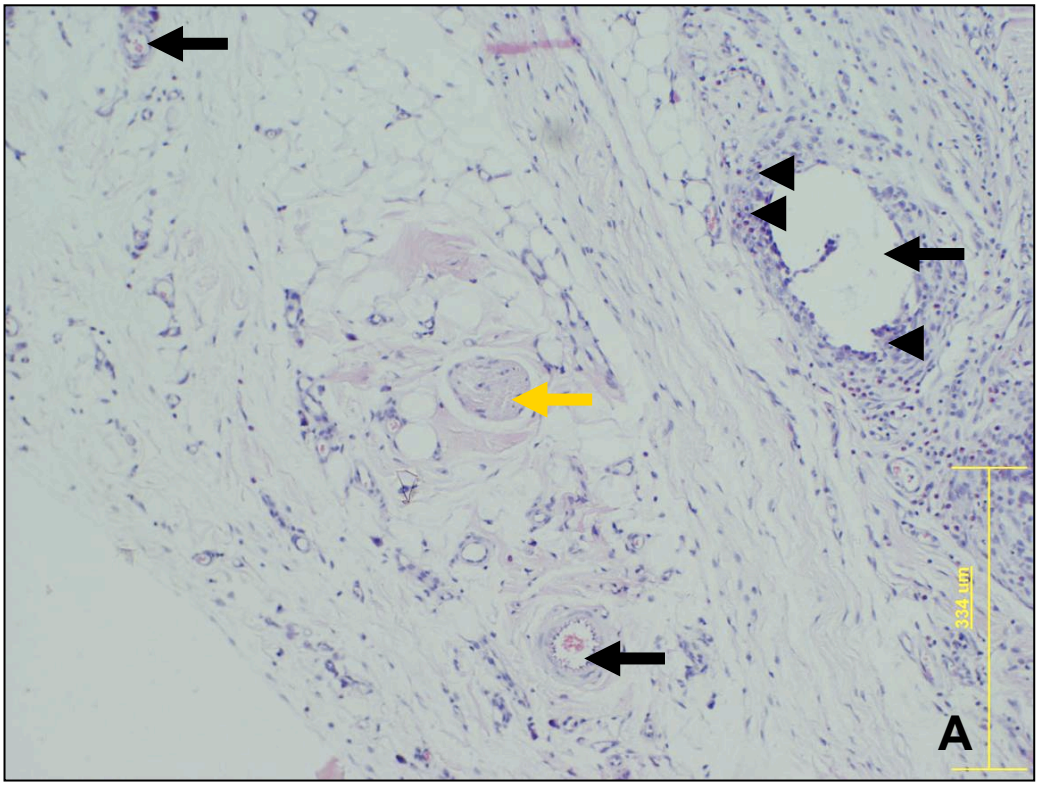


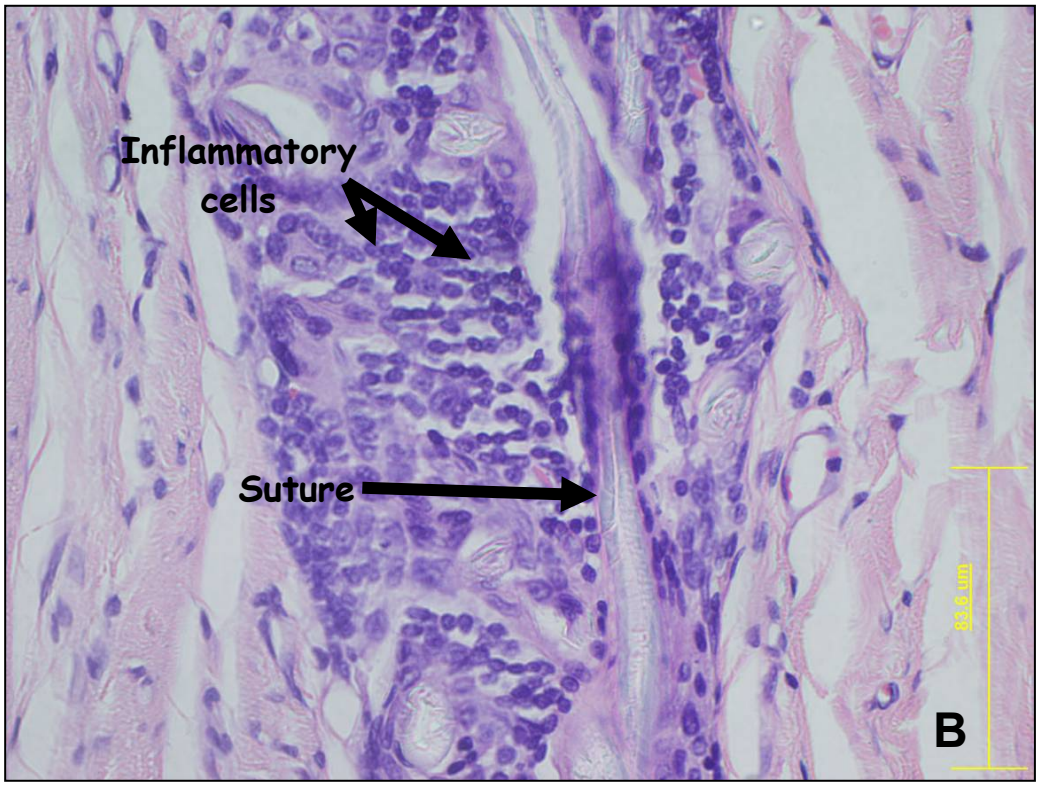


**Fig. 27** H&E staining of the scaffold harvested four weeks post-implantation. A: black arrows - blood vessels within the graft with endothelial lining and vascular wall of smooth muscle cells, yellow arrow - acellular nerve infiltrated with cells resembling native neural layout, black arrow heads – inflammatory cells around big vessels within the graft; B: inflammatory cells around the sutures. Yellow bar indicates the scale of the image.

#### 4.3.1.2.2. Picro Sirius red/Miller's elastin staining

Picro Sirius red staining showed well preserved collagen within the scaffold. The fibres were green, green-to-yellow, yellow, and yellow-to-orange when viewed under polarised light. Two weeks post-implantation thin green fibres were predominant at the edges of the scaffold. Some green fibres were also found between orange fibres in central parts of the grafts **(Fig. 28A)**. Faint elastin staining was also seen in two-week old grafts **(Fig. 28B)**.

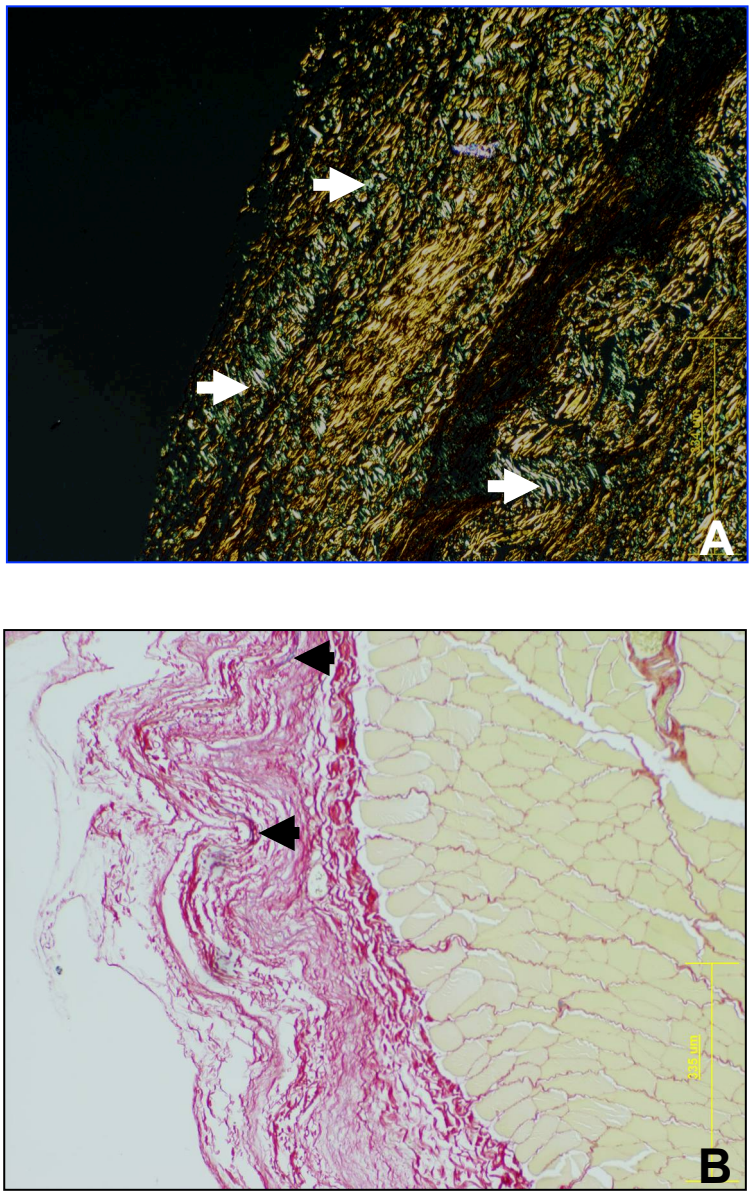


**Fig. 28** Picro Sirius red and Miller's elastin staining of the scaffold harvested two weeks after implantation. A: white arrows – thin green collagen fibres at the edges and in some central parts of the cross section; B: black arrows – blue, elastin staining. Yellow bar indicate the scale of the images.

The distribution and state of the collagen fibres at four weeks post-implantation were also the same as in acellular scaffold. However, grafts harvested eight weeks post-surgery showed abundant amount of thick, orange and red fibres, especially in close proximity of the blood vessels **(Fig. 29 A)**. Green fibres were still present mostly at the edges of cross sections of the specimen. Elastin was easily identifiable in many newly created blood vessels **(Fig. 29 B)**.

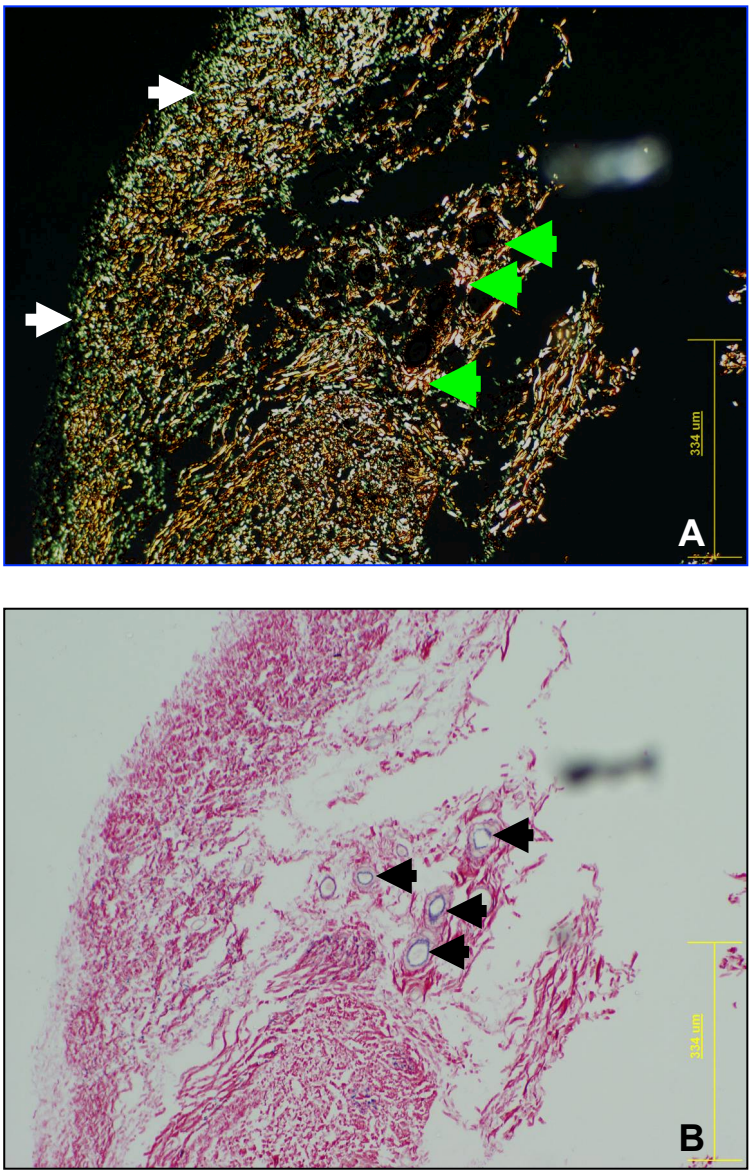


**Fig. 28** Picro Sirius red and Miller's elastin staining of the scaffold harvested four weeks after implantation. A: white arrows – thin green collagen fibres at the edges of the cross section, green arrows – thick red and bright orange collagen fibres around the new blood vessels; B: black arrows – blue, elastin staining of the blood vessels. Yellow bar indicate the scale of the images

#### *4.3.1.3. Immunohistochemical*

IHC staining proved that cells residing in the grafts obtained at all three time points expressed the proliferation marker (Ki67). However, up to two months post-implantation there were no cells that had differentiated towards either intestinal epithelium (CK8), or nerve tissue (S-100) in the specimen. Encouragingly, as early as two weeks after implantation of scaffolds, neo-vessels were positive for αSMA. After the first two weeks *in vivo* some cells in the walls of bigger veins and arteries were expressing αSMA **(Fig. 30 A)**. By the end of the fourth week post implantation most of the newly created vessels were positive for αSMA **(Fig. 30 B)**, and at the end of the experiment bigger vessels had well differentiated αSMA-positive, thick, muscular walls **(Fig. 30 C)**.

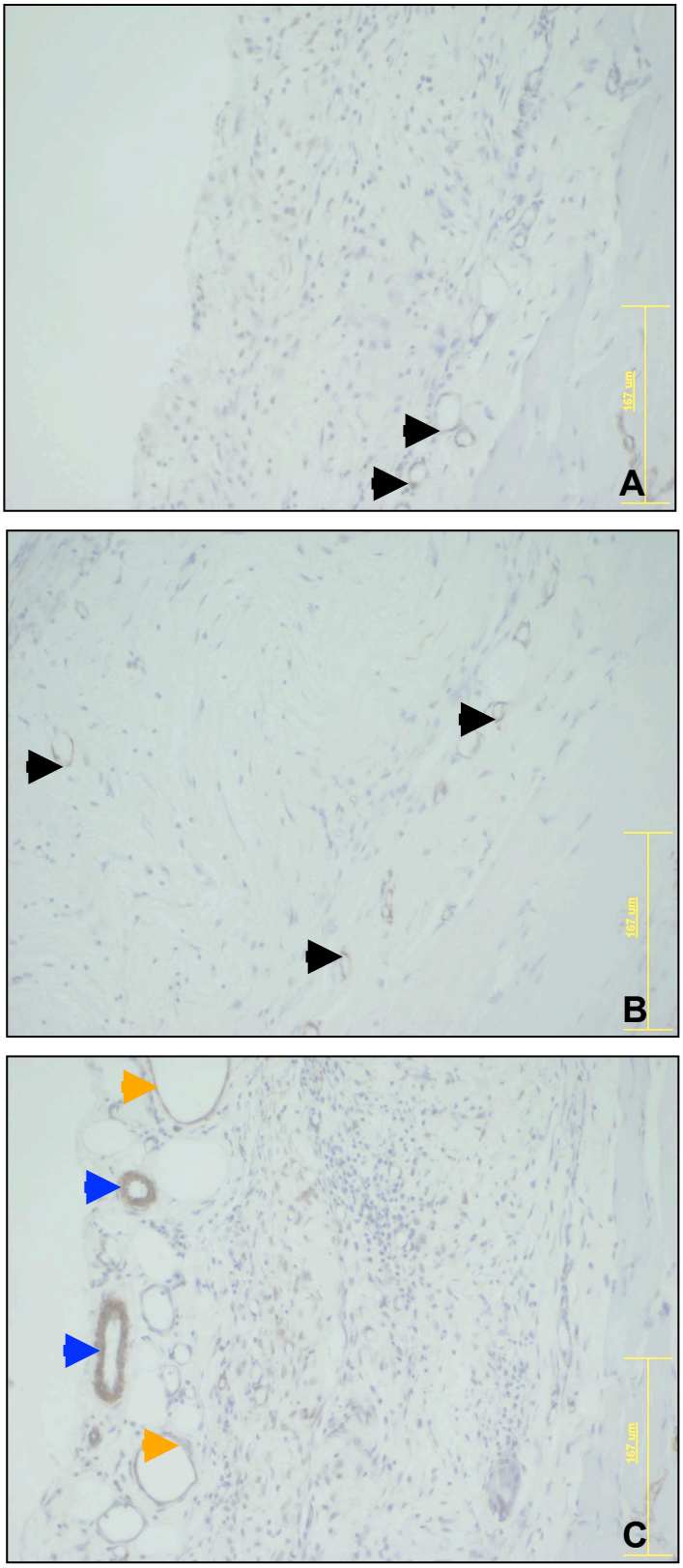


**Fig. 30** IHC staining of αSMA in grafts harvested two weeks (A), four weeks (B), and eight weeks (C) post-implantation; black arrows – brown-stained smooth muscle cells in neo-vessels, blue arrows – smooth muscle cells of arteries, yellow arrows – smooth muscle cells of veins. Yellow bar indicates the scale of the images.

As soon as two weeks post-implantation some of the cells lining the circumference of the neo-vessels were FVIII-positive. However, only eight-week old grafts expressed endothelial marker within full circumference of the vessels **(Fig. 31)**.

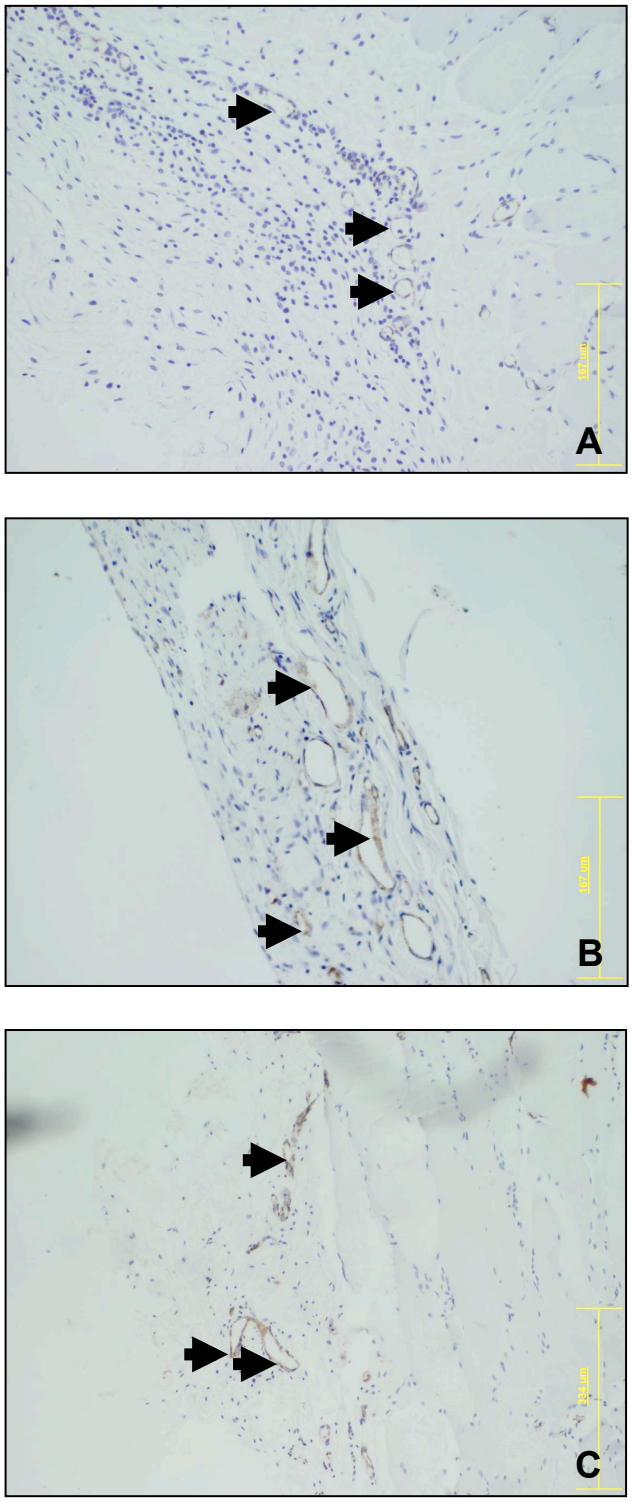


**Fig. 31** IHC staining of FVIII in grafts harvested two (A), four (B), and eight (C) weeks post-implantation; black arrows – brown-stained endothelial cells in neo-vessels. Yellow bar indicates the scale of the images.

Analyses of VEGF expression indicate that it is retained in the de-cellularised intestine **(Fig. 32)**. It has been shown in the grafts harvested at each time point with a visible time-related increase in staining intensity **(Fig. 33)**. What is more, the section of the grafts harvested two weeks after surgery show expression of VEGF that is not restricted to angiogenic activity (newly created, small vessels).

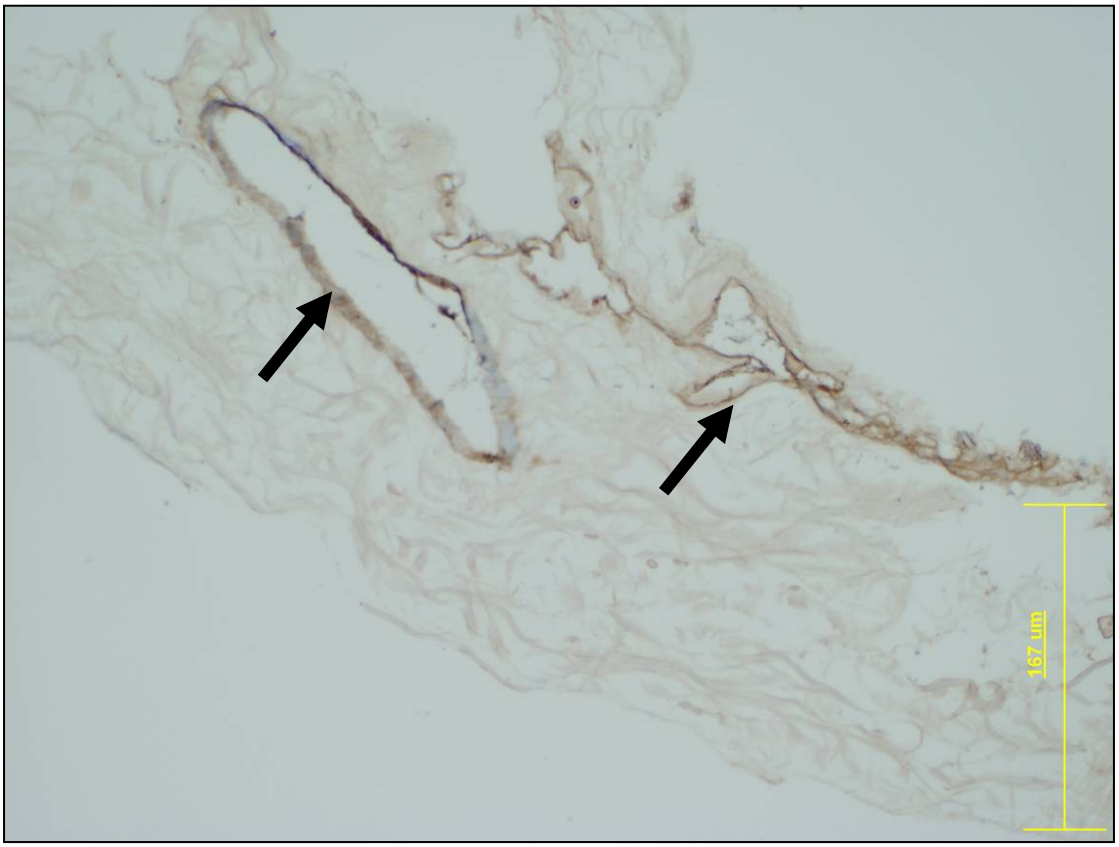


**Fig. 32** IHC staining of VEGF within de-cellularised intestinal blood vessels (arrows). Yellow bar indicates the scale of the image.

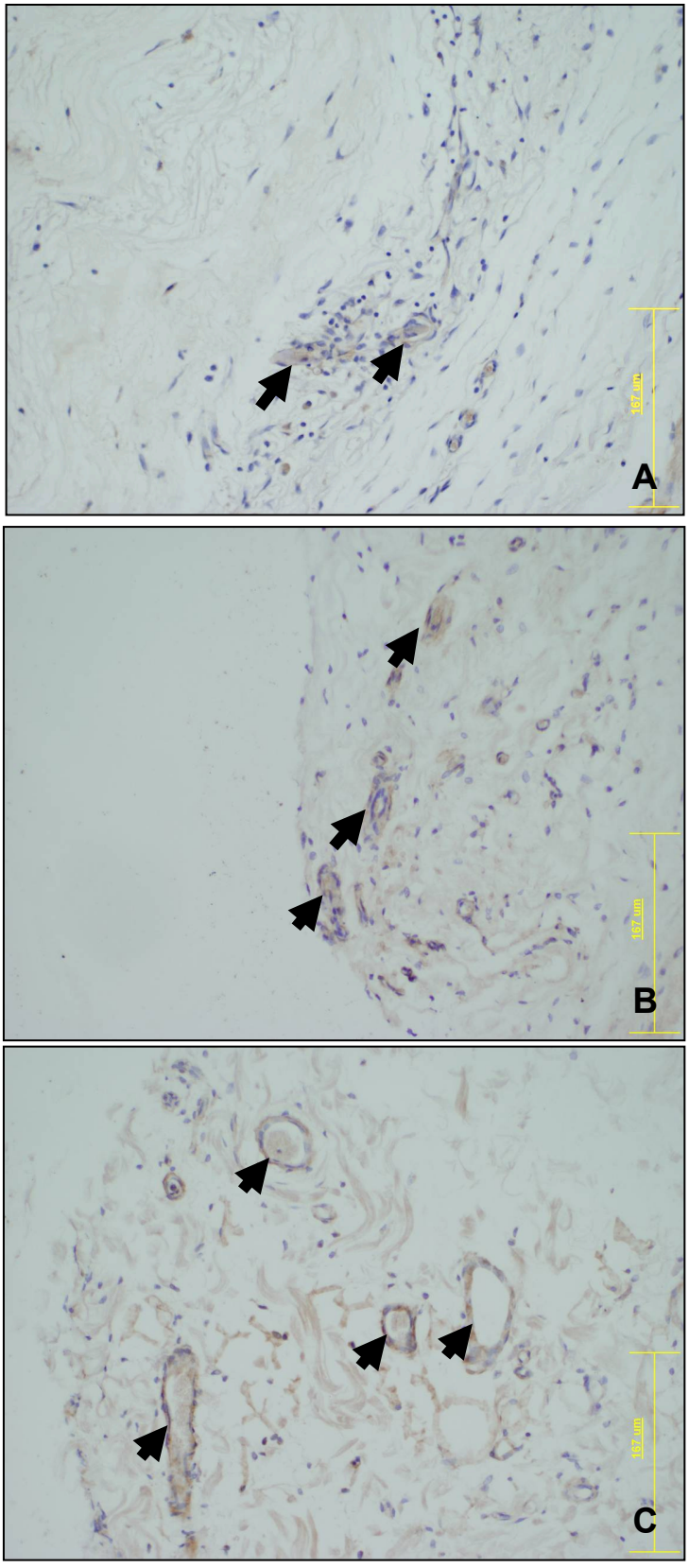


**Fig. 33** IHC staining of VEGF in grafts harvested two weeks (A), four weeks (B), and eight weeks (C) post-implantation; black arrows – brown-stained VEGF within neo-vessels. Yellow bar indicates scale of the images.

There were very few VEGF-R-positive cells in the grafts harvested two weeks after implantation. Their amount gradually increased with time. Four weeks post-surgery positive cells were randomly repopulating the scaffold. Some cells expressing the receptor were located on the lumenal surface of the blood vessels. After eight weeks, considerably high amounts of VEGF-R- positive cells were present mostly in the close proximity of the blood vessels, with some lining possible places of previous blood vessels **(Fig. 34)**.

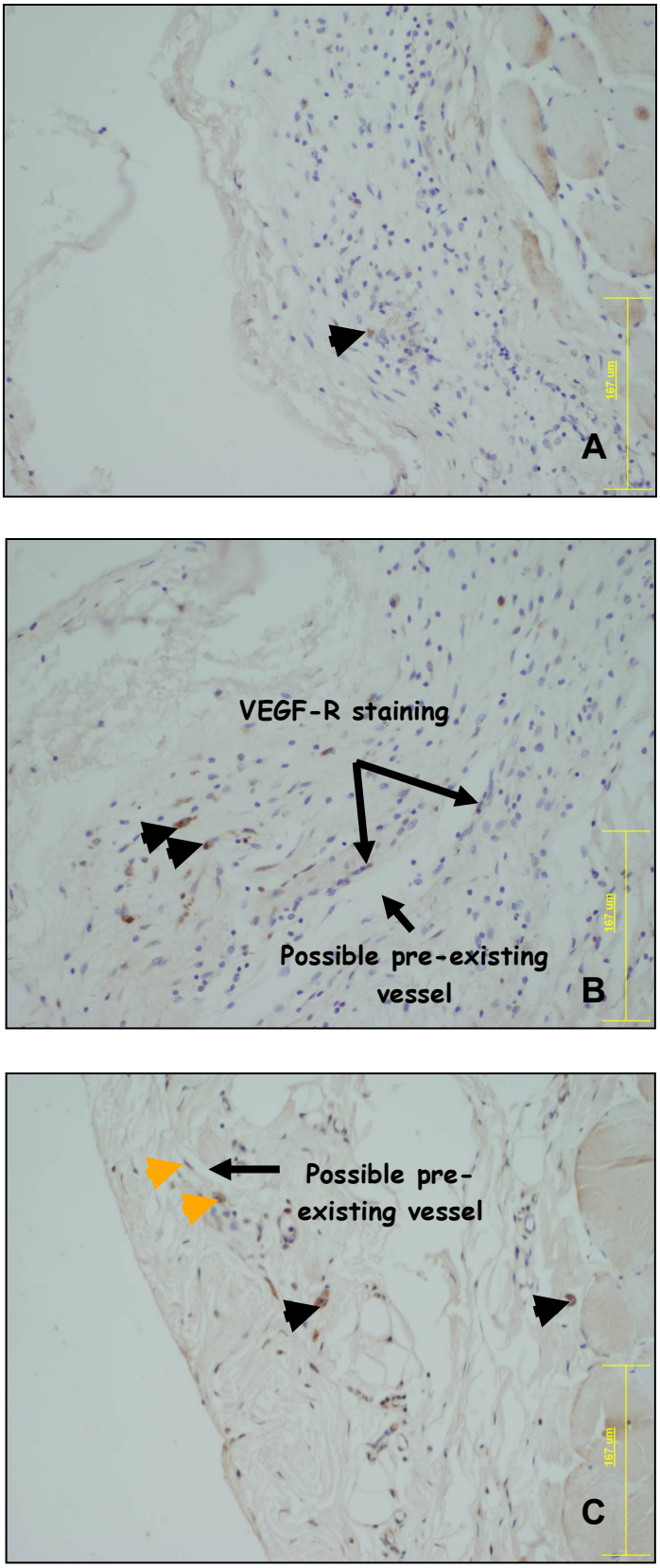


**Fig. 34** IHC staining of VEGF-R in grafts harvested two weeks (A), four weeks (B), and eight weeks (C) post-implantation; black arrows –VEGF-R -positive cells not associated with blood vessels, yellow arrows – VEGF-R-positive cells lining pre-existing vessels. Yellow bar indicates the scale of the images.

## 4.4. Discussion

ECM scaffolds are commonly used for reconstructive and regenerative applications in clinical and pre-clinical studies (62). Acellular intestinal matrix has been proven to provide smart remodelling which is an important prerequisite for tissue maturation and regeneration (151). When de-cellularised scaffold is implanted as a naturally occurring biopolymer, it stimulates angiogenesis, growth and differentiation of connective and epithelial tissue, as well as deposition, organization, and maturation of ECM components, which results in blocking cell-mediated contraction of the site and induces remodelling towards tissue in its natural physiological state (152).

Biocompatibility tests performed in rat model proved to induce angiogenesis, cellular infiltration and secretion of new ECM without inducing chronic immune response. This proved the possibility of using de-cellularised ileum as a potential scaffold in tissue engineering. It appeared to be non-immunogenic and served as a good matrix for cellular ingrowth. Implants were well tolerated and they induced much lower levels of inflammation or immune response than the implants presented in Chapter 2. As early as two weeks post-surgery all the implants were infiltrated with cells, which were distributed evenly within the implants (no 'empty' spaces could be seen) in all of the grafts at any time. H&E staining showed re-populating cells initially having characteristics of inflammatory cells (polymorphonuclear), but failed to induce chronic inflammation. Moreover, lack of fibrotic encapsulation or scar tissue formation suggests that any foreign body reaction had resolved. The above result proves that even though the scaffold contained traces of DNA material, its amount was below the threshold needed to stimulate a foreign body reaction, or DNA was degraded during first two weeks post-implantation.

Non-cross-linked ECM-scaffolds were described as completely absorbable (153), however the graft could be well-distinguished from surrounding tissue up to two months post-implantation. The collagen analysis showed that collagen at the edges of the grafts (thin green fibres) undergoes gradual degradation. However, its rate gives the re-populating cells enough time to produce new ECM, indicated by depositions of thin, green collagen in the centre of the two-week-old grafts. New fibres gradually mature, which is shown by bright orange-to-red colours of Picro Sirius stained collagen at eight weeks post-implantation.

Most of the cells were proliferating, and some of them started to appear within acellular nerves or ganglions. Their morphology resembled that of nervous tissue; however, they were not positive neural markers (S-100). In explants harvested at each time point spontaneous angiogenesis was taking place, which could have been a factor that limited the immune reaction. Within a few weeks most of the new vessels developed endothelial lining (positive for F VIII), and a well-defined vascular wall containing elastin and expressing smooth muscle markers (αSMA). Analysis of VEGF showed that de-cellularised matrix retained VEGF, which could be one of the reasons why remodelled material promotes such rapid angiogenic ingrowth. VEGF expression in the grafts harvested at the two-week time point was not associated with the existing blood vessels and there were hardly any VEGF-R-positive cells. It could indicate that 'unrelated' staining was in fact residual VEGF remaining in the tissue after de-cellularisation. Moreover, some of the VEGF and VEGF-R expression was centred at the possible pre-existing vessels of the scaffold, which may suggest that internal cues and retained functional proteins directed the neo-vascularisation of the grafts. There is a positive correlation between the amount of retained ECM GAG's and VEGF expressed in a scaffold (154). Therefore, the presence of VEGF expression within the

de-cellularised ileum proves that the method of de-cellularisation described in the previous chapter allows retention of the sufficient amounts of GAG's to guarantee some of the bioactive function of the ECM. VEGF is crucial for neo-vascularisation of grafts. Post-implantation blood vessels permeability to cells and macromolecules within the scaffold increases. This causes coagulation, enabling platelets to disintegrate and shed their contents, among which are several inflammatory mediators such as VEGF. In response to this chemotactic factors neutrophils, followed by macrophages migrate towards the site of angiogenesis. At the same time, angiogenic factors that were released by platelets and secreted by attracted cells stimulate local vascularisation. However, if the scaffold is not supplied with VEGF in the first place that initial attraction by the cells and macromolecules does not take place. Therefore, biomaterials that do not express growth factors are often less compatible and do not promote cellularisation and angiogenesis as efficiently as the biological matrices (155). The fact that the de-cellularisation process preserved VEGF in the scaffold is the reason of immediate blood vessel penetration of the matrix. Time-related increase in VEGF expression was caused by intensive platelet deposition and infiltration of cells expressing VEGF-R (endothelial cells, fibroblasts, keratinocytes, macrophages, mast cells, platelet and polymorphic neutrophils), first in the part of the grafts adjoining native muscle and later in other parts. In synthetic scaffolds loaded with VEGF, the expression of the growth factors is difficult to control. This is because too much VEGF alone leads to immature, leaky vessels (156). This problem is non-existent when ECM scaffolds are used, where release of molecules is gradual and occurs in the same manner as in native tissues.

*In vivo* routes and origin of new vessels within the acellular tissues will never be described, unless a method of permanent labelling of the de-cellularised blood

vessels is discovered. Nevertheless, careful histological examination can promote some ideas. The above studies seem to show that most of the neo-vascularisation happens in the close proximity of the recipient tissue, with adjoining vessels growing into the scaffold. However, there are some cells that line the pre-existing conduits. Examination of these cells is most exciting as it proves that the concept of using ECM scaffolds extends far beyond them being only natural, non-toxic biopolymers with pre-loaded biomolecules. The fact that the direction and differentiation of the cells re-populating ECM scaffolds can be directed towards the tissue of origin is very exciting in the field of bio-engineering, but yet it remains to be proven.

Biocompatibility within human body of acellular ileum can not directly be assured by the above results (namely the immunologic differences between human and rat). However, the method presented in the previous chapter show that it is possible to produce scaffold that is well tolerated in rat model and promotes smart remodelling in contrast to being immunologically rejected. These properties are key factors and requirements when designing a scaffold for tissue engineering application.

# Chapter 5.

# Stereological analysis of scaffold performance *in vivo*

## *5.1. Background and aims*

A stereological approach can provide an objective unbiased assessment of structural changes in biological systems. In this chapter stereological analysis was incorporated to assess time related changes of biological activity within the implanted scaffold. The focus was on host tissue infiltration, immunological active cell numbers and changes of the volume of porcine de-cellularised ileum implanted subcutaneously into the rat recipients. As research in the field of tissue engineering progresses, and new scaffolds continue to be manufactured it is essential to develop an unbiased analytical method of *in vivo* performance.

### 5.1.1. Concept of unbiased stereology

Stereology was developed to describe the methodologies that allowed access to 3D information about biological (or other geometrical) structures based upon observation made on 2D sections (157). In stereology, quantification is considered the objective method to describe a structure, compare two structures, study structural change and relate the structure to the function. Stereological probes such as the dissector can provide unbiased estimates of numerical density and if volume is known

estimates of total numbers within an object. A stereology-compatible sample must be representative of the entire structure (158). Unbiased sampling procedures must also be applied uniformly at every stage of tissue processing, sectioning and selecting of fields of view. A test-system needs to be superimposed onto an image before counting, so that a stereological formula can be subsequently applied (159). Thus, unbiased samples (sections) were mounted on the histological slides and analysed using stereological parameters.

Subsequently, the challenge faced is determining which stereological parameter is relevant to the particular question being asked. The stereological parameters fall into two categories. These are absolute: volume, surface area, length and number (e.g. number of neurons in rat brain) or relative: volume density, surface density and number density (e.g. number of neurons per cubic millimetre) (160).

#### *5.1.1.1. Absolute volume*

The 'safest' (allowing the best interpretation of the results) method that could be applied for the analysis of the porcine scaffolds implanted subcutaneously into rats (explants described in chapter 4) was estimation of absolute numbers of certain cells per implant. The absolute volume was measured to check if the implanted ECM scaffolds shrank within eight weeks post-surgery, as well as to obtain a reference parameter for absolute number analysis.

The absolute volume of an explant can be calculated by weight and specific gravity or by liquid displacement using the Archimedes' Principle (161). However this method cannot be applied to tissues that can not displace water after immersion (lungs), are too small (blood capillaries) or are trapped/attached to other structures (brain cortex). In such cases, volume can be estimated using Cavalieri's Principle,

which states: "the volume of an arbitrary shaped object can be estimated in an unbiased manner from the product of the distance between planes and the sum of the areas on systematic random parallel sections through the object" (162). This means that the scaffold needed to be serially sectioned at known distances (*T*), parallel to an originally randomly chosen section (in an interval *0*-*T*) plane **(Fig. 35)**. Only one face of each section can be measured and the areas ($A_i$) are determined by point counting (161).

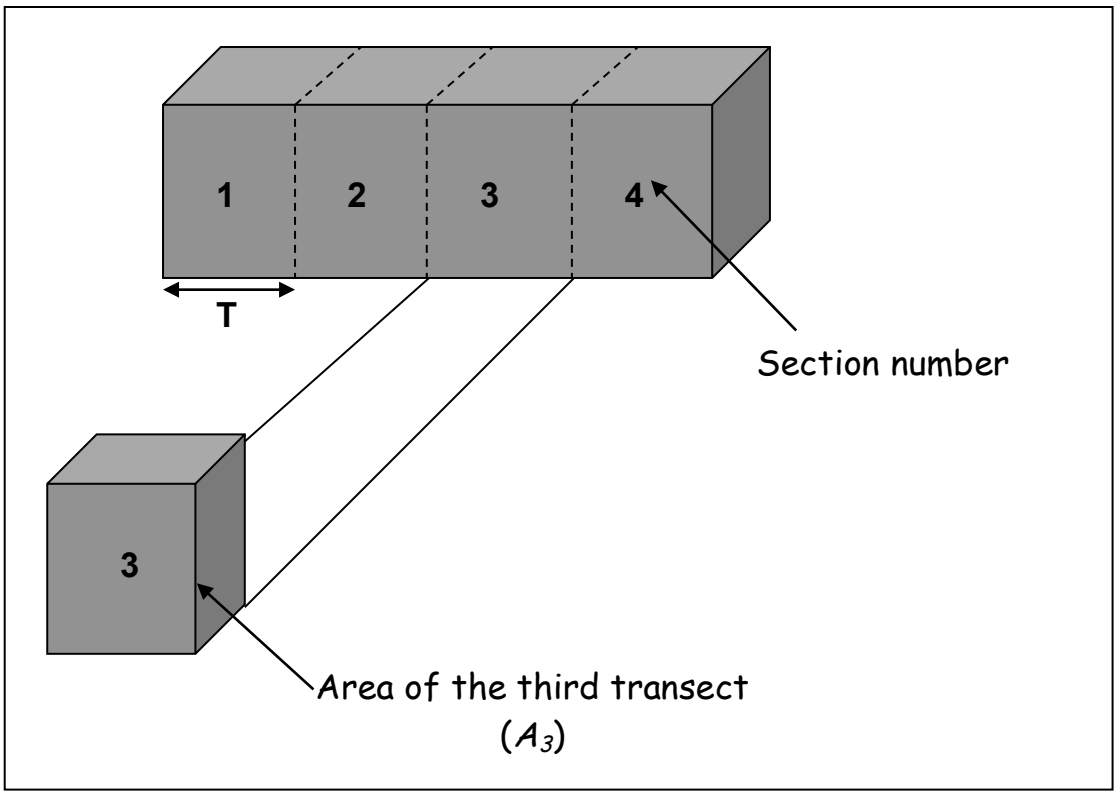


**Fig. 35** Cavalieri's Principle; The absolute volume can be calculated by the product of the distance between planes (*T*) and the sum of the areas ($A_i$) on systematic random sections through the object.

The volume of the object is estimated by summing the areas and multiplying by the slice thickness:

$$V = (TA_1) + (TA_2) + \ldots + (TA_m) = T\sum_{i=1}^{m} A_i$$

In point counting, a suitable test system is placed on the image and the area occupied by the object is measured by counting the points that fall onto the object (*P*). Given random positioning of the array, the total number of points, which falls on the profiles (slices of the scaffold) provides an unbiased estimate of their total area. The exact relation is:

$$A_i = \sum Pa(p)$$

where *a(p)* is the area equivalent of one test point (area associated with the point). Therefore the absolute volume of an object can be calculated:

$$V = Ta(p) \sum_{i=1}^{m} P_i$$

The application of the above equation will give an unbiased estimation of the scaffold's absolute volume, irrespective of the shape and of cutting direction (161). Only four to eight systematic sections can guarantee a coefficient error of the estimate of about 5-10% when using the Cavalieri's estimator (163).

#### *5.1.1.2. Number density*

Number is a dimensionless entity. Thus, when counting objects, the smallest unique feature that is readily identifiable (e.g. nucleus when counting *Eucaryota* cells) should be used (164). However, that object could be present in more than one section if the sections are thin enough (160). Conventional object counting of each slide will result in an overestimation. Stereology provides the solutions to the problem. One of

them is the optical brick method which was used to perform analysis of the implanted scaffolds.

#### 5.1.1.2.1. The optical brick

The optical brick has been created to prevent overestimation of particle counting. It relies on the optical section 'scanning' method which increases the practical efficiency of counting object numbers. Using light microscopy, 'optical sections' can be continuously scanned, which provides a direct count (160). In practice, the microscopical plane of focus is moved up and down within one thick section (15-30 μm) of the object. The microscope used for number analysis should be fitted with the microcator, which is used to measure depth in the *z* direction (the optical axis of the microscope) by the microscope stage. In light microscopy, the highest numerical aperture lens should be used as this provides the thinnest possible optical section. A depth of focus of approximately 0.5μm can be achieved using oil immersion lens (x 100) and a condenser. When applied to a thick histological section only a thin slice of the section is in focus, which in practice means that the objects appear and disappear as the section is focused through (160).

#### 5.1.1.2.2. Unbiased counting rule

The objects are counted on the basis of the unbiased counting rule, using an unbiased 'brick', rather than by a 2D unbiased counting frame. The unbiased brick is generated be moving an unbiased counting frame through the thick histological section of an object. It consists of three acceptance planes and five forbidden surfaces **(Fig. 36)**. The particles (e.g. nuclei) are counted if they are within the counting frame and do not intersect any of the forbidden planes **(Fig. 37)** (160).

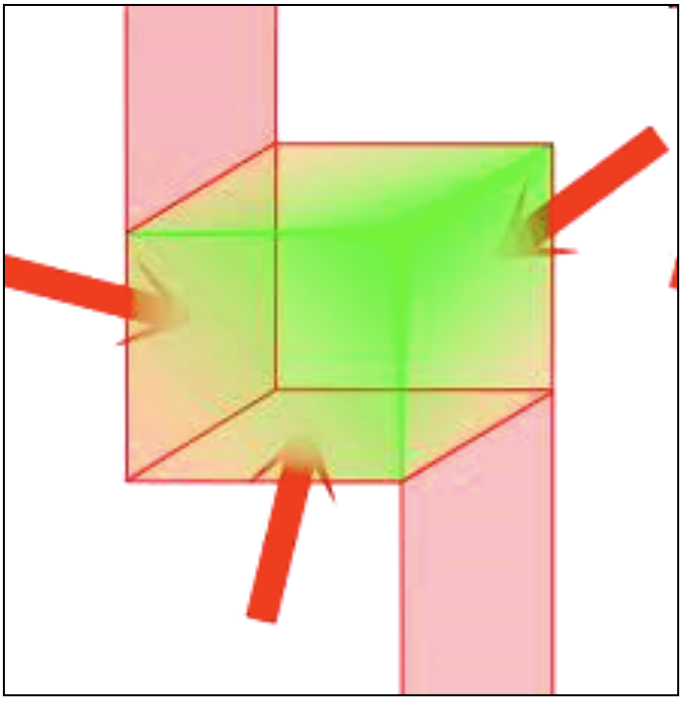

**Fig. 36** A schematic illustration of the unbiased brick. The brick consists of the central volume, bounded by three acceptance surfaces (green), and five forbidden planes (red). http://www.stereology.info/optical-disector-unbiased-brick/

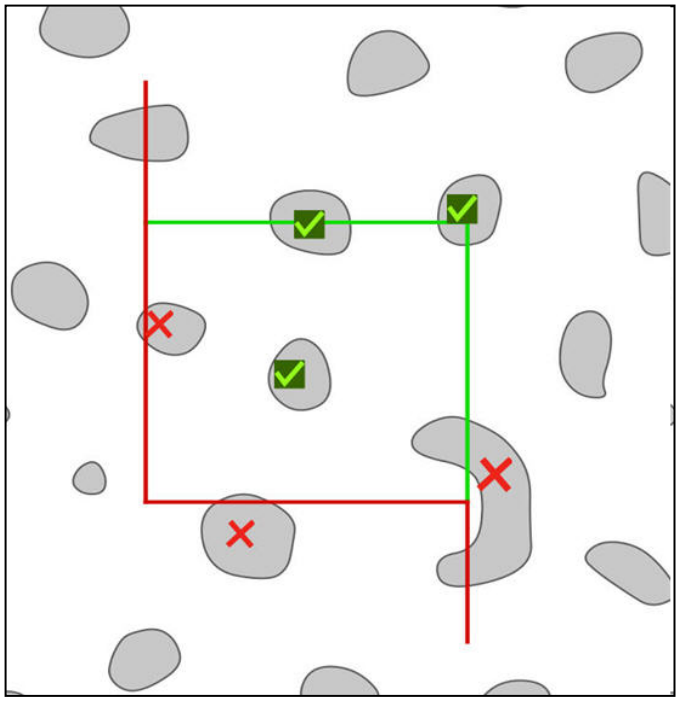

**Fig. 37** A schematic illustration of the unbiased counting rule. The unbiased counting frame consists of a red forbidden and green acceptance line. Objects falling inside the frame or intersect the acceptance line are counted (green ticks). Particles touching the forbidden lines are not counted (red crosses). http://www.stereology.info/criteria-for-counting-cells

In practice, the unbiased counting brick is superimposed onto a thick section and the microcator is set to zero. The section is scanned downwards at a defined distance (optical dissector height). It is important to count the objects only within the unbiased counting brick when they are in their maximal focus. Only then they are recorded as 'new events' and counted.

Numerical density ($N_v$) can be estimated by dividing the total number of objects counted ($\sum Q$) by the number of the dissector ($\sum P$) multiplied by the dissector volume. The dissector volume is obtained by multiplying the area of the unbiased counting brick ($A_f$) by the optical dissector height ($h$). Thus, a number per unit volume is obtained:

$$N_v = \frac{\sum Q^-}{\sum P(A_f h)}$$

#### *5.1.1.3. Absolute number*

The absolute number of objects ($N_{TOT}$) within the reference parameter (e.g. absolute volume) can be estimated by multiplying numerical density ($N_v$) by the absolute volume ($V$) of the object of interest (e.g. scaffold).

$$N_{TOT} = N_v V$$

#### *5.1.1.4. Coefficient of Error*

The efficiency of the stereological methods incorporated into analysis of an object can be defined by calculating the Coefficient of Error ($CE$) for each step (volume estimation and density estimation).

Volume $CE$ is obtained:

$$CE_V = \frac{\sqrt{3\sum(P_iP_i) + \sum(P_iP_{i+1}) - 4\sum(P_iP_{i=2)})/12}}{\sum P_i}$$

where *Pi* stands for the number of points within the object.

Numerical density *CE* is obtained:

$$CE_{(N_v)} = \sqrt{\frac{n}{n-1}\left[\frac{\sum(Q^-)^2}{\sum Q^- \sum Q^-} + \frac{\sum(P)^2}{\sum P \sum P} - \frac{2\sum(Q^-P)}{\sum Q^- \sum P}\right]}$$

where *n* is the number of section of an object, *P* is the total number of dissectors within the object and *Q* is the total number of the particles counted per object (160).

### 5.1.2. Macrophage phenotype as a determinant of biologic scaffold remodeling.

Quantification of inflammatory cells in terms of presence/absence and time frame of occurrence indicates the nature of inflammatory reaction and scaffold integration (164). Macrophages are critical antigen presenting cells that play pivotal roles in host responses to biomaterial implants. The control of macrophage phenotypic balance from proinflammatory M1 to reparative M2 (described in Chapter 1) is a goal of investigators to optimize the host response to scaffolds for tissue engineering purposes (165). The processing method used during the manufacturing of a biologic scaffold, tissue source and species of origin can have a profound influence upon the macrophage phenotype profile and downstream remodeling events (166). Biomaterials directly influence innate and adaptive immune cell adhesion, reactive

oxygen intermediate production, cytokine secretion, nuclear factor-kappa B nuclear translocation, gene expression, and cell surface markers, all of which are likely to affect allogeneic rejection or acceptance responses (167). Routine histological examination alone is inadequate to determine the phenotype of mononuclear cells that participate in the host response to the scaffold.

The presence of large numbers of macrophages in the tissue and their multinucleate giant-cells counterpart is one of the hallmarks of chronic inflammation. Typically, the host inflammatory response to an implanted biomaterial followed a predictable sequence of events, which resulted in foreign body reaction and fibrosis. That was before phenotypic and functional polarization of the mononuclear phagocyte cell population was described (59). The M1 (pro-inflammatory) and M2 (immunoregulatory) phenotypes of macrophages gave a new insight into immune activity in the acute phase of host response to biomaterials. Further investigations proved that although morphologically indistinguishable, mononuclear macrophages from these two pathways can be identified and differentiated according to their cell surface markers and their cytokine and gene expression profiles (60).

Macrophages are a plastic cell population capable of changing sequentially their polarization in response to local stimuli during the process of wound healing (168). These stimuli can originate from other cells infiltrating the scaffold, microbial or toxic agents, biomaterial epitopes and its degradation products (169). The effects of macrophage phenotype upon the tissue-remodeling outcome following the implantation of a biomaterial are largely unknown, but recognition of the predominant phenotypic profile may provide a tool by which a constructive and functional tissue remodeling outcome can be predicted and/or promoted.

The objective of the experiments presented in this chapter was to examine the changes of the macrophage phenotype within the first eight weeks post-implantation of a porcine de-cellularised scaffold into a rat recipient. Moreover, using stereological analysis it was possible to quantify the cellular infiltration of the implants with not only macrophages but also other cells. The changes of ratio of M1 and M2 macrophages within implanted scaffold in a time related manner have been proven to predict the biomaterial's fate *in vivo* (166). The objective of this chapter was to show this changes of M2/M1 ratio, which in case of significant increase could suggest that there is a documented somewhere else chance for smart remodelling and positive long-term outcome. The aim was to show if the de-cellularised intestine can induce better than described negative controls (cross-linked matrices inducing long-term rejection) and show similar pattern of residual macrophages populations to positive control (autologous tissue) *in vivo*. Quantitative data in existing reports is based on straightforward counting in 2D of M1 and M2 macrophages within fields of microscopical view, which is linked to assumptions which are highly biased and therefore difficult to interpret.

## *5.2. Methodology*

### 5.2.1. Materials

The list of materials and equipment used in experiments described in this chapter is presented in **Appendix 4**.

## 5.2.2. Animal husbandry

All animals were maintained and handled similarly to the procedure presented in Chapter 2 (2.2.2).

## 5.2.3. Tissue slides preparation

The blocks of tissue harvested two, four and eight weeks post-implantation (Chapter 4) were measured and cut into four equal segments **(Fig. 37)**. Tissue was processed and prepared for histological staining in the way described in sub-chapter 3.2.6.2. The blocks embedded in wax were cut into 15 μm (sections undergoing staining for chemokine receptor 7: CCR7 antigens) or 25μm (sections undergoing staining for CD68 and CD163 antigens) thick histological sections and mounted onto 5% APTS-covered slides.

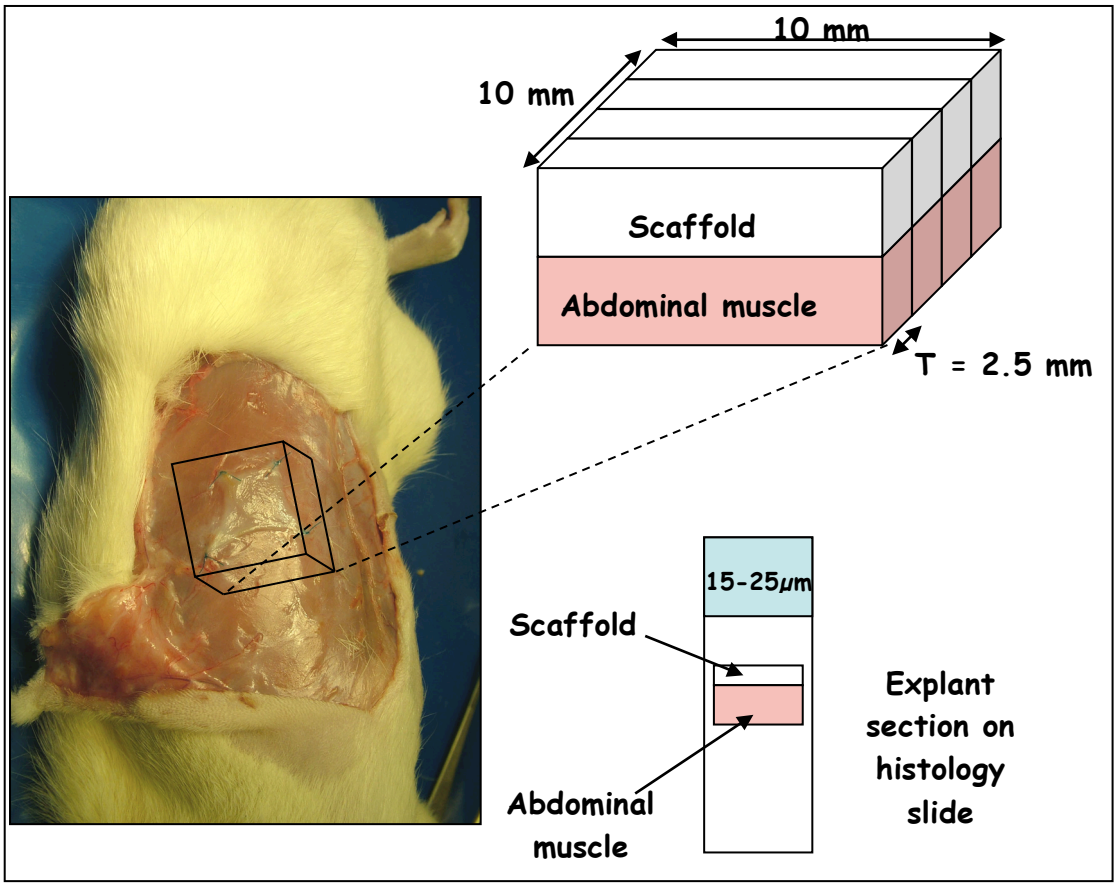


**Fig. 38** A schematic illustration of the scaffold explantation eight weeks post-surgery and preparation of sections for stereological analysis. The scaffold was resected with underlying abdominal muscle and the blocks of tissue were cut into four equal segments, each measuring ~2.5mm (length) and 10 mm (width). The segments were embedded in wax facing longer (10mm) side.

## 5.2.4. Immunohistochemistry

The staining was performed in a way described in sub-chapter 3.2.6.3. IHC-staining was optimized using first the control tissue (rat spleen) and then 5µm thick sections of the test tissue (explants). The optimal protocols used for IHC staining are described in **Appendix 9**, **Table 8.** Sections were stained with CD68 (pan macrophage marker), CCR7 (M1 profile marker) and CD163 (M2 profile marker). The optimal protocol for CCR7-labelling involved the use of harsh antigen retrieval treatment. 25µm thick sections were not resistant to high temperature exposure and the sections did not remain attached to the slide. Thus, thinner (15 µm) sections were cut and stained with CCR7 antibodies.

Prior to stereological quantification each section was analysed for its precise thickness using microcator, the antibody penetration of its whole thickness and length. Sections with average thickness less than 15μm, which showed incomplete penetration of the antibodies or any damage of the stained tissue were re-cut and re-stained.

### 5.2.5. Stereological quantification of changes of scaffold volumes *in vivo*

The volume of the scaffold pre-implantation was calculated based on their measurements. The volumes of the scaffolds harvested at each time point were estimated according to Cavalieri's principle. The areas were estimated using microfiche reader superimposed with a grid of quadratic points calibrated using a microscopic grid, and *a(p)* was calculated. $A_i$ of each explant were estimated in single H&E stained sections of each segment of each subdivided into four scaffolds ($T$ = 2.5 mm), counting and summing the points interposed on each of them ($P_i$). The absolute volumes of explanted scaffolds were then calculated considering their total length of 10mm. *CE* of the estimates was calculated.

### 5.2.6. Stereological quantification of cellular infiltration, macrophages content and M1/M2 ratio within scaffold implanted into rat recipients

The numerical densities of cells infiltrating the scaffold, staining positively for CD68, CD163 and CCR7 were estimated using a 3D stereological technique. Sections were viewed at a microscope magnification of 1000 (oil immersion lens). An unbiased

counting frame (60% of the image total area) generated by a digital software package (Kinetic Imaging Stereology 5.0) was projected onto IHC-stained image. Each image was brought into maximum focus of the first nucleus and the microcator was zeroed. The unbiased optical brick technique was used for the estimation of positive and negative for the appropriate macrophage marker cell densities. All nuclei seen in maximum focus at their largest diameter and contained within unbiased counting frame and defined brick depth of 15 μm were counted, starting at the top left corner and following a tessellating pattern of 3mm (optimized in pilot study). For each slide 13 optical bricks were sampled and the number of negative and positive for each marker cells was recorded. This ensured that for a single scaffold 52 unbiased optical bricks were sampled.

Total number of negative CD68+, CD163+ and CCR7+ cells within each scaffold was estimated by multiplying the volume of each scaffold with the numerical density. M2/M1 ratio changes in time post-implantation were also estimated.

## 5.2.6. Statistical analysis

All continuous data was expressed as the mean ± Standard Error of the Mean (SEM) and $p<0.05$ was taken as significant. $p$ values were estimated using two-way ANOVA with post hoc Tukey intergroup comparison, and all computations were performed using GraphPad Prism 4 and Microsoft Office Excel software.

## 5.3. Results

### 5.3.1. Stereological quantification of changes of scaffold volumes *in vivo*

The volumes of scaffold pre-implantation are as follows [$mm^3$]: 720, 680, 600, 590, 600, 640, 650, 650, 670, 800, 550, 570, 600, 640, 580, 680, 700 and 600. This gave mean volume of 640 $mm^3$ (STDEV=62.02 $mm^3$). The estimated volumes of each explanted scaffold along with CE values are shown in **Table 14 (Appendix 13).** Pooled data from each of the three harvests (two, four and eight weeks after subcutaneous implantation) are shown in **Table 15.**

**Table 15.** Estimated average volumes of the scaffolds explanted at each time point post-implantation.

| *Time post-implantation [week]* | *Mean Volume [$mm^3$]* | *STDEV* |
|---|---|---|
| 2 | 561.6 | 120.5 |
| 4 | 632.3 | 137.3 |
| 8 | 659.7 | 97.28 |

Statistical analysis showed no significant changes ($p$>0.05) in scaffold volume at any time point **(Fig. 39)**. There was no implant shrinkage even after eight weeks post-surgery, with mean volume oscillating around value of 600$mm^3$ (640, 561.6, 632.3 and 659.7 $mm^3$) at any given time.

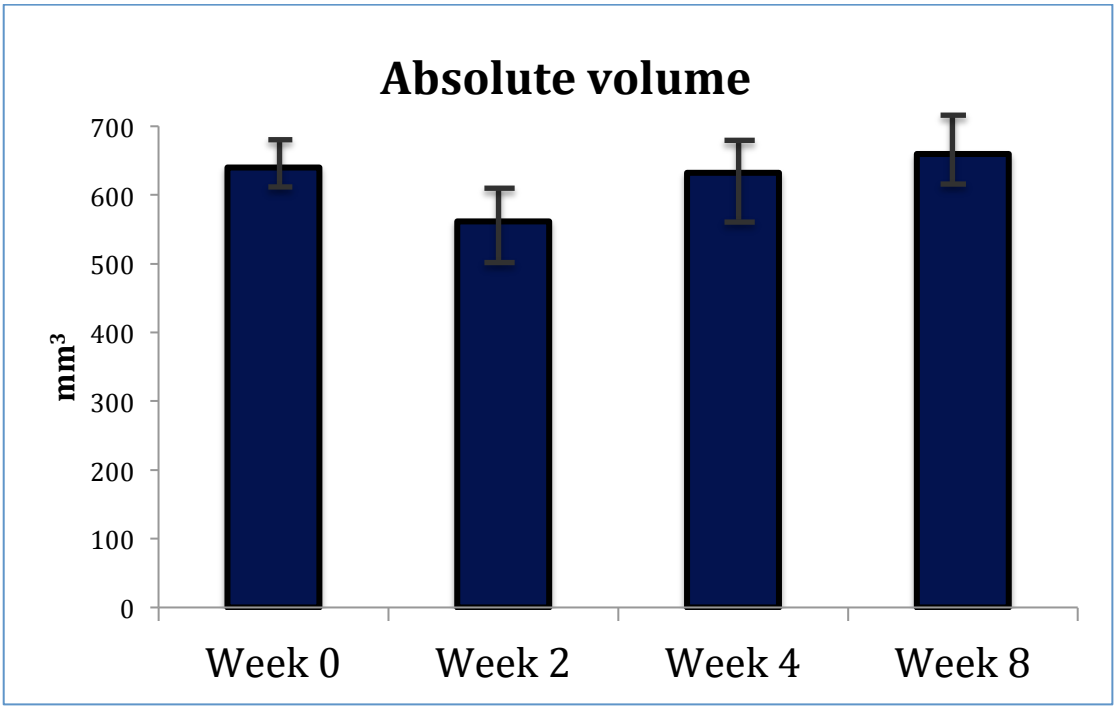


**Fig. 39** Estimated volumes of scaffolds pre-implantation (week 0) and at 2, 4, and 8 weeks post-implantation into rodent recipient. No significant difference could be seen between any of the columns.

## 5.3.2. Stereological quantification of cellular infiltration, macrophages content and M1/M2 ratio within scaffold implanted into rat recipients

The densities of negative, and positive CD68, CD163 and CCR7 cells were estimated. Along with CE are presented in **Table 16 (Appendix 14).** The total numbers of negative and positive for CD68, CD163 and CCR7 cells within each of the scaffold are presented in **Table 17 (Appendix 15).** Pooled data from each of the three harvests (two, four and eight weeks after subcutaneous implantation) are shown in **Table 18.**

**Table 18.** Average total number of cells, pan, M1 and M2 macrophages within the scaffolds explanted at each time point post-implantation.

| Time post-implantation [week] | Mean Total Cells $N_{TOT}$ | STDEV | Mean CD68 $N_{TOT}$ | STDEV | Mean CD163 $N_{TOT}$ | STDEV | Mean CCR7 $N_{TOT}$ | STDEV |
|---|---|---|---|---|---|---|---|---|
| 2 | 9.69 E-10 | 2.37 E-10 | 3.92 E-10 | 1.00 E-10 | 1.29 E-10 | 4.22 E-11 | 1.36 E-10 | 4.44 E-11 |
| 4 | 8.15 E-10 | 1.36 E-10 | 3.3 E-10 | 1.1 E-10 | 9.88 E-11 | 2.82 E-11 | 9.03 E-11 | 1.86 E-11 |
| 8 | 8.56 E-10 | 1.08 E-10 | 3.19 E-10 | 3.38 E-11 | 1.35 E-10 | 1.24 E-11 | 4.25 E-11 | 2.36 E-12 |

Two-way ANOVA analysis proved there was no significant difference at two, four or eight weeks post-implantation ($p>0.05$) in the total numbers of cells infiltrating the scaffold, number of pan macrophages or M2 macrophages within the scaffold **(Fig. 40)**. However, the total number of CCR7+ cells decreased significantly after four ($p<0.05$) and eight ($p<0.001$) weeks comparing to the number of CCR7+ cells within the scaffold at two weeks post-implantation. There was also statistically significant drop in total number of CCR7+ macrophages within the scaffold between fourth and eight week *in vivo* ($p<0.05$) The total number of CD163+ showed some trend towards increase, but this was not statistically significant difference.

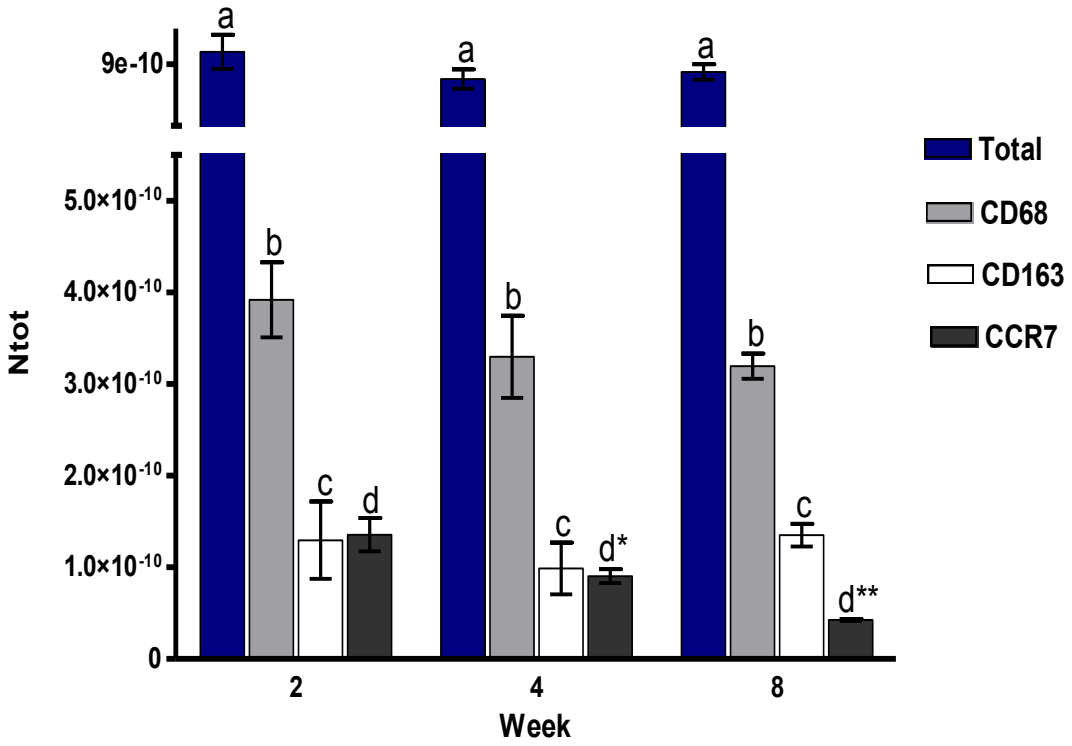


**Fig. 40** Estimated total numbers of cells within explanted scaffolds at 2, 4, and 8 weeks post-implantation into rodent recipient. No significant difference could be seen between total numbers of cells infiltrating the scaffolds, pan and M2 macrophages at any given time point. There was a significant drop in total number of M1 macrophages both at four (*) and eight (**) weeks post-implantation.

At every time point there was a significant difference ($p$<0.001) between number of total cells having infiltrated the scaffold and CD68+ cells, CD163+ cells and CCR7+ cells. There was also significant difference between the number of pan macrophages and CD163+ cells at two and four *(*$p$<0.001*)* as well as eight weeks post-implantation *(*$p$<0.01*)*. $p$ value < 0.001 was constant for difference in the number of pan macrophages and CCR7+ cells at all three time points. There was no significant difference in the number of CCR7+ and CD163+ macrophages at two and four weeks *in vivo* ($p$>0.05)**.** However, at eight weeks post-implantation the number of CCR+ cells was significantly lower ($p$<0.05) than the number of CD163+ cells within the scaffold **(Fig. 41)**.

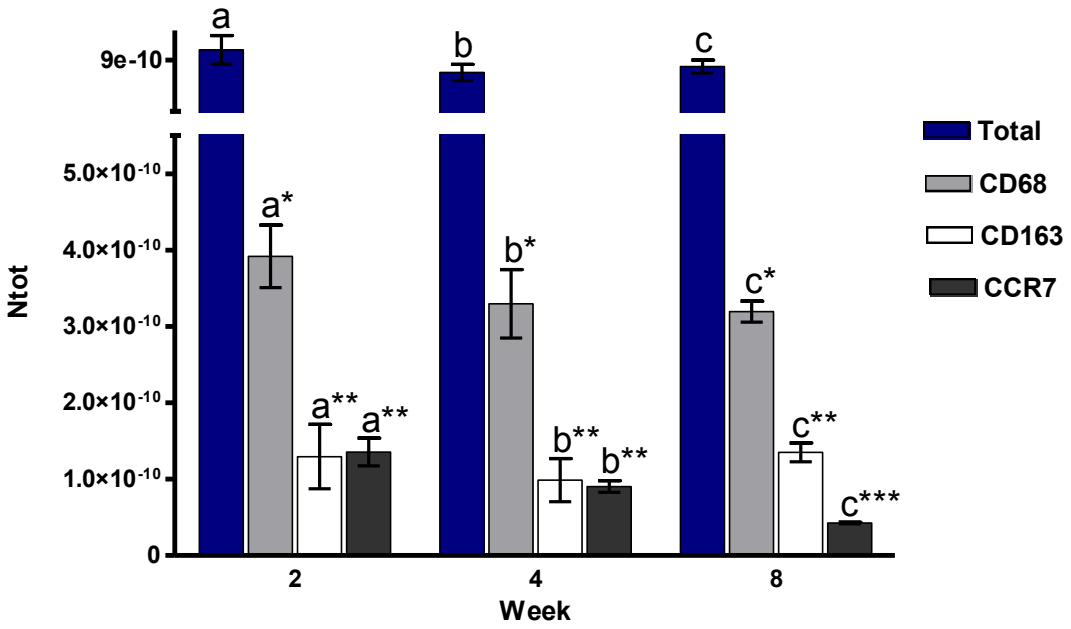


**Fig. 41** Estimated total numbers of cells within explanted scaffolds at 2, 4, and 8 weeks post-implantation into rodent recipient. Significant difference could be seen between total numbers of cells infiltrating the scaffolds and CD68+ (a-c vice a*-c*), CD163+ and CCR7+ (a-c vice a**-c**) cells at any given time point. There was also a significant difference between number of pan and M1 or M2 macrophages at any given time (a-c* vice a-c**). There was no significant difference in number of CD163+ and CCR7+ cells at two or four weeks (a**-b**). However, there was a significant drop of CCR7+ in relation to CD163+ cells at eight weeks post-implantation (c** vice c***).

The changes of ratio of M2/M1 macrophages confirmed that the switch from pro-inflammatory to pro-remodeling phenotype occurred eight weeks post-implantation when ratio of M1/M2 total numbers significantly increased ($p<0.01$) from 1.1 to 3.2 **(Fig. 42)**.

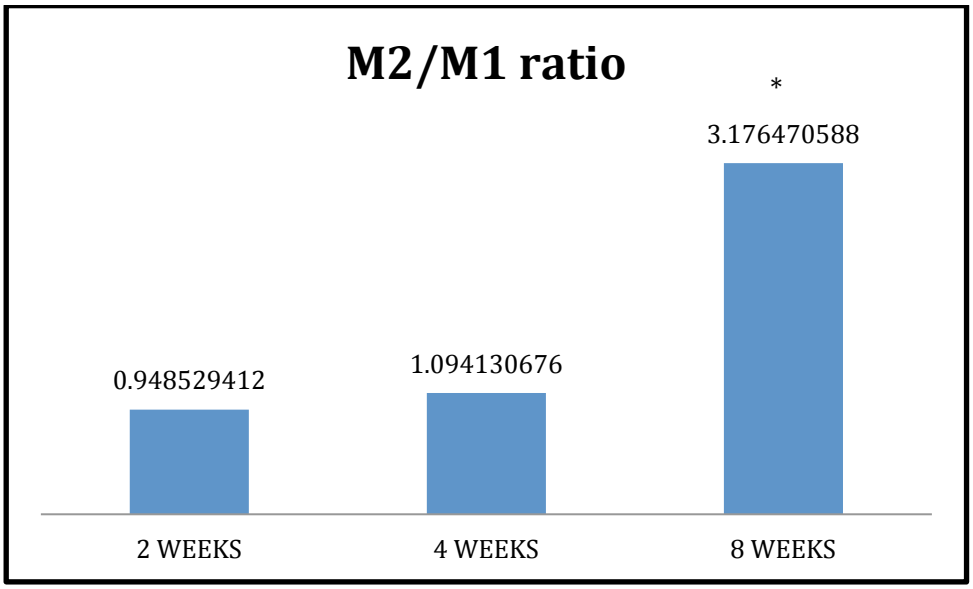


**Fig. 42** Changes of M2/M1 macrophages ratio, showing significant ($p<0.01$) increase at eight weeks post implantation into rat recipient showing switch from pro-rejection to pro-acceptance response.

40% of cells re-populating the scaffolds at two and four weeks post-implantation were macrophages stained positively for CD68. That percentage decreased slightly at the time of the last harvest **(Fig. 43)**. CD 163+ cells constituted to 13, 12 and 16% of total number of cells infiltrating the scaffolds, which was equal to 32, 30 and 43% of pan macrophages at two, four and eight weeks respectively **(Fig. 43 and 44)**. The number of CCR7+ cells decreased from 14% of total cells infiltrating the implant at two weeks *in vivo* to 11% at four weeks and 5% at eight weeks. They represented 35% of the pan macrophages at first harvest, 28% at second and 14% at third **(Fig. 43 and 44)**.

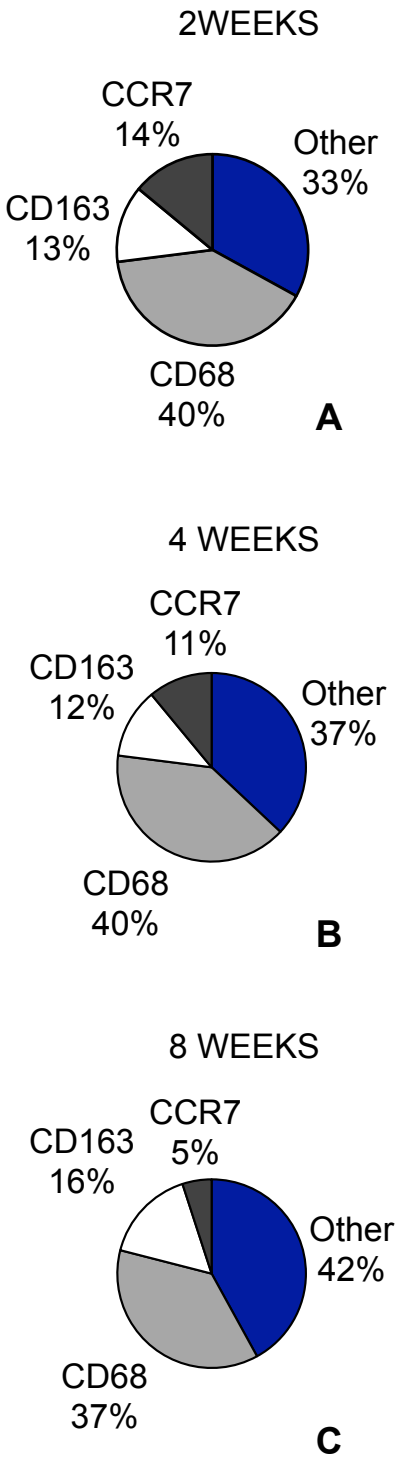


**Fig. 43** Pie chart of total number of cells infiltrating the scaffolds at two (A), four (B) and eight (c) weeks post-implantation into rodent recipient.

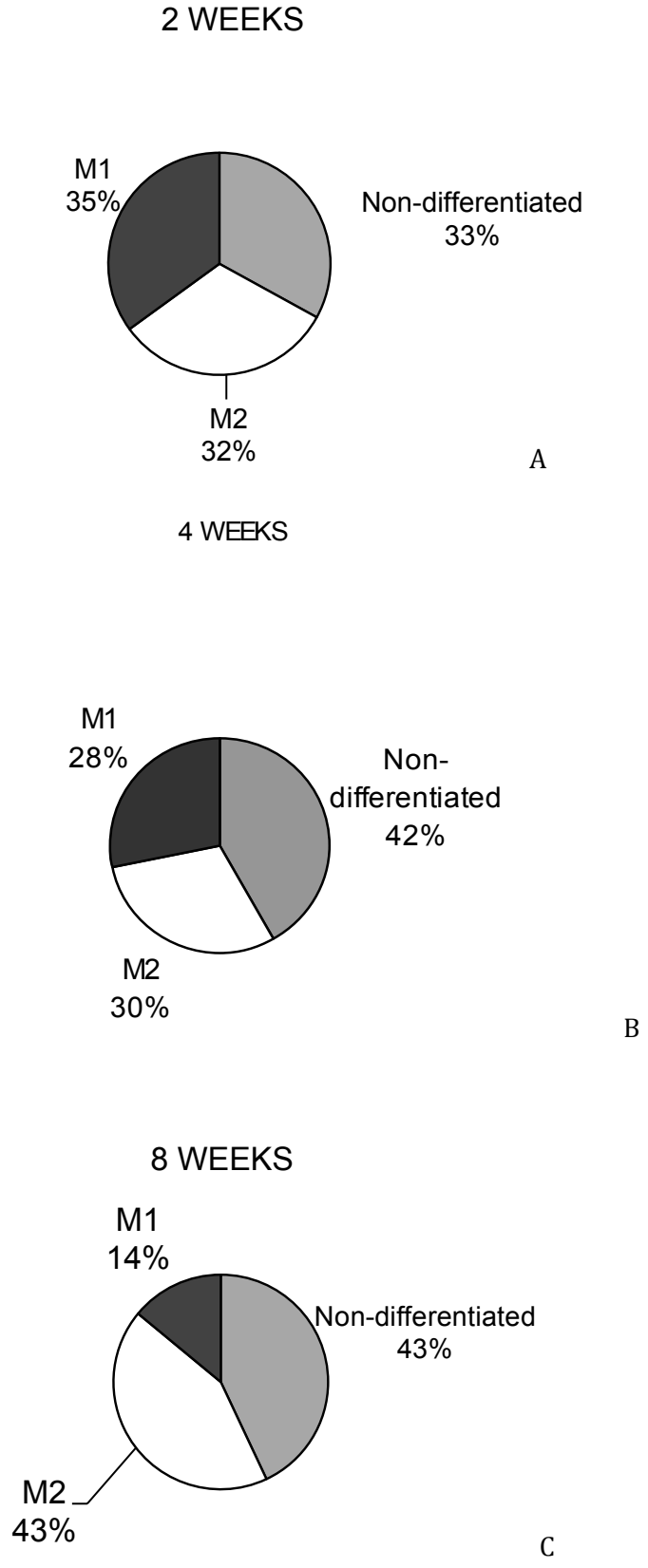


**Fig. 44** Pie chart of total number of macrophages infiltrating the scaffolds at two (A), four (B) and eight (c) weeks post-implantation into rodent recipient.

## 5.4. Discussion

In a recent study that compared the host tissue response to five biologic scaffold materials currently marketed for orthopaedic applications, it was shown that an intense mononuclear macrophage response in the early post-implantation period was common to all five products. However, the long-term remodeling outcome differed greatly between the scaffold materials. The tissue showed chronic inflammation, fibrosis, scarring, and encapsulation with some materials and the formation of organized, site-appropriate tissue for other materials (170). The presence of a cell population that is typically associated with cytotoxicity and inflammation was not necessary predictive of the long term remodeling outcome. Following studies showed that the phenotype of mononuclear macrophages that participate in the host response to biologic scaffold materials can differ markedly and that the method of material processing was an important variable (166). The surface topology and molecular organization of a scaffold was shown to affect macrophages, and cell-surface interactions, which in turn can change the quantity and identity of secreted pro-inflammatory cytokines and chemokines, the gene expression pattern, and downstream remodeling events (171). For example, Badylak et al. (166) showed that chemical cross-linking of SIS resulted in a switch from an M2-dominant profile (pro-acceptance) to a M1-dominant one (pro-rejection) and a change in the long term (16 weeks) remodeling outcome from constructive remodeling to chronic inflammation. M1 cells are crucial in matrix destruction and tissue reorganisation at injured tissues via the production of a variety of enzymes such as matrix metalloproteinase, collagenase, elastase, and hyaluronidase (165). This allows them to quickly migrate through the injured tissues to clear pathogens and debris. However, prolonged activation of M1 macrophages can lead to tissue injury. Therefore, mechanisms have

evolved to replace the inflammatory profiles with reparative or alternatively activated (beneficial for tissue engineered constructs) M2 macrophages at later stages of inflammation to facilitate tissue remodeling. The extent of plasticity of macrophages in changing their phenotype is yet to be determined. It is known though that a variety of absorbed proteins including fibronectin, vitronectin, albumin, fibrinogen, and VWF play a pivotal role in the response of macrophages to biomaterial (165). As shown in Chapter 4 some of these factors have been preserved in intestinal scaffold, which may suggest possibility of polarisation towards M2 phenotype. The M2 response is associated with an organized, site-appropriate tissue-remodeling outcome and an absence of persistent inflammation. However, the specific ligand-receptor interaction between macrophages and the scaffold surfaces are yet to be discovered.

Mononuclear cells are commonly observed and are expected participants in the host response to biomaterials, including those that are used as scaffold for tissue reconstruction. "The term mononuclear cell is a generic morphologic description for a population of cells with a single nucleus, a round or oblong shape, and variable amounts of cytoplasm." In tissue they are usually considered to have phagocytic or macrophage capability (166).

The proposed earlier paradigm for M1 and M2 differentiation is based upon observations of differential cytokine expression profiles and cell surface markers. M1 phenotype expresses CD68, CD80, and CCR7 cell surface markers in rats, and M2 phenotype expresses CD68 and CD163 surface markers in rats (species differences exist). This chapter presents the changes of macrophages accumulations within the implants, which could possibly be translated into predictions of the viability of the implant (166). In addition to the fact that rat and mouse are the only animal models characterised for M1/M2 markers, the rationale for the model choice should be

confirmed by the fact that rats pan macrophages demonstrate the highest degree of chemotaxis in response to complement-activating chemoattractants. This makes them the most robust and safest from the clinical translation point of view model for investigation of macrophage-based responses (213).

Previous reports characterizing the macrophage population that participated in the remodeling responses as a function of the M1 and M2 polarization schemes in rat model were based on counting cells stained with IHC markers within microscopical fields of view. This is very biased method and only a stereological approach could definitely prove or disprove it. Stereology is powerful because it provides 3D data which makes the interpretation of results more effective. Stereological estimates have two important statistical qualities: they are unbiased in general and they are efficient. Moreover, wherever 3D information is required from slice images, stereology should be the method of choice (161). It has been applied successfully in other disciplines of biology. However its potential has not been realized in the evaluation of tissue response to bio-engineered scaffolds. Stereological methods can be successfully employed in order to understand the dynamics and complexity of tissue-scaffold interactions in an objective quantitative manner. The state of the art is now such that there is no excuse for confining measurement to the planar areas like in other studies investigating M1 and M2 profiles in the tissue, which could be accused of less effective in, repeatability, groups' comparison, efficiency and what follows interpretation of scaffold behaviour *in vivo*.

An important aim in designing a research animal experiment is to obtain statistically relevant results with the use of a minimal number of animals (163). It was suggested that a conservative starting point is five specimens per experimental group (n=5). The reason being that "if something is found to increase (or decrease) in all

five cases, the probability that this is due to chance is $p=(1/2)^{n=5}<0.005$, and the experiment could be conclusive" (172). In stereology the same number can be applied to the number of blocks per animal, sections per block or fields per slide to obtain statistically relevant data. In this study we used six cases per time point, four blocks per case and 13 fields of view per block, which in total gave 52 optical bricks per case, 104 per animal and 312 counts per time point for each of the markers. Thus, the statistical and stereological relevance of the analysis was achieved.

Estimates of the absolute volume of the scaffolds implanted subcutaneously into rat recipients for two, four and eight weeks showed no significant difference at any given time point. This also corresponds with the macroscopic observations of the scaffolds at the explantation time. This indicates that there was no significant matrix shrinkage between two, four and eight weeks. What is more, there is a trend indicating increase in absolute volume of the scaffolds in time, which may suggest that infiltrating cells secrete new structural ECM proteins. This corresponds with the results of Picro Sirius red staining of the explants showing new, thin, green collagen fibres in the populated by the cells parts of the scaffold (Chapter 4). However, this trend was not statistically significant. The efficiency of the Cavalieri's Principle incorporated into absolute volume analysis over other planimetric methods is well documented (163). The CE should ideally be around 5%. Most of the CE values were around 10% with only couple of counts reaching 13 and 15%. This was due to the restricted grid size (the smallest available used) and the count of four slides per case.

There was also no significant difference in the total number of cells within the scaffold. The total number of CD68+ remained statistically unchanged over the duration of the study. Furthermore, there was no significant difference in the total number of CD163+ cells at any time point *in vivo*. The amount of M2-profiled

macrophages seemed to remain the same up to two months post-implantation. On the other hand, there was a significant drop in the total number of CCR7+ cells after four, and then again after eight weeks post-implantation. This strongly suggests that the presence of M1-profiled macrophages in the scaffold implanted *in vivo* was negatively correlated with the time. This was confirmed by the analysis of macrophages ratios that showed significant switch towards M2-pro-acceptance profile. This in terms of M2/M1 time related switch placed the scaffold closer to the positive control rate than the negative one presented by others (169). This implies that: M1 macrophages were either migrating out of the scaffold or trans-differentiating into pan or M2 macrophages over time. The percentage analysis suggests that it was the former, as the percentage of the pan macrophages remained almost the same during eight weeks in vivo with only small (3%) drop at eight weeks. At the same time the percentage of M1 profile dropped from 14% to 5% of pan macrophages during the same time. Simultaneously the percentage of M2 macrophages within the population of CD68+ cells increased from 30% to 43%. Said differently there was a 9% drop in M1 phenotype, and increase of 13% M2 phenotype within the population of undifferentiated macrophages, which amount stayed almost unchanged over the period of study.

Two-way ANOVA analysis proved as well that the ratio of M1 and M2 macrophages remained the same at two and four weeks post-implantation. However, after eight weeks *in vivo* there were significantly less pro-inflammatory macrophages than macrophages inducing constructive remodeling. It is hypothesised that the ratio of M1:M2 cells may be more important than the total number of cells, as there is clearly a correlation of the M1:M2 ratio to remodeling outcome (169). Thus, the analyses of two-way ANOVA were performed, and the switch from M1 to M2 profile

could be established on the time scale at four weeks post-implantation. Other studies investigating M1:M2 ratio in acellular scaffolds showed that this switch can be achieved as soon as one week post-implantation. Nevertheless, these observations were based on a biased and unreliable planimetric method of counting positive cells in the fields of microscopic view (169). Interestingly, the same authors state that any cellular (even autologus) material elicits a predominantly M1 type of response and results in deposition of dense connective tissue and scarring, which is contradictive with many tissue-engineering reports showing smart remodeling using seeded with autologus cells matrices (173). Nevertheless, this study suggests that the involvement of a cellular component can alter the ultimate response against the implant, but the underlying mechanism is not clear. It is possible that dendritic cells may contribute to the preferentially M1 response in the presence of cellular components by uptaking the codelivered cells near the implant site and becoming activated. They may also respond to maturation-inducing danger signals released by the transplanted cells from the construct. The maturation of the dendritic cells and the subsequent adaptive immune response may cross-talk with macrophages and result in M1 phenotype (165). Nevertheless, these results are based on biased methods and only thorough investigation using more effective and reliable methods, such as stereology could shed some light on the above hypothesis.

The sum of M1 and M2 immunopositive cells' numbers did not always equal the number of CD68+ cells, which is similar to what others reported using non-stereological methods (166). It could mean that CD68+ macrophages that were not yet determined to be an M1 or M2 phenotype would remain negative for the CD163 or CCR7 marker. It is unknown whether macrophages that were not committed to the M1 or M2 phenotype were recruited to the site of scaffold remodeling and then

stimulated to differentiate locally or whether phenotype-committed macrophages were selectively recruited to the site of remodeling depending upon the antigens or substrates that were present (166).

The analysis of cellular densities were characterised by CE values of 10-20%. Normally they should oscillate around 10%. Nevertheless, the counts were performed on 52 optical bricks per case which makes the results reliable and statistically relevant.

There were a couple of limitations in this study. First, the control group was not analysed for inflammation or constructive remodeling, and therefore the ultimate fate of the graft could not be predicted with certainty. Nevertheless, the quantitative data of M1 and M2 phenotypes in the control and test groups using a rat model was described by others (166). Therefore, the relative changes in the macrophages sub-population within the same range of time using the same animal model can be compared to this existing data suggesting link between M2 response and a favourable remodelling of the scaffold. Some of the other studies checked the expression of cytokines in the implants. However, using the stereological approach in this case it was crucial to preserve the whole explants (as they were relatively small pieces of tissue) for unbiased sampling. Thus, no material could be sacrificed to perform additional measurements. Nevertheless, the quantitative method employed is the best existing one in obtaining reliable and efficient results.

Work presented in this chapter highlights the method of predicting the fate of biomaterials using short-term and simple *in vivo* studies. This technique can be easily applied to any other tissue-engineered graft or implant. It proves it is important to consider not only the simple presence of macrophages (which number has not significantly changed over two months *in vivo*) at the site of remodeling, but also the

phenotype of this important cell population when attempting to predict downstream remodeling outcomes. The scaffold that was obtained by the method presented in Chapter 5 proved to provoke M2 response as soon as four weeks post-implantation. Even though the switch towards pro-remodeling phenotype took place later than in studies reported by others, it was very significant and proved using an advanced and considerably superior method.

# Chapter 6.

# *In vivo* evaluation of scaffold biocompatibility in the porcine model

## 6.1. Background and aims

One of the most limiting aspects of the existing approaches to tissue engineering of complex tissues and organs is the ability to provide for a functional circulatory system when *in vivo* studies are performed. The method of obtaining a scaffold with an intact acellular vasculature described in chapter 3 could possibly eliminate this obstacle. Every de-cellularisation process changes the properties of ECM and what follows, mechanobiological properties of the tissue (145). The ultimate test for bio-engineered tissues and organs, containing their vascular tree, is the introduction of systemic perfusion in order to test their potential *in vivo* (174). Performing scaffold implantations it was possible to test the behaviour of the vascular and intestinal part of the scaffold under physiological loading of systemic perfusion. Because the scaffold is composed of a vascular and intestinal part, characterised by significant differences in their ECM structure, it was crucial to test the behaviour of both. The biocompatibility test of the scaffold described in chapter 4 was the first step in estimating its *in vivo* behaviour. To verify the conceptual assumption that the presented scaffold could provide an immediate blood-supply post-implantation and to

check if the vessels' lumens remain open and their walls resistant to rupture, a vascular anastomosis between acellular scaffold and donor porcine renal pedicle were performed. The place of implantation was chosen primarly due to the vessels size compatibility. Moreover, nephroctomy is one of the least invasive procedures and linked with high recovery rate. An additional advantage was the fact that implanted scaffold, onced left in vivo for longer than one-hour, could rest in the kidney cavity.

The ultimate goal is to use the scaffold described in chapter 3 to create an *in vitro* system where the vascular tree could be seeded with endothelial cells and acellular ileum with intestinal stem cells, and then the whole construct could be used as an *in vitro* model or transplanted into a recipient. Blood vessels seeded with endothelium are less prone to induce blood coagulation and the resulting thrombosis. However, bare collagen is highly thrombogenic (175), and therefore the anticoagulation protocols had to be applied in the presented here, preliminary *in vivo* studies.

The first procedure was planned to last one hour, which was enough for the full re-perfusion of the scaffold. The aim of this implantation was to check if the concept resulting in de-cellularising the intestine with intact mesentery granted immediate blood distribution within the whole graft post-implantation. As the experiment finished with a success the next objective was to check if the viable blood perfusion within the graft can be obtained for periods longer than one-hour. The scaffold has been implanted for one week, and the animal was kept under mild anticoagulation. This was estimated to be long enough to characterise cellular compatibility of the matrix post-implantation within the porcine model. Poor results promoted further investigation into variables impacting on grafts survival. It was obvious that before advancement into longer studies the one-hour-long implantations

needed to be repeated and the satisfactory outcome replicated in three separate experiments. This also allowed finding denominator for the successful perfusion of the graft with blood over prolonged periods of time and resulted in advancement towards recovery studies. This time the understanding of the perfusion biocompatibility of the scaffold was greater.

The behaviour of the scaffold exposed to systemic perfusion is crucial when planning transition into more complex models. Thus, the investigation of the de-cellularised scaffold was described in detail, including all, even unsuccessful transplantations. The chronology of the experiments was also preserved.

## *6.2. Methodology*

### 6.2.1. Materials

The list of materials and equipment used in experiments described in this chapter is presented in **Appendix 4**.

### 6.2.2. Animal husbandry

All animals were maintained and handled similarly to the process presented in Chapter 3 (3.2.2).

Animals that underwent recovery studies received post-operatively analgesia using intravenous Carprofen (4mg/kg body weight) and Cefuroxime (14mg/kg) to prevent post-operative sepsis.

### 6.2.3. Acellular scaffold implantation into porcine recipient

A Large White Landrace crossbreed pig (55-75kg) underwent a right sided nephrectomy via a midline incision. The vascular part (main artery and vein of ileal pedicle) of de-cellularised and sterilized scaffold construct was anastomosed in an end-to-end fashion to the appropriately renal artery and vein using 8-0 Ethicon, Prolene suture. The anastomosis site as well as the mesenteric vasculature of implanted scaffold construct was checked for any bleeding and Mersilk ties were put in places of excess blood loss. Once the blood perfusion within the graft was obtained the implant was placed into the kidney cavity for one hour before explantation of the graft and termination of the animal by lethal injection of sodium pentobarbitone (100mg/kg). If signs of severe clotting were seen, the graft was immediately removed and the animal was terminated.

After the first successful procedure (terminal), the vascular tree of the scaffold was implanted for seven days into a porcine recipient (first recovery studies). Following three successful one hour implantations (terminal procedures) into the porcine recipient the scaffold-construct was implanted for 24 hours (second recovery studies). The implant was placed into the kidney cavity and the abdominal muscle layers were closed using intramuscular suture (3.0 Vicryl) and skin using horizontal mattress suture (3.0 Mersilk). Post-operatively, the animal received analgesia using intravenous Carprofen (4mg/kg body weight). Following the grafts' explantation the animals were terminated.

## 6.2.4. Development of anti-coagulation protocol

The anti-coagulation protocol used was composed of pre-treatment with anti-thrombotic drugs prior and during surgical procedure, as well as pre-conditioning the vascular part of the implant by injecting it with either neat or dissolved solution of heparin sodium in saline **(Table 19)**. The pig that underwent the first recovery study received additional treatment of Aspirin post-implantation.

**Table 19** Anticoagulation protocols used while implanting acellular constructs.

| *Animal Number* | *Type of procedure (terminal/recovery)* | *Weight of the pig [kg]* | *Heparin sodium administrated systemically during implantation [U]* | *Heparin sodium applied into the scaffold prior to implantation [U]* | *Total heparin sodium received by an animal/kg/h of surgical procedure* | *Additional anti-coagulative /platelet-formation drugs received by an animal [U/kg/h]* |
|---|---|---|---|---|---|---|
| *1.* | Terminal | 55 | 1. Post-incision: 7.000<br>2. Prior to releasing the vascular clamps: 1.000 | 1.000 | 55 | - |
| *2.* | Recovery (7 days) | 55 | 1. Post-incision: 7.000<br>2. Prior to releasing the vascular clamps: 1.000<br>3. Prior to placing the implant into kidney cavity: 1.000<br>4. 1h after placing the implant in the kidney cavity: 2.000 | 1.000 | 82 | 1. Aspirin 40mg/day, post-surgically |
| *3.* | Terminal | 60 | 1. Post-incision: 7.000<br>2. Prior to releasing the vascular clamps: 2.000 | 1.000 | 51 | - |

| | | | | | | |
|---|---|---|---|---|---|---|
| ***4.*** | Terminal | 73 | 1. Post-incision: 7.000<br>2. Prior to releasing the vascular clamps: 2.000<br>3. Administrated into graft's feeding artery: 2.000 | 1.000 | 82 | 1. Warfarin: 12mg/day starting 3 days prior to surgery |
| ***5.*** | Terminal | 70 | 1. Post-incision: 10.000<br>2. Prior to releasing the vascular clamps: 10.000 | 30.000 | 260 | 1. Warfarin: 12mg/day starting 3 days prior to surgery |
| ***6.*** | Terminal | 70 | 1. Post-incision: 10.000<br>2. Prior to releasing the vascular clamps: 10.000 | 30.000 | 260 | 1. Warfarin: 12mg/day starting 3 days prior to surgery |
| ***7.*** | Terminal | 75 | 1. Post-incision: 10.000<br>2. Prior to releasing the vascular clamps: 10.000 | 35.000 | 298 | 1. Warfarin: 12mg/day starting 2 days prior to surgery<br>2. Clexane: 120mg on the day of surgery |
| ***8.*** | Recovery (24 hours) | 55 | 1. Post-incision: 10.000<br>2. Prior to releasing the vascular clamps: 2.000 | 30.000 | 255 | 1. Warfarin: 12mg/day starting 3 days prior to surgery |

## 6.2.5. Histological analysis of the grafts

The explants were first fixed in 10% neutral buffered formalin solution for 48h, and then intestinal part of the grafts was open longitudinally and histology samples were taken in a uniform matter **(Fig. 45)**.

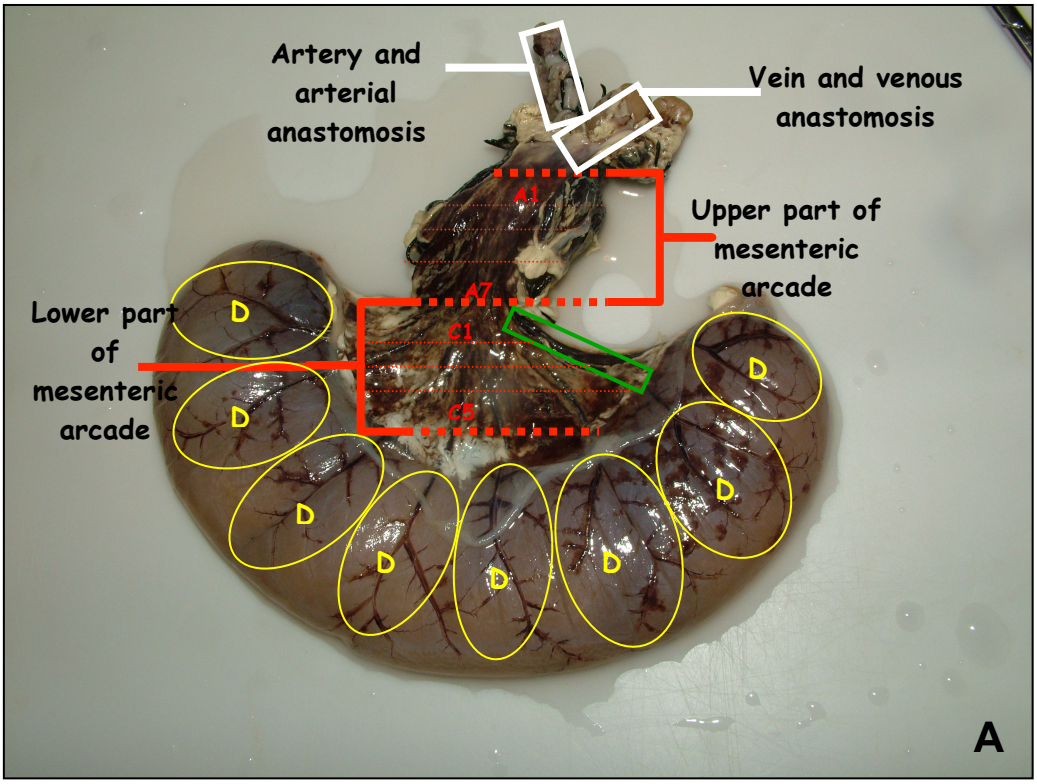


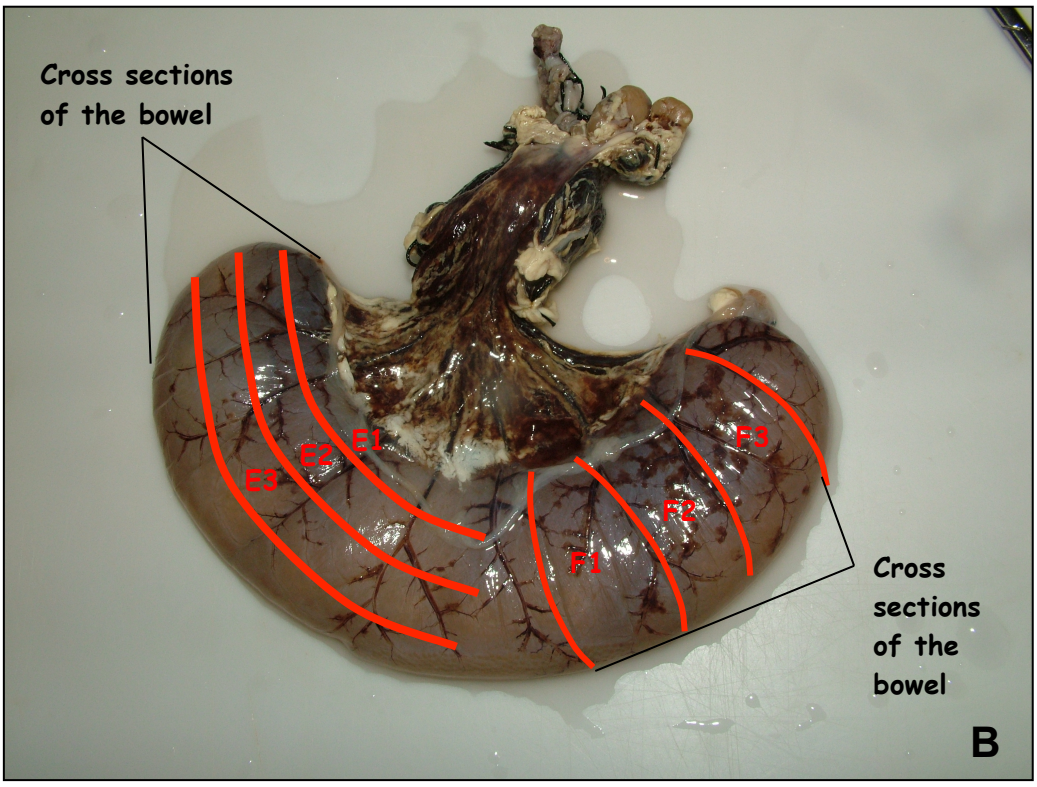


**Fig. 45** Layout of the sampling sites for the histological analysis of porcine grafts (animals:1, 3-8) fixed in 10% formalin solution. A, B two sides of the explant; A: white rectangles indicate places of the sampling within the main artery and vein (cross sections) and their anastomotic sites (longitudinal sections); red brackets include the cross sections of the upper (A1-A7) and lower (C1-C5) mesenteric arcade; green rectangle shows site of longitudinal sections of mesenteric vessels; yellow ovals present places of sampling for "flat embedding" of the bowel segments (D1-D8). B: sequential cross sections of the bowel in two different directions (direction E and F).

The sampling pattern enabled progressive analysis of the blood perfusion within the vascular and intestinal part of the scaffold-construct. Starting from the arterial side, longitudinal sections of the arterial anastomosis were prepared for histological analysis. Moving with the direction of the blood flow, serial sections of the main artery as well as the mesenteric arcade were taken. Moreover, longitudinal section of mesenteric arcade was analysed. Longitudinal sections of the venous anastomosis and cross sections of vein were also prepared. The bowel part of the scaffold was cut along and samples from one side were embedded flat in order to longitudinally analyse the vessels within the bowel **(Fig. 46)**. The other side was used to produce cross sections of the bowel in two different orientations **(Fig. 45B)**.


**Fig. 4**6 Flat embedding of intestinal part of the scaffold-construct.

The sampling of the graft harvested seven days post-implantation was dictated by its appearance and is presented in **Fig. 47**.

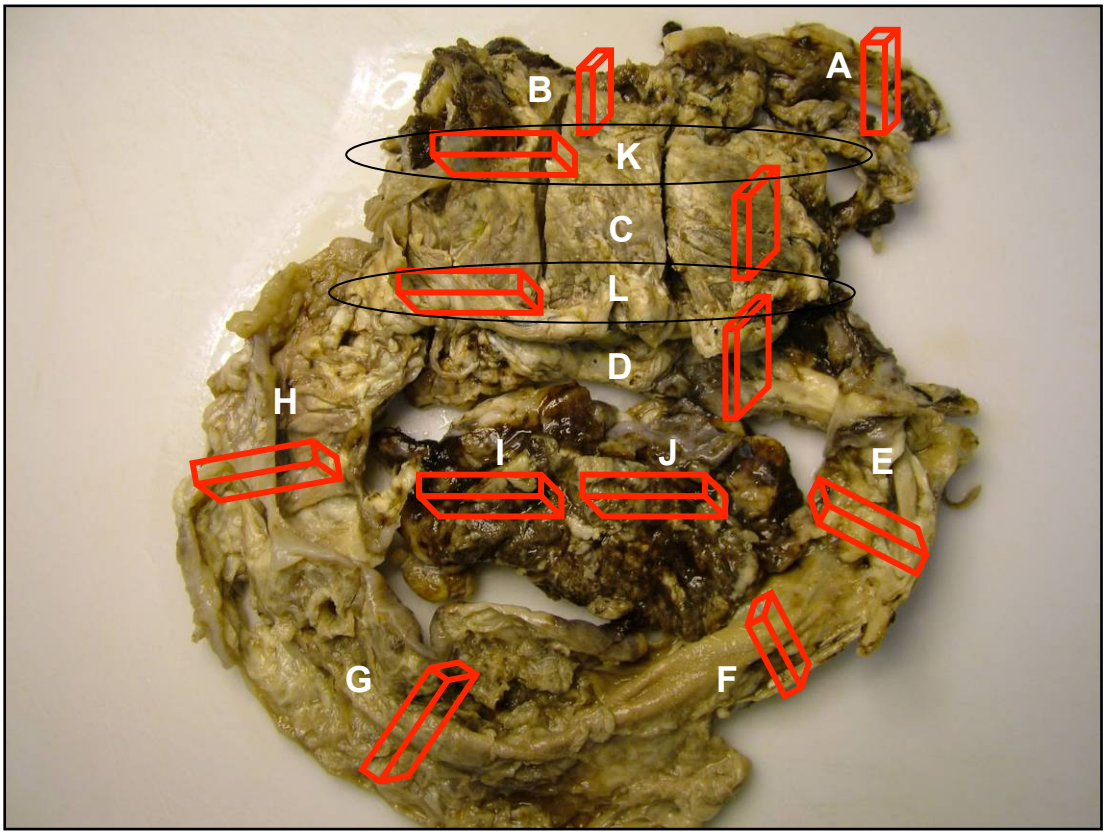


**Fig. 47** Layout of sampling sites for histological analysis in porcine graft harvested 1 week post-implantation (animal number 2), and fixed in 10% formalin solution. Letters A-L show morphologically different regions of the graft. Six sequential sections were harvested from each region. Red cubes show orientation of the samples.

Tissue was processed and prepared for histological staining in the way described in subchapter 3.2.6.2. Samples of grafts underwent H&E and Picro Sirius red/Miller's elastin staining.

## 6.2.6. Immunohistochemical analysis of the grafts

IHC staining was incorporated in order to visualize endothelial and endothelial progenitor cells, smooth muscle actin, macrophages and VWF within the grafts. Some sections of interest (based on H&E results) were chosen and stained with different markers: CD133 for endothelial progenitor cells (all grafts), CD68 for macrophages (grafts harvested 1 and 24 hours post-implantation), VWF (grafts harvested 1 and 24 hours post-implantation, scaffold-construct as a reference tissue) for blood vessels and

α smooth muscle actin (αSMA; grafts harvested 1 and 24 hours post-implantation) and endothelial cells (CD31; grafts harvested 7 days post-implantation). Protocols were initially tested on porcine control tissue. The staining was performed in a way described in sub-chapter 3.2.6.3. Specific IHC protocols are summarised in **Table 8 (Appendix 9)**.

## *6.3. Results*

### 6.3.1. Acellular scaffold implantation into porcine recipient

All procedures resulted in successful end-to-end anastomosis of the de-cellularised feeding artery and draining vein to the appropriate renal artery and vein of the recipient animal. Releasing the arterial clamps resulted in partial re-perfusion of the grafts, which was followed by positioning the scaffold into the kidney cavity.

In six out of eight scaffolds complete blood re-perfusion was obtained within one hour from implantation. Five grafts remained perfused for the time of the experiment (animals number: 1, 5-8); macroscopically no blood coagulation could be characterised **(Table 20)**.

**Table 20** Outcome of the implantations of the scaffold-constructs into porcine recipients.

| **Animal number** | ***Outcome of the implantation*** | | | |
|---|---|---|---|---|
| | ***Successful anastomosis*** | ***Re-perfusion with blood*** | ***Clot formation*** | ***Excessive bleeding*** |
| 1. | + | + | - | - |
| 2. | + | + | + | - |
| 3. | + | - | + | - |
| 4. | + | - | + | - |
| 5. | + | + | - | - |
| 6. | + | + | - | - |
| 7. | + | + | - | +++ |
| 8. | + | + | - | + |

All parts of the scaffold-construct (including vascular micro-connections within the de-cellularised bowel) were uniformly re-perfused and maintained blood flow for the duration of the experiment **(Fig. 48)**, which was confirmed by the microscopically observed blood perfusion *in vivo*. Three grafts re-perfused within ten minutes, and other two had to be placed into the kidney cavity to allow the completion of the process.

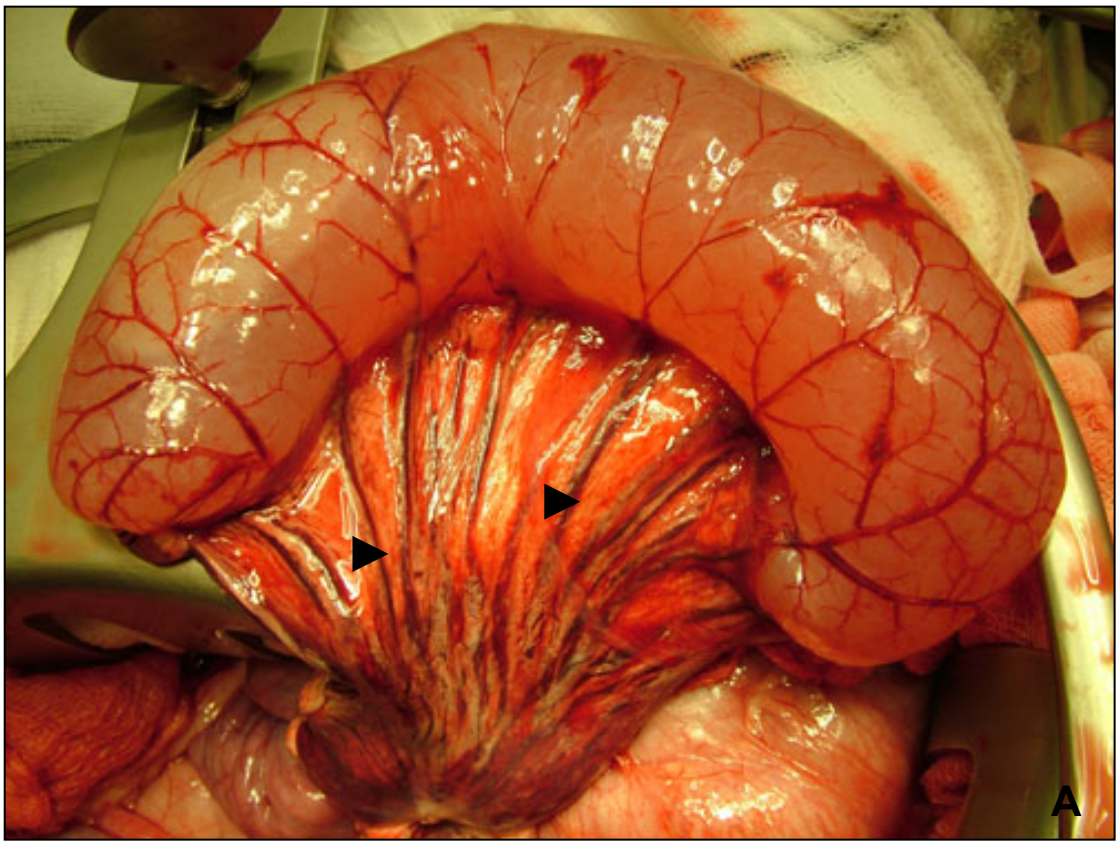


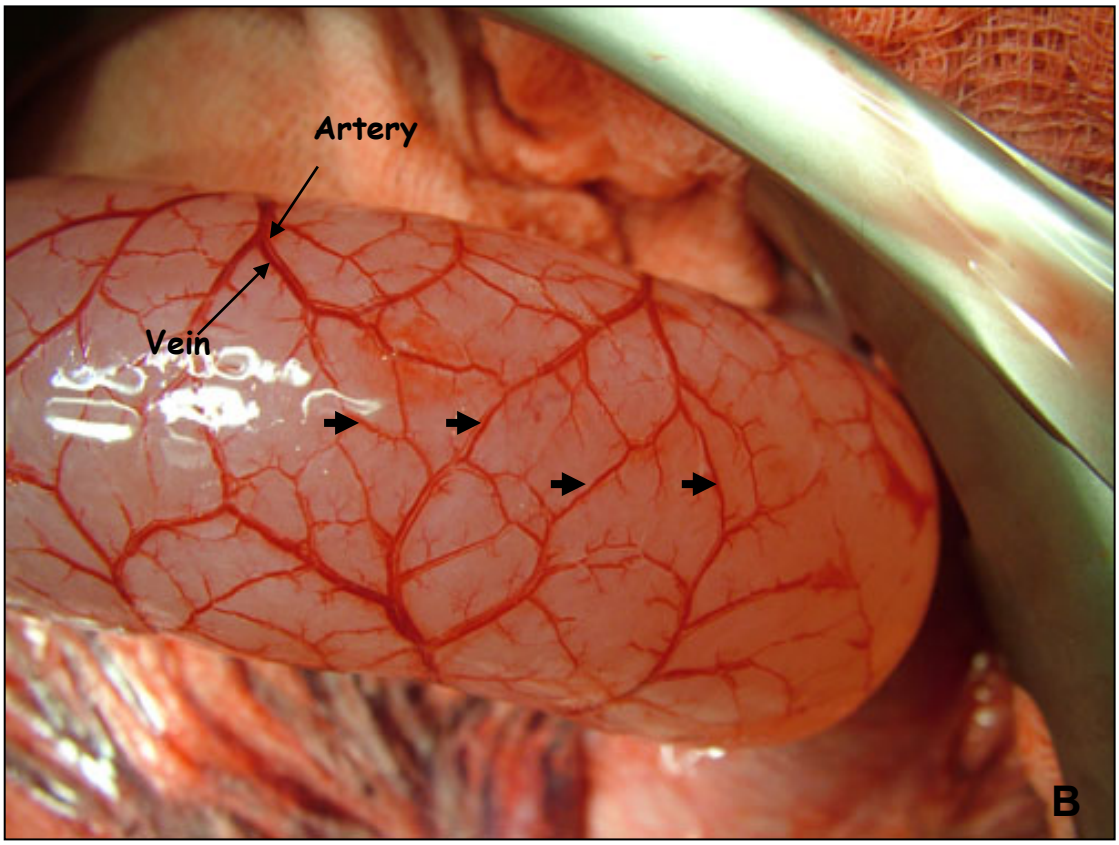


**Fig. 48** Completely and evenly re-perfused with systemic blood scaffold one hour post implantation A - arrow heads – clot-free mesenteric vessels, B - arrows – intestinal micro-connections with distinguishable de-cellularised vessels: wider veins and narrower arteries.

Two of the procedures resulted in a complete loss of the vessels perfusability caused by the blood coagulation as early as ten minutes after introducing the systemic perfusion and failed to completely re-perfuse with blood (animal number 3 and 4) **(Fig. 49)**. Within one of the re-perfused grafts excessive bleeding occurred (animal number 7), and the planned recovery study could not be carried on.

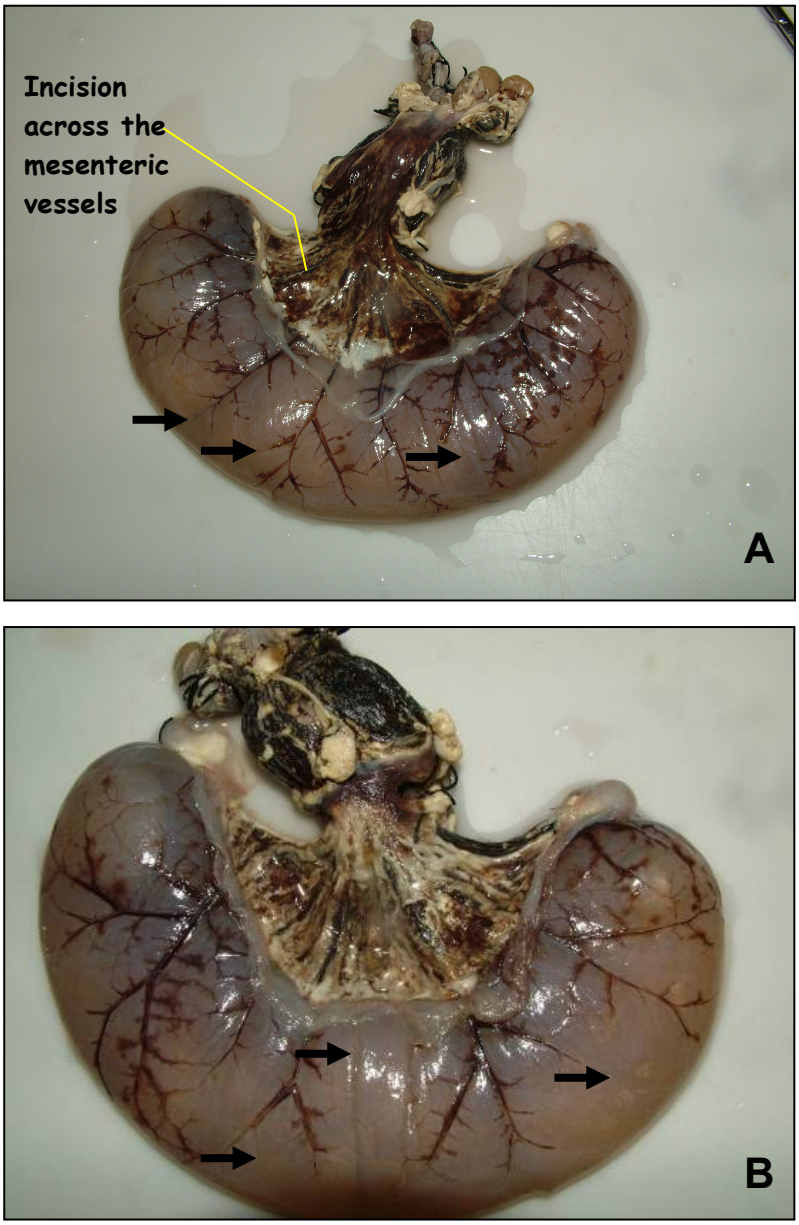


**Fig. 49** Porcine graft implanted for one hour (animal number 3) and fixed in 10% formalin solution for 24 hours, both sides (A, B). A - Mesenteric arcade with coagulated blood, what was confirmed by the incision across the mesenteric vessels. Black arrows – non-perfused parts of the graft.

In all the grafts some bleeding from the de-cellularised vessels into the spaces underneath the serous membrane was observed. Even though blood filled the spaces between the serosa and the submucosa in the intestinal part, and between two serous layers of mesenteric arcade of the grafts in animals: 1, 5-8 **(Fig. 50),** striping off the serosal layer and closer examination showed an undisturbed rate of the perfusion. Within a few minutes of removing the serosal layer, the extravascular leakage stopped, and all five grafts were fully perfused with circulating blood till the end of the experiments.

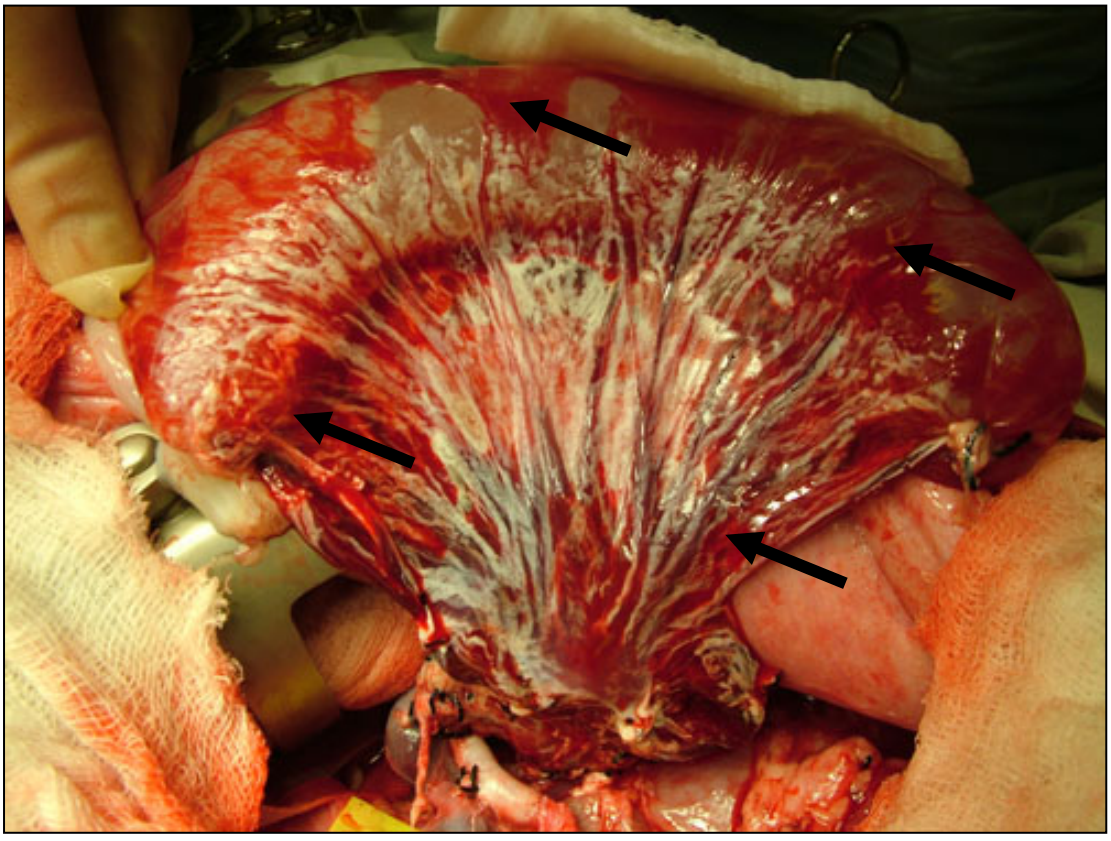

**Fig. 50** Porcine graft implanted for one hour (animal number 5) showing extravascular bleeding in between serous membranes. Black arrows – blood gathering under intestinal serosa and within mesentery.

The lumens of the vessels of the graft left *in vivo* for 24 hours were perfused at the time of explantation **(Fig. 51)**. There was some bleeding from the implant into the abdomen, however there were no adverse clinical signs during the time of the

experiment. There was no excess blood within the intestinal lumen of any of the grafts.

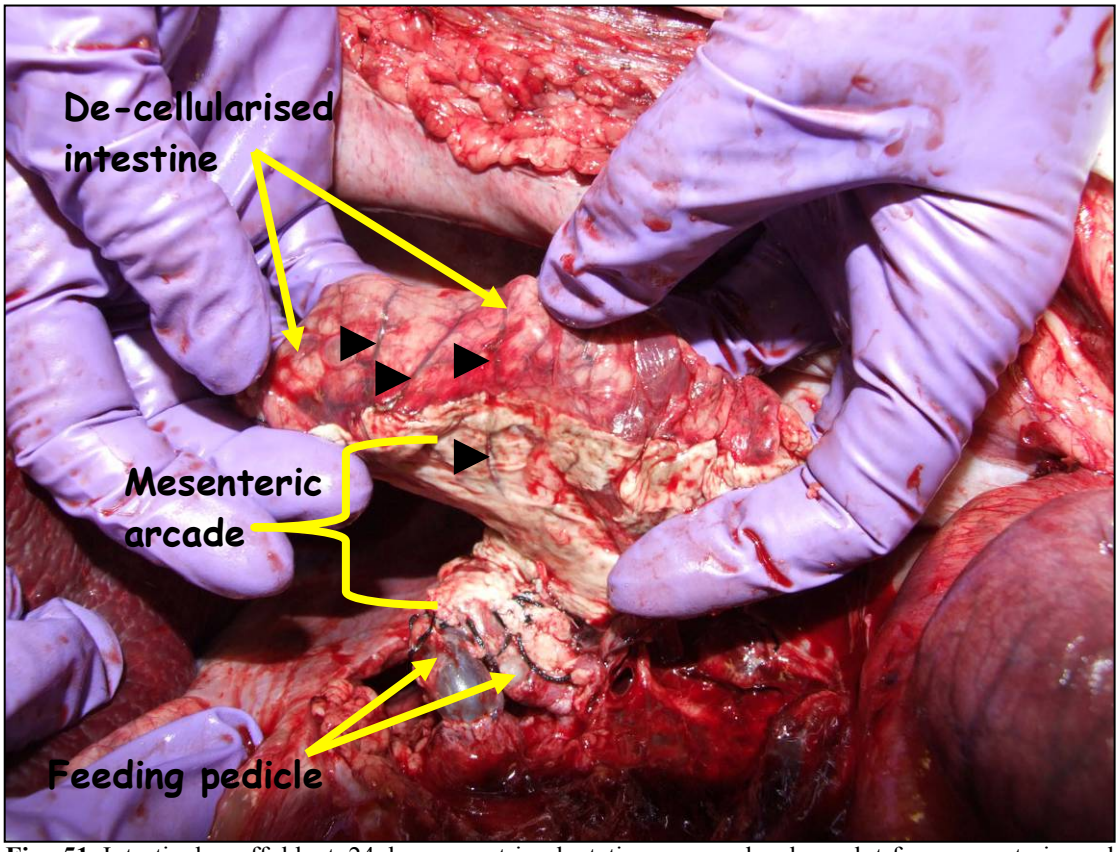


**Fig. 51** Intestinal scaffold at 24 hours post-implantation, arrow heads - clot-free mesenteric and intestinal vessels showing good blood flow.

The animal that underwent the seven-day-long recovery study survived till the planned termination date without showing any signs of systemic infection or other alerting symptoms. Over the study period the animal was feeding well, gained 5kg of body weight and as soon as 1 day post-surgery passed urine.

While the graft could not be recognized easily at first sight on explantation, after a more thorough examination it was found where implanted. Excessive adhesions to surrounding tissues and fibrosis were identified. However, post implantation the scaffolds structure and all its parts (including sutures) could be named and visualized **(Fig. 52)**.

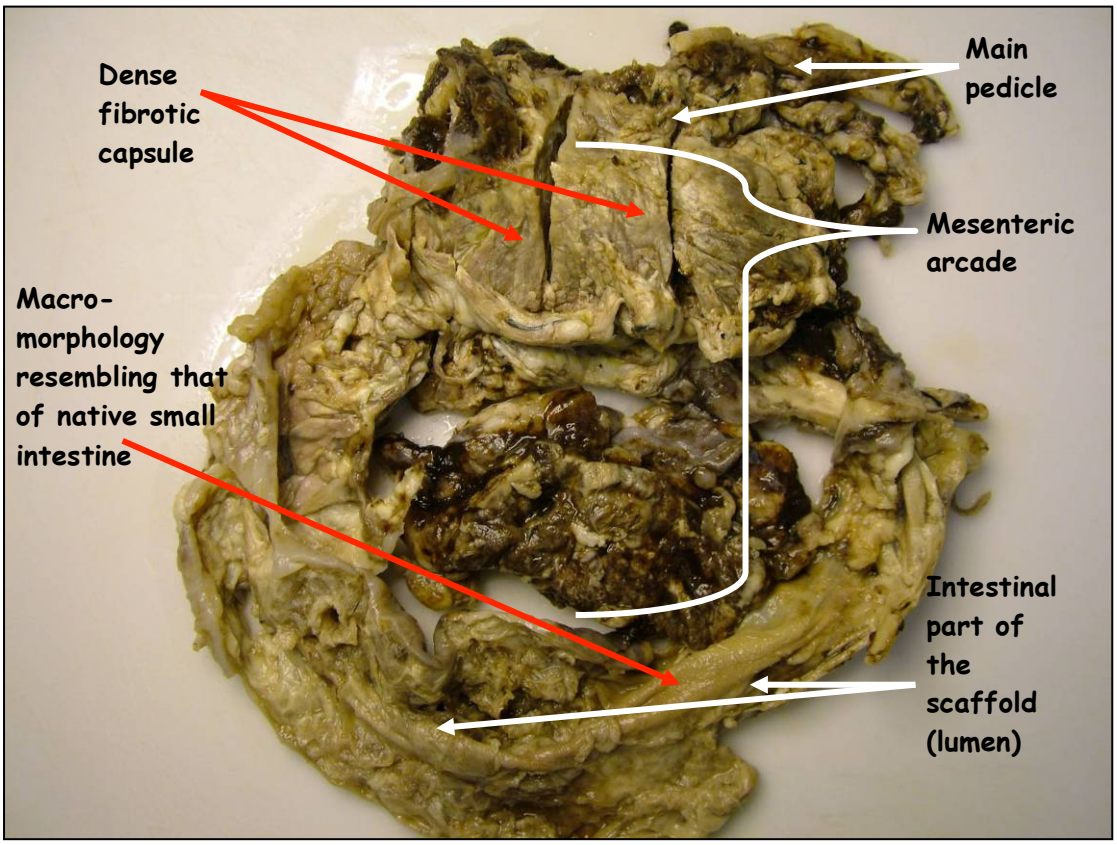


**Fig. 52** Porcine graft harvested 1 week post-implantation, and fixed in 10% formalin solution. White arrows show parts of the scaffold-construct that could be identified at the time of explantation.

## 6.3.2. Development of anti-coagulation protocol

The re-perfusion of the grafts with systemic blood was obtained in five out of eight cases. The unsuccessful re-circulations were caused by clotting of the mesenteric vessels, which took place shortly after introducing systemic blood to the scaffold-construct. The most successful protocols combined oral pre-medication of the animals with 12mg/day of Warfarin, pre-conditioning of the scaffold construct with 30.000U of neat sodium heparin and intravenous infusion of 12 000 – 20 000U of sodium heparin. The animals where the total heparin intake (calculated based on the weight of the animals and the length of the surgical procedure) was 255-260U/kg/h were anticoagulated most sufficiently. Nevertheless, the procedure performed on the animal that received only 55U/kg/h also had a satisfactory outcome

with complete re-perfusion of the de-cellularised vessels **(Table 20)**. It appeared that the additional variable was the length of the de-cellularised feeding artery and draining vein **(Table 21)**. The outcome of the implantations of shorter vessels was more successful and the grafts, which had the highest intake of heparin per body weight, per time of the study and per length of the donor pedicle, were mostly clot-free. The grafts with the lowest heparin intake considering the length of the pedicle developed clots at the early stages of the experiments.

**Table 21** Total heparin received by an animal in regards to the lengths of the de-cellularised feeding artery and draining vein of the scaffold-construct.

| Animal number | Length of the pedicle [cm] | | Average length of implanted vessels | Total heparin received by an animal regarding length of the implanted vessels [U/kg/h/cm] |
|---|---|---|---|---|
| | Artery | Vein | | |
| 1. | 1 | 0.5 | 0.75 | 73 |
| 2. | 3.0 | 2.5 | 2.75 | 30 |
| 3. | 3.5 | 2.5 | 3 | 17 |
| 4. | 3 | 2.35 | 2.675 | 30 |
| 5. | 2 | 1.95 | 1.975 | 131 |
| 6. | 1.9 | 1.9 | 1.9 | 137 |
| 7. | 1.95 | 1.95 | 1.95 | 153 |
| 8. | 2 | 1.85 | 1.925 | 132 |

Three successful implantations (animals number: 1, 5 and 6) confirmed good mechano-biological behaviour of the scaffold-construct, and plans regarding the next step involved recovery studies (animal number 7). Due to unrelated experimental circumstances the recipient animal could not receive three but only two doses of

Warfarin (2x12mg/day). With regards to properly anti-coagulating the animal, an extra dose (120mg=12 000U) of low molecular heparin (Clexane) was injected subcutaneously prior to making the midline incision. There was no reduction in the amount of heparin sodium injected during the surgical procedure, which in total gave 298U/kg/h of heparin received by the animal. This protocol appeared to be too strong as the animal lost a considerable amount of blood and could not be expected to perform satisfactorily in recovery studies **(Fig. 53)**. Therefore four hours after implantation the decision was made to remove the graft and terminate the recipient animal.

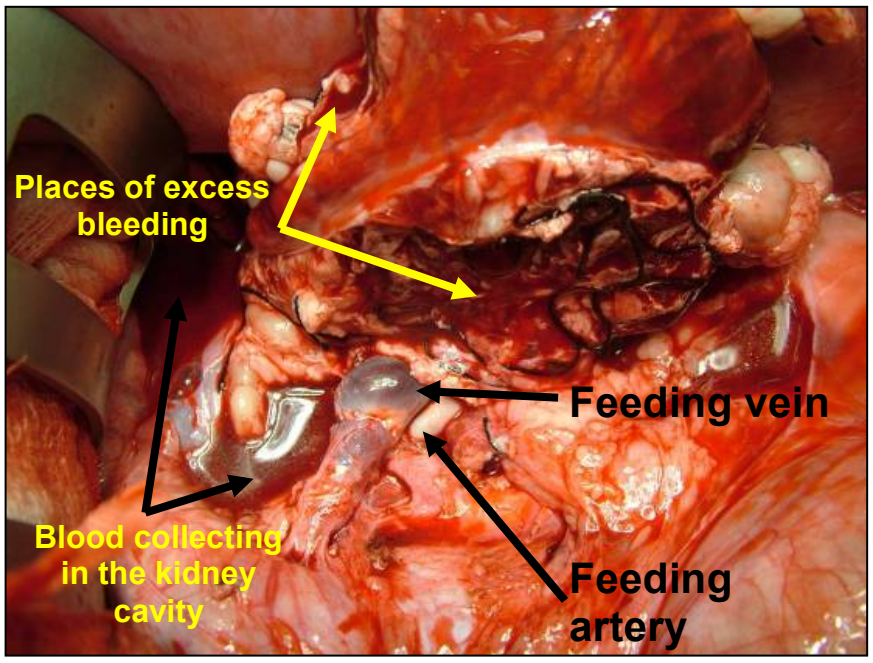


**Fig. 53** Porcine graft during implantation into porcine recipient (animal number 7); excessive bleeding from mesenteric arcade caused the termination of the recipient animal.

The anticoagulation of the graft implanted in the first recovery study was most probably insufficient, which caused complete lost of lumen's perfusion. However, the outcome of the second recovery study was successful and the vessels within the graft stayed open. There were no signs of severe anti-coagulative activity even in the micro-vasculature up to 24 hours post-implantation.

The anticoagulation protocol incorporated into the animal studies influenced greatly the outcome of the implantations. The biologic activity of blood within the grafts was confirmed by the histological findings.

## 6.3.3. Histological analysis of the grafts

H&E staining was performed mostly in order to check the uniformity and rate of grafts' re-perfusion with blood and visualize the lack or presence of coagulative activity within the de-cellularised vessels. Blood vessels were considered clotted when the entire lumen or its majority was filled with a blood clot. A clot is characterized by changes of red blood cells morphology (single cells can not be distinguished) and uneven distribution of white blood cells (they are usually gathering to disintegrate the coagulated blood). Implanted scaffold-constructs were also examined for the character and extensity of infiltration with the host cells.

### *6.3.3.1. Histological analysis of the grafts harvested one hour post-implantation*

Histological findings showed that all the parts of the explants harvested from animals number: 1, 5-8 were fully perfused with blood. Only the smallest vessels in the intestinal parts of the grafts showed minimal anticoagulative activity, with majority of lumen containing morphologically unchanged erythrocytes.

H&E staining of anastomotic sites and main pedicle just above the suture line showed no signs of clotting (animals number: 1, 5-7) **(Fig. 54)**.

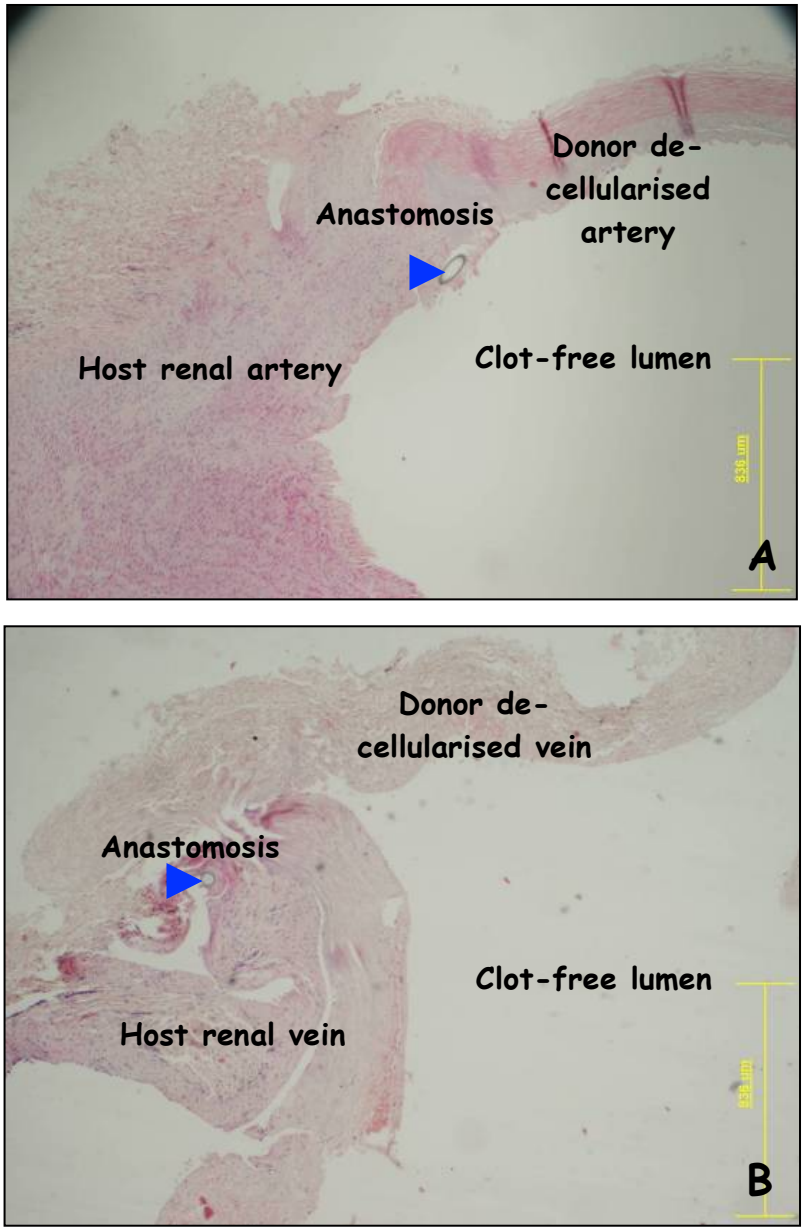


**Fig. 54** H&E stained cross sections of the anastomotic sites of the graft harvested one hour post-implantation (animal number 5): A – arterial anastomotic site with no clot formation; B – venous anastomotic site with no clot formation. Blue arrow heads indicate the suture. Yellow bars indicate the scale of the images.

White blood cells were distributed evenly throughout the lumen and the morphology of the red blood cells was unchanged with no indication towards their phagocytosis and autolysis within the main pedicle and most of the mesenteric vessels (animal number 1, 5-7) **(Fig. 55)**. Furthermore, small vessels within the intestinal part of the scaffold were also clot-free.

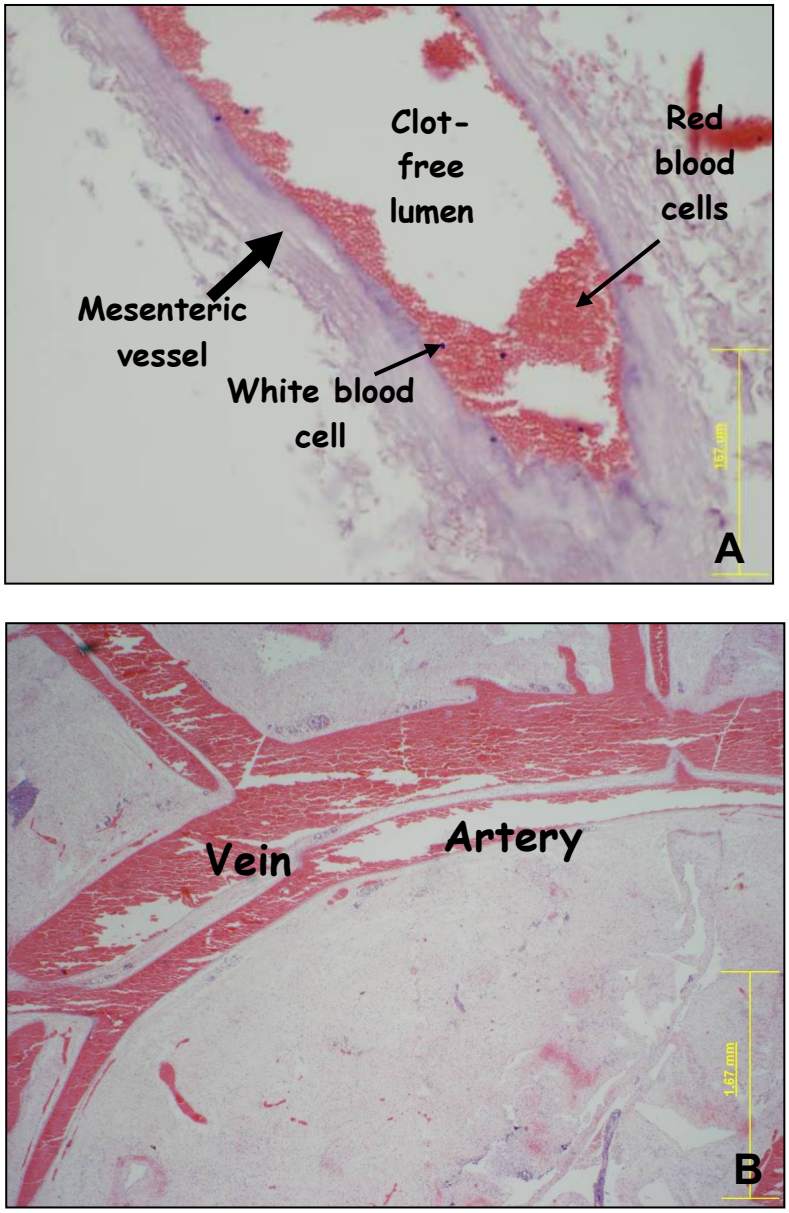


**Fig. 55** H&E analysis of mesenteric arcade of the scaffold implanted for one hour into porcine recipient (animal number 6). A- cross section of the mesentery with no signs of clotting,; B- longitudinal section of mesenteric vein and artery with clot-free lumens. Yellow bars indicate the scale of the images.

The majority of the intestinal vessels were evenly and fully filled with blood. Moreover most of them contained no blood clots with only few showing minimal coagulative activity **(Fig. 56).**

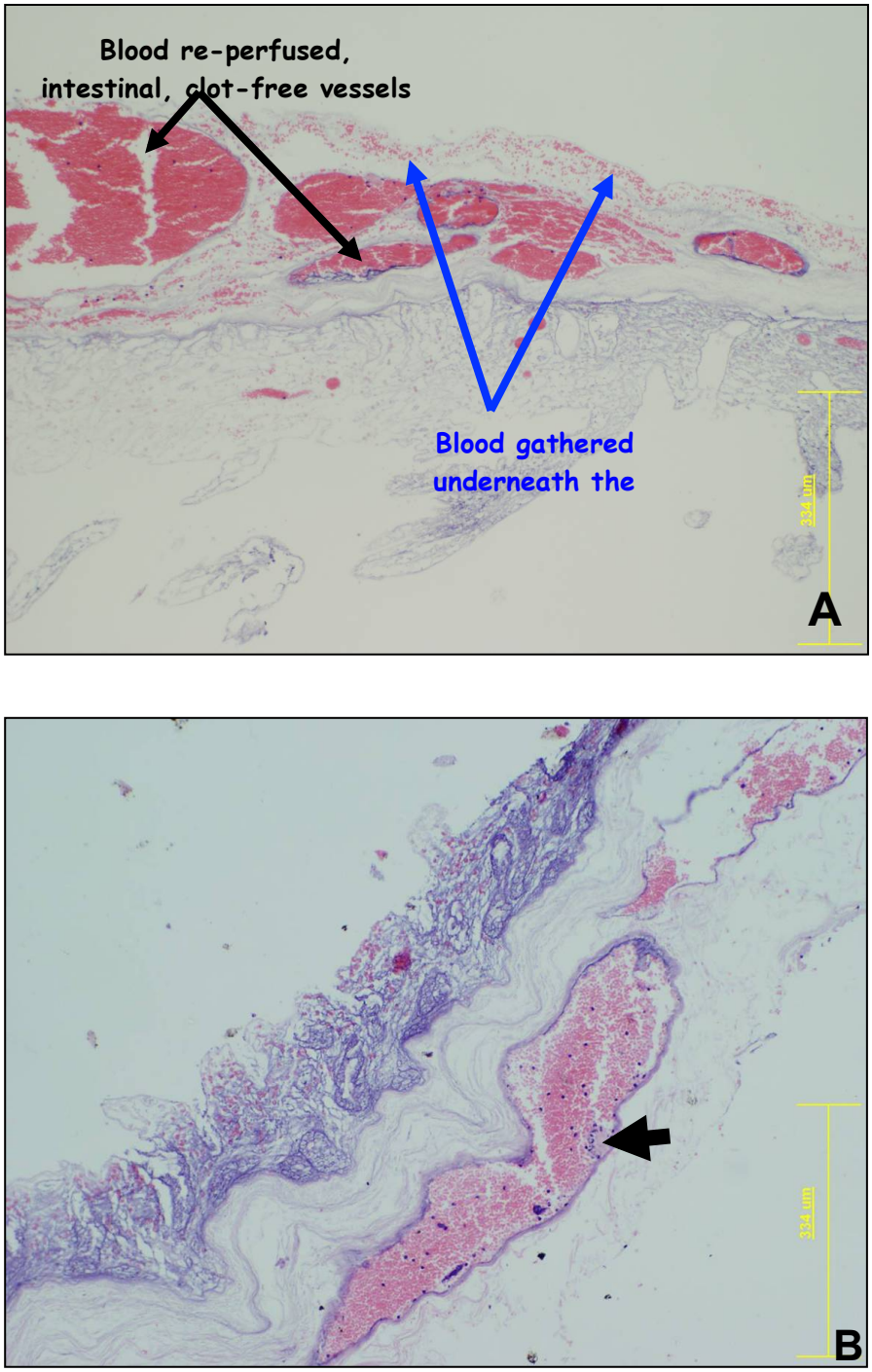


**Fig. 56** H&E stained cross section of de-cellularised bowel of the graft implanted for one hour into porcine recipient (animal number 1). A- blood-perfused, clot-free intestinal vessels; B- intestinal vessels showing minimal blood clot-formation (arrow). Yellow bars indicate the scale of the images.

Miller's elastin staining proved that clotting within the grafts harvested from animals number 1, 5-7 was mostly triggered in places where the vascular wall or internal elastin was interrupted **(Fig. 57)**.

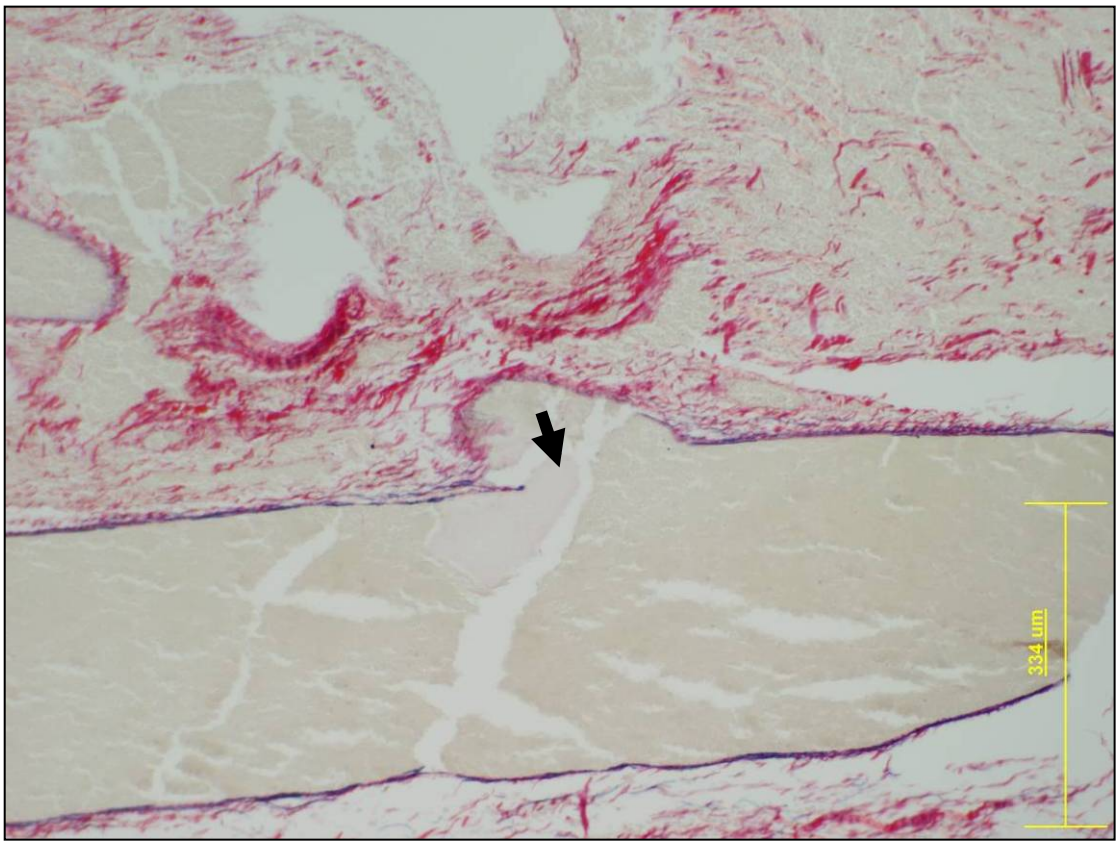


**Fig. 57** Picro Sirius red/Miller's elastin stained section of the small-diameter vessel within intestinal part of the graft one hour post-implantation; interrupted elastin (blue staining) causing coagulation of the blood (arrow). Yellow bar indicates the scale of the image.

Histological analysis of the vasculature of the grafts that showed macroscopic signs of clotting during the surgical procedure (animal numbers: 3 and 4) proved partial or complete loss of ability to perfuse caused by blood-clot formation in many places. Major clot formation could already be seen in longitudinal sections of anastomotic sites **(Fig. 58).**

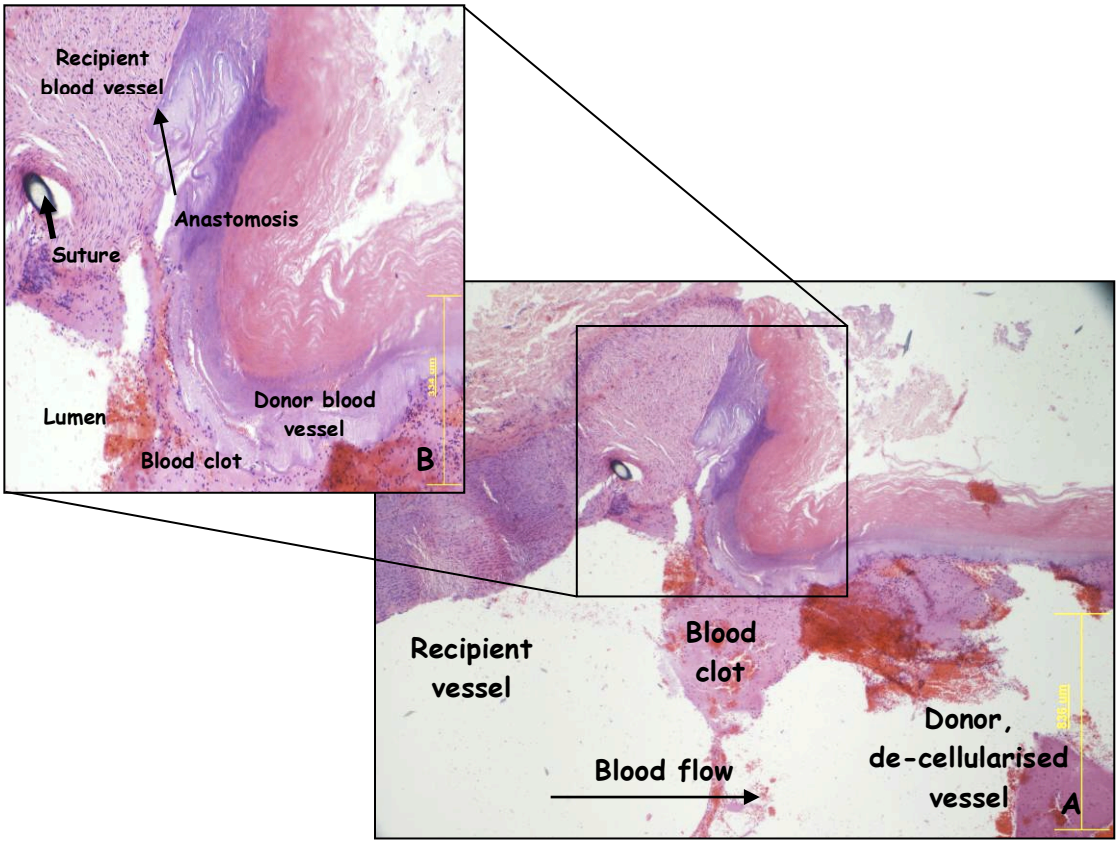


**Fig. 58** H&E stained longitudinal section of arterial anastomotic site of the graft harvested one hour post-implantation (animal number 4): A - blood coagulation within the lumen of the de-cellularised donor artery, no blood coagulation in the recipient tissue, blood could still flow through the graft but the diameter of the donor vessel was drastically reduced; B – magnified place of anastomosis with visible clotting only within the recipient vessel. Yellow bars indicate the scale of the images.

Similarly, the majority of the mesenteric and intestinal vessels were filled with blood at some stage of coagulation or non-perfused at all **(Fig. 59)**.

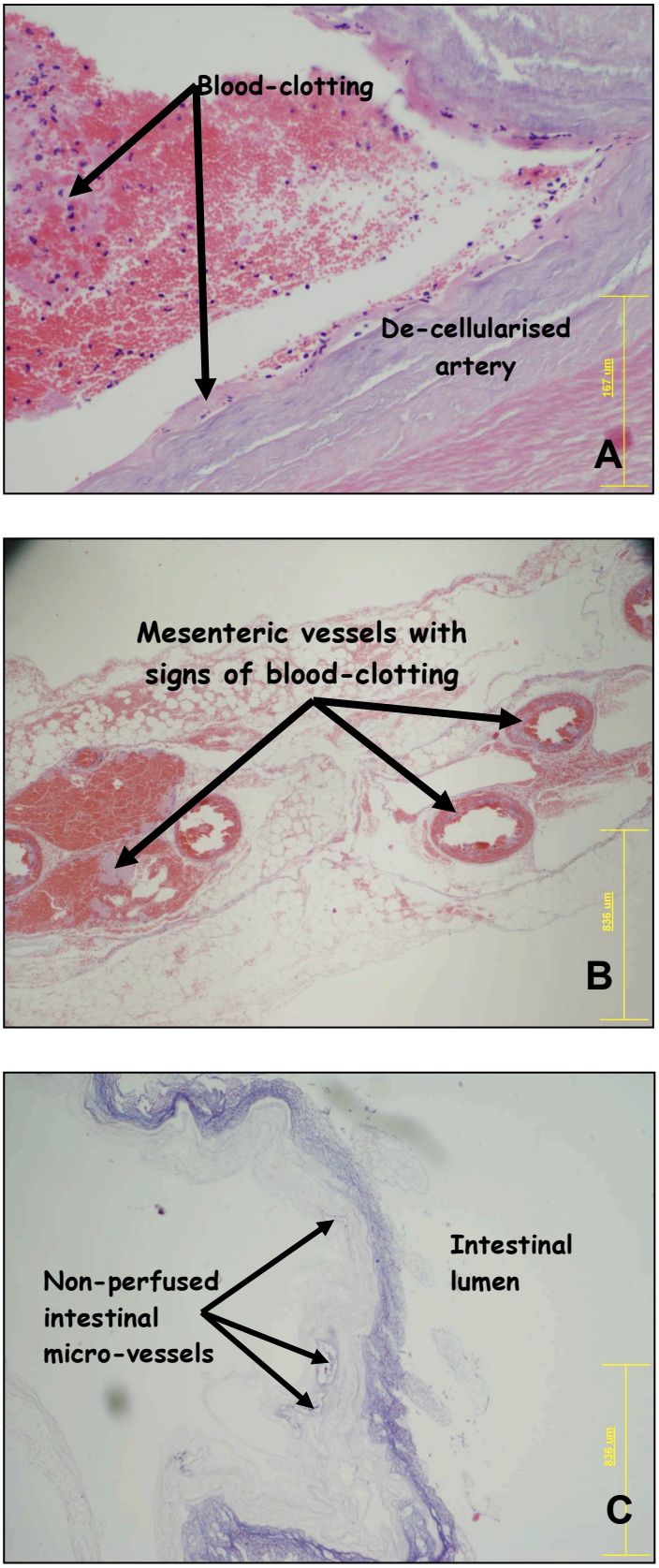


**Fig. 59** H&E stained sections of the graft harvested one hour post-implantation (animal number 4): A – anastomosed artery with early signs of blood clotting in the central and peripheral part of the lumen; B – mesenteric vessels showing signs of blood-coagulation; C – cross section of the intestinal part of the graft with non-perfused with the blood intestinal vessels. Yellow bars indicate the scale of the images.

As soon as one hour post-implantation, recipient cells were present in the anastomosed acellular vessels **(Fig. 60)**.

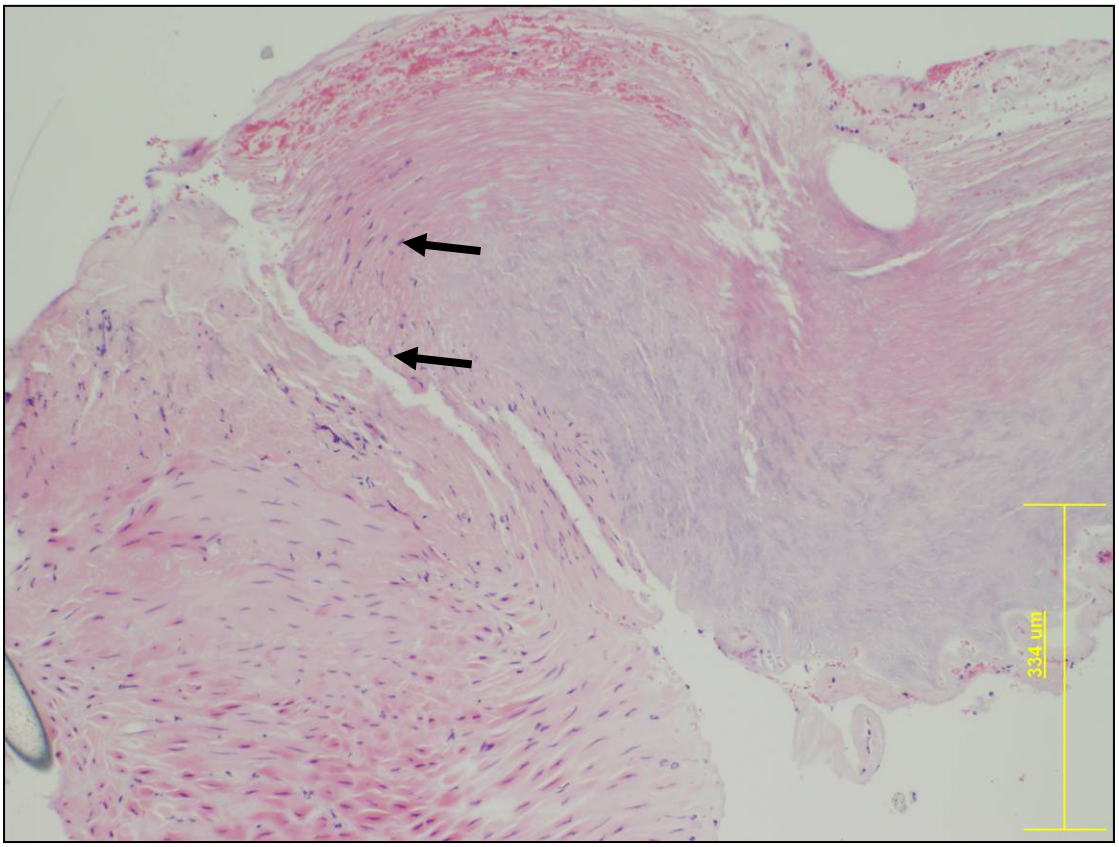


**Fig. 60** H&E stained longitudinal section of the arterial anastomotic site of the graft harvested one hour post-implantation from porcine recipient (animal number 1): arrows – host cells infiltrating de-cellularised superior mesenteric artery. Yellow bar indicates the scale of the image.

### *6.3.3.2. Histological analysis of the graft harvested one week post-implantation*

H&E-stained samples obtained from the region of anastomosis and the graft's main pedicle showed a clotted major part of the main artery, with visible signs of calcification and fibrotic capsule around the pedicle **(Fig. 61)**. However, some thrombus and clot-free sections of the main pedicle could also be identified **(Fig. 62).**

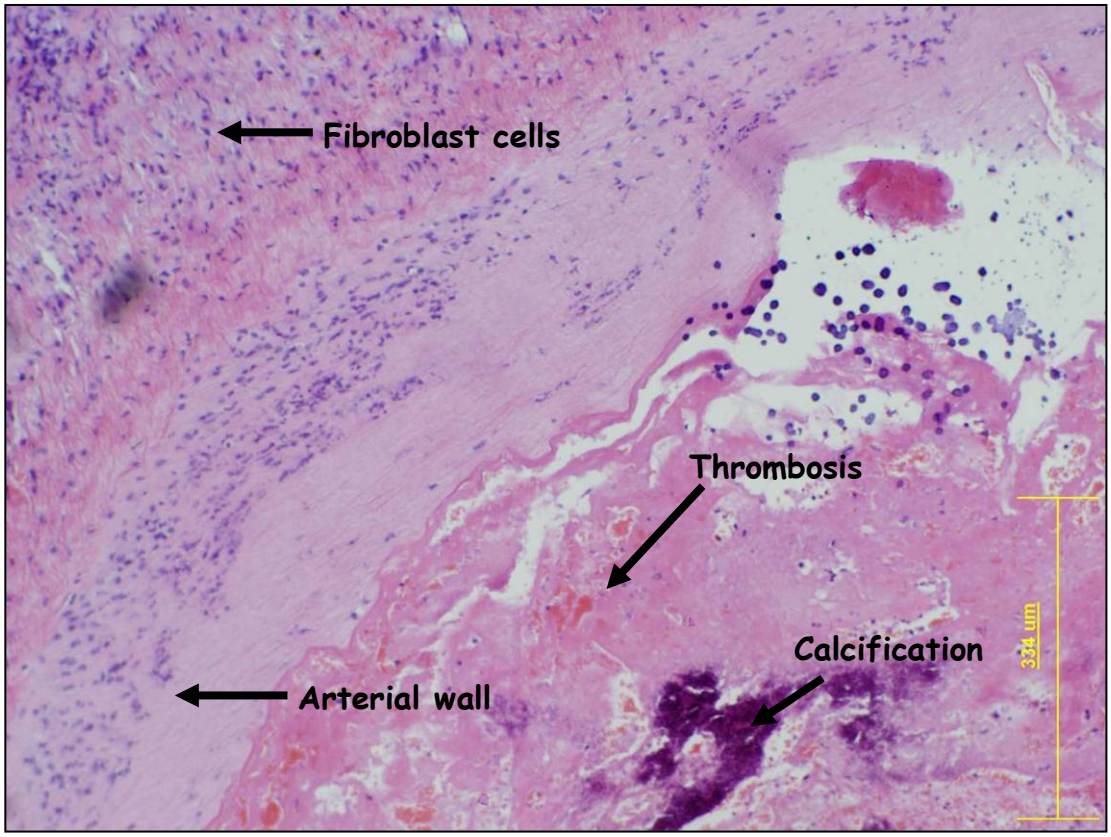


**Fig. 61** H&E stained cross section of the graft harvested one week after the implantation (animal number 2) showing thrombosed and partially calcified feeding artery. Yellow bar indicates the scale of the image.

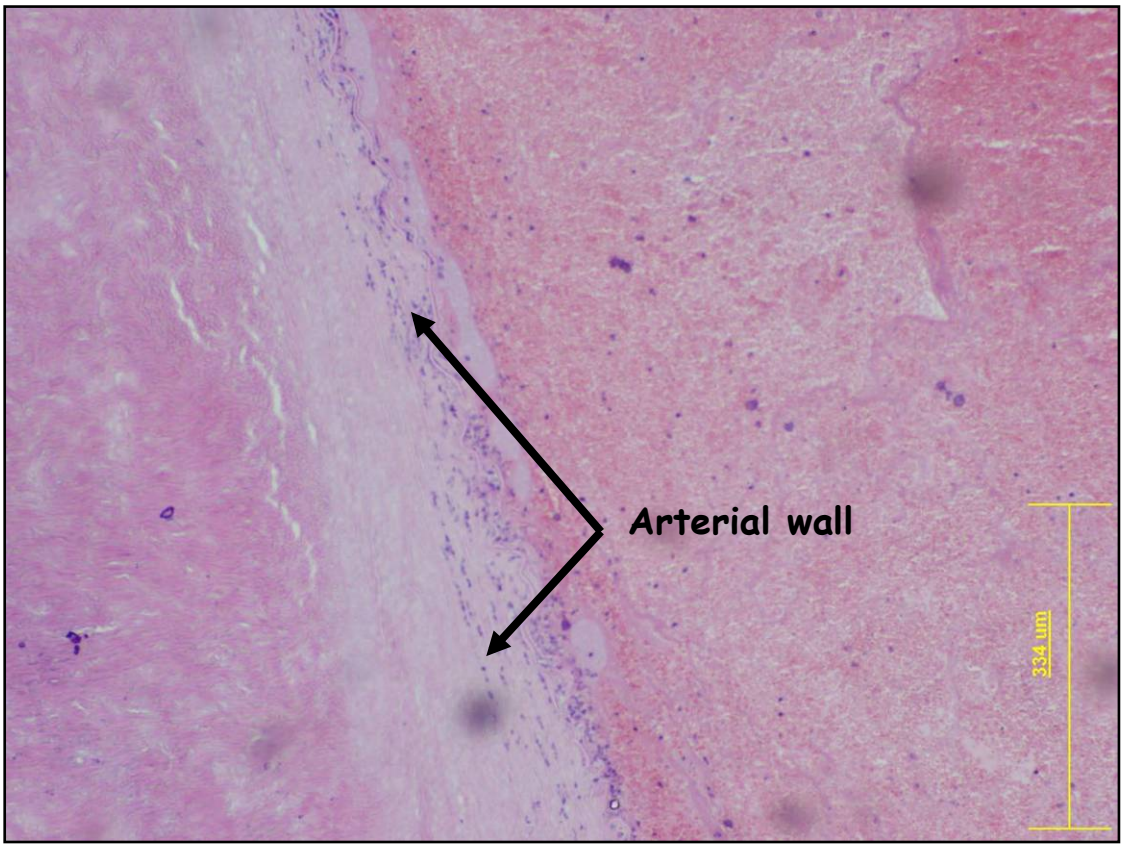


**Fig. 62** H&E stained cross section of the graft harvested one week after the implantation (animal

number 2) showing some places where clots were not formed, and the vessels were perfusing. Yellow bar indicates the scale of the image.

Most of the graft's mesenteric vessels were not open at the time of explantation. Infiltration with cells was restricted to the scaffold-constructs external parts, where there was evidence of intensive neo-vascularisation **(Fig. 63)**. Fibroblasts aggregation could be seen at the outer parts of the mesenteric arcade.

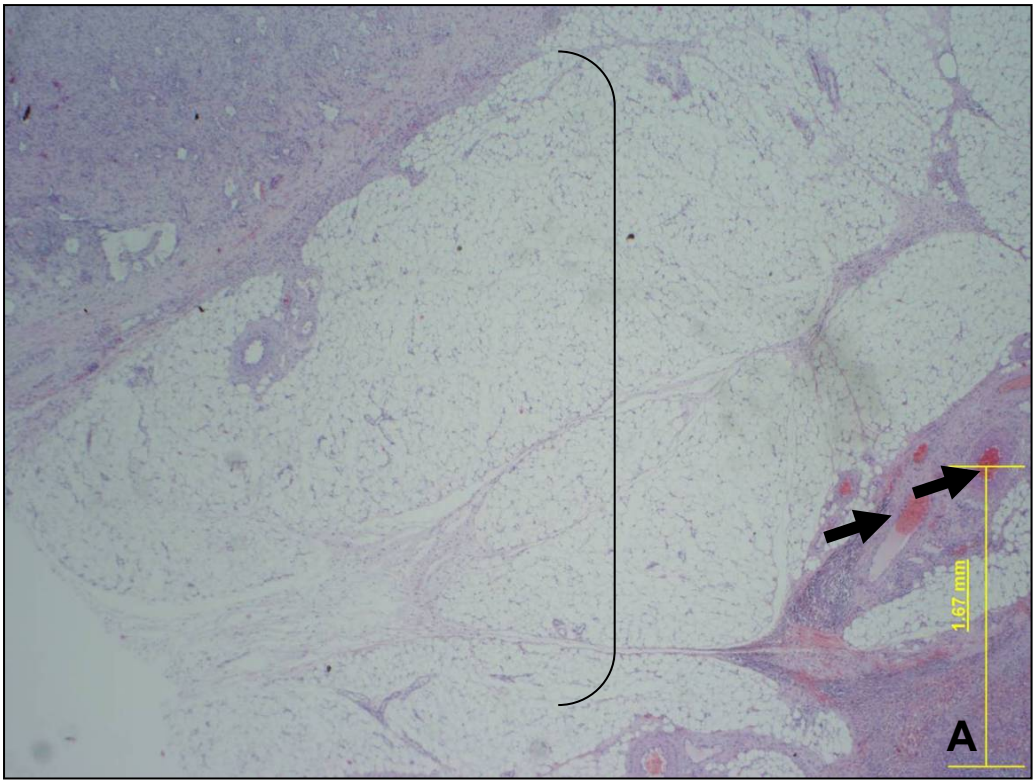

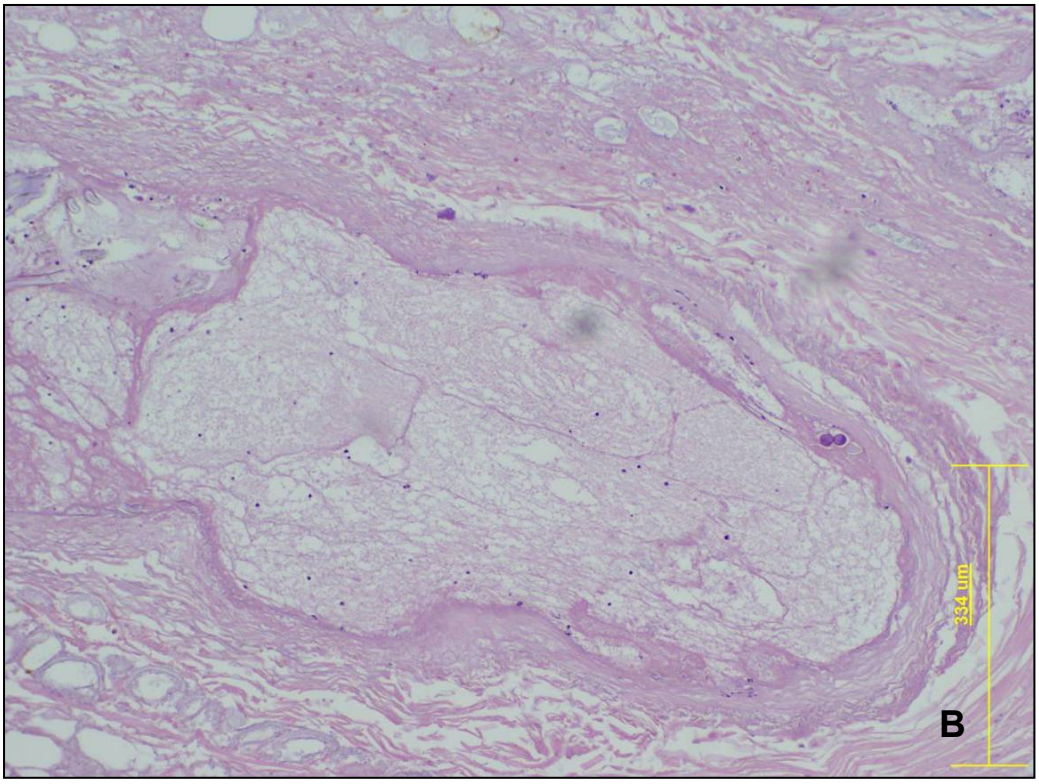


**Fig. 63** H&E stained cross section of the mesentery of the graft harvested one week post-implantation (animal number 2). A- non-infiltrated with the cells middle part of the explant (bracket), and neo-vascularisation (arrows) in the external, populated with the cells part of the graft; B- non-perfused mesenteric vessel. Yellow bars indicate the scale of the images.

Huge amounts of inflammatory polymorphonuclear cells could be found in places of graft re-population **(Fig. 64)**.

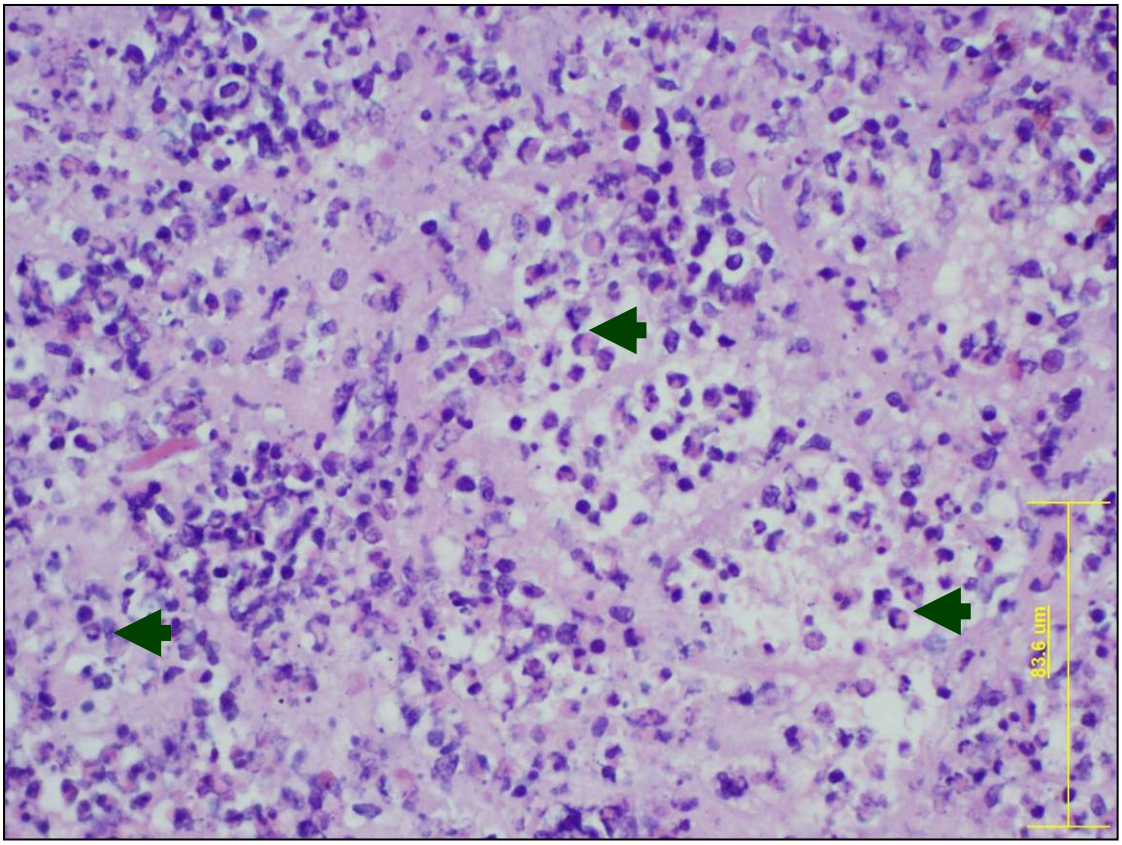


**Fig. 64** H&E staining of intestinal section of the graft harvested one week post-implantation showing abundance of polymorphonuclear cells (arrows). Yellow bar indicates the scale of the image.

Furthermore, most of the intestinal parts of the graft were filled with loose, spongy ECM fibres. Histology confirmed that the periphery of the graft was fibrotic. The only exception was the part of the bowel in region F in Fig. 36. H&E analysis showed that at this specific region all the acellular intestinal layers (villi, submucosa/muscularis externa and serosa) still could be identified post one week *in vivo*, and no fibrotic reaction or extensive polymorph infiltration was present **(Fig. 65)**. This was the only part of the bowel where there were signs of functional, blood-perfusing vessels.

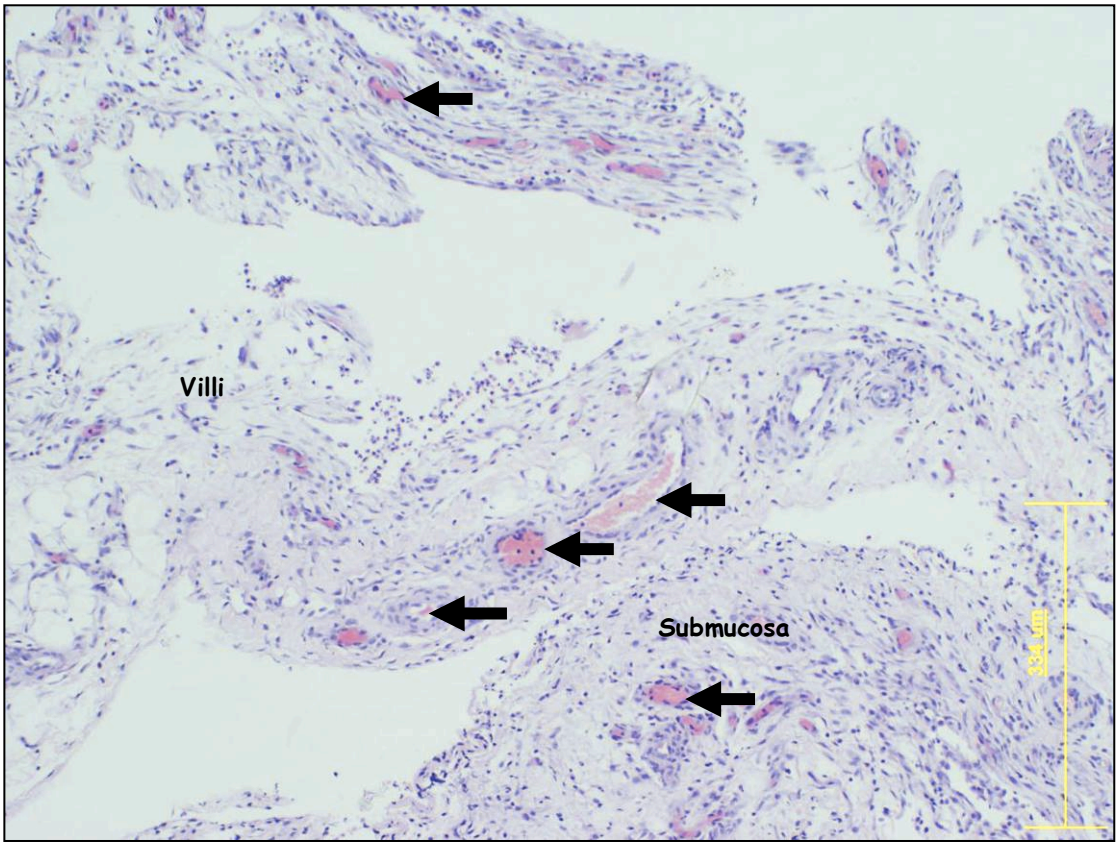


**Fig. 65** H&E staining of the intestinal part of the graft (region F in Fig. 36) harvested one week post-implantation. Arrows – blood-filled vessels within the graft. Yellow bar indicates the scale of the image.

### *6.3.3.3. Histological analysis of the graft harvested 24 hours post-implantation*

The last scaffold-construct was implanted for 24 hours. The histological analysis showed that all of its sections were perfused with blood and most of the de-cellularised vessels were clot-free. The rate of the cellular infiltration was significantly higher than in the grafts implanted for one hour. The wall of the vein was evenly infiltrated with cells some of which were fibroblast-like cells **(Fig. 66)**.

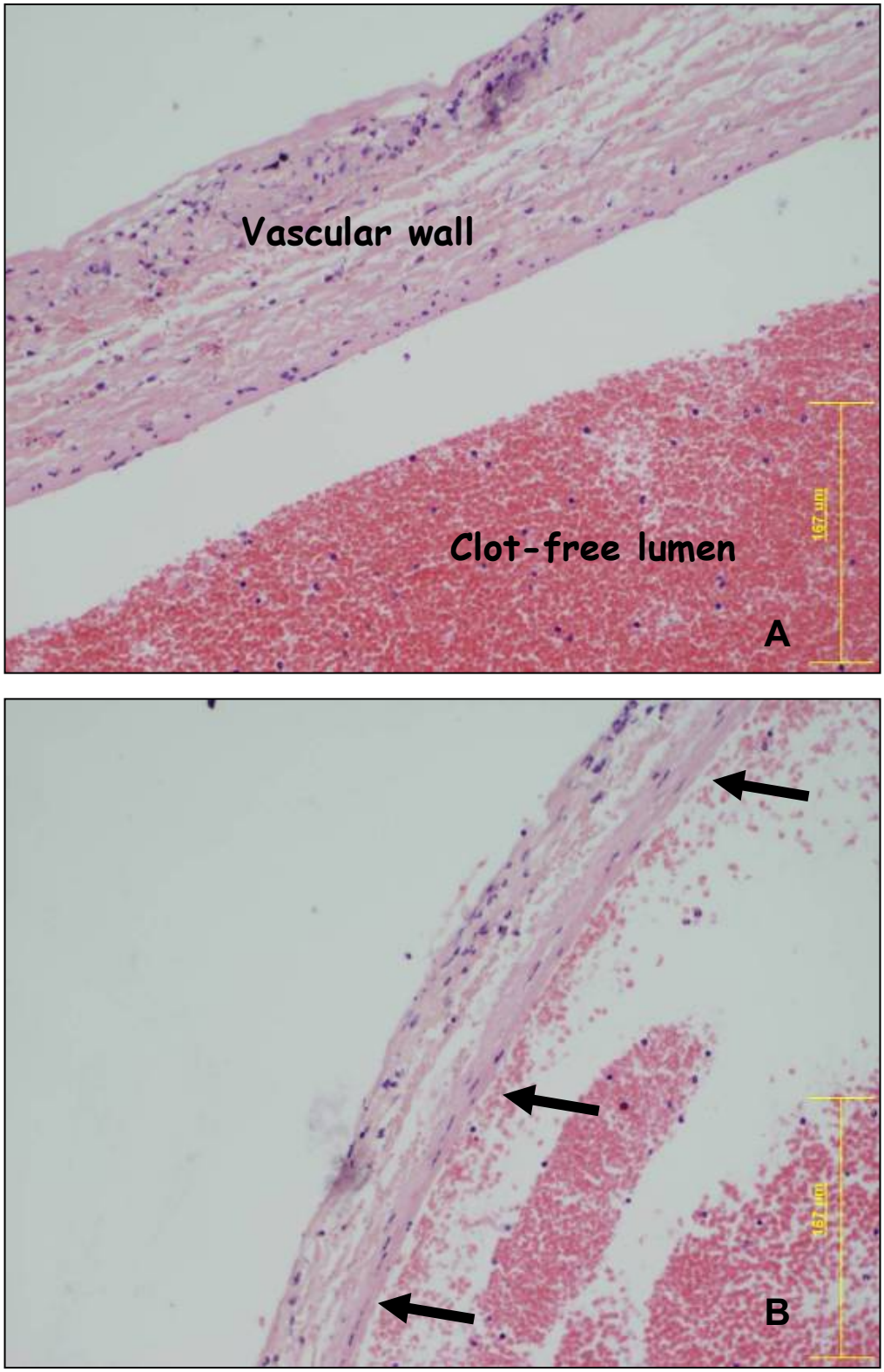


**Fig. 66** H&E stained cross sections of the main vein of the graft harvested 24 hours post-implantation (animal number 8): A – evenly infiltrated with cells wall of the de-cellularised vein showing no signs of blood-clotting; B –elongated, fibroblast-like cells situated within the venous wall (arrows). Yellow bars indicate the scale of the images.

The graft's anastomosed artery (proximal and distal parts) was also infiltrated with cells. However, throughout the whole length of the vessel the middle section of the wall showed no signs of cellular presence **(Fig. 67)**.

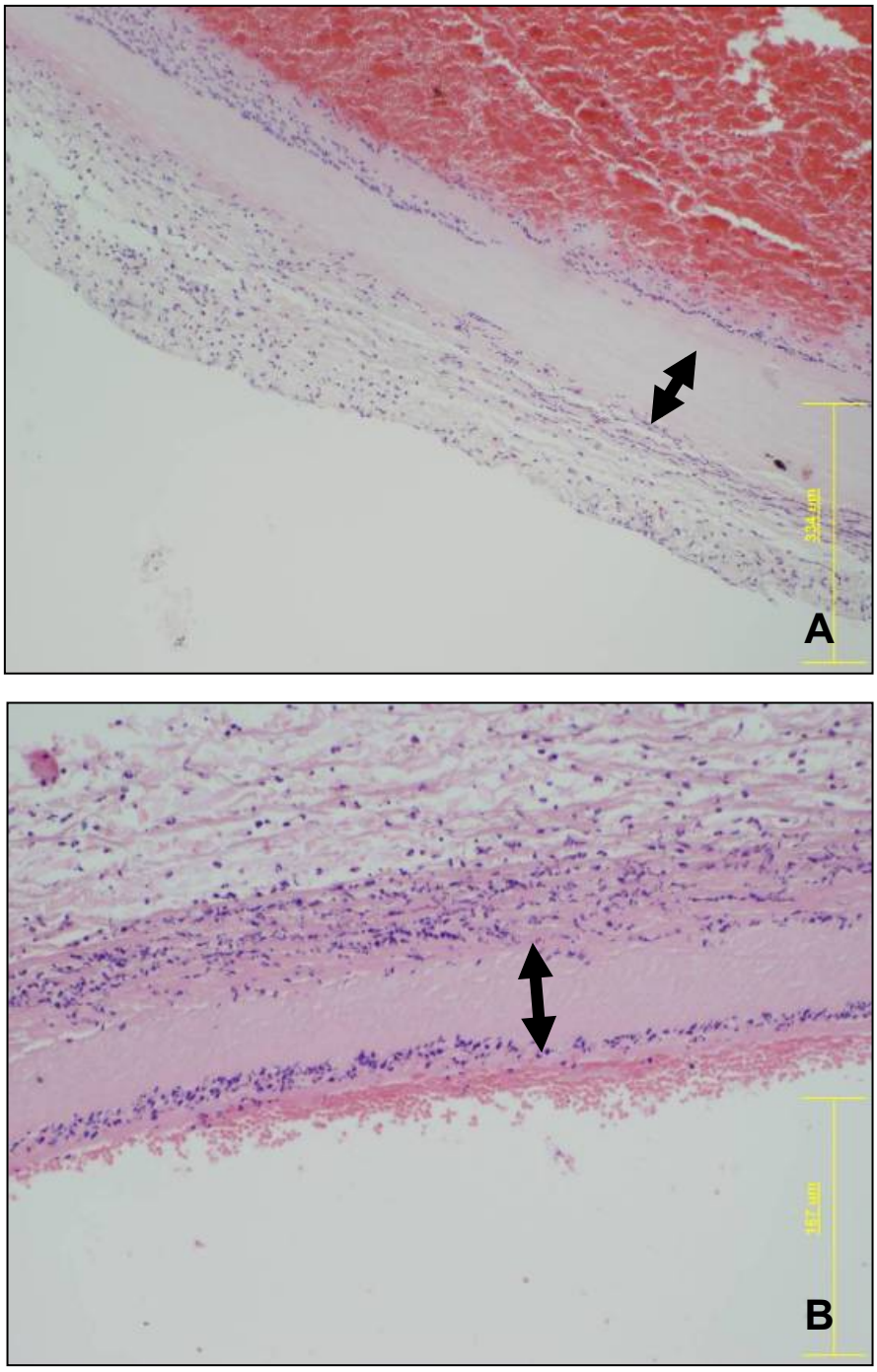


**Fig. 67** H&E stained cross sections of the main artery of the graft harvested 24 hours post-implantation (animal number 8): cells infiltrating the wall of the de-cellularised artery with no signs of clotting within the lumen, double arrows - non-infiltrated by cells part of the arterial wall within proximal (A), and distal (B) end. Yellow bars indicate the scale of the images.

The mesenteric vessels were also well perfused and showed no blood-coagulation. The blood released into ECM was restricted to some small intestinal vessels, but there was no major bleeding within any part of the graft **(Fig. 68)**. Most of the vessels infiltrating the mesenteric and the intestinal part of the graft were the polymorphonuclear cells.

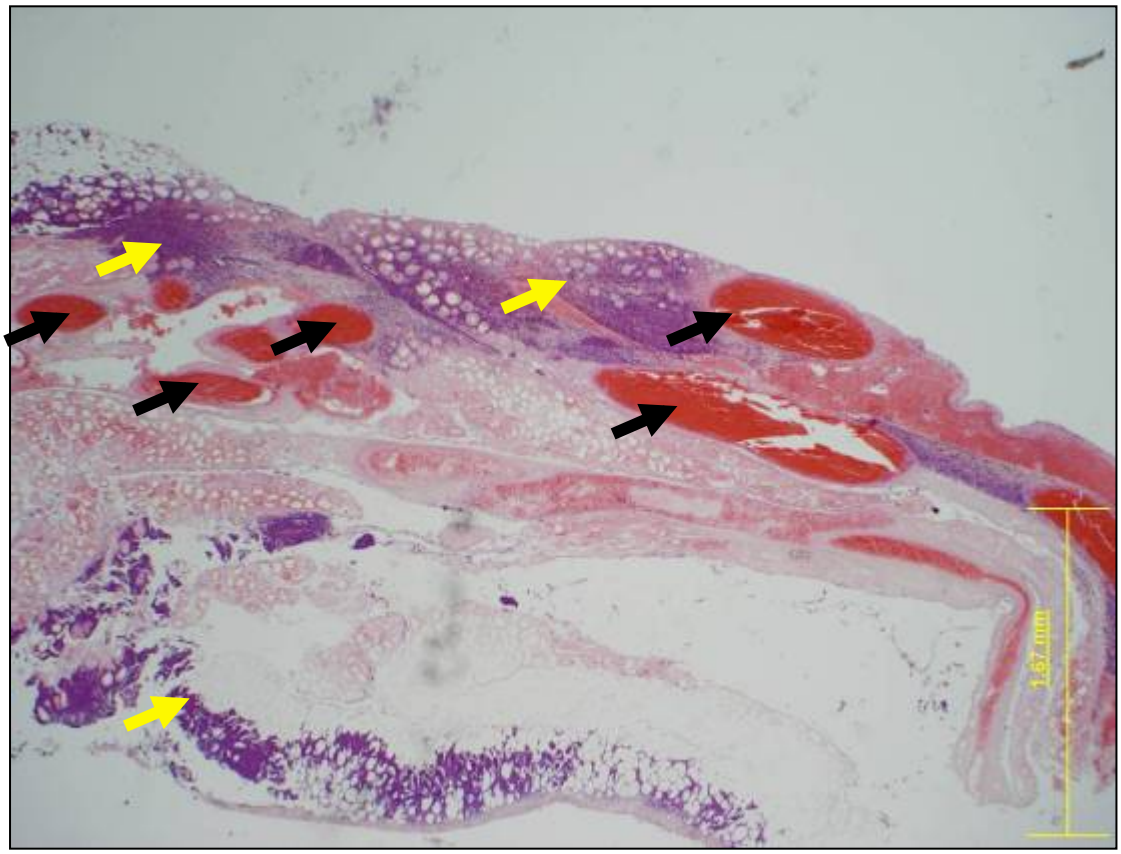

**Fig. 68** H&E stained cross section of the mesenteric arcade of the graft harvested 24 hours post-implantation (animal number 8): clot-free vessels (black arrows) and inflammatory cells infiltrating the outer parts of the graft (yellow arrows). Yellow bar indicates the scale of the image.

Moreover, micro-vessels of intestinal part of the graft were fully perfused with blood and, even the small ones were free of clots. Nevertheless, not all of the micro-vessels were clot-free. In some even though perfusion of blood was still present early signs of clot formation started to appear **(Fig. 69).**

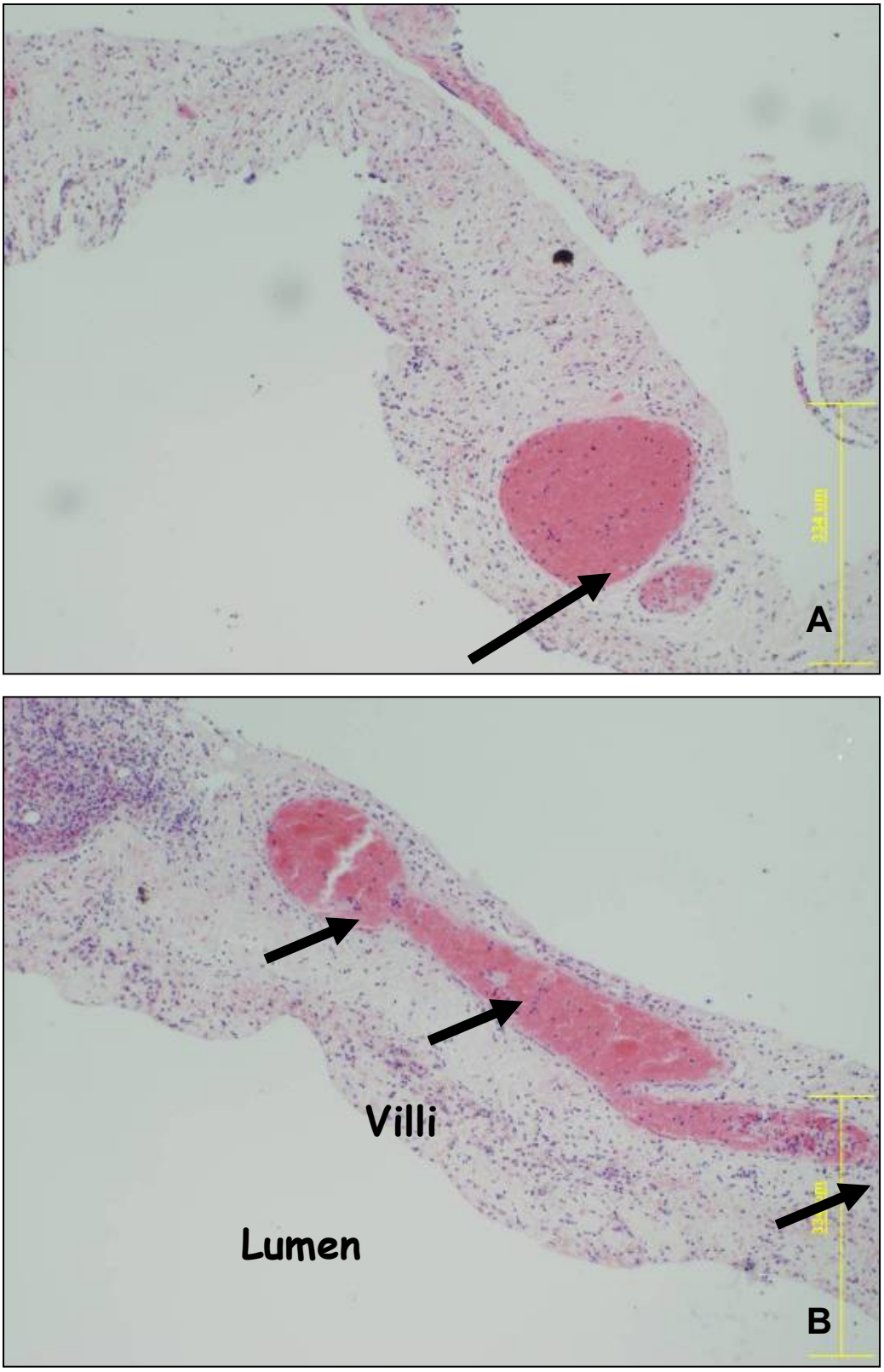


**Fig. 69** H&E stained cross sections of the intestinal part of the graft harvested 24 hours post-implantation (animal number 8): A – clot-free section (arrow indicates no clot formation within fully perfused intestinal vessel), B – early signs of clotting within some of the intestinal vessels (arrows indicate small blood clots). Yellow bars indicate the scale of the images.

Bleeding from leaking vessels was present in limited amounts in the intestinal part of the graft **(Fig. 70)**. All parts of the graft were infiltrated with inflammatory cells.

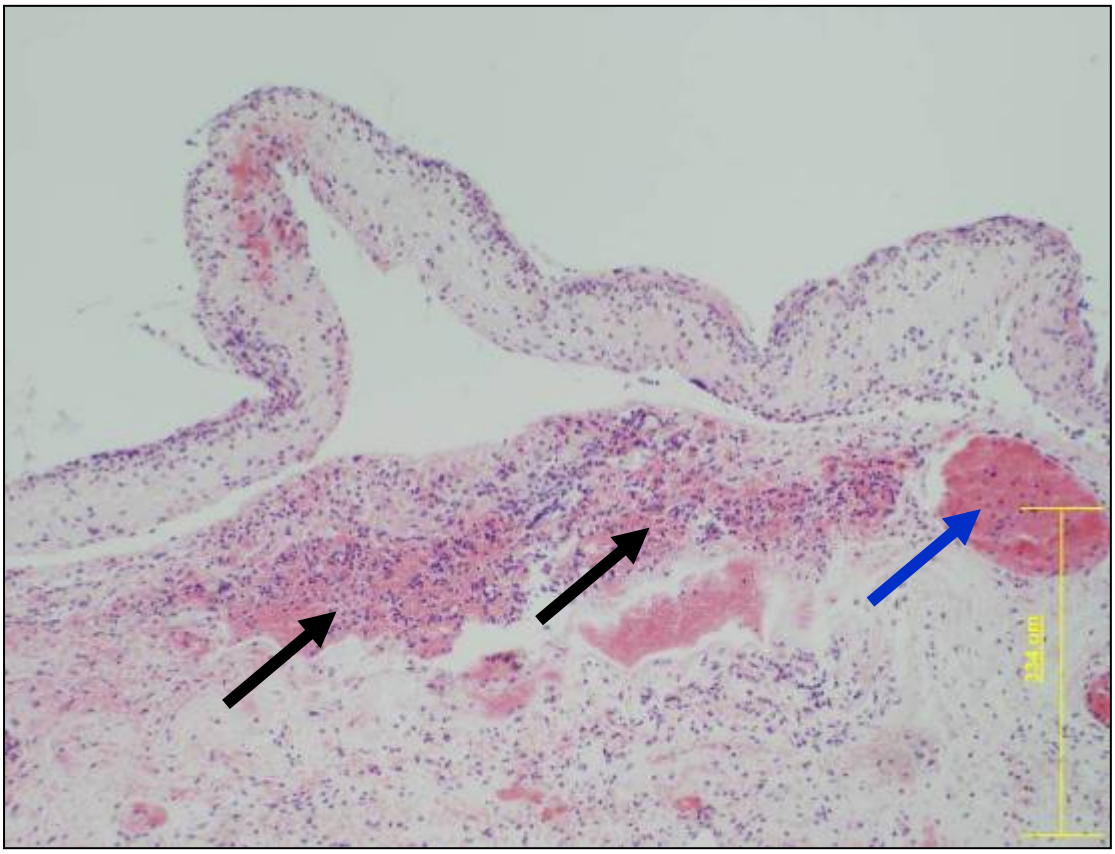

**Fig. 70** H&E stained cross sections of intestinal part of the graft harvested 24 hours post-implantation (animal number 8): black arrows indicate bleeding in between the ECM fibres, blue arrow indicates blood-perfused intestinal vessel. Yellow bar indicates the scale of the image.

### 6.3.4. Immunohistochemical analysis of the grafts

All sections of the implants were stained with CD68 as a marker of macrophages. The CD68-positive (CD68+) cells were present in almost all sections of the grafts implanted for one and 24 hours. Even within one hour post-implantation the donor de-cellularised tissue was infiltrated with CD68+ cells. On the cross section of the anastomotic site, almost all the cells infiltrating the donor arteries and veins were CD68+ and almost no CD68+ could be found within the renal arteries or veins of the recipients. The infiltration with CD68+ cells was also intense in mesenteric arcade

and intestinal parts of the grafts. Many positive cells were involved either in breaking down the blood-clots, gathered on the luminal surface of the vessels, or in the close proximity **(Fig. 71)**. The infiltration of monocytes was even more intense at 24 hours post-implantation.

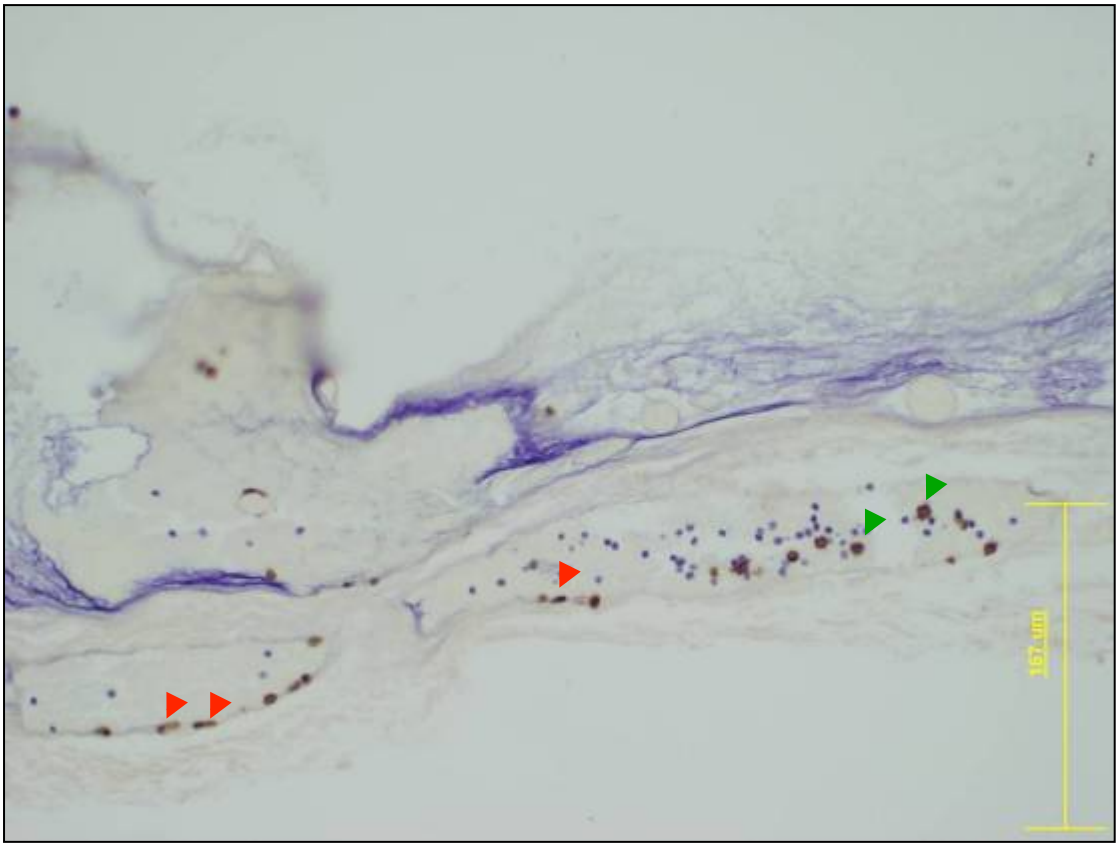


**Fig. 71** Immunohistochemical analysis of the intestinal part of the graft harvested one hour post implantation (animal number 6). Red arrow heads indicate elongated CD68+ cells gathering on the luminal surface of the de-cellularised vessel; green arrow heads indicate round, mononuclear CD68+ macrophages within the lumen of the re-perfused vessel. Yellow bar indicates the scale of the image.

IHC showed that endothelial progenitor cells were present in all of the parts of all grafts harvested one and 24 hours post-implantation. Some were lining the lumen and some could be found in the wall of the vessels. Most of the endothelial progenitor cells (CD133+) lining the lumens of the de-cellularised vessels were of elongated shape. No CD133+ cells could be seen within the recipient vessels. The distal end of

the anastomosed vessels was less populated with CD133+ cells. There were also places where endothelial progenitor cells could not be found **(Fig. 72)**.

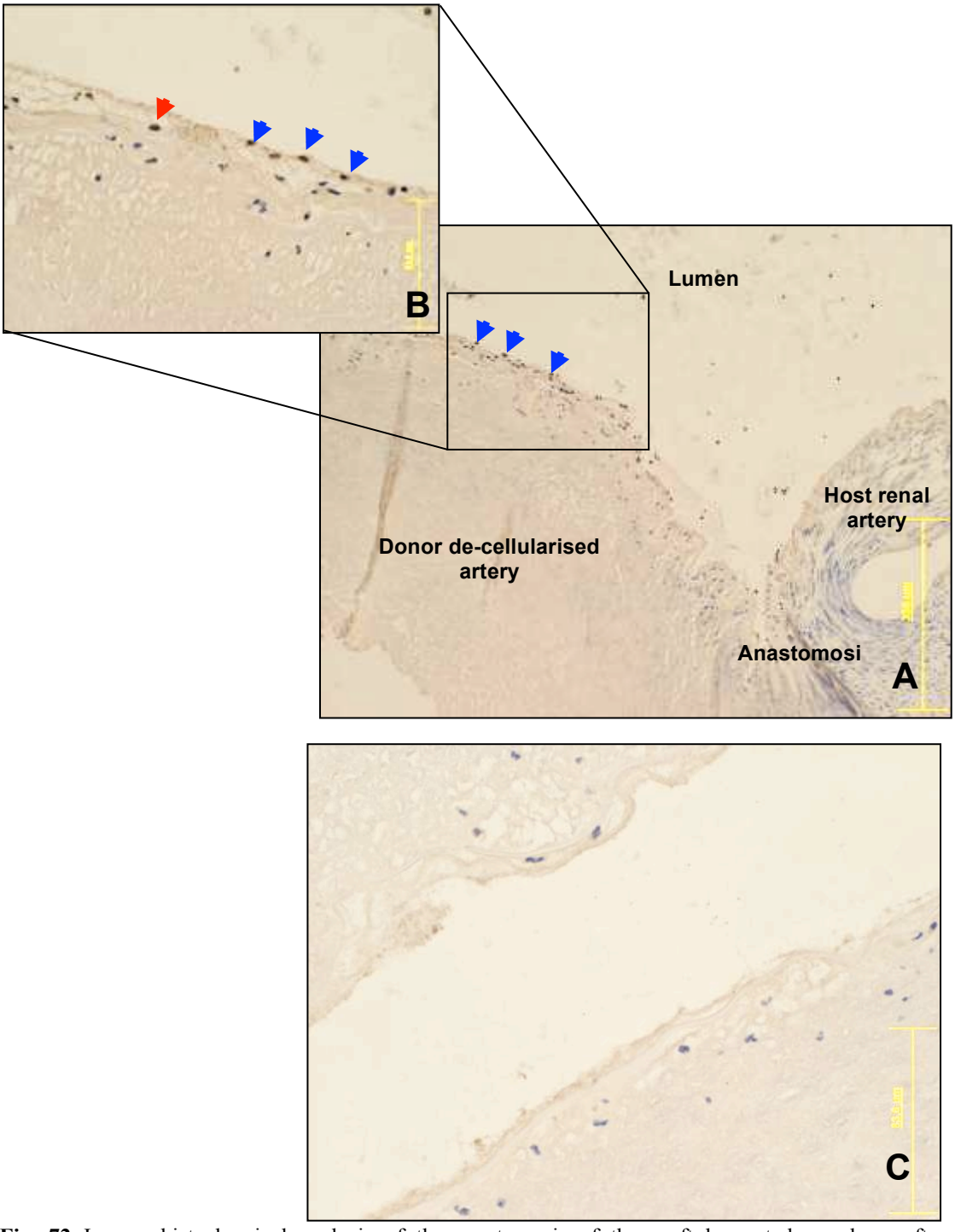


**Fig. 72** Immunohistochemical analysis of the anastomosis of the graft harvested one hour after implantation (animal number 6). A – CD133+ cells line the lumen of the graft's proximal artery (blue arrows); no positive cells could be found in the wall of recipient renal artery; B – magnified de-cellularised artery: CD133+ cells present in the wall of the vessel (red arrow); C – distal end of the anastomosis with no CD133+ cells. Yellow bars indicate the scale of the images.

The sections of the graft harvested 24 hours post-implantation showed more intense infiltration with CD133+ cells, which were present in the feeding pedicle, mesenteric vessels and intestinal micro-vessels. Especially in larger vessels the progenitor cells were located mostly on the luminal surface **(Fig. 73)**.

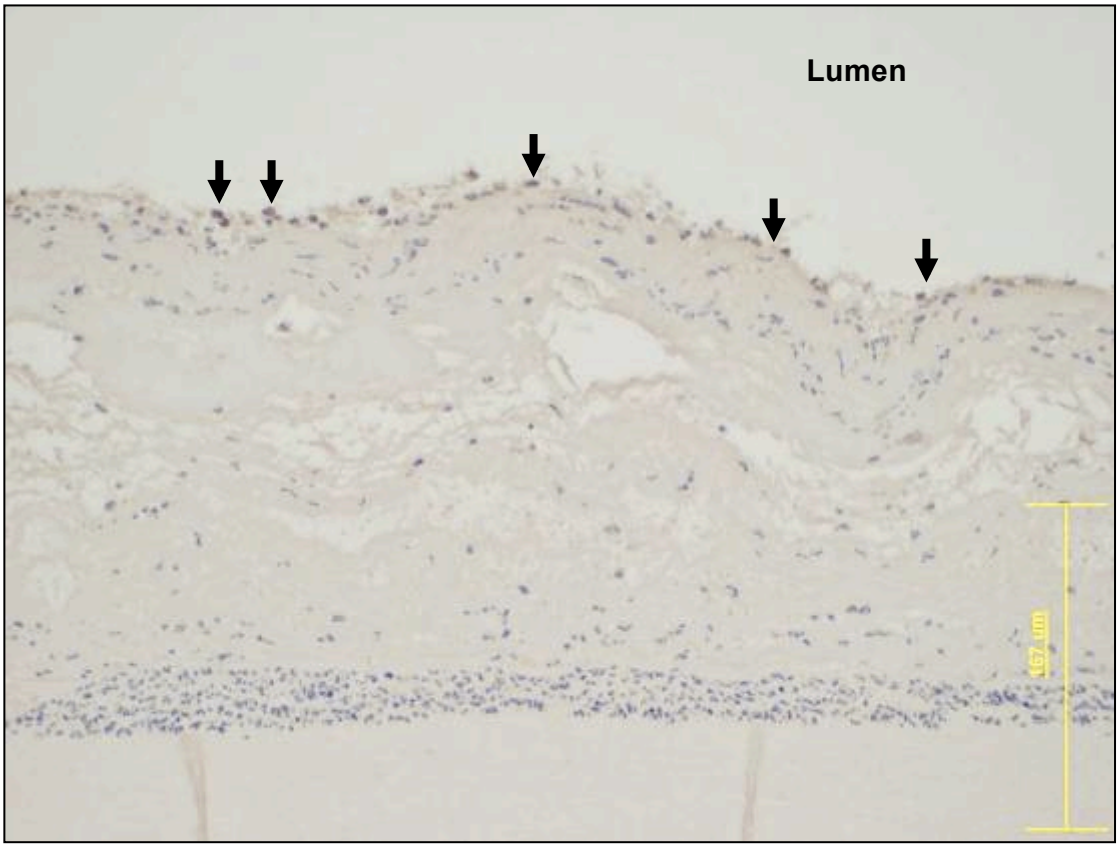


**Fig. 73** Immunohistochemical analysis of the anastomosis of the graft harvested 24 hours after implantation (animal number 8). Arrows - CD133+ cells lining lumen of the donor de-cellularised artery. Yellow bar indicates the scale of the image.

There were some CD133+ cells spread within some parts of the graft harvested one week post-implantation (animal number 2). However, little staining was seen in pre-existing vascular conduits, but was seen at the peripheral parts of the graft where neo-vascularisation was taking place.

Von Willebrand Factor is a glycoprotein present in endothelium and subendothelial connective tissue. All sections of grafts harvested one and 24 hours

post-implantation were marked with anti-VWF antibodies. For comparison non-implanted sections of the scaffold-construct were negative for VWF.

As soon as one hour post-implantation the luminal surface of the graft's de-cellularised vessels was positive for VWF (VWF+). Sections of anastomotic site showed similar amount of VWF+ staining in donor and recipient main pedicle. However, no staining was detected when non-implanted de-cellularised main artery and vein were analysed. Vessels that collapsed or were clotted during the period of the experiment were not positive for VWF. WVF positivity was found only on clot-free surfaces. No VWF+ could be detected within non-implanted mesenteric arcade **(Fig. 74)**. Blood vessels of the graft implanted for 24 hours were also VWF+.

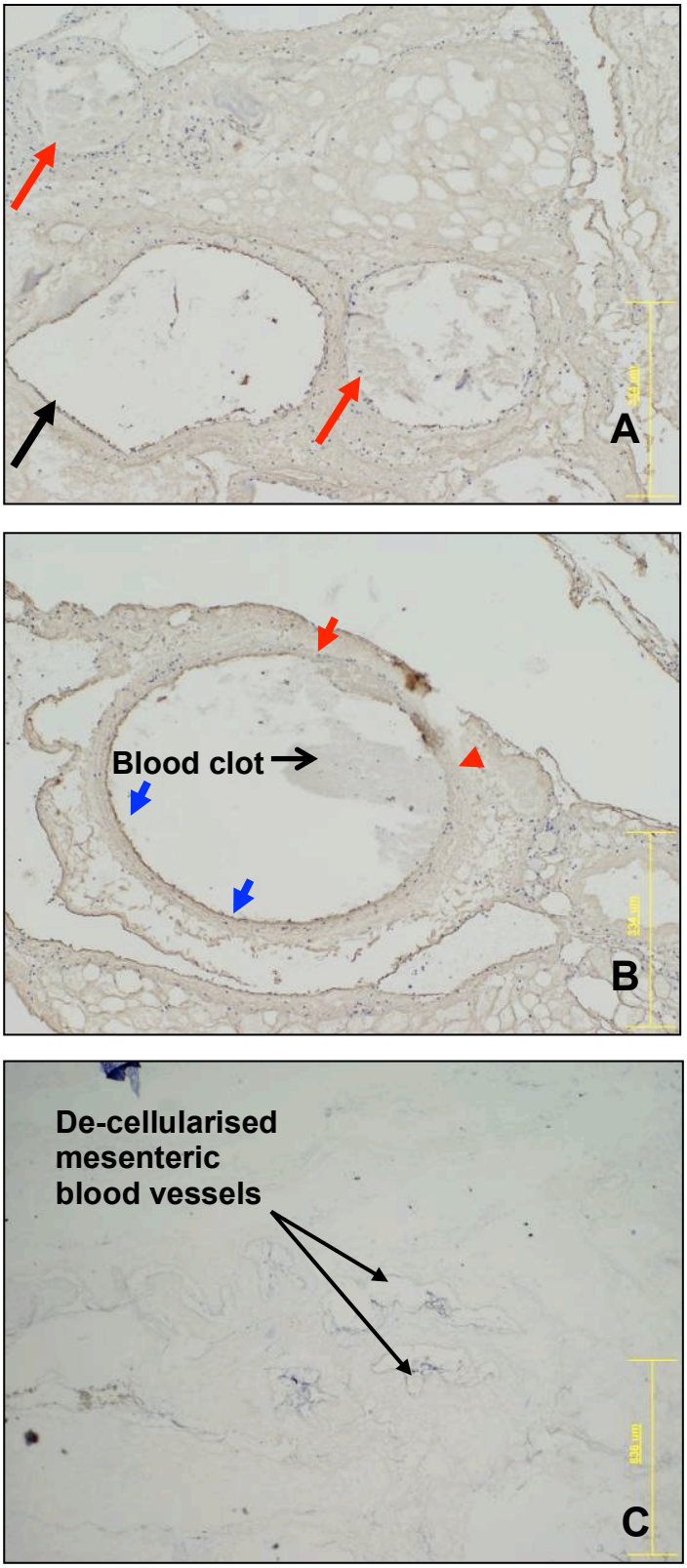


**Fig. 74** IHC analysis of VWF: A - the cross section of the mesentery of the graft harvested one hour after implantation (animal number 1): VWF+ present in perfusable vessels without blood clotting (black arrow) and absent in clotted vessels (red arrows); B – the cross section of mesenteric vessel partly clotted: the VWF+ restricted to non-clotted parts of it (blue arrows); C – the cross section of the mesentery of a scaffold prior-to-implantation showing no VWF+ staining within its vessels. Yellow bar indicates scale of the images.

The staining of the graft harvested one week after implantation expressed endothelial cells' marker (CD31) only in functioning vessels. No smooth muscle cells were detected in any of the scaffolds implanted for either one or 24 hours.

## 6.4. Discussion

Orthotopic implantation of de-cellularised organs is increasingly considered as a more relevant test of mechano-biological properties of the de-cellularised (through the vasculature) tissues and organs than any *ex vivo* experiments (174). These matrices should have the requisite strength and properties to enable them to function adequately under physiological loading. Vascularised scaffolds need to be not only biocompatible, but also minimally thromboreactive, which is the greatest immediate concern. It is well established that platelet activation occurs when platelets come in contact with collagen. Platelets directly adhere by binding platelet collagen receptor to integrins on collagen, and the intrinsic clotting cascade is initiated when prekallikrein, kininogen, factor XI and XII are exposed to collagen (175). Lack of an endothelial lining can make the anastomosed vessels highly thrombogenic, and too gentle an anticoagulation protocol can cause blood clot development in the early stages of surgical procedures.

At the moment, there is no commercially available system that could be successfully incorporated into *in vitro* models of small intestine bio-engineering using de-cellularised porcine ileum. Therefore, the only way to test a scaffold's biomechanical behaviour was introduction of the systemic perfusion *in vivo*. Ongoing studies are focused on pre-seeding vascular and intestinal parts of the scaffold with different cell types (endothelial and organoid units) which in future will be tested *in vivo*. Seeding anti-thrombogenic precursors or heparin lining of capillaries may avoid

coagulation while implanting the scaffold-constructs. However, at present none of the above techniques are ready to be incorporated in the studies and thus, the application of anticoagulants was necessary.

Coagulation of blood and consequential loss of vessels un-clotted was a worry while performing implantations into porcine recipients. Pigs have the most reactive blood coagulation mechanism, clotting the fastest and lysing the slowest (176). This makes them both: perfect to check scenarios of grafts perfusion-ability, and at the same time extremely difficult in terms of obtaining positive outcomes. While no anticoagulation protocol must be applied in studies of ECM-scaffolds under high-sheer and high-pressure (142) when implanting small-diameter, acellular grafts in positions with lower flow velocity and pressure values anticoagulation treatment is necessary (177).

The presented results show that the mechano-biological features of the developed scaffold made it easy to implant and re-perfuse with blood. The developed anticoagulation protocol was sufficient to keep implants perfused for the duration of experiment, without causing excessive bleeding. When other acellular scaffolds composed of vascular tree were implanted, lack of anticoagulation activated thrombosis within 30 minutes post-anastomosis. The only way to eliminate this negative outcome would have been to pre-seed and culturing the vasculature of the scaffold with endothelial cells or progenitors (178). Nevertheless, even in this group preliminary studies involved implantation of seven un-seeded scaffolds into porcine recipient. Moreover, all seven implants resulted in immediate and excessive bleeding from the vasculature, suggesting, that the applied process of de-cellularisation damaged the structure of ECM, especially elastin of the scaffolds vascular tree. As collagen fibres are highly thrombogenic, places of disrupted tunica interna and

internal elastin were inducing clot formation in grafts implanted for one hour. Therefore, it was of high importance to design the de-cellularisation process to preserve these features of ECM and at the same time remove antigenic epitopes. When heparin was used as an anti-coagulative agent the outcome of the implantations was much more positive (174).

The preliminary outcome of the first anastomosis showed great potential, and therefore the decision to conduct a first recovery study was taken. Inefficient anticoagulation and rapid loss of vessels ability to get perfused post-implantation were the cause of the grafts negative outcome. Nevertheless, even these seemingly unsuccessful experiment proved that in places where perfusion was present for the whole time, were well infiltrated with cells, and did not show extensive inflammation or fibrosis. However, it was obvious that the mechanism of this primary perfusion needs to be well established before committing to longer than one hour studies.

The series of following procedures proved that the outcome of testing biological products/scaffolds can very often depend on the donor animals and their anatomical and physiological variability. Therefore, the methods incorporated into the experimental model needed optimizing for a range of biological differences that could contribute to the general outcome of the study. It appeared that while implanting the de-cellularised scaffold the first successful procedure could not be repeated without optimizing anticoagulation protocol. Moreover, additional criteria such as recipient blood pressure, or the length of grafted vessels were the reason for the negative outcome of the graft. Nevertheless, four similar and satisfactory outcomes in the terminal procedures (one hour implantations) could be achieved. What is more, a recovery study using the same protocol resulted in very promising data.

Two short term operations were unsuccessful. The main reason of the failure of the first one was early clotting within the mesenteric arcade. The second implant was unsuccessful largely due to the hypotension within the recipient renal vessels, which in combination with unsatisfactory heparinisation caused early vascular obstruction.

Surprisingly, the length of the anastomosed donor capillaries appeared to be an additional variable, which influenced the outcome of the implantations. Distal parts of the grafts with longer pedicles were characterised with lower blood pressure, which triggered blood clotting within smaller vessels. Taking into consideration all the variables it was possible to optimize dosage of heparin/Warfarin that had to be introduced into the system (through the recipient and the scaffold) to prevent blood clots formation. Some authors suggest that anticoagulation is not recommended for SBS patients, especially children (179), however at this stage of the project it was more important to check the graft's biomechanical behaviours, to prove the concept that it can be re-perfused immediately after implantation, rather then design a viable clinical protocol.

Only when heparin intake was increased to 250-260U/kg/h the anticoagulation was strong enough to prevent clot formation even in intestinal micro-vessels. On the other hand, too harsh an anticoagulation protocol caused excessive bleeding from the graft (animal number 7), and recovery studies could not be continued. Dose of heparin oscillating around 250-260U/kg/h with addition of 12mg/day of Warfarin for three days prior to surgery appeared to be a mostly reliable and an optimal protocol which prevented clotting, but did not cause excessive bleeding within the graft. Even after 24 hours the vasculature was unobstructed and only few vessels contained small blood-clots. At the time of harvest there was small amount of blood within the kidney cavity,

which suggested that the leakage was originating from the graft. Such a state in longer studies (e.g. few days or weeks) could induce overt clinical symptoms. The bleeding could have been caused by the animal placing too much physiological tension on the fragile de-cellularised vessels while moving. Moreover, high doses of the anticoagulative drugs would prevent blood from clotting and naturally strengthening the acellular vessels. In future it would be advisable to separate fragile scaffold from abdominal content by use of surgical bowel bags.

There was some leakage from the vascular channels into the matrix. However most of the fluid was exiting via the venous outflow. Most of the blood was gathered underneath the serosa. Similar problems were encountered when Peterson et al. performed *in vivo* studies of de-cellularised lung tissue in rat model (180). Nevertheless, the bleeding from the intestinal scaffold was significantly limited after 24 hours post-implantation. In long term studies while vessels are re-cellularised, new ECM is being produced and there is less leakage from the loose collagen fibres of micro-vessels (181). Moreover, as the endothelium is being formed, or vessels are seeded prior to implantation the need for anticoagulation is lower.

Little information is available on the re-cellularisation of plain de-cellularised biological scaffolds in the systemic circulation. This study proves that the ingrowth from the host tissue happens immediately after implantation, but the deposition of the progenitor cells and macrophages from the blood stream is also possible. All the successfully integrated grafts proved to be highly biocompatible and as soon as one hour post-implantation the proximal ends of anastomosed vessels were re-populated with the host cells. It has been shown that the majority of the cells residual in the tissue engineered grafts come from host tissue rather than the seeding process (182).

Comparing the histological sections of the scaffolds that stopped perfusing blood within the first half hour *in vivo*, with the ones that stayed clot-free, the rate of the scaffold infiltration with host cells was lower. Many more cells were always visible within the anastomotic site than in other parts of the implants, which indicated that cells were coming from direct tissue-tissue rather than blood-tissue contact. Yet, cells were also visible in distal parts of the grafts, in the vicinity of open, blood perfusing vessels. The cells infiltrating the scaffold-construct within first hour post-implantation are mainly polymorphonuclear cells and macrophages. Immunohistochemical analysis proved that majority of the cells repopulating grafts implanted for one and 24 hours into porcine recipient were macrophages and monocytes. Recently, as stated in the previous chapter it has been identified that macrophages' activity is very important in constructive remodelling of the graft and as well inducing rejection of the implant it also can promote regeneration or site specific tissue formation (183). Moreover, macrophages are very plastic cells and are responsive to cell-cell and cell-matrix cross-talk: *in vivo* that monocytes and macrophages can have the propensity for endothelial trans-differentiation (184). Moreover, 24 hours post-implantation endothelial progenitor cells could be found on luminal surfaces. In grafts explanted after one hour CD68+ cells were found in abundance. As a result of exposure to higher sheer-stress levels endothelial progenitors and macrophages were mobilized, which was confirmed by differences in re-population with CD133+ and CD68+ cells within arterial and venous anastomotic sites. More endothelial progenitors were present in proximal parts of the acellular vessels. However, some were delivered with systemic perfusion into distal, smaller mesenteric vessels, as one of the roots for re-endothelialisation (185).

Absent in non-implanted scaffolds VWF+ staining was found on clot-free luminal surfaces of vessels within the grafts implanted for one and 24 hours. This means that the staining is indicating the dynamic surface of the blood activity rather than subendothelial proteins. VWF is blood glycoprotein involved in haemostasis, and its expression within the vasculature of the implants was a consequence of its interaction to collagen and not indication of endothelial activity. Moreover, the implants showed infiltration with progenitor cells which over time could possibly become mature endothelium with all the trans-membranous proteins, but this differentiation has been reported to last at least two weeks (175).

All parts of the graft were infiltrated with cells 24 hours post-implantation. Some of the ones present on the lumenal surface and within the vascular wall had elongated shape, similar to endothelial and fibroblast-like cells. However, except some randomly placed cells on the periphery of the vascular wall no other αSMA+ staining was detected.

Interestingly, there was one part of the graft that did not get re-populated with any cells. It was the media (central part of the vascular wall) of grafted main artery (**Fig. 67**). The cells were lining the lumen and re-populating the outer part of the wall. However, not even one cell was seen in middle section. That kind of selective infiltration pattern was reported when other de-cellularised vessels were tested *in vivo* (186). One explanation could be the fact that highly organised ECM of central part of the vascular wall is more resistant to cellular infiltration. It is possible that this organisation of fibres is very specific to smooth muscle-like cells.

The 24 hours old graft was infiltrated with inflammatory cells, but no severe immune response could be seen in any of its parts. Nevertheless, the period of experiment was too short to definitely say that no chronic reaction was expected.

After 24 hours *in vivo* there was less macrophages within the arterial anastomotic site than within the venous one. On the other hand, high numbers of CD133+ cells were still present in the arterial anastomotic site and not many CD133+ cells were seen within the grafted vein. It could suggest that in the first instance the macrophages re-populate de-cellularised tissue and induce ECM remodelling which then attracts progenitor cells. The rate of infiltration with host cells of arterial anastomotic site was higher than the venous one in all the grafts (181).

Taking everything into account it was demonstrated that the de-cellularised tissue was easy to implant and re-perfuse (using adequate anticoagulation protocol) and trigger cellular infiltration and possible differentiation towards functional endothelium. It is a satisfying initial phase of constructing complex tissue constructs. It could be a good proof of principle for incorporating the scaffold into *in vitro* phase, where vasculature and intestinal segment can be separately and simultaneously seeded and cultured in a bioreactor.

# Chapter 7.

# Isolation and characterisation of porcine organoid units and endothelial cells

## *7.1. Background and aims*

The epithelial lining of the gastrointestinal tract is the most rapidly proliferating tissue in the body. As described in Chapter 1 this constant state of renewal of differentiated epithelial cells is sustained by a continual supply of progeny from multipotent progenitors that originate from stem cells located within the intestinal crypts. In addition to supporting normal epithelial homeostasis, intestinal stem cells are thought to play an important role in the rapid expansion of the gut during development, tissue regeneration following injury or surgical loss, and malignancy (187).

The above caused a tremendous increase in the study of stem cells in both homeostatic and disease states in the past decade. Our understanding of intestinal adult stem cell biology and (how stem cells fit into a niche, and how that niche influences them) has significantly increased. However, this knowledge results largely from indirect measurements of their behaviour, as very little is known about the specific markers that could be used to isolate and characterise intestinal stem cells. Furthermore, their specific location and function within a well-established intestinal stem cells niche makes it difficult to culture them *in vitro*. Thus, growing of intestinal

epithelium containing stem cells has many limitations. Established cell lines are predominantly fetal or transformed and bear little resemblance to normal adult intestine in terms of growth factor responses, susceptibility to apoptosis, gene expression, and differentiation (116). Currently the only method to isolate intestinal stem cells, and preserve their ability to proliferate and differentiate into adult intestinal epithelium has been described by Evans et al. (73). As mentioned before intestinal OU isolated from neonatal rats (73) or juvenile pigs (80) with preserved intact stem cells and their niche have been shown to generate mature tissue *in vivo* (116).

The recent description of several potential markers and the use of transgenic mice and advances in neomucosa creation have provided a tremendous advancement in current understanding of these cells. The first such marker identified in the small intestine, Musashi-1 (Msi-1), is expressed within a broad region of the stem cell zone of the crypt (187). *Lgr5* was initially identified as a Wnt target gene expressed in colon cancer, and is the first marker to identify the cells between the Paneth cells (188). *Lgr5*-positive cells were shown to be active in the cell cycle, dividing once approximately every 24 hours. Lineage tracing experiments showed that *Lgr5*-positive cells were capable of generating the entire villus epithelium (187). Recently doublecortin and CaM kinase-like-1 (DCAMKL-1), a microtubule associated kinase in postmitotic neurons, has been shown to colocalize with Msi-1 staining, however with a more restricted expression (189).

The aim of the experiments presented in this chapter was to establish the method of isolation of porcine intestinal organoid units, and using available stem cell markers to localise them within isolated clusters. Organoid units were isolated from juvenile and adult donors. The obtained populations could be used in future

experiments for seeding de-cellularised intestine to promote neomucosa creation, which would be a completely novel approach in targeting small intestine tissue engineering. The method of isolation adult, porcine, intestinal organoid units has not been described before.

Moreover, the isolation, and *in vitro* propagation of endothelial cells was characterised with the aim of incorporating them into future experiments for seeding the vascular part of the scaffold presented in chapter 3.

The experiments presented in this chapter characterise the structure, but the functionality of isolated OU and cells is yet to be proven.

## *7.2. Methodology*

This chapter describes the method of isolating porcine OU from a piglet and three adults, characterization of their yield and IHC labelling of intestinal stem cells.

The isolation of endothelial cells was carried out once as the methods of obtaining relevant amounts of endothelial cells are well described in literature. Nevertheless, it was important to optimise and make ready the protocols for harvesting and characterising cells prior to the seeding experiments.

### 7.2.1. Materials

The list of materials and equipment used in experiments described in this chapter is presented in **Appendix 4**.

## 7.2.2. Animal husbandry

All animals were maintained and handled similarly to the process presented in Chapter 3 (3.2.2).

## 7.2.3. Solutions

Solutions used in experiments presented in this chapter are described in **Appendix 16**.

## 7.2.4. Isolation and characterisation of porcine intestinal organoid units

### *7.2.4.1. Isolation of porcine organoid units*

Under sterile conditions 10 cm of jejunum (n=1) was resected from a 6 weeks old piglet (11 kg), 10 cm of jejunum (n=3) and ileum (n=3) from an adult White Crossbred pig. First, the lumens were flushed with room temperature saline solution and then with cold Hank's Balanced Salt Solution (HBSS) to clean the luminal content. The specimens were then cut into 1mm$^2$ squares using a tissue cutter. These were washed three times with 4ºC HBSS, sedimenting for at least 1 minute between washes. Subsequently the specimen was digested with enzyme solution on an orbital shaker at 37 ºC for 30 minutes (piglet) or 2.5 hours (adult pig). The digestion was immediately stopped with three washes of a 4ºC Dulbecco's Modified Eagle's Medium (DMEM) solution. The organoid units were centrifuged between washes at 150 rpm for 5 minutes, discarding the supernatant. Finally the organoid units were reconstituted in DMEM solution and their yield was checked and histological smears were prepared.

### *7.2.4.2. Characterization of the yield of porcine intestinal organoid units*

To establish the yield of the isolation process, OU were counted in the haemocytometer and their viability was checked. Immediately after isolation, 100µl of organoid units' solution was spun down and the pellet was re-suspended in PBS. Trypan blue solution was added to the suspension to obtain 1:1 dilution. The pellet was broken down by pippeting up and down and 10µl of the prepared solution was placed in a haemocytometer. The number of intestinal organoids seen in five separate grid squares was recorded. The organoid units' viability was checked by counting units, which did not stain with the dye against the dead ones that appeared blue. Each grid square measured 1mm x 1mm with a depth of 0.1mm corresponding to a volume of 0.1µm. Since the total volume of resulting OU suspension was known, the yield was calculated per 10cm of intestine.

### *7.2.4.3. Immunohistochemical visualization of intestinal stem cells within the porcine organoid units*

Organoid units reconstituted in DMEM were spun down and re-suspended in PBS. Subsequently smears of cell clusters were prepared on APTS slides by placing 40µl (one drop) of solution onto the slide. The liquid was gently spread out using a pipette tip on a slide surface and left to dry overnight. The following day the slides were fixed in 1:1 solution of ice-cold acetone and methanol for 2 minutes at 4 ºC and left to dry at room temperature overnight.

Fixed slides underwent IHC staining of intestinal stem cells within the organoid units using DCAMKL-1 antibody **(Table 8, Appendix 9)**. The staining was performed in a way described in sub-chapter 3.2.6.3.

## 7.2.5. Isolation and culture of porcine endothelial cells and their characterisation

### *7.2.5.1. Preparation of gelatin-coated glass coverslips*

Gelatin solution was autoclaved and cooled down to room temperature. Glass coverslips were heated in nitric acid solution, and rinsed under running distilled water. Then they were transferred to a conical tube containing 70%EtOH solution and stored till the day of the experiment. Two hours prior to the cells isolation coverslips were placed in the wells of the culture plates and rinsed twice with sterile distilled water. The culture surfaces of the coverslips were coated with gelatin solution (10μl/$cm^2$) and allowed to dry at least for two hours (with lid partially open) under the laminar flow, before introducing cells and medium.

### *7.2.5.2. Isolation of porcine endothelial cells*

Under sterile conditions a 5cm segment of jugular vein was resected from an adult White Crossbred pig. First it was flushed with Dulbecco's PBS (D-PBS) and filled with Collagenase F solution. The vein was then incubated at 37°C (gassed with 5% $CO_2$ at 100% humidity) for 15 minutes. The endothelial cells solution was placed in centrifugation tubes, and the collagenase activity was stopped by adding supplemented standard medium. After centrifugation at 1000rpm for 5 min, the supernatant was discarded and the pellet resuspended in PBS. This procedure was repeated twice before the pellet was suspended in endothelial cell growth medium. Cells were seeded onto 6-well-plates supplemented with gelatin-coated coverslips and

cultured at 37°C (gassed with 5% $CO_2$ at 100% humidity) for two weeks. The culture was passaged twice (day 5 and 10), and the medium was changed every second day.

#### *7.2.5.3. Yield and viability analysis of harvested and cultured endothelial cells*

Harvesting of cells from gelatin-coated coverslips was performed by incubation for 5 minutes in 37°C trypsin solution. Trypsin was inactivated by adding supplemented standard medium to wells. Following trypsin solution treatment cells were centrifuged and washed in PBS. Their yield and viability were checked on day 0, 5, 10 and 14 using haemocytometer in a similar matter as described above.

At the end of the experiment the coverslips were removed, washed in PBS, fixed in ice cold acetone and methanol (1:1) for 10 minutes at -20°C, and air dried.

#### *7.2.5.4. Immunocytochemical characterisation of cultured endothelial cells*

The cells identity was confirmed performing immunocytochemical staining (ICC) using anti-Factor VIII antibody (A0082). First cells were washed three times in PBS and immobilized for 10 minutes using Triton X solution. Then coverslips were washed 3 x 3min in PBS and non-specific staining was blocked with Dako Protein Block for 30 min. The primary antibodies were applied in dilution of 1:200 overnight. On the following day the coverslips were washed 3 x 3 min in PBS and incubated with Anti-mouse ImmPRESS kit for 30 min. Following three washes in PBS (3 x 3min) coverslips were incubated with chromogen (DAB) for 3 minutes and washed with distilled water. Coverslips were then counterstained with Harri's haematoxylin and mounted onto histological slides.

## 7.3. Results

### 7.3.1. Isolation of porcine intestinal organoid units

The process of isolating the organoid units from jejunum of a piglet was successful, however the digestion of the tissue needed to be harsher and longer when using small intestine of an adult animal. The isolated organoid units were clusters of mesenchymal and epithelial cells of different size **(Fig. 75)**. Some were very similar in appearance to rat organoid units **(Fig. 75 A)** measuring 50 (width) -200 (length) µm, others appeared to be as big as single intestinal crypt/villi. Their lengths exceeded 350 µm **(Fig. 75 B)**. Nevertheless they were always composed of a mesenchymal core and external epithelial layer.

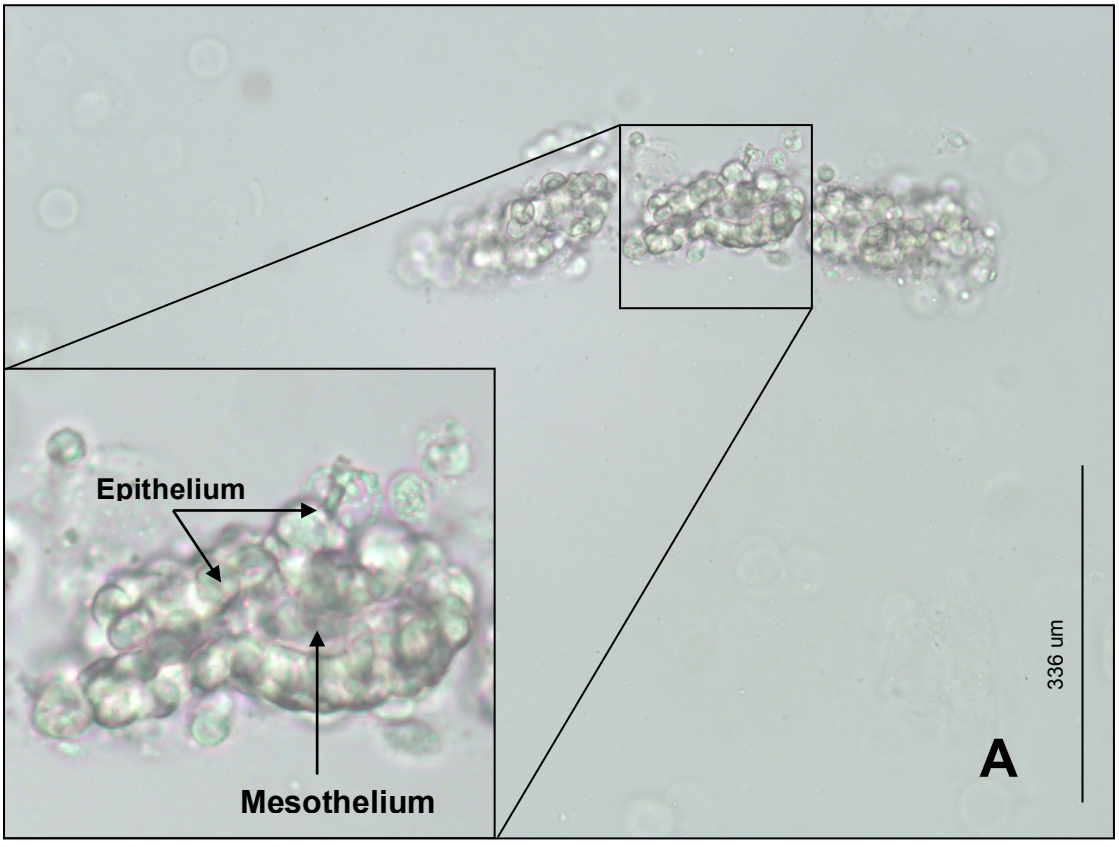

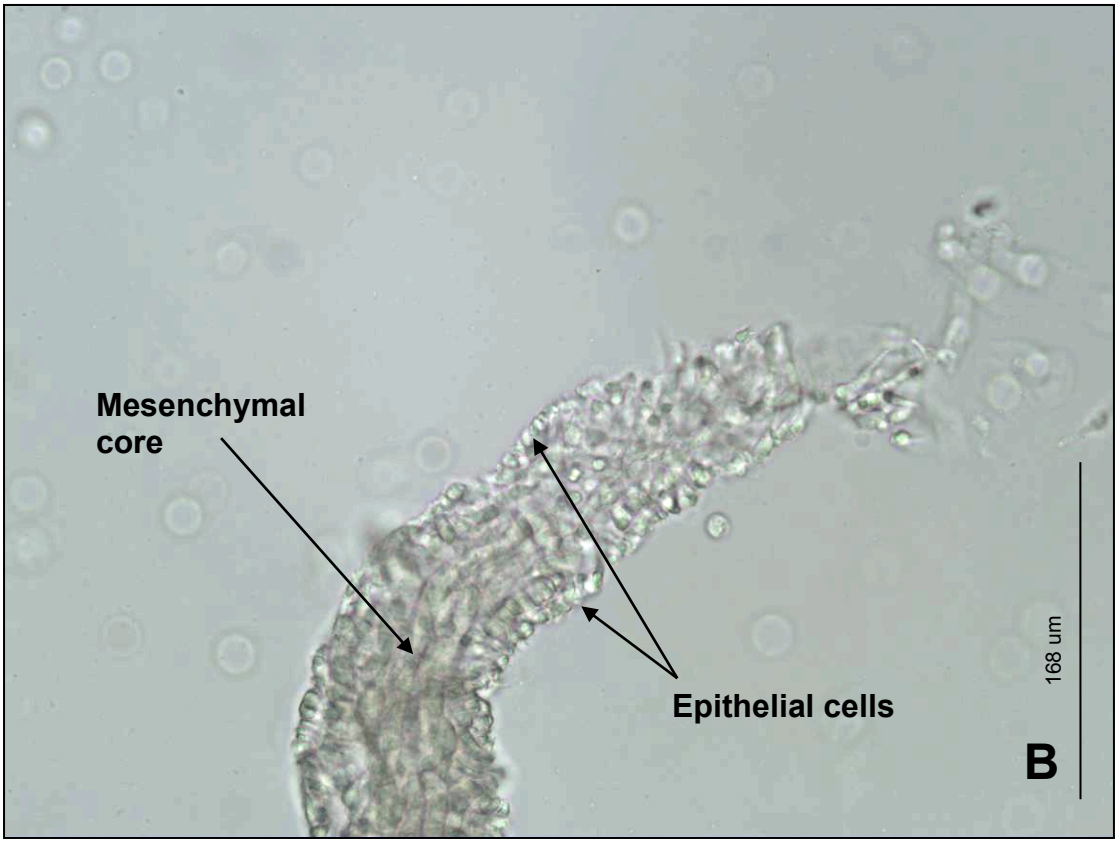


**Fig. 75** Intestinal organoid units isolated from an adult pig, containing mesenchymal cells in the centre and epithelial layer on the periphery: A – small units measuring 50-200µm; B – large, crypt-size units measuring more then 350 µm in length (for comparison of crypts morphology see **Fig. 1**). Bars indicate the scale of the images.

Final suspensions of OU obtained from adult intestines contained much more cellular components (both epithelial and mesenchymal), as well as some unbroken sections of *muscularis mucosae.*

## 7.3.2. Characterization of the yield of porcine intestinal organoid units

Using a more gentle protocol the amount of organoid units isolated from piglet jejunum was comparable with the amount of OU harvested from the ileum of an adult animal. It was possible to obtain 250 000 OU per ml of PBS which was equal to 5 000 000 OU isolated from 10cm-long segment of jejunum. The average amount of the intestinal OU isolated from ileum of an adult pig was 263 333 OU/ml which was equal to 5 266 667 OU per 10cm of ileum **(Table 22)**. On average much less organoid

units could be obtained using the same protocol from jejunum of an adult pig (170 000 OU/ml = 3 400 000 OU/10cm of jejunum). However, high standard deviation values showed high variation within that group, with one procedure resulting in isolating 280 000 OU/ml (5 600 000 OU/10cm of jejunum) whilst another as little as 80 000 OU/ml (1 600 000 OU/10cm of jejunum).

**Table 22** Yield analysis of intestinal organoid units isolated from adult pigs; STDEV – standard deviation.

| *Tissue* | *Animal weight [kg]* | *Organoid units/ml of PBS [OU/ml]* | *Average OU/ml (STDEV)* | *Total organoid units in 10cm of small intestine* | *Average OU/10cm of small intestine (STDEV)* |
|---|---|---|---|---|---|
| *Ileum* | 55 | 270 000 | 263 333 (11 547) | 5 400 000 | 5 266 667 (230 940) |
| | 65 | 250 000 | | 5 000 000 | |
| | 62 | 270 000 | | 5 400 000 | |
| *Jejunum* | 50 | 280 000 | 170 000 (101 489) | 5 600 000 | 3 400 000 (2 029 778) |
| | 65 | 80 000 | | 1 600 000 | |
| | 60 | 150 000 | | 3 000 000 | |

Viability tests showed that isolated OU were intact and contained a majority of viable cells, although some of the epithelial cells of the isolated OU were not viable - which is to be expected with this type of isolation **(Fig. 76)**. Nevertheless none of the analyzed organoid units were composed of only dead cells. Most of the mesenchymal and epithelial cells had intact cytomembrane and did not show any trypan blue intake.

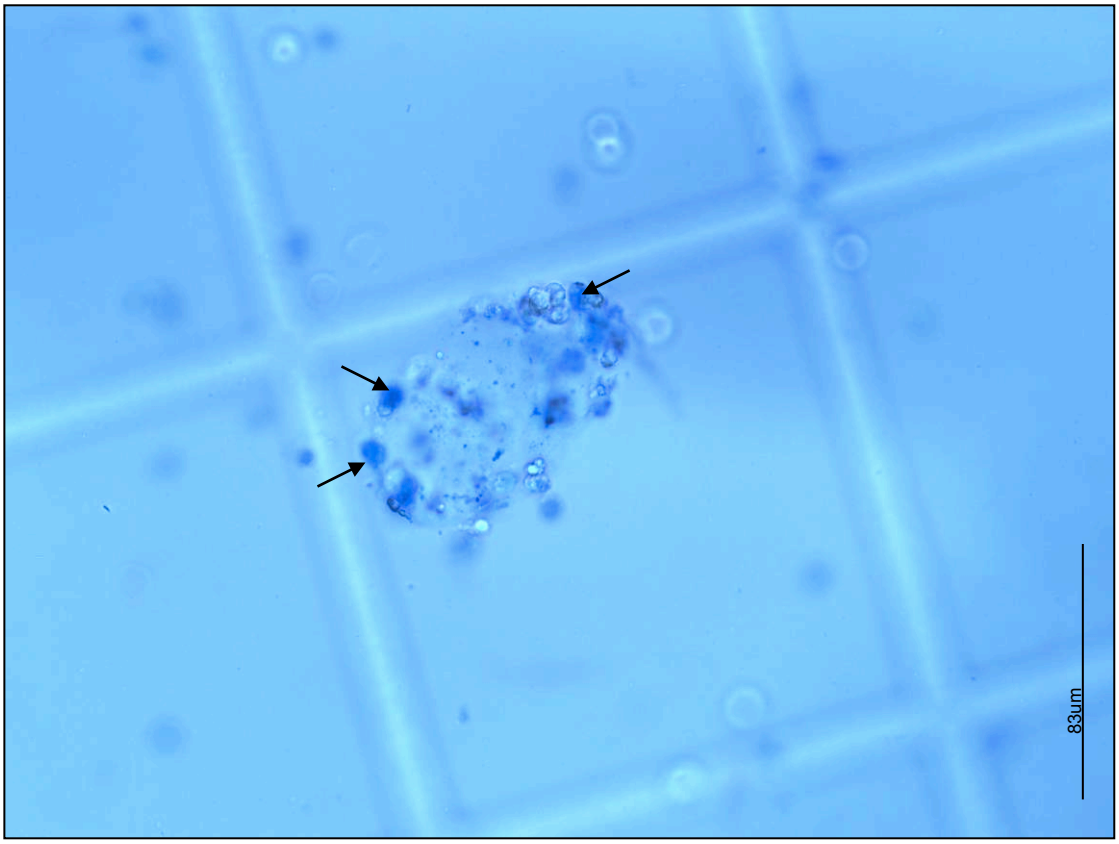


**Fig. 76** Trypan blue-stained intestinal organoid units isolated from an adult pig, some dead (blue) cells can be seen on the periphery of the cluster (arrows), however most of the cells within the unit stayed alive. Bar indicates the scale of the image.

### 7.3.3. Immunohistochemical visualization of intestinal stem cells within the porcine organoid units

The intestinal stem cells were successfully identified in both small intestine and intestinal organoid units **(Fig. 77, 78).** The DCAMKL-1+ cells were present in OU isolated from both: piglets and adult animals. However, not all OU contained DCAMKL-1+ cells. Some organoids had the morphology of the OU but contained no stem cells **(Fig. 79)**. The DCAMKL-1+ cells found in the small intestine were mostly restricted to the intestinal crypts. Nevertheless, some odd cells could be also seen towards the villi **(Fig. 78)**.

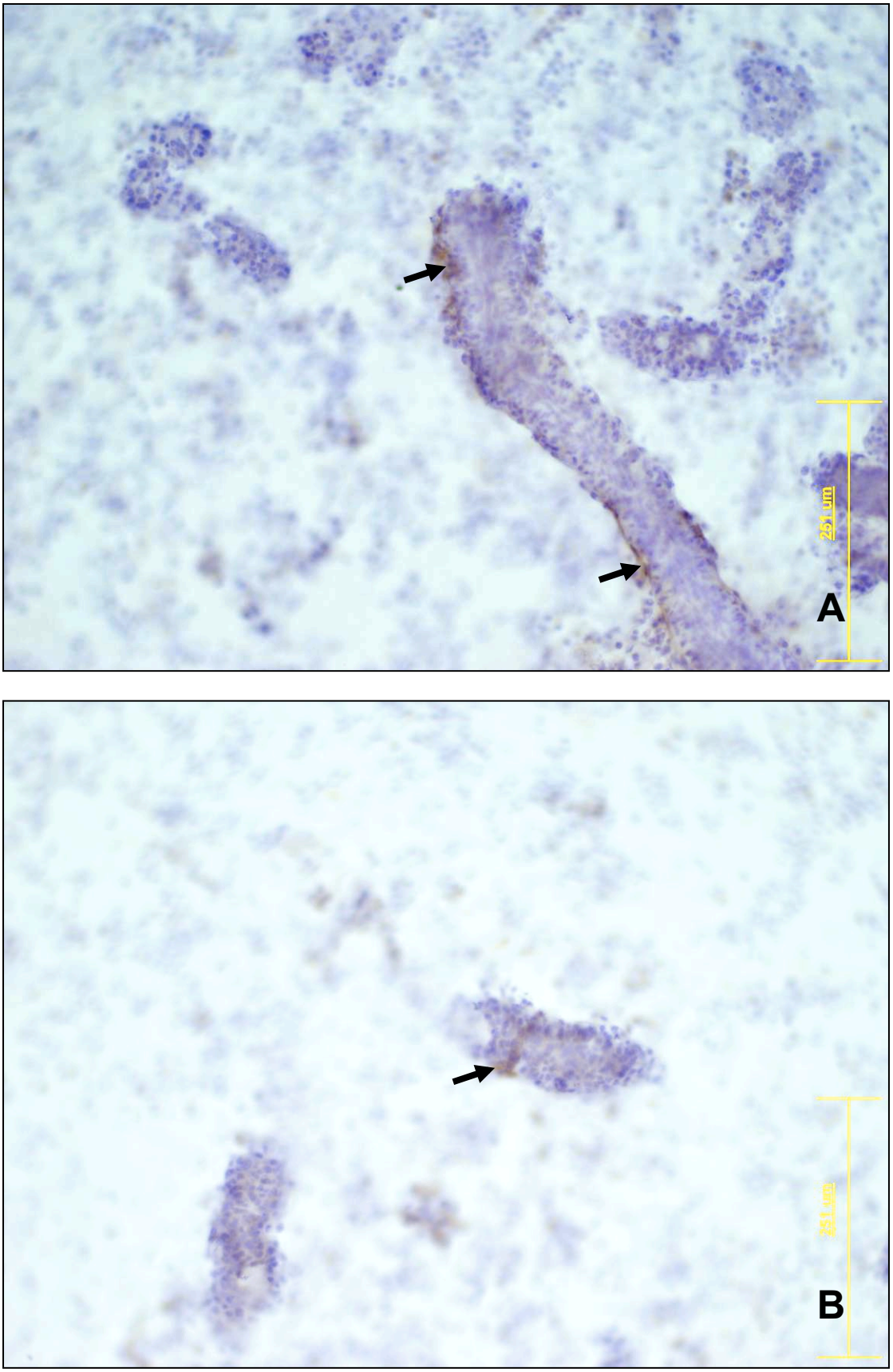


**Fig. 77** IHC analysis of the intestinal stem cells within the isolated from an adult pig intestinal organoid unit. A – large, crypt-like units; B – smaller OU. Arrows indicate brown, positively stained with anti-DCAMKL-1antibodies cells within the OU. Bars indicate the scale of the images.

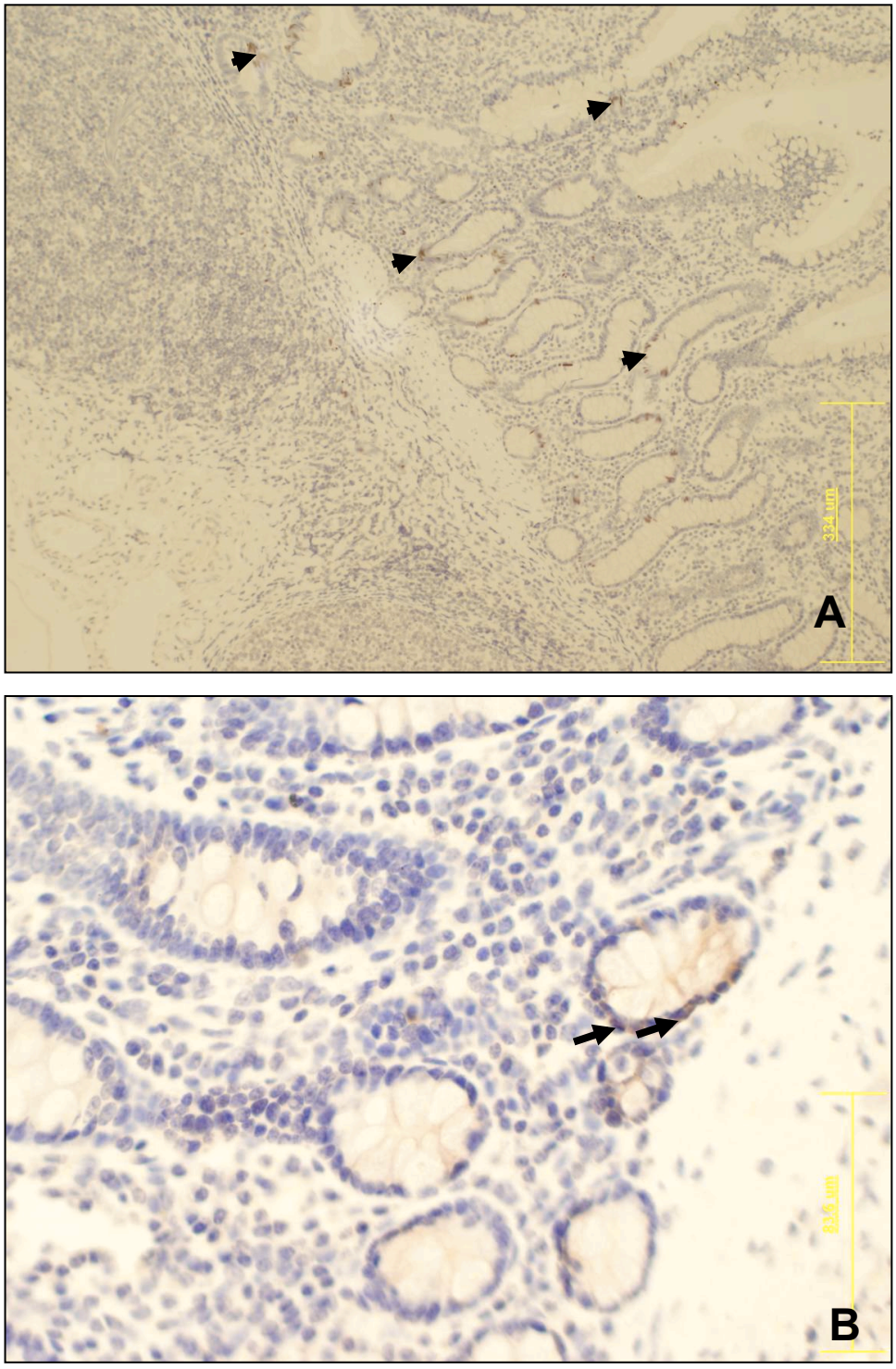


**Fig. 7**8 IHC analysis of intestinal stem cells within the ileum of an adult pig. A- low magnification; B – high magnification. Arrows indicate brown, positively stained with anti-DCAMKL-1antibodies cells. Bar indicates the scale of the image.

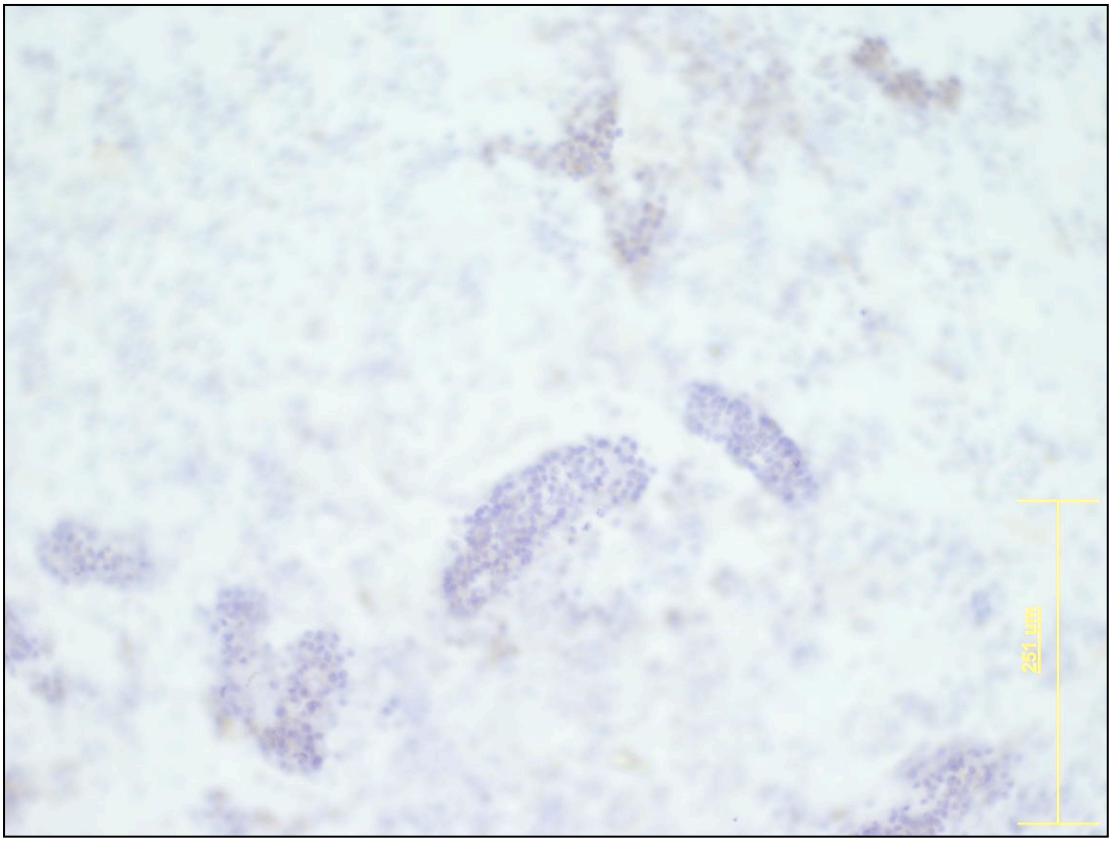


**Fig. 79** IHC analysis of intestinal stem cells within the isolated from an adult pig, intestinal organoid units. No brown, positively stained with anti-DCAMKL-1antibodies cells within some of the OU. Bar indicates scale of the image.

## 7.3.4. Isolation of endothelial cells and their characterisation

The process of isolation of endothelial cells from a 5 cm long segment of porcine jugular vein was conducted once and resulted in the yield of 240 000 cells and high viability **(Table 23)**. Endothelial cells were successfully seeded onto gelatin-coated glass coverslips and maintained in the culture for two weeks. Their yield was checked while passaging on day 5 and 10 and at the end of experiment. The six-fold increase in the yield of the endothelial cells was recorded two weeks into the culture. The cells viability remained high (83-95%) throughout the experiment **(Table 23)**.

**Table 23** The yield and viability of endothelial cells cultured in a monolayer on a gelatin-coated glass coverslips.

| **Day of culture** | **Yield** [CN*] | **Viability** [%] |
|---|---|---|
| 0 (isolation) | 240 000 | 83 |
| 5 (1st passage) | 950 300 | 95 |
| 10 (2nd passage) | 1 102 000 | 90 |
| 14 (final harvest and end of the experiment) | 1 124 500 | 91 |

**CN- total cell number originating from 5cm long segment of porcine jugular vein*

The cultured cells remained in their differentiated state throughout the experiment, which was confirmed performing ICC labelling of endothelial marker **(Fig. 80)**.

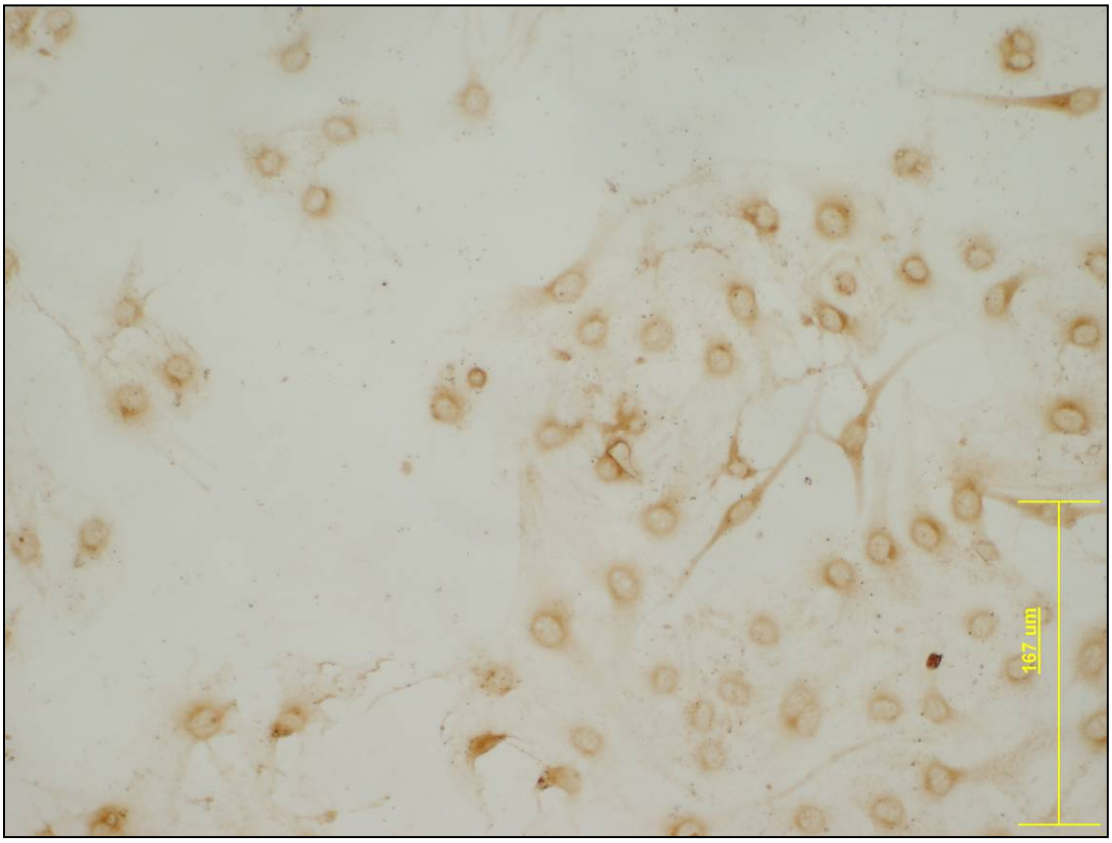


**Fig. 80** ICC analysis of porcine endothelial cells cultured in monolayer for two weeks. All the cells remained in their differentiated state expressing FVIII (brown staining). Bar indicates the scale of the image.

## 7.4. Discussion

The intestinal epithelium is a continuously replacing tissue. The cells responsible for this replacement are the stem cells located towards the base of the small intestinal crypt or at the very base of a colonic crypt (116).

As described before, OU are multicellular clusters, originating from gastrointestinal tissue, predominantly containing epithelial cells based around a mesenchymal core. When seeded on an appropriate scaffold, either in a rodent (190) or pig (80) model they have been reported to form neo-tissue which replicates the architecture of the native organ (stomach and intestine).

The secret of success of OU in their proliferating capacities is the preservation of mesenchyme-epithelial integrity. Beyond fetal development, balanced gut maturation depends on that cross-talk (191). Only the preservation of intestinal stem cell niche and support of mesenchymal-derived cells is crucial for preservation of the balance between the high rate of production and apoptosis of intestinal cells and the regulation of their proliferation and differentiation. This interaction is vital for maintaining crypts and villi morphology and therefore the gut functionality (192). Pericryptal mesoderm is composed of fibroblasts, which are key cells supporting the intestinal stem cells. Characteristically they form a protective fenestrated sheath around the stem cell compartment, creating the stem cell niche – the optimal environment for stem cells to renew themselves and to give rise to differentiated progeny (191). Thus, the mesenchymal core of OU is a major source of instructive signalling to the intestinal epithelium. Growth factors and cytokines secreted by it promote epithelial restitution and proliferation (192). Mesenchymal derived cells are required for long-term culture of intestinal stem cells. Intact Wnt and Notch signalling, which are active in the niche, were confirmed to be necessary *in vitro*

(193). This key feature of OU was granted by gentle isolation, which results in preservation of the niche containing stem cells.

It was possible to isolate the OU whilst preserving the stem cell niche from both: piglet and an adult animal. The age of the piglet was chosen as it corresponds (in terms of establishing all cell lines of the small intestine) to the age of suckling rats used by Evans and colleagues (73) and the age of pigs used by Sala et al. (80). The obtained clusters resembled in their appearance OU reported by Sala et al. (80). They were also similar in their structure to OU isolated from rodents (190). There was neither noticeable difference in the appearance of the clusters isolated from a piglet and adult animals, nor between OU obtained from jejunum and ileum. The dissimilarity among jejunal and ileal tissue appeared in the yield of the isolation procedure. Use of the same protocol resulted in a much lower yield of OU isolated from jejunum. However, the high standard deviation values suggest the result could not be interpreted into a firm conclusion. Two out of three variables within that group are similar to the values of the OU isolated from the ileum, and exclusion of the lowest number would bring these assessments to equilibrium. The average yield of OU isolated from a six weeks old piglet by Sala et al. (80) was similar to the one obtained here (5 845 000 vice 5 000 000). It was also comparable to the yield of OU harvested from an adult ileum (5 266 667).

Even though the isolation process of OU from an adult gut was significantly longer than any other previously reported, there was no compromise on OU viability.

The isolation procedures were similar to that reported in the other study (80), however the time and the concentration of enzymatic agents had to be drastically increased while isolating clusters from the adult animals (for both: ileum and jejunum). Even though Evans et al. (73) reported large numbers of mesenchymal cells

from the *lamina priopria* of a suckling rat, which were present as single cells and smaller clusters, it appeared that while harvesting OU from adult intestine the contamination with mesenchymal and epithelial cells is much higher. This was caused by the fact that porcine intestine harvested from an adult contains much thicker mucosal, submucosal and muscular layers which are more resistant to the gentle digestion by collagenase/dispase cocktail. Higher enzyme concentrations and longer digestion time allowed OU to be obtained in the desired cluster-form, but some superficial cells, exposed to these high doses were easily disconnected from main core of the tissue. Moreover, big undigested sections of *muscularis mucosae* were still present in the supernatant of the OU solution. While isolating OU from the rodents all the non-OU debris can be eliminated by simple sedimentation. This technique worked well in case of the piglet intestine but when using adult guts the supernatant still contained non-OU tissue sections and large amounts of cells. All of the intestinal tissue engineering studies to date have isolated OU from either neonatal rat intestine which contained small blunt villi but no well-developed crypts, or piglets intestine with much thinner than in adults tissue intestinal layers (80).

No other report investigates the isolation of OU from adult animals, and the presented protocol is the optimum method while preserving the stem cells niche and organoids morphology without incorporating complex and time consuming steps. However, it is not known if the function of the intestinal stem cells within isolated OU is preserved. The fetus and newborns have significant regenerative capability different from adults (194). Therefore, the activity of the adult intestinal stem cells within isolated OU may not be as efficient in generating intestinal epithelium as the reported neonatal tissue. Furthermore, the *in vitro* or *in vivo* role of 'contaminating' cells and mesenchymal sections remains to be tested.

In many reports describing generation of neo-intestine when using OU in rodent models it was uncertain whether any functional stem cells survived the isolation procedures or the subsequent culture period (116). It was not until recently that a putative molecular maker for intestinal epithelial stem cells *in situ* within intact tissue sections was suggested. Msh-1 was reported as that candidate. It is a neural RNA-binding protein that controls *Drosophila* external sensory organ development by regulating target genes post-transcriptionally and controls asymmetric cell division (195). The expression pattern of Msh-1 has been examined in mouse small intestine using IHC and *in situ* hybridization. The Msh-1 positive cells were located not only within the expected stem cell niche but also above the theoretical location, which suggest that some daughter cells also express the epitope (196). Moreover, the Msh-1 expression could not be examined *ex situ* and only small amounts of Msh-1 are normally found in gut (197). The only way to identify these cells was to localize them in a very selective expected place of residence. The improvement in the field of antibodies used for visualization of specific antigens within the tissue is much slower in the field of pre-clinical than clinical studies. Antibodies specific for animals and especially for rodents (huge cross-reactivity) take longer to be tested for specific applications and introduced to the market. Working on a rat tissue it was impossible to use Msh-1 to visualize intestinal stem cells within OU isolated even from suckling pups. However, moving towards large animal models it was achievable using a different, better tested marker. It appeared that intestinal stem cells identified by the putative stem cell marker - DCAMKL-1, are one of the major components of an intact intestinal stem cell niche. First to characterize this microtubule associated kinase, expressed in post-mitotic neurons as an intestinal stem cell marker were May et al. (198). This chapter characterises the expression of this marker in either: the native

small intestine (of a piglet and an adult) and within isolated OU (piglet and an adult). DCAMKL-1 expression in colon has been restricted to a single cell within the crypt. However, in the small intestine it was reported in more than one location of intestinal crypt, and even within crypt/villus junction (189). Multicenter staining of DCAMKL-1+ cells was also reported by Sala et al. (80). This unspecific to stem cell niche staining was also observed in this experiment. Nevertheless, not all of the isolated units contained positive DCAMKL-1 cells. Each individual OU may consist of a mixture or one type of the proliferating cell populations, stem cells or differentiated cells (199) which explains why some of the OU were negative for DCAMKL-1.

The method presented in this chapter for isolation and *in vitro* propagation of endothelial cells has been previously described by Mall et al. (200). The ultimate goal of the project focuses on constructing a cellular implant that could be generated *in vitro* for *in vivo* application. As future work will mostly be focused on engineering a bioreactor and seeding the scaffold, it was important to optimize methods of isolation and characterise both types of cells needed for seeding a scaffold that has intact vascular conduits. The presented method may not be ideal for clinical use but at this stage it was more important to create a reliable method of obtaining endothelial cells rather than an applicable method of their harvesting from the patients. SBS patients very often lack the vessels that could be used as source of endothelial cells due to the PN-dependency. There are well-described techniques of differentiating bone marrow stem cells into functional endothelium (9), however pulsatile stimulation of seeded vessels is an unavoidable requirement. Thus, it cannot be achieved without more complex equipment.

The yield of isolated and cultured cells was high and it was proved that it is possible to culture these cells without compromising their differentiated state for at

least two weeks. Moreover, the six-fold increase in the yield from a single isolation procedure is a very satisfactory result (200).

The presented technique of OU isolation is a broad variation first presented by *Evans et al.* (73), however it was possible to adjust the process to obtain a morphological equivalent of intestinal OU in an adult porcine model. OU seeded on appropriate scaffold, that could be also vascularised *in vitro* would be an alternative option to existing therapies of SBS. There are still many problems yet to be resolved before small intestine tissue engineering finds its way into clinical applications. Unless sources of autologus epithelial cells, or stems that give rise to them, can be harvested from the patients, standard SBS treatments will remain necessary. Harvesting a sufficient amount of these cells can be difficult in patients with diseased or damaged intestine that has led to massive resection. It may be possible to harvest small amounts of OU from the remnant small intestine over a period of time that could then be expanded *in vitro*. None of the existing studies have ever reported the construction of lengths bigger than 1cm, which would be clinically beneficial for SBS patients. Therefore the methods used today will not be applicable when treating humans, unless ways can be found to expand either the number of OU or isolate stem cells that can differentiate into intestinal epithelium capable of producing mucosa. Up to this point researchers experienced difficulties with expanding OU in the culture as their proliferative and differential capacities depend on the competence of each OU separately as well as an appropriate 3D environment (201).

The method presented here for isolating OU from adult animals allows preservation of intestinal stem cells and in the future it will hopefully be used as an additional tool in investigating yield and the regenerative capacities of mature tissue, which is much easier to obtain in a clinical situation.

Nonetheless, the *in vitro* culturing conditions of OU harvested from a pig are not optimized yet. Rat OU has been reported to survive under flow conditions (96). Nevertheless, the method of simultaneous culture of OU and endothelial cells remains to be validated. Progressing to an adult, large animal model has undoubtedly many advantages. Unanswered questions, like establishing long-term stability and functionality of the tissue-engineered constructs with autologus-cells, as well as regulation of molecular turnover responsible for the occurrence of the disease in the first place could be tested in a model that resembles morphologically and physiologically of human patients. Such construct could also find it applications in studying pathogenic states *in vitro* or screening of therapeutic agents (202).

# Chapter 8.

# General conclusions and discussion

## *8.1. Conclusions*

There is an abundance of evidence in the bioengineering field in the advantages in using de-cellularised structures as natural scaffolds to replace failing organs and tissues. Small intestinal tissue engineering is a fledgling technology, which may in the future provide an adjunct to medical and surgical therapies for intestinal failure resulting from small bowel syndrome. The experiments described in this thesis confirm that:

- it is possible to de-cellularise porcine ileum with intact mesenteric arcade while preserving the structural and functional integrity of the ECM,
- the presented de-cellularisation process results in biocompatible and non-toxic matrix, that upon implantation triggers cellular infiltration and angiogenesis, without inducing foreign body reaction and fibrosis,
- de-cellularised scaffold primarily induces pro-remodelling type of mononuclear response,
- intestinal organoid units can be harvested from adult and neonatal porcine donors with reproducible yield,
- intestinal stem cells can be characterised within isolated neonatal and adult porcine organoid units.

## *8.2. Discussion*

This chapter will initially describe the models used in investigating the bioengineering of the small intestine and the reasons behind the transition from rodent to porcine preclinical model presented in this thesis. Then it will discuss the progress made in the development of a biological, ready-to-vascularise scaffold for applications in large animal models, as well as simultaneous biocompatibility and toxicity studies. Finally the conclusions of the presented work will be specified and the future developments, that will be required before the techniques can be progressed further, discussed.

### 8.1.1. *In vivo* and *in vitro* models in development of bioengineered small bowel

Tissue engineering is a rapidly emerging field that combines the established disciplines of engineering, biology and medicine with the goal of fabricating viable tissues and organs. Although initially targeted for applications in regenerative medicine, a novel application of this technology has been to generate experimental model systems for studying biological mechanism and testing the efficacy of potential therapies. Nevertheless, the ultimate goal of the field is the development of vital tissues and organs that can be used to restore, maintain, or improve diseased or worn-out native counterparts (16). To date, numerous organ prototypes have been bio-engineered, including heart valves, blood vessels, nerves, skin, cartilage, bone, cornea, liver, pancreas, bladder and gastrointestinal tract.

The most prevalent biological model systems incorporated into tissue engineering include those based on cultured cells, tissues and organs, and on whole animals. A chief advantage associated with reductionist models based on cultured

cells is the ability to precisely control the microenvironment to which the cells are exposed. In intestinal physiology, for example, cultured monolayer of Caco-2 cells have been used extensively as models of intestinal absorptive and secretory epithelium (203). Much of the current understanding of intracellular signals transduction mechanisms regulating intestinal epithelial transport is derived from studies based on these and related models. However, it is important to remember that reductionist models rely on immortalised or transformed cells residing in an artificial microenvironment, each of which bear little resemblance to their normal counterparts. Thus, the behaviour of this Caco-2 line can not be extrapolated to those of normal enterocytes residing in a complex, 3D and multicellular milieu (202).

The isolation of organoid units was a considerable step towards creation of intestinal replacement. However, the early excitement was extinguished by the difficulties in establishing long-term culture of the viable intestinal epithelium. Therefore, most of the researches focused on *in vivo* studies.

*Ex vivo* models of tissue and organ culture allow preservation of normal tissue architecture and still make it possible to control a local environment but they have limited throughput and viability compared to simple *in vitro* models. However, this is a step in the right direction towards bioengineering of a gastrointestinal tract, which has not yet been described or clarified.

On the other hand, *in vivo* models can allow for long-term studies of complex processes under physiological relevant conditions. In intestinal physiology, models based on intestinal intubation or cannulation, isolated intestinal loops, and gross nutrient balances have been used to study absorption (204). In many cases, studies conducted under physiological relevance using these models yielded findings that are dramatically opposed to those based on non-physiological models (202). At present,

the experience of small intestine tissue engineering remains limited to experiments using animal models, principally small rodents, such as those described in Chapter 2. As mentioned in Chapter 1 there are two approaches to generate neointestinal tissue. First, the use of scaffolds (mostly SIS and other acellular matrices) as interposition grafts, second, the transplantation of intestinal organoid units onto implanted scaffold or denuded bowel. Both techniques have advantages and disadvantages, which have been highlighted before. Nevertheless, in general it has become clear that development of more complex, multi-layered tissues, such as intestine may be promoted and achieved quicker using biologically derived scaffolds. ECM structure of acellular tissues was suggested to facilitate the growth of correctly orientated mucosa, smooth muscle and serosal layers, while allowing the development of adequate vasculature and lymphatic tissue (105).

The development of a tissue-engineered construct requires the performance of several preclinical studies prior to an evaluation in human subject. Some preclinical studies can function as a proof of concept and are usually followed by expanded studies that are designed to evaluate efficacy in a relevant or well-accepted model. Usually, parallel studies are also performed to evaluate safety (205). An experimental model of intestinal regeneration using organoid units harvested from a neonatal rat has been previously achieved and served as a proof of concept for the work presented in this thesis (94). Following a new trend of de-cellularised native organs as tissue-specific scaffolds promoted the use of an *in vivo* model using a de-cellularised rat intestine seeded with organoid units. However, the intestine-derived scaffold was mechanically weak and therefore it failed to provide neomucosa development when seeded with organoid units and implanted subcutaneously. Further advancement of the experimental model described in Chapter 2 required strengthening of the ECM

scaffold. This could be achieved by creating a hybrid scaffold done by coating the acellular intestine with a porous polymer. Preliminary studies of this design were less than encouraging as the polymer showed unusual stiffness and did not provide adequate permeability for cellular infiltration. As a result the scaffold appeared non-biocompatible and the seeded organoid units did not survive and generate neomucosa. At this point it was crucial to estimate future perspectives of the project balancing technical difficulties and progress towards viable replacement therapy for intestinal failure.

For many tissue-engineered constructs, the pivotal preclinical studies designed to demonstrate efficacy involve a transition from the use of small animals to large-animal models. The need for large animals may be dependant on a need to evaluate responses to the construct under conditions that better simulate a physiologic match with the human clinical condition. Thus, a decision was made to place the emphasis on the development of porcine model, where the mechanical weakness of the scaffold was less likely to be an issue. As a result a biologically derived, ready-to-vascularise porcine scaffold, described in Chapter 3 has been developed.

In contrast, the safety and biocompatibility studies are focused on evaluating toxicity, either locally or systemically, and sometimes they also can provide assessment of the effects of storage or sterilisation on the properties of the construct (205). Therefore, at this stage simultaneously a small animal model described in Chapters 4 and 5 was incorporated into biocompatibility and toxicity studies of porcine de-cellularised ileum. The relevance of the results described in these chapters are summarised below.

### 8.1.2. Possibilities and advantages of using capillarised, biological, acellular scaffold for small intestine tissue engineering

The field of tissue engineering is constantly evolving putting hope into alternative to transplantations methods of treatment for end-stage tissue and organ failures. Ideally, surgeons would replace defective tissues with identical ones, recapitulating completely their structure and function. Nevertheless, when building biological structures from scratch, such an advance may become unachievable. The approach adopted in this thesis was to regenerate and then replace damaged tissue with an information rich scaffold into which adjacent cells migrate to create a replacement bowel. This material, ideally, should closely recapitulate the structure and function of the defective tissue while providing a safe, biocompatible material for tissue replacement (206). The information rich environment of the ECM was proved to provide the key signals and cues needed to restore damaged tissues to their natural state (207). However, this approach quickly evolved into the necessity of incorporating *ex vivo* seeding of reconstructive matrices with appropriate cells. ECM scaffolds started to be used not only as prosthetic and repair materials, but created a whole new source of scaffolds for the generation of off-the-shelf tissues and organs. As soon as the difficulties with *in vivo* incorporation of created *ex vivo* structures started to emerge, researchers reached for biomaterials that could contribute to scaffold turnover *in vivo*, preserving viability of seeded cells and at the same time actively directing the local cells to migrate and proliferate to where they are needed. It became obvious that the integration of the host tissues with the implanted construct is an important milestone in creating viable clinically treatment options not only for SBS patients, but for everyone with end-stage organ failure.

An ideal material for soft tissue reconstruction must be strong, easy to handle and biocompatible while supporting the growth of the new tissue. Natural ECM of the intestine provides the components necessary to direct the healing response allow for the proliferation of new, healthy tissue and restore tissue integrity to the damaged site. The 3D organization of these extracellular components distinguishes them from synthetic materials and is associated with constructive remodeling instead of scar tissue formation. Common features of this ECM-assisted tissue remodeling include angiogenesis, recruitment of inflammatory and circulating progenitor cells and constructive remodeling of damaged tissue structures (40). Therefore, ECM scaffolds have started to be widely used to create replacement tissues and organs using both *in vitro* and *in vivo* models. Thanks to the technique of de-cellularisation even complex tissues can be generated using this relatively simple approach. Even though this simple strategy does not offer a universal regenerative solution, it has resulted in many significant advancements across the field. One of the first of these was the de-cellularisation of the whole rat heart, and *in vitro* regeneration of its contractile function by seeding the ECM with cardiac or endothelial cells (133). In February 2011 the BBC broadcasted a program entitled: "Horizon – How to Mend a Broken Heart" featuring the de-cellularising of a whole human heart in order to repeat the approach originally tested on an animal model. Dr. Doris Taylor explained how a prepared 'ghost-heart' could help patients which are at risk of dying whilst waiting for the available donor organs. Furthermore, three years ago, Claudia Castillo, a 30-year-old mother of two became the first person to receive a transplant organ created from autologus stem cells seeded onto a de-cellularised cadaveric trachea. This was followed by performing a similar implantation in ten-year-old Kieran at Great Ormond Street Hospital in London. In contrast with traditional transplant surgery, the

de-cellularisation protocol solved the problem of tissue rejection by removing virtually all traces of human leukocyte antigens, meaning the patients required no immunosuppressive drugs. As well as immediately restoring airway function, the constructs facilitated rapid development of an internal cellular lining and blood vessel network (62).

Although so far the focus within the field of intestinal tissue engineering was on scaffolds designed and assembled in 'bottom-up' mode from synthetic polymers, de-cellularised tissue offered distinct and important benefits in recreating neomucosal function. In addition to the fact that ECM materials compared to synthetic scaffolds have advantageous characteristics for cellular migration and differentiation upon implantation, they also provide the vital intestinal layered 3D structure important for recreation. The scaffold introduced in Chapter 3 has one more, very unique benefit. It contains intact vascular conduits, which were preserved by a customised de-cellularisation protocol. The implantation of de-cellularised vasculature of this scaffold described in Chapter 6 proved to provide immediate blood supply to all parts of the matrix. What is more, even without recreating vascular morphology but using pharmacological agents it was possible to maintain the ability to re-perfuse of de-cellularised vessels for up to at least 24 hours post-implantation. At that time most of the scaffold was infiltrated with the inflammatory and progenitor cells. The majority of the migrating cells originated from systemic perfusion, which showed how important it was to keep even the smallest vessels within the scaffolds unobstructed.

The use of the rodent model described in Chapter 4 and 5 allowed investigation of the behaviour of the de-cellularised ileum *in vivo* for periods of time longer than 24 hours. Simple subcutaneous implantations proved that antigens and the agents used for de-cellularisation were removed from the ileum and the scaffold

proved to be safe, non-toxic, and most importantly biocompatible. This meant that biomolecules crucial for constructive remodelling were preserved whilst de-cellularisation and they actively promoted cell-cell and cell-matrix interactions *in vivo*. Most of these functional molecules have a short half-life in the circulation (208) hence the need for them to be delivered through the biomaterial and released at low concentrations on a timescale of weeks. This was confirmed by some of the quantitative and qualitative analysis of the scaffolds structural and functional elements presented in Chapter 4.

Chapter 5 confirmed the switch of pro-inflammatory to pro-remodelling immunological phenotype as soon as four weeks post-implantation. The incorporation of a stereological unbiased quantitative tool into the model can result in more reliable way to predict *in vivo* fate of the tissue-engineered constructs. This quantitative and reproducible functional assay is pivotal in the preclinical stage and cannot be underestimated, especially when it can be used as a mean to reduce animal use in tissue-engineering without compromising efficacy of the studies (205).

The results discussed herein demonstrate the importance of the ECM environment in determining cell behaviour, and highlight the need for regenerative materials to provide cells with not only biological cues but also supply them with nutrients immediately after implantation. In light of the above mentioned clinical applications, the development of intelligent materials is often guided in the first instance by the surgical applicability and potential of improving the outcome for the patient. Thus, the scaffold presented here partially targets the biggest obstacle in the development of viable therapy for SBS by enabling production of 20-30cm long constructs, which can be easily implanted and immediately supplied with blood. Even though, the generation of thick and heterogeneous intestinal tissue will require further

innovations, the scaffold described in this thesis presents a possible platform for further development of the tissue-engineered small bowel.

### 8.1.3. Sources of intestinal regeneration

As a result of recent advances in identification and culture of putative stem cells, interest in *in vitro* models of intestinal epithelial cells has been rejuvenated. In particular, there is a considerable relevance in the regenerative potential of intestinal stem cells and organoid units (116). Identification of factors and pathways involved in controlled differentiation of stem/progenitor cells into tissue-specific lineages is expected to contribute immensely to effective clinical protocols. However, it is not possible to identify intestinal stem cells on the basis of simple histology alone. Recently many immunohistochemical and genetic markers have been described in literature as selective, putative, intestinal stem cell markers (195). Most of these candidates have been characterised in rodent models. There are many species-related differences in the expression of surface markers. For example, the focus of many recent reports Msh-1 antigen has been identified as an intestinal stem cells marker in mouse and rat but not in any other species (195). When porcine specific anti-Msh-1 antibody was used in IHC analysis of porcine small intestine (data not shown) the positive staining could not be described either in a neonate or an adult animal. At the same time, the control tissue (cortex) showed expected, positive staining. Sala et al. (80) used a putative stem cell marker: DCAMKL-1 while characterising regenerative potential of neonatal, porcine, intestinal organoid units *in vivo*. The antigen proved to be present on the surface of a very selective population of proliferating cells at the base of the porcine intestinal crypt.

The method presented in Chapter 7 for OU isolation was tailored for adult porcine tissue. It is believed that this is the first description of intestinal OU that were harvested from an adult porcine tissue. Moreover, anti-DCAMKL-1 antibodies were successfully used to visualise the intestinal stem cells residual within control intestinal tissue of a neonatal and adult pig as well as some of the isolated OU.

The prospect of isolating OU from adult intestine opens a whole world of possibilities for involving autologous OU into tissue-engineered constructs. At the moment one of the major obstacles facing the future of intestinal regeneration is the issue of yield needed to rebuild neomucosal layer. If it was possible to harvest OU from adults, at the time of bowel resection the yield of isolation could be increased. OU harvested from only ten centimetres of neonatal, porcine small intestine allowed regeneration of 1.5-3cm of bowel. If harvest at the resection technique could be employed in clinics, even up to 30cm of autologous bowel could be bioengineered from 100cm of resected tissue. Implantation of 30-50 cm long segments of bowel could allow SBS patients to be weaned off PN (202).

The individuals most desperately needing a new alternative to bowel transplantations are children. The donor shortage is even more predominant in this group. The technique presented in Chapter 7 is adequate for isolating OU from adult tissue, however the method of obtaining juvenile OU has been described elsewhere (80). The marker used for identification of putative stem cells within the intestinal OU has been checked in neonatal and adult tissue. Such specific targeting of intestinal stem cells by the antibody can in the future be used to isolate a pure population of intestinal stem cells or pure populations of DCAMKL-1+ OU to better understand their role in epithelial proliferation and differentiation, as well as conditions important for their growth *in vitro*.

As discussed previously it is possible that an alternative to using intestinal stem cells will need to be employed in tissue engineering of the small intestine. Ultimately, it may become achievable to generate intestinal progenitor cells from other autologous pluripotent cell lines such as bone marrow or blood derived stem cells.

### 8.1.4. Limitations of the current concept of small intestine tissue engineering – is it possible to create bioengineered small intestine?

Successful tissue engineering begins with a clear and precise definition of the clinical demand or problem being addressed. The incidence, prevalence and demographics of the SBS indicate the need for successful therapy. Current intestinal tissue management either through PN or transplantations do not seem efficient enough in 21$^{st}$ century. At the same time it needs to be considered how innovative and complex therapy will benefit the SBS patients and if it will be advantageous over the existing treatment methods. For example, long-term graft and patient survival needs to be considerably higher for implantations of tissue-engineered constructs than for intestinal transplantation to turn the novel technique into common and widely available practice. The management of patients with severe chronic intestinal failure should aim to optimise long-term survival, minimise the incidence of complications and maximise the quality of life for the patient. Perhaps tissue engineering will need to integrate with existing medical and surgical therapies in order to achieve these goals.

The concept presented in this thesis is based on creating a scaffold that could be used to grow long segments of neomucosa. This would be beneficial to SBS

patients, however there are many obstacles, which still have to be addressed when considering recreation of the anatomical integrity of the small intestine. The major hurdle will be the recreation of the intestinal contractibility and subsequently motility. The presented here ECM scaffolds has a potential to provide a good environment for *in vitro* propagation of more than one types of tissue. Its biocompatibility has already been proven, so it is very probable that it will be a good matrix for ingrowth not only porcine and rat cells, but also human ones. The findings presented in this chapter are all linked to specific limitations, which are highlighted in the following sub-chapter. However, the general concern of transforming animal and *in vitro* studies into viable clinical therapies remains.

However, recreating the alimentary tract is not a simple task. Successful application of tissue-engineered small intestine in humans requires overcoming many unique challenges. As a result, clinical application of engineered intestinal tissue still remains a number of years away. The understanding of how to optimally harvest relevant cell populations and how to expand and culture them in a 3D environment is crucial (116). The difficulty of propagating cell lines of normal intestinal epithelium has impeded research into the molecular mechanism underlying differentiation of stem/progenitor cells into a various intestinal lineages (202). In all the examples provided in Chapter 1 there is a lack of long-term epithelial and/or stem cultures of intestine. With an expanding role of stem cells in the treatment of degenerative disorders, there is a critical need for additional efforts to develop *in vitro* models of well-characterised and marked stem/progenitor epithelial cells of gut or other cells that could be differentiated into all lineages of neo-intestine.

Several, earlier described studies demonstrated long-term propagation of primary epithelial cell and OU cultures derived from rodents (202). Some of them

showed long-term replication potential and functional differentiation, suggesting that the cultures might have contained stem cell populations, although such characterisation was not performed. More recently, intestinal epithelial cells expressing certain stem cell markers have been described, but the cells failed to develop into cell lines and died after 3-4 passages (116). The difficulty in producing stable cell lines most likely relates to imperfect knowledge of tissue dissociation methods, culture conditions, inclusion of appropriate structure and third dimension into the culture as well as lack of reliable intestinal stem cell markers (202). Furthermore, all the *in vitro* studies of intestinal regeneration have been performed on a rodent, mostly neonatal tissue.

The yield and methods of expansion of intestinal epithelium or growth of OU *in vitro* also remains an obstacle. It is possible that a better understanding of the inter- and extra-cellular interactions within the intestinal crypts may facilitate targeted augmentation of *in vitro* stem cells replication via the use of specific molecules and/or scaffolds. Such methods could then be used in conjunction with *in vivo* techniques to increase the volume of neomucosal tissue in artificial bowel-constructs. This may be done by the use of highly biocompatible vectors, that can be supplied with nutrients, and integrated with the host environment immediately after implantation, and methods proved to induce intestinal adaptation such as GLP-2 or growth factors delivery (209).

Even though ECM scaffolds used in bioengineering of intestinal tissue have only been tested as acellular matrices it is possible that a combined approach in which intestinal OU were transplanted onto the sections of de-cellularised ileum, might allow for the creation of compatible, long segments of neointestine. The autologous OU would allow the cellularisation of the central section of the scaffold *in vitro*, and after implantation tissue could grow inwards from the adjacent healthy jejunum.

It may also be possible to create sections of tissue engineered colonic mucosa and implant this in continuity with remnant small intestine. Tissue engineered colonic mucosa has been created in rodent models using techniques similar to those used to produce tissue engineered small intestine (116). Although bioengineered colonic mucosa would not have the same absorptive capacity as small intestinal mucosa, it might improve fluid and electrolytes absorption and also provide hormonal stimuli for small intestinal adaptation (202).

We must also learn how to build intestinal structures composed of a dynamic and complex epithelial lining over a fully innervated muscular tube. At the moment there are no studies that approach the issue of appropriate gross geometry of bioengineered bowel in order to have adequate functional capacity for peristalsis. The use of more advanced, de-cellularised materials may be particularly helpful in this regard, by providing the cues for all the epithelial, muscular and neural components.

Also unknown is a method of delivery and ultimate positioning of segments of tissue-engineered small intestine. The muscular and neural regeneration may be very slow or even non-existent. Creation of a pouch or use of a de-functional intestinal loop rather than straightforward lengthening by interposition may appear a more viable option. At the same time it is important to introduce bioengineered grafts to intestinal content in order to provoke functional differentiation. However, all the studies of interposition of acellular tubular scaffolds longer than few centimetres in large animal models resulted in high mortality. Moreover, exposure of the construct to the luminal content of the gastrointestinal tract may result in anastomotic leakage or partial digestion/damage of the construct. Noteworthy is the question of whether the scaffold will be able to withstand the intraluminal pressure of the small intestine?

All of this is largely dependant on the scaffold used for intestinal regeneration. The de-cellularised ileum presented in this thesis is a good candidate to be considered for this purpose. It has been proven to be compatible, which means it would allow considerably quick integration with host tissue. It can be obtained in lengths clinically viable for SBS patients and provide immediate re-perfusion with the host blood post-implantation. Finally, intestinal tissue for de-cellularisation can be harvested either from cadavers or as xenografts. The first implants of bioengineered tissues are behind us, and therefore it is important to provide the regulations of organ and tissue donations for not only transplantations but also tissue de-cellularisation and scaffold harvesting. The solution may be adoption of the legislation executed in Spain, where the government made everyone a potential organ donor. Furthermore, agreement needs to be reached such that the organs and tissues which failed to serve as transplantation material can serve as de-cellularisation specimen. Even though the porcine anatomy is very similar to human, it is crucial to move towards de-cellularising human tissues and creating 'ghost-organs' which could be re-populated with patients' own cells.

Ultimately, if tissue engineering is to become a clinically viable therapy in the management of intestinal failure secondary to SBS in adults or children, it will be essential to combine the techniques described in this thesis with ones existing in the literature to produce a section of biologically active tissue.

Although the evolution of the technology to a point where it could be used in humans appears to be distant, recent reports of successful clinical experiments using tissue engineered bladders and tracheas allude to the potential of the technique (210;211).

### 8.1.5. Limitations of the studies

The preliminary rodent model presented in Chapter 2 highlighted the many technical difficulties of creating a biocompatible and non-immunogenic hybrid scaffold. Within two weeks post-implantation seeded with organoid units ECM-polymer scaffolds induced a foreign body reaction and failed to show signs of neomucosal creation. The synthetic scaffold was not the only target of inflammatory reaction. OU seeded onto control, non-coated with polymer scaffolds also seemed to induce a host response. The results of similar experiments, but using inbred OU-donor and recipient rats were different with signs of OU survival and neomucosal generation (94). To thoroughly test the strength and compatibility of the new hybrid scaffold the experiment would have to be repeated using an inbred rodent model, and most probably less rigid polymer. However, at the same time the urge to start developing a large animal model resulted in rapid advancement in the process of de-cellularisation of porcine small intestine. The transition to the porcine model was inevitable and it was also linked to there being no-need for strengthening of the scaffold by polymer coating.

As mentioned previously presented in Chapter 3 ileal scaffolds have many advantages over other matrices for intestinal regeneration used so far. It follows the trend in the field of tissue engineering of providing vascular conduits, important in the development of big constructs and whole organs (lung heart). The tailored de-cellularisation process resulted in complete removal of cellular components. It also removed the majority of DNA, residuals preserving the collagen structure and a considerable amount of GAGs. Nevertheless, the collagen analyses were only based on qualitative and not quantitative data. The de-cellularisation of the ileum was very demanding in terms of adjusting the process for different tissues involved in the

process. At the same time numerous scaffolds had to be delicately and carefully harvested and prepared in the process of protocol optimisation. It became clear that 'ideal' de-cellularisation would be impossible to achieve. The process had to be based on the balance between removing the cells, preserving the ECM and preserving the de-cellularised vessels ability to perfuse. It is noteworthy to say that the animal-to-animal differences were always present and the exact protocol (e.g. pulsatile rate of the de-cellularisation pumps) depended greatly on small adjustments that had to be made separately for each scaffold. This also means that the reproducibility of the result may be highly dependant on the person performing the experiment. This can decrease the chance of the technique to be easily transferred into common use when treating the patients. However, it can be a starting point for de-cellularising human bowels, and human-to-human differences or their management may not be less dominant than in the case of the pigs.

The obvious limitation of the rodent *in vivo* studies presented in Chapter 4 and 6 is the lack of well-defined control groups. Cross-linking the scaffolds prior to the implantation could create the negative control group. As stated before, cross-linking induces foreign body reaction and fibrosis rather than constructive remodelling *in vivo* (32). At the same time implantation of autologous tissue is regarded as negative control in terms of inducing adverse immune response. Nevertheless, the histological results were confirmed by an in house pathologist who due to his expertise in the field of scaffold cellular responses could confirm the character of the host reaction to the implants. Furthermore, as described in Chapter 5, the quantification of different populations of macrophages could be compared to results of the studies using identical *in vivo* model and *ex vivo* staining that had well-described positive and negative control groups.

Vascular anastomoses presented in Chapter 6 were performed in eight animals, five of which resulted in re-perfusion of the graft and vessels unobstructed state throughout the time of the experiment. These results gave good understanding of the biomechanical performance of the scaffold, however it is yet to be determined how the seeding of the vasculature with endothelial cells characterised in Chapter 7 will influence that outcome.

The experiments described in Chapter 7 demonstrate that it is possible to create porcine intestinal OU in a reproducible fashion. However, the OU yield obtained from one harvest of 10cm long segment of adult jejunum needs to be tested for its regenerative potential *in vivo* or *in vitro*. A better understanding of the dynamics of the intestinal crypt will help to identify what role DCAMKL-1+ cells play in intestinal OU replication and development. Presented here are early experiments that need to be tested in appropriate models. However, they indicate the possibility of 'reusing' adult resected bowel to generate intestinal OU containing putative stem cells.

## *8.3. Future work*

The work described in this thesis, coupled with the discussion above, encourages a number of further studies. The further tests of the de-cellularised tissue are needed to estimate scaffold biomechanics, before incorporating it into complex *in vitro* systems. There is the potential for complete *in vitro* maturation of intestinal tissue in bioreactor (202). Not only will *in vitro* maturation allow for a precise study of intestinal tissue development, it will allow for a potentially limitless supply of the off-the-shelf intestinal tissues for SBS patients. OU isolated from neonatal rat have been cultured in flow bioreactor for up to three days (96). The next step within the

project should focus on designing and manufacturing two circuits (vascular and intestinal) pulsatile perfusion bioreactor. Porcine OU described in Chapter 7 could be seeded onto the ileal lumen and endothelial cells onto the vascular lumens of the porcine acellular scaffold and cultured to obtain optimal seeding growth. It has been shown that endothelial cells described in Chapter 7 can grow for up to two weeks. To sustain their differentiated state an incorporation of mechanical or electrical stimuli would be required. This could be done by seeding the endothelial cells onto the lumen of the de-cellularised mesenteric vessels introduced to the pulsatile flow of bioreactor. Separation of the two circuits in the bioreactor could allow simultaneous, dynamic seeding of two different type of cells, as well as culture using two different (specific for given cells) mediums and mechanical preconditioning (different pulse and flow rates).

Such a system could also be used as a tool to optimise minimal yield of the cell/OU isolation required for sufficient seeding of the scaffold, without performing costly and time-consuming *in vivo* studies. Depending on the outcome of seeding procedures thought needs to be dedicated to eventual improvement in the yield for the isolation process.

If the efficiency of employing OU units into creating artificial bowel is low, then the characterisation of different sources of cells, such as previously described mesenchymal stem cells or even embryonic stem cells need to be considered.

Furthermore, there is another important advantage of operating within *in vitro* models. A clinician of the future might apply a tissue-engineered model system to facilitate tailoring therapies for individual patients (e.g. the culture of harvested via

endoscopy OU could be used for high-throughput screening of the drugs for inflammatory bowel disease patients) (96).

Possibly one of the most achievable goals within the project, before the *in vitro* models is created, is seeding the lumen of the de-cellularised ileum and intraperitoneal implantation of cellular constructs into porcine recipients with and without the immunosuppression. Immunosuppressive drugs may alter the regenerative potential of seeded OU, but at the same time without them OU isolated from different animals may not survive *in vivo*. Therefore, the role of immunosuppressants needs to be validated.

The perfect solution would involve obtaining autologous sources of cells and performing the OU isolation and implantation during one surgical procedure, as done by Sala et al. (80). The alternative is the use of immunodeficient porcine recipients of tissue-engineered bowel constructs, but this is a very costly requirement.

The first steps in obtaining tissue-engineered small intestine using large animal model has been achieved. In future using tools developed here (scaffold and cellular components) it may be very possible to create the replacement products *in vitro* and ultimately check their biocompetence performing interposition studies in porcine recipients. Ultimately the protocols and techniques can be adjusted for clinical use.

# Appendices

## *Appendix 1*

## *De-cellularisation methods used for organs and tissues*

**Table 1. De-cellularisation methods used for organs and tissues**

| METHOD | ORGAN/TISSUE |
|---|---|
| **2. Physical** | |
| • Agitation and sonification | Liver |
| • Mechanical or pressure massage | Bladder |
| • Freezing and thawing | Nerve tissue |
| | Liver |
| • Irradiation | Nerve tissue |
| **2. Chemical** | |
| • Acetic acids | Small intestine submucosa |
| | Bladder |
| | Liver |
| | Pericardium |
| • Alkaline acids | Small intestine submucosa |
| • Non-ionic detergents | |
| ✓ Triton X-100 | Skin |
| | Liver |
| | Aortic valve |
| | Pericardia |
| | Ligament-Bone |

| | |
|---|---|
| ✓ Polyethylene glycol (PEG) | Heart |
| • Ionic detergents | |
| ✓ SDS | Vein |
| | Ligament-Bone |
| | Bladder |
| | Heart |
| | Tendon |
| | Esophagus |
| | Ureter |
| ✓ Sodium deoxycholate | Valve |
| | Liver |
| | Muscle |
| ✓ Triton X-200 | Nerve tissue |
| • CHAPS | Artery |
| • Sulfobetaine-10 and -16 | Nerve tissue |
| | Liver |
| • Tri(n-butyl)phosphate | Tendon |
| • Hypotonic and hypertonic solutions | Artery |
| | Amniotic membrane |
| | Pericardium |
| | Small intestine submucosa |
| • Tributyl phosphate (TnBP) | Ligament-Bone |
| • EDTA and EGTA | Small intestine submucosa |
| **3. Biological** | |
| • Trypsin | |
| ✓ 0.05% | Valve |
| | Liver |
| ✓ 0.25% | Skin |
| ✓ 0.5% | Aortic valve |

| | |
|---|---|
| • Endo- and exonucleases | Valve |
| | Amniotic membrane |
| | Bladder |
| | Pericardium |
| | Muscle |
| | Esophagus |
| • Dispase | Skin |
| • Collagenase | Cartilage |
| | Pericardium |
| • Pronase | Cartilage |

* De-cellularisation methods are not specific for the described organs. The table presents most commonly used agents to de-cellularise specific tissues. The agents may be the only part of the process or a major one in the combined method.

# *Appendix 2*

## *Preclinical and clinical applications of ECM scaffolds*

**Table 2** Preclinical and clinical applications of ECM scaffolds in repair and restoration of organs and tissues.

| DECELLULARIZED ORGAN | DONOR SPECIES | APPLICATION | HOST SPECIES |
|---|---|---|---|
| SKIN | Rat | Dermal substitute | Rat |
| | | Full thickness burns healing | |
| | Pig | Full thickness burns healing | Pig |
| | | Diaphragmatic prostheses treatment | Rat |
| | Bovine | Repair of mucosa defect otolaryngology | Human |
| | Human | Treatment of hallux rigidus | Human |
| | | Urethral reconstruction | |
| SMALL INTESTINE SUBMUCOSA | Pig | Achilles tendon reconstruction | Dog |
| | | Hernia repair | Rabbit |
| | | | Human |
| | | Vocal cord reconstruction | Dog |
| | | Intervertebral disc regeneration | Human |
| | | Repair of cecal wound | Rat |
| | | Meniscal regeneration | Dog |

| | | | |
|---|---|---|---|
| | | Diaphragmatic prostheses | Rat |
| | | Urinary tract repair | Pig |
| | | Peyronie's disease treatment Anastomotic dilatation, fistula repair, urethroplasty, soft tissue repair and reinforcement, dura matter repair, skin grafting, vaginal slings | Human |
| NERVE TISSUE | Rat | Peripheral nerve repair | Rat |
| AMNIOTIC MEMBRANE | Rabbit | Surgical patch with a whole range of uses (e.g. soft tissue replacement, body wall repair, cardiovascular applications, wound dressing) | Human |
| | | Fetoscopic closure of iatrogenic defects in fetal membranes | Rabbit |
| DIAPHRAGM | Human | Abdominal wall defect repair | Rabbit |
| PERICARDIUM | Bovine | Tissue engineering /patches for clinical application | Mouse |
| | Dog | Tissue engineering /patches for clinical application | Rat |
| | | Pulmonary | Sheep |

| | | | |
|---|---|---|---|
| | | bioprostheses | |
| BLADDER | Pig | Full thickness wound repair | Rat |
| | | Hypospadia repair | Human |

# *Appendix 3*

## *Commercially available ECM scaffold materials*

**Table 3.** Commercially available ECM scaffold materials.

| *Product* | *Material* | *Use* |
|---|---|---|
| AlloDerm | Dry sheet of cross-linked human skin | Abdominal wall, breast, head and neck reconstructions, grafting |
| AlloPatch® | Dry sheet of human fascia lata | Soft tissue augmentation patch |
| Axis™ dermis | Dry sheet of human dermis | Pelvic organ prolapse |
| Bard® Dermal Allograft | Dry sheet of cadaveric human dermis | Pelvic organ prolapse |
| CuffPatch™ | Hydrated sheet of cross-linked SIS | Soft tissue reinforcement |
| DurADAPT™ | Dry sheet of cross-linked horse pericardium | Dura matter repair |
| Dura-Guard® | Hydrated sheet of bovine pericardium | Spinal and cranial repair |
| Durasis® | Dry sheet of SIS | Dura matter repair |
| Durepair® | Dry sheet of fetal bovine skin | Cranial or spinal dura repair |
| FasLata® | Dry sheet of cadaveric fascia lata | Abdominal repair and vaginal prolapse |
| Graft Jacket® | Dry sheet of human skin | Foot ulcers |
| Oasis® | Dry sheet of SIS | Partial and full thickness wounds, superficial and second degree burns grafting |
| OrthADAPT™ | Dry sheet of cross linked | Soft tissue reinforcement, |

| | | |
|---|---|---|
| | horse pericardium | repair and reconstruction in orthopaedic applications |
| Pelvicol® | Hydrated sheet of cross linked porcine dermis | Pelvic organ prolapse |
| Peri-Guard® | Dry sheet of cross-linked bovine pericardium | Pericardial and soft tissue repair |
| Permacol™ (Zimmer Collagen Patch in USA) | Hydrated sheet of cross-linked porcine dermis | Soft connective tissue repair |
| PriMatrix™ | Dry sheet of fetal bovine skin | Wound management |
| Restore™ | Dry sheet of SIS | Soft tissue reinforcement |
| Stratasis® | Dry sheet of SIS | Treatment of urinary incontinence |
| SurgiMend™ | Dry sheet of fetal bovine skin | Surgical repair of damaged or ruptured soft tissue membranes |
| Surgisis® | Dry sheet of SIS | Soft tissue repair and reinforcement |
| Suspend™ | Dry sheet of human fascia lata | Urethral sling |
| TissueMend® | Dry sheet of fetal bovine skin | Surgical repair and reinforcement of soft tissue in rotator cuff |
| Vascu-Guard® | Dry sheet of cross-linked bovine pericardium | Reconstruction of blood vessels in neck, legs and arms |
| Veritas® | Hydrated sheet of cross-linked bovine pericardium | Soft tissue repair |
| Xenform™ | Dry sheet of fetal bovine skin | Repair of colon, rectal, urethral, and vaginal prolapse, pelvic reconstruction, urethral sling |

# *Appendix 4*

# *Laboratory equipment and reagents*

## 1. Laboratory equipment

### *1.1. Tissue preparation and histology*

- Balance-HF-300 (A&D Instruments)
- Cassets and slides writer-Lamb MicroWriter (RaymondALamb)
- Hotplate (RaymondALamb)
- Microtome-Retraction AS325 (Shandon)
- Waterbath (RaymondALamb)
- Tissue Processor-TissueTek VIP (Miles Scientific)
- Embeding centre-Tissue Tek III (Miles Scientific)

### *1.2.Immunohisto- and Immunocytochemistry*

- Vortex-Genie 2 (Scientific Industries)
- Magnet stirrer/hotplate-RCT basic (Kika Werke)
- pH meter-3505 (Jeway)
- Semi-automatic pipettes (Eppendorf, Fisher Brand, Gilson)

### *1.3. Microscopy and stereology*

- Microfish-100 (Canon)
- Microscope-Laborlux S (Leitz)
- Microscope-BH-2 (Olympus)
- Fluorescent microscope-Optihot-2 (Nikon)

- Microcator (Heidenhain)

### *1.4. Preparation of acellular matrix*

- Incubator-Windsor Incubator, range 37-70ºC (Sandrest)
- Pump-pulsatile, perfusion pump SCIQ 323, range 1-300rpm (Watson Marlow)
- Dissecting microscope (Leica)

### *1.5. Molecular biology*

- Microwave-800W (Panasonic)
- Micro-centrifuge-FugeOne (Eppendorf)
- Centrifuge-Avanti 30 (Beckman)
- UV illuminator-Dual Intensity Transilluminator (UVP)
- Power station for electrophoresis-PowerPac HC (BioRad)
- Thermo block-Dri Block DB-2D (Techne)
- Microscale-Sartorius 2001MFZ (SBDHRD-Asset)

### *1.6. Tissue/cell isolation and culture*

- $CO_2$ incubator-Galaxy R (Jencons Millenium)
- Hybridisation Oven/Shaker-SI20H, range 25-80º (Stuart Scientific)
- Centrifuge-Harrier 15/80 (MSE)
- Inverted microscope-Axiovert 25 (Zeiss)
- Tissue chopper-McILWAIN (The Mickle Laboratory Engineering LTD)
- Microflow Biology Safety Cabinet (Prior Laboratory Supplies LTD)
- Dymax 5 Vacum Pump (Fisher Scientific)

## 2. Laboratory reagents

### *2.1. Tissue preparation and histology*

- Xelene (Genta Medicals)
- IMS (Genta Medicals)
- Gill's Haematoxylin (PioneerResearch Chemicals)
- Harris's Haematoxylin (PioneerResearch Chemicals)
- Eosin (Sigma)
- HCl(Fisher Scientific)
- DPX (Surgipath)
- Water based mounting medium- Immu-Mount (Shandon)
- Potassium Permanganate (Sigma)
- Sulfuric Acid (Sigma)
- Oxalic Acid (Sigma)
- Miller's Stain (Pioneer Research Chemicals)
- Weighert's Haematoxylin: Solutions A and B (PioneerResearch Chemicals)
- Sirius Red (Sigma)
- Saturated Aqueous Solution of Picric Acid (Sigma)
- Histology Wax (Leica)
- 10% NBF (Genta Medicals)
- EtOH(Fisher Scientific)
- IPA (Genta Medicals)
- 'Fairy' liquid (Proctor & Gamble)
- PFA (Sigma)
- Vectashield HardSet MountingMedium with DAPI (Vector Laboratories)

### *2.2.Immunohisto- and Immunocytochemistry*

- 30% $H_2O_2$aqueous solution (Sigma)
- MeOH (Fisher Scientific)
- 2.5% Normal Horse Serum (Vector Laboratories LTD)
- ImmPress Anti-Rabbit Ig (peroxidase) Kit (Vector Laboratories LTD)
- ImmPress Anti-Mouse Ig (peroxidase) Kit (Vector Laboratories LTD)
- ImmPACT DAB (Vector Laboratories LTD)
- Non-specific protein block (Dako)
- Vectastain Elite ABC kit (Vector Laboratories LTD)
- Acetone (Sigma)
- APTS (Sigma)
- PBS (Sigma)
- Trizma Base (Sigma)
- Tween-20 (Sigma)
- Anti-α-SMA antibody, clone 1A4 (Sigma)
- Anti-Col I antibody, clone COL-1 (AbCam)
- Anti-Col III antibody, ab778 (AbCam)
- Anti-Ki67 antibody, ab833 (AbCam)
- Anti-S-100 antibody, clone SH-B1 (Sigma)
- Anti-CK 8 antibody, clone phosphor AE3 (AbCam)
- Anti-CD163 antibody, clone ED2 (Cambridge Bioscience)
- Anti-CCR7 antibody, clone Y59 (Insight Biotechnology)
- Anti-CD68 antibody, ED1 (AbDSerotec)
- Anti-DCAMKL-1 antibody, AP72196 (Abgent)
- Anti-VEGF antibody, clone A-20 (Santa Cruz)
- Anti-VEGF-R antibody, ab2349 (AbCam)

- Anti-CD133 antibody, SC19365 (Insight Biotechnology)
- Anti-CD31 antibody, 250589 (Bioquote LTD)
- Anti-FVIII antibody, CP099C (Biocar Medical)
- Anti-FVIII antibody, A0082 (Dako)
- Anti-VWF antibody, MCA 127 (Serotec)
- Proteinase K (Dako)
- Citric acid (Sigma)
- Trypsin 250 (Defco)
- Vector Unmasking Solution (Vector Laboratories)
- BSA (Sigma)
- NaCl (Sigma)
- KCl (Sigma)
- Biotinylated Anti-Rabbit antibodies (Vector Laboratories)
- Biotinylated Anti-Mouse antibodies, rat absorbed (Vector Laboratories)
- Biotinylated Anti-Goat antibodies (Vector Laboratories)

### *2.3.Preparation of acellular matrix and hybrid scaffold*

- Chloroform (Fisher Scientific)
- SDS (Sigma)
- EDTA (Sigma)
- PA (Sigma)
- DNaseI (Sigma)

### *2.4. Tissue/cell isolation and culture*

- HBSS (Sigma)

- D-glucose (Sigma)
- Dispase (Gibco)
- Collagenase Type I (Sigma)
- Collagnase F (Sigma)
- DMEM (Sigma)
- FBS (Sigma)
- Sorbitol (Sigma)
- Penicillin/Streptomycin (Sigma)
- EGF (Pepro Tech EC LTD)
- HGF (Pepro Tech EC LTD)
- VEGF (Pepro Tech EC LTD)
- FGF (Pepro Tech EC LTD)
- R3IGF (Pepro Tech EC LTD)
- Essential amino acids mix (Sigma)
- Endothelial cell basal medium 2 with supplement pack (PromoCell)
- Ascorbic Acid (Sigma)
- Insulin (Sigma)
- ECM Gel (Sigma)
- Porcine mucosal heparin (Sigma)
- 0.4% Trypan Blue aqueous solution (Sigma)
- Percoll (Sigma)
- M199 Medium (Sigma)
- Gelatin (Sigma)
- Nitric acid (Sigma)
- Copper (II) sulphate

- D-PBS (Sigma)

### *2.5. Molecular biology*

- Agarose (Sigma)
- TBE (Sigma)
- Gel Loading Buffer (BioLabs)
- Ethidium Bromide (Sigma)
- DNA Ladder (BioLabs)
- GenElute Mammmalian Genomic DNA Miniprep Kit (Sigma)
- GAG's Blyscan Assay (Biocolor)
- Papain (Sigma)
- Cystein (Sigma)

# *Appendix 5*

# *Xylene-based tissue processing*

**Table 4.** Procedure for xylene-based processing to wax.

| *REAGENT* | *TIME* | *TEMPERATURE* |
|---|---|---|
| 10% NBF | 2 hours | Room temperature |
| 70% IMS* | 1 hour | Room temperature |
| 90% IMS | 1 hour | Room temperature |
| 100% IMS | 1 hour | Room temperature |
| 100% IMS | 1 hour | Room temperature |
| 100% IMS | 1 hour | Room temperature |
| IMS / Xylene | 1 hour | Room temperature |
| Xylene | 30 minutes | Room temperature |
| Xylene | 1 hour | Room temperature |
| Xylene | 30 minutes | Room temperature |
| 56ºC paraffin wax | 30 minutes | 60ºC |
| 56ºC paraffin wax | 90 minutes | 60ºC |
| 56ºC paraffin wax | 90 minutes | 60ºC |

**IMS-Industrial Methylated Spirits*

# *Appendix 6*

# *Xylene-based histology-slides preparation*

**Table 5.** Protocol for de-waxing and rehydration (xylene-based protocol). Slides were bathed sequentially in the solutions below.

| | ***REAGENT*** | ***TIME*** |
|---|---|---|
| 1. | Xylene 1 | 5 minutes |
| 2. | Xylene 2 | 2 minutes |
| 3. | 100% IMS | 2 minutes |
| 4. | 95% IMS | 2 minutes |
| 5. | 70% IMS | 2 minutes |
| 6. | Running water | 2 minutes |

# *Appendix 7*

# *H&E staining*

**Table 6.** H&E staining. Slides were bathed sequentially in the solutions below.

| | ***REAGENT*** | ***TIME*** |
|---|---|---|
| 1. | Gill's Haematoxylin | 90 seconds |
| 2. | Running water | 5 minutes |
| 3. | 1% HCl* in 70% IMS | 3 seconds (agitate) |
| 4. | Running water | 4 minutes |
| 5. | 0.5% aqueous Eosin | 5 minutes |
| 6. | Running water | 20 seconds (agitate) |
| 7. | Dehydrate and mount with DPX** | |

**HCl-hydrochloric acid; **DPX- Di-N-Butyle Phthalate in Xylene*

# *Appendix 8*

# *Picro-Sirius Red/Miller's Elastin staining*

**Table 7.** Protocol for Picro-Sirius Red/Miller's Elastin staining. Rehydrated slides were bathed sequentially in the following solutions.

| | *REAGENT* | *TIME* |
|---|---|---|
| 1. | Acid Potassium Permanganate* | 5 minutes |
| 2. | Distilled water | 1 minutes |
| 3. | 1% aqueous solution of Oxalic acid | 2 minutes |
| 4. | Distilled water | 5 minutes |
| 5. | 70% IMS | 1 minute |
| 6. | 90% IMS | 1 minute |
| 7. | Miller's stain | 1 hour |
| 8. | 95% IMS | 1 minute |
| 9. | Tap water | 2 minutes |
| 10. | Weighert's Haematoxylin** | 10 minutes |
| 11. | Tap water | 1 minute |
| 12. | 1% HCl in 70% IMS | 5 seconds |
| 13. | Tap water | 5 minutes |
| 14. | Distilled water | 30 seconds |
| 15. | Picro Sirius Red*** | 45 minutes |
| 16. | Dehydrate and mount with DPX | |

**0.25% Potassium permanganate in aqueous solution of 1.5% sulphuric acid;**A and B solutions-1:1 ratio;***1% Sirius Red in Saturated aqueous solution of picric acid*

# Appendix 9

# Immunohistochemical stainings

**Table 8.** IHC staining protocols.

| *Primary antibody specificity* | *Cell/protein target* | *Tissue/species* | *Antigen retrieval* | *$H_2O_2$ solution [%] (time of incubation)* | *Wash buffer* | *Non-specific block (incubation time)* | *Primary antibody dilution (time of incubation)* | *Secondary antibody (dilution/time of incubation)* | *DAB incubation time* | *Chapter number* |
|---|---|---|---|---|---|---|---|---|---|---|
| **αSMA** | Smooth muscle actin | Subcutaneous implants/Rat | - | 3% (30 min) | PBS* | 2.5% normal horse serum (30 min) | 1:4 000 (30 min) | Anti-mouse ImmPRESS kit (30 min) | 30 sec | 4 |
| **αSMA** | Smooth muscle actin | Acellular matrix grafts/Pig | - | 3% (30 min) | PBS | 2.5% normal horse serum (30 min) | 1:4 000 (30 min) | Anti-mouse ImmPRESS kit (30 min) | 20 sec | 6 |
| **CCR7** | Activated B and T lymphocytes and M1 macrophages | Subcutaneous implants/Rat | 5 min 0.25% citrate buffer[a] | 10% (30 min) | PBS | 2.5% normal horse serum (75 min) | 1:100 (overnight) | Biotinylated anti-rabbit 1:100 followed by ABC (1 h) | 35 sec | 5 |

| | | | | | | | | | | |
|---|---|---|---|---|---|---|---|---|---|---|
| **CD31** | Endothelial cell intercellular junction | Acellular matrix grafts/Pig | 20 min 0.5% citrate buffer[a] | 10% (30 min) | PBS | 2.5% normal horse serum (30 min) | 1:10 (overnight) | Anti-rabbit ImmPRESS kit (30 min) | 15 sec | 6 |
| **CD68** | Macrophages | Subcutaneous implants/Rat | 1 min Proteinase K[b] | 10% (30 min) | PBS | 2.5% normal horse serum (1 h) | 1:100 (2 h) | Biotinylated anti-mouse 1:100 followed by ABC (1 h) | 35 sec | 5 |
| **CD68** | Macrophages | Acellular matrix grafts/Pig | Trypsin digestion[c] | 3% (30 min) | PBS | 2.5% normal horse serum (30 min) | 1:100 (2 h) | Anti-mouse ImmPRESS kit (30 min) | 20 sec | 6 |
| **CD133** | Hematopoietic stem cells, endothelial progenitor cells, | Acellular matrix grafts/Pig | 5 min Proteinase K[c] | 10% (1 h) | TBS-T** | 2.5% normal horse serum (2 h) | 1:10 (overnight) | Biotinylated anti-goat 1:100 followed by ABC (1 h) | 7 sec | 6 |
| **CD163** | M2 macrophages | Subcutaneous implants/Rat | 3 min Proteinase K[c] | 10% (30 min) | PBS | 2.5% normal horse serum (75 min) | 1:10 (overnight) | Biotinylated anti-mouse 1:100 followed by ABC (1 h) | 2 min | 5 |

| | | | | | | | | | | |
|---|---|---|---|---|---|---|---|---|---|---|
| **CK8** | Epithelial cells | Subcutaneous implants/Rat | - | 3% (30 min) | PBS | 2.5% normal horse serum (30 min) | 1:100 (1 h) | Biotinylated anti-mouse 1:150 followed by ABC (1 h) | 30 sec | 4 |
| **COL I** | Collagen type I | Acellular matrix /Pig | Vector unmasking solution[d] | 3% (30 min) | PBS | 2.5% normal horse serum (30 min) | 1:200 (2 h) | Anti-mouse ImmPRESS kit (1 h) | 20 sec | 3 |
| **COLIII** | Collagen type III | Acellular matrix /Pig | - | 3% (30 min) | PBS | 2.5% normal horse serum (30 min) | 1:100 (overnight) | Anti-rabbit ImmPRESS kit (30 min) | 20 sec | 3 |
| **DCAMKL-1** | Intestinal stem cells | Organoid units and small intestine/Pig | 2 min Proteinase K[c] | 10% (1 h) | PBS | Streptavidin/biotin block followed by 2.5% normal horse serum (30 min) | 1:50 (overnight) | Biotinylated anti-rabbit 1:200 followed by ABC (1 h) | 20 sec | 7 |
| **FVIII** (CP099C) | Blood vessels | Subcutaneous implants/Rat | 2 min Proteinase K[c] | 15% (30 min) | TBS-T | 2.5% BSA*** in TBS (1h) | 1:50 (1 h) | Biotinylated anti-rabbit 1:150 followed by ABC (30 min) | 70 sec | 4 |

| | | | | | | | | | | |
|---|---|---|---|---|---|---|---|---|---|---|
| **Ki67** | Proliferating cells | Subcutaneous implants/Rat | 10 min 0.25% citrate buffer[a] | 3% (30 min) | PBS | 2.5% normal horse serum (30 min) | 1:100 (1 h) | Biotinylated anti-rabbit 1:100 followed by ABC (30 min) | 30 sec | 4 |
| **S-100** | Neuronal progenitors | Subcutaneous implants/Rat | 1 min Proteinase K[c] | 3% (30 min) | PBS | 2.5% normal horse serum (30 min) | 1:100 (2 h) | Biotinylated anti-mouse 1:150 followed by ABC (1 h) | 5 sec | 4 |
| **VEGF** | Vascular endothelial growth factor | Subcutaneous implants/Rat | - | 3% (30 min) | PBS | 2.5% normal horse serum (2 h) | 1:50 (overnight) | Biotinylated anti-rabbit 1:100 followed by ABC (1 h) | 10 sec | 4 |
| **VEGF** | Vascular endothelial growth factor | Acellular intestinal scaffold/Pig | - | 3% (30 min) | PBS | 2.5% normal horse serum (2 h) | 1:50 (overnight) | Biotinylated anti-rabbit 1:100 followed by ABC (1 h) | 25 sec | 4 |

| | | | | | | | | | | |
|---|---|---|---|---|---|---|---|---|---|---|
| **VEGF-R** | Receptor for vascular endothelial growth factor | Subcutaneous implants/Rat | 15 min 0.25% citrate buffer[a] | 3% (30 min) | PBS | 2.5% normal horse serum (30 min) | 1:50 (overnight) | Biotinylated anti-rabbit 1:200 followed by ABC (1 h) | 10 sec | 4 |
| **VWF** | Blood vessels | Acellular matrix grafts/Pig | 2 min Proteinase K[c] | 3% (30 min) | PBS | 2.5% normal horse serum (45 min) | 1:400 (1 h) | Anti-rabbit ImmPRESS kit (45 min) | 10 sec | 6 |

[a]citrate buffer, pH 6.0 at 95°C followed by 15 minutes of cooling down the sections submerged in citrate buffer solution
[b]Proteinase K digestion in 25°C
[c]5min in distilled water at 37ºC followed by 30 min in 1% trypsin solution in TBS, pH 7.8 at 37ºC
[d]Vector Unmasking Solution for 15 minutes at 80°C0.01M
** PBS-Phosphate Buffer Saline (5 tablets in 1l of distilled water)*
*** TBS-T-Tris-Buffer Saline with Tween-20 (6% Trizma base, 9% sodium chloride (NaCl), pH7.6, 0.5%Tween-20)*
****BSA-Bovine serum albumin*

# *Appendix 10*

# *Solutions used in Chapter 2*

## Solutions used in experiments described in Chapter 2

- **Wash solution**
  - Hank's Balanced Salt Solution (HBSS) with low calciur magnesium
  - 2% D-glucose
  - 0.035% sodium carbonate ($NaHCO_3$)
- **Enzyme solution, pH 7.4**
  - HBSS
  - 0.01% Dispase
  - 0.02% Collagenase type XI-S
- **DMEM solution**
  - Dulbecco's Modified Eagle's Medium (DMEM)
  - 5% Fetal Bovine Serum (FBS)
  - 2% Sorbitol
  - 0.6% Penicillin/Streptomycin cocktail
- **Growth medium**
  - Dulbecco's Modified Eagle's Medium (DMEM)
  - 5% Fetal Bovine Serum (FBS)
  - 2% Sorbitol
  - 0.6% Penicillin/Streptomycin cocktail
  - 0.000 005% HGF

- 0.00025% Insulin
- 0.01% Porcine Mucosal Heparin
- ECM gel (½ volume of DMEM)

- **Soap Water**
  - Distilled water
  - 1.7% ‘Fairy’ liquid

# *Appendix 11*

# *Xylene-free tissue processing*

**Table 9.** Procedure for xylene-free tissue processing.

| *REAGENT* | *TIME* | *TEMPERATURE* |
|---|---|---|
| 10% NBF | 30 minutes | 35ºC |
| 10% NBF | 30 minutes | 35ºC |
| 50% EtOH* | 1 hour | 35ºC |
| 50% EtOH | 1 hour | 35ºC |
| 50% EtOH | 1 hour | 35ºC |
| 80% EtOH in IPA** | 1 hour | 35ºC |
| 80% EtOH in IPA | 1 hour | 35ºC |
| 80% EtOH in IPA | 1 hour | 35ºC |
| IPA | 1 hour | 35ºC |
| IPA | 1 hour | 35ºC |
| 56ºC paraffin wax | 30 minutes | 60ºC |
| 56ºC paraffin wax | 90 minutes | 60ºC |
| 56ºC paraffin wax | 90 minutes | 60ºC |

**EtOH-ethanol*
***IPA-isopropanol*

# *Appendix 12*

# *Solutions used in Chapter 3*

## Solutions used in experiments described in Chapter 3

- **0.05% Trypsin solution, pH 7.5**
  - PBS
  - 0.05% Trypsin
  - 0.05% ethylene-diamine-tetraacetic acid (EDTA)

- **0.2% Trypsin solution, pH 7.5**
  - PBS
  - 0.2% Trypsin
  - 0.05% ethylene-diamine-tetraacetic acid (EDTA)

- **Triton X-100 solution**
  - PBS
  - 1% Triton X-100

- **0.075% SDS solution**
  - PBS
  - 0.075% sodium dodecyl sulphate (SDS)

- **1.5% SDS solution**

- PBS
- 1.5% SDS

- **SDX solution**
  - PBS
  - 4% sodium deoxycholic acid solutions (SDX)

- **Antibiotics solution**
  - PBS
  - 0.2% Streptomycin/Penicillin cocktail (penicillin: 100IE/ml; streptomycin:100µg/ml)

- **DNase I solution**
  - PBS
  - 2.000 U /l deoxyribonuclease type I (DNase I)

- **PA solution**
  - Sterile PBS
  - 0.1% paracetic acid (PA)

- **Evans Blue solution**
  - Distilled water
  - 0.01% Evans Blue solution

# Appendix 13

## Volumes of implanted scaffolds

**Table 14.** Estimated volumes along with CE values of explanted scaffolds.

| Animal number | Scaffold | Volume [$mm^3$] | CE [%] |
|---|---|---|---|
| 1 | P5914-1 | 323.76 | 11 |
| 1 | P5914-2 | 574.56 | 15 |
| 2 | P5915-1 | 611.04 | 9 |
| 2 | P5915-2 | 647.52 | 10 |
| 3 | P5916-1 | 638.4 | 13 |
| 3 | P5916-2 | 574.56 | 9 |
| 4 | P5983-1 | 893.76 | 9 |
| 4 | P5983-2 | 633.84 | 10 |
| 5 | P5984-1 | 551.76 | 9 |
| 5 | P5984-2 | 611.04 | 10 |
| 6 | P5985-1 | 497.04 | 12 |
| 6 | P5985-2 | 606.48 | 10 |
| 7 | P6033-1 | 647.52 | 10 |
| 7 | P6033-2 | 611.04 | 11 |
| 8 | P6034-1 | 775.2 | 10 |
| 8 | P6034-2 | 601.92 | 10 |
| 9 | P6035-1 | 542.64 | 10 |
| 9 | P6035-2 | 779.76 | 9 |

# *Appendix 14*

# *Cell-densities of implanted scaffolds*

**Table 16**. Estimated densities along with CE of cells infiltrating the scaffolds implanted subcutaneously into rat recipients.

| Animal number | Scaffold | Total cells $N_v$ [1/mm$^3$] | Total cells CE [%] | CD68 $N_v$ [1/mm$^3$] | CD68 CE [%] | CD163 $N_v$ [1/mm$^3$] | CD163 CE [%] | CCR7 $N_v$ [1/mm$^3$] | CCR7 CE [%] |
|---|---|---|---|---|---|---|---|---|---|
| 1 | P5914-1 | 1.57E-12 | 9 | 6.05E-13 | 14 | 2.18E-13 | 13 | 2.09E-13 | 9 |
| 1 | P5914-2 | 1.68E-12 | 9 | 6.88E-13 | 12 | 2.03E-13 | 13 | 2.27E-13 | 11 |
| 2 | P5915-1 | 1.81E-12 | 9 | 7.2E-13 | 12 | 1.61E-13 | 16 | 3.18E-13 | 9 |
| 2 | P5915-2 | 1.7E-12 | 9 | 6.82E-13 | 13 | 2.2E-13 | 13 | 2.39E-13 | 12 |
| 3 | P5916-1 | 1.79E-12 | 11 | 7.29E-13 | 17 | 2.72E-13 | 15 | 2.5E-13 | 11 |
| 3 | P5916-2 | 1.72E-12 | 11 | 7.61E-13 | 15 | 3.06E-13 | 11 | 1.87E-13 | 13 |
| 4 | P5983-1 | 7.13E-13 | 15 | 3.02E-13 | 20 | 5.98E-14 | 22 | 1.22E-13 | 18 |
| 4 | P5983-2 | 1.19E-12 | 11 | 4.51E-13 | 16 | 1.37E-13 | 17 | 1.66E-13 | 16 |
| 5 | P5984-1 | 1.53E-12 | 9 | 5.33E-13 | 18 | 2.46E-13 | 13 | 1.49E-13 | 14 |
| 5 | P5984-2 | 1.72E-12 | 11 | 9.04E-13 | 15 | 1.72E-13 | 20 | 1.73E-13 | 12 |
| 6 | P5985-1 | 1.56E-12 | 10 | 5.55E-13 | 13 | 1.9E-13 | 15 | 1.35E-13 | 14 |
| 6 | P5985-2 | 1.37E-12 | 11 | 4.96E-13 | 15 | 1.93E-13 | 18 | 1.2E-13 | 17 |
| 7 | P6033-1 | 1.25E-12 | 10 | 4.86E-13 | 16 | 2.29E-13 | 13 | 6.85E-14 | 19 |
| 7 | P6033-2 | 1.44E-12 | 10 | 5.32E-13 | 10 | 2.02E-13 | 14 | 7.23E-14 | 17 |
| 8 | P6034-1 | 1.25E-12 | 13 | 4.85E-13 | 19 | 1.91E-13 | 16 | 5.78E-14 | 20 |
| 8 | P6034-2 | 1.34E-12 | 11 | 4.81E-13 | 16 | 1.97E-13 | 16 | 7.07E-14 | 17 |
| 9 | P6035-1 | 1.28E-12 | 10 | 5.19E-13 | 13 | 2.52E-13 | 12 | 7.28E-14 | 20 |
| 9 | P6035-2 | 1.25E-12 | 10 | 4.22E-13 | 14 | 1.74E-13 | 19 | 5.1E-14 | 15 |

# *Appendix 15*

# *Total cell numbers of implanted scaffolds*

**Table 17**. Total number of cells infiltrating each of the scaffolds, and pan, M1 and M2 macrophages within the implants.

| Animal number | Scaffold | Total cells $N_{TOT}$ | CD68 $N_{TOT}$ | CD163 $N_{TOT}$ | CCR7 $N_{TOT}$ |
|---|---|---|---|---|---|
| 1 | P5914-1 | 5.06879E-10 | 1.9594E-10 | 7.04502E-11 | 6.7504E-11 |
| 1 | P5914-2 | 9.64744E-10 | 3.95412E-10 | 1.16521E-10 | 1.30253E-10 |
| 2 | P5915-1 | 1.10806E-09 | 4.39704E-10 | 9.8133E-11 | 1.94555E-10 |
| 2 | P5915-2 | 1.10111E-09 | 4.41868E-10 | 1.42713E-10 | 1.54628E-10 |
| 3 | P5916-1 | 1.1458E-09 | 4.65394E-10 | 1.73709E-10 | 1.59345E-10 |
| 3 | P5916-2 | 9.8652E-10 | 4.36953E-10 | 1.757E-10 | 1.07443E-10 |
| 4 | P5983-1 | 6.37519E-10 | 2.69826E-10 | 5.34468E-11 | 1.09039E-10 |
| 4 | P5983-2 | 7.55411E-10 | 2.85735E-10 | 8.69628E-11 | 1.05027E-10 |
| 5 | P5984-1 | 8.43476E-10 | 2.94143E-10 | 1.35898E-10 | 8.23226E-11 |
| 5 | P5984-2 | 1.04842E-09 | 5.5238E-10 | 1.04793E-10 | 1.05893E-10 |
| 6 | P5985-1 | 7.73146E-10 | 2.75758E-10 | 9.42388E-11 | 6.71501E-11 |
| 6 | P5985-2 | 8.29968E-10 | 3.01057E-10 | 1.17233E-10 | 7.25957E-11 |
| 7 | P6033-1 | 8.10954E-10 | 3.14954E-10 | 1.48347E-10 | 4.43227E-11 |
| 7 | P6033-2 | 8.80997E-10 | 3.25257E-10 | 1.23186E-10 | 4.41782E-11 |
| 8 | P6034-1 | 9.65357E-10 | 3.76127E-10 | 1.48373E-10 | 4.47678E-11 |

| | | | | | |
|---|---|---|---|---|---|
| 8 | P6034-2 | 8.04165E-10 | 2.89343E-10 | 1.18578E-10 | 4.25377E-11 |
| 9 | P6035-1 | 6.94362E-10 | 2.81467E-10 | 1.36474E-10 | 3.94933E-11 |
| 9 | P6035-2 | 9.77663E-10 | 3.28981E-10 | 1.35522E-10 | 3.97756E-11 |

# *Appendix 16*

# *Solutions used in Chapter 7*

## Solutions used in experiments described in Chapter 7

- **Enzyme solution for isolation of OU from a piglet, pH 7.4**
  - HBSS with low calcium and magnesium
  - 0.025% Dispase
  - 6.4% Collagenase type I
- **Enzyme solution for isolation of OU from an adult pig, pH 7.4**
  - HBSS
  - 0.08% Dispase
  - 10% Collagenase type I
- **DMEM solution**
  - DMEM
  - 10% FBS
  - 4% Sorbitol
- **Gelatin solution**
  - Distilled, autoclaved water
  - 0.2% gelatin
- **Nitric acid solution**
  - Distilled water
  - 10% Nitric acid
- **Collagenase F solution**
  - PBS

- 0.5% Collagenase type F

- **Supplemented standard medium**
  - RPMI medium
  - 10% FBS

- **Endothelial cells growth medium**
  - 50% DMEM
  - 50% Endothelial Cell Basal Medium 2 with supplement pack

- **Trypsin solution**
  - PBS
  - 0.005% Trypsin
  - 0.02% EDTA

- **Triton X-100 solution**
  - PBS
  - 10% Triton X-100

# Reference List

(1) Nightingale J, Woodward JM. Guidelines for management of patients with a short bowel. Gut 2006 Aug;55 Suppl 4:iv1-12.

(2) Sudan D. Advances in the nontransplant medical and surgical management of intestinal failure. Curr Opin Organ Transplant 2009 Jun;14(3):274-9.

(3) Goulet O, Sauvat F. Short bowel syndrome and intestinal transplantation in children. Curr Opin Clin Nutr Metab Care 2006 May;9(3):304-13.

(4) Rickham PP. Massive small intestinal resection in newborn infants. Hunterian Lecture delivered at the Royal College of Surgeons of England on 13th April 1967. Ann R Coll Surg Engl 1967 Dec;41(6):480-92.

(5) Wallander J, Ewald U, Lackgren G, Tufveson G, Wahlberg J, Meurling S. Extreme short bowel syndrome in neonates: an indication for small bowel transplantation? Transplant Proc 1992 Jun;24(3):1230-5.

(6) Hanson WR, Osborne JW, Sharp JG. Compensation by the residual intestine after intestinal resection in the rat. I. Influence of amount of tissue removed. Gastroenterology 1977 Apr;72(4 Pt 1):692-700.

(7) Messing B, Crenn P, Beau P, Boutron-Ruault MC, Rambaud JC, Matuchansky C. Long-term survival and parenteral nutrition dependence in adult patients with the short bowel syndrome. Gastroenterology 1999 Nov;117(5):1043-50.

(8) Quiros-Tejeira RE, Ament ME, Reyen L, Herzog F, Merjanian M, Olivares-Serrano N, et al. Long-term parenteral nutritional support and intestinal adaptation in children with short bowel syndrome: a 25-year experience. J Pediatr 2004 Aug;145(2):157-63.

(9) Schalamon J, Mayr JM, Hollwarth ME. Mortality and economics in short bowel syndrome. Best Pract Res Clin Gastroenterol 2003 Dec;17(6):931-42.

(10) Byrne TA, Morrissey TB, Nattakom TV, Ziegler TR, Wilmore DW. Growth hormone, glutamine, and a modified diet enhance nutrient absorption in patients with severe short bowel syndrome. JPEN J Parenter Enteral Nutr 1995 Jul;19(4):296-302.

(11) Sudan D. Long-term outcomes and quality of life after intestine transplantation. Curr Opin Organ Transplant 2010 Jun;15(3):357-60.

(12) Middleton SJ, Pollard S, Friend PJ, Watson C, Calne RY, Davies M, et al. Adult small intestinal transplantation in England and Wales. Br J Surg 2003 Jun;90(6):723-7.

(13) Nucci A, Burns RC, Armah T, Lowery K, Yaworski JA, Strohm S, et al. Interdisciplinary management of pediatric intestinal failure: a 10-year review of rehabilitation and transplantation. J Gastrointest Surg 2008 Mar;12(3):429-35.

(14) Vantini I, Benini L, Bonfante F, Talamini G, Sembenini C, Chiarioni G, et al. Survival rate and prognostic factors in patients with intestinal failure. Dig Liver Dis 2004 Jan;36(1):46-55.

(15) Atala A. Engineering organs. Curr Opin Biotechnol 2009 Oct;20(5):575-92.

(16) Langer R, Vacanti JP. Tissue engineering. Science 1993 May 14;260(5110):920-6.

(17) Hasetine W. A brave new medicine. A conversation with William Haseltine.. Interview by Joe Flower. Health Forum J 1999 Jul;42(4):28-5.

(18) Polak JM, Bishop AE. Stem cells and tissue engineering: past, present, and future. Ann N Y Acad Sci 2006 Apr;1068:352-66.

(19) Bergsma JE, Rozema FR, Bos RR, Boering G, de Bruijn WC, Pennings AJ. In vivo degradation and biocompatibility study of in vitro pre-degraded as-polymerized polyactide particles. Biomaterials 1995 Mar;16(4):267-74.

(20) Lanza R, Langer R, Vacanti JP. Principles of Tissue Engineering. Third ed. Elsvier; 2007.

(21) Atala A. Autologous cell transplantation for urologic reconstruction. J Urol 1998 Jan;159(1):2-3.

(22) Griffith LG, Naughton G. Tissue engineering--current challenges and expanding opportunities. Science 2002 Feb 8;295(5557):1009-14.

(23) Cilento BG, Freeman MR, Schneck FX, Retik AB, Atala A. Phenotypic and cytogenetic characterization of human bladder urothelia expanded in vitro. J Urol 1994 Aug;152(2 Pt 2):665-70.

(24) Chen HC, Hu YC. Bioreactors for tissue engineering. Biotechnol Lett 2006 Sep;28(18):1415-23.

(25) Portner R, Nagel-Heyer S, Goepfert C, Adamietz P, Meenen NM. Bioreactor design for tissue engineering. J Biosci Bioeng 2005 Sep;100(3):235-45.

(26) Vunjak-Novakovic G, Freed LE. Culture of organized cell communities. Adv Drug Deliv Rev 1998 Aug 3;33(1-2):15-30.

(27) Hoerstrup SP, Sodian R, Sperling JS, Vacanti JP, Mayer JE, Jr. New pulsatile bioreactor for in vitro formation of tissue engineered heart valves. Tissue Eng 2000 Feb;6(1):75-9.

(28) Powell CA, Smiley BL, Mills J, Vandenburgh HH. Mechanical stimulation improves tissue-engineered human skeletal muscle. Am J Physiol Cell Physiol 2002 Nov;283(5):C1557-C1565.

(29) Torok E, Pollok JM, Ma PX, Kaufmann PM, Dandri M, Petersen J, et al. Optimization of hepatocyte spheroid formation for hepatic tissue engineering on three-dimensional biodegradable polymer within a flow bioreactor prior to implantation. Cells Tissues Organs 2001;169(1):34-41.

(30) Badylak SF. In vivo studies to evaluate tissue engineering techniques. Ann N Y Acad Sci 2002 Jun;961:302-4.

(31) Orwin EJ, Hubel A. In vitro culture characteristics of corneal epithelial, endothelial, and keratocyte cells in a native collagen matrix. Tissue Eng 2000 Aug;6(4):307-19.

(32) Badylak SF, Grompe M, Caplan AI, Greisler HP, Guldberg RE, Taylor DA. In vivo remodeling: breakout session summary. Ann N Y Acad Sci 2002 Jun;961:319-22.

(33) Peters MC, Polverini PJ, Mooney DJ. Engineering vascular networks in porous polymer matrices. J Biomed Mater Res 2002 Jun 15;60(4):668-78.

(34) Nerem RM. Tissue engineering: the hope, the hype, and the future. Tissue Eng 2006 May;12(5):1143-50.

(35) Guldberg RE, Ballock RT, Boyan BD, Duvall CL, Lin AS, Nagaraja S, et al. Analyzing bone, blood vessels, and biomaterials with microcomputed tomography. IEEE Eng Med Biol Mag 2003 Sep;22(5):77-83.

(36) Pioletti DP. Biomechanics and tissue engineering. Osteoporos Int 2011 Jun;22(6):2027-31.

(37) Guilak F. Functional tissue engineering: the role of biomechanics in reparative medicine. Ann N Y Acad Sci 2002 Jun;961:193-5.

(38) Butler DL, Goldstein SA, Guldberg RE, Guo XE, Kamm R, Laurencin CT, et al. The impact of biomechanics in tissue engineering and regenerative medicine. Tissue Eng Part B Rev 2009 Dec;15(4):477-84.

(39) McDevitt CA, Wildey GM, Cutrone RM. Transforming growth factor-beta1 in a sterilized tissue derived from the pig small intestine submucosa. J Biomed Mater Res A 2003 Nov 1;67(2):637-40.

(40) Hodde J. Naturally occurring scaffolds for soft tissue repair and regeneration. Tissue Eng 2002 Apr;8(2):295-308.

(41) Bernard MP, Chu ML, Myers JC, Ramirez F, Eikenberry EF, Prockop DJ. Nucleotide sequences of complementary deoxyribonucleic acids for the pro alpha 1 chain of human type I procollagen. Statistical evaluation of structures that are conserved during evolution. Biochemistry 1983 Oct 25;22(22):5213-23.

(42) Bissell MJ, Hall HG, Parry G. How does the extracellular matrix direct gene expression? J Theor Biol 1982 Nov 7;99(1):31-68.

(43) Laurie GW, Horikoshi S, Killen PD, Segui-Real B, Yamada Y. In situ hybridization reveals temporal and spatial changes in cellular expression of mRNA for a laminin receptor, laminin, and basement membrane (type IV) collagen in the developing kidney. J Cell Biol 1989 Sep;109(3):1351-62.

(44) Badylak SF, Freytes DO, Gilbert TW. Extracellular matrix as a biological scaffold material: Structure and function. Acta Biomater 2009 Jan;5(1):1-13.

(45) Badylak SF. Xenogeneic extracellular matrix as a scaffold for tissue reconstruction. Transpl Immunol 2004 Apr;12(3-4):367-77.

(46) Badylak S, Kokini K, Tullius B, Whitson B. Strength over time of a resorbable bioscaffold for body wall repair in a dog model. J Surg Res 2001 Aug;99(2):282-7.

(47) Gilbert TW, Stewart-Akers AM, Simmons-Byrd A, Badylak SF. Degradation and remodeling of small intestinal submucosa in canine Achilles tendon repair. J Bone Joint Surg Am 2007 Mar;89(3):621-30.

(48) Badylak SF, Vorp DA, Spievack AR, Simmons-Byrd A, Hanke J, Freytes DO, et al. Esophageal reconstruction with ECM and muscle tissue in a dog model. J Surg Res 2005 Sep;128(1):87-97.

(49) Niyibizi C, Kavalkovich K, Yamaji T, Woo SL. Type V collagen is increased during rabbit medial collateral ligament healing. Knee Surg Sports Traumatol Arthrosc 2000;8(5):281-5.

(50) Li F, Li W, Johnson S, Ingram D, Yoder M, Badylak S. Low-molecular-weight peptides derived from extracellular matrix as chemoattractants for primary endothelial cells. Endothelium 2004 May;11(3-4):199-206.

(51) Gilbert TW, Sellaro TL, Badylak SF. Decellularization of tissues and organs. Biomaterials 2006 Jul;27(19):3675-83.

(52) Schenke-Layland K, Vasilevski O, Opitz F, Konig K, Riemann I, Halbhuber KJ, et al. Impact of decellularization of xenogeneic tissue on extracellular matrix integrity for tissue engineering of heart valves. J Struct Biol 2003 Sep;143(3):201-8.

(53) Badylak SF, Gilbert TW. Immune response to biologic scaffold materials. Semin Immunol 2008 Apr;20(2):109-16.

(54) Jones KS. Effects of biomaterial-induced inflammation on fibrosis and rejection. Semin Immunol 2008 Apr;20(2):130-6.

(55) Brennan EP, Reing J, Chew D, Myers-Irvin JM, Young EJ, Badylak SF. Antibacterial activity within degradation products of biological scaffolds composed of extracellular matrix. Tissue Eng 2006 Oct;12(10):2949-55.

(56) Chen F, Yoo JJ, Atala A. Acellular collagen matrix as a possible "off the shelf" biomaterial for urethral repair. Urology 1999 Sep;54(3):407-10.

(57) Li F, Li W, Johnson S, Ingram D, Yoder M, Badylak S. Low-molecular-weight peptides derived from extracellular matrix as chemoattractants for primary endothelial cells. Endothelium 2004 May;11(3-4):199-206.

(58) Zheng MH, Chen J, Kirilak Y, Willers C, Xu J, Wood D. Porcine small intestine submucosa (SIS) is not an acellular collagenous matrix and contains porcine DNA: possible implications in human implantation. J Biomed Mater Res B Appl Biomater 2005 Apr;73(1):61-7.

(59) Anderson CF, Mosser DM. A novel phenotype for an activated macrophage: the type 2 activated macrophage. J Leukoc Biol 2002 Jul;72(1):101-6.

(60) Mosser DM. The many faces of macrophage activation. J Leukoc Biol 2003 Feb;73(2):209-12.

(61) Traphagen S, Yelick PC. Reclaiming a natural beauty: whole-organ engineering with natural extracellular materials. Regen Med 2009 Sep;4(5):747-58.

(62) Macchiarini P, Jungebluth P, Go T, Asnaghi MA, Rees LE, Cogan TA, et al. Clinical transplantation of a tissue-engineered airway. Lancet 2008 Dec 13;372(9655):2023-30.

(63) Brunicardi FC, Andersen DK, Billiar TR, Dunn DL, Hunter JG, Pollock RE. Schwartz's Principles of Surgery. 8th ed. McGraw-Hill Professional; 2004.

(64) Day RM. Epithelial stem cells and tissue engineered intestine. Curr Stem Cell Res Ther 2006 Jan;1(1):113-20.

(65) Cheng H, Leblond CP. Origin, differentiation and renewal of the four main epithelial cell types in the mouse small intestine. V. Unitarian Theory of the origin of the four epithelial cell types. Am J Anat 1974 Dec;141(4):537-61.

(66) Hall PA, Coates PJ, Ansari B, Hopwood D. Regulation of cell number in the mammalian gastrointestinal tract: the importance of apoptosis. J Cell Sci 1994 Dec;107 ( Pt 12):3569-77.

(67) Leedham SJ, Brittan M, McDonald SA, Wright NA. Intestinal stem cells. J Cell Mol Med 2005 Jan;9(1):11-24.

(68) Leblond CP. The life history of cells in renewing systems. Am J Anat 1981 Feb;160(2):114-58.

(69) Withers HR, Elkind MM. Microcolony survival assay for cells of mouse intestinal mucosa exposed to radiation. Int J Radiat Biol Relat Stud Phys Chem Med 1970;17(3):261-7.

(70) Potten CS, Loeffler M. Stem cells: attributes, cycles, spirals, pitfalls and uncertainties. Lessons for and from the crypt. Development 1990 Dec;110(4):1001-20.

(71) Kayahara T, Sawada M, Takaishi S, Fukui H, Seno H, Fukuzawa H, et al. Candidate markers for stem and early progenitor cells, Musashi-1 and Hes1, are expressed in crypt base columnar cells of mouse small intestine. FEBS Lett 2003 Jan 30;535(1-3):131-5.

(72) Booth C, Potten CS. Gut instincts: thoughts on intestinal epithelial stem cells. J Clin Invest 2000 Jun;105(11):1493-9.

(73) Evans GS, Flint N, Somers AS, Eyden B, Potten CS. The development of a method for the preparation of rat intestinal epithelial cell primary cultures. J Cell Sci 1992 Jan;101 ( Pt 1):219-31.

(74) Chen DC, Agopian VG, Avansino JR, Lee JK, Farley SM, Stelzner M. Optical tissue window: a novel model for optimizing engraftment of intestinal stem cell organoids. J Surg Res 2006 Jul;134(1):52-60.

(75) Weiser MM. Intestinal epithelial cell surface membrane glycoprotein synthesis. I. An indicator of cellular differentiation. J Biol Chem 1973 Apr 10;248(7):2536-41.

(76) Tait IS, Flint N, Campbell FC, Evans GS. Generation of neomucosa in vivo by transplantation of dissociated rat postnatal small intestinal epithelium. Differentiation 1994 Apr;56(1-2):91-100.

(77) Patel HR, Tait IS, Evans GS, Campbell FC. Influence of cell interactions in a novel model of postnatal mucosal regeneration. Gut 1996 May;38(5):679-86.

(78) Tait IS, Penny JI, Campbell FC. Does neomucosa induced by small bowel stem cell transplantation have adequate function? Am J Surg 1995 Jan;169(1):120-5.

(79) Sattar A, Robson SC, Patel HR, Angus B, Campbell FC. Expression of growth regulatory genes in a SCID mouse-human model of intestinal epithelial regeneration. J Pathol 1999 Jan;187(2):229-36.

(80) Sala FG, Kunisaki SM, Ochoa ER, Vacanti J, Grikscheit TC. Tissue-engineered small intestine and stomach form from autologous tissue in a preclinical large animal model. J Surg Res 2009 Oct;156(2):205-12.

(81) Agopian VG, Chen DC, Avansino JR, Stelzner M. Intestinal stem cell organoid transplantation generates neomucosa in dogs. J Gastrointest Surg 2009 May;13(5):971-82.

(82) Kim SS, Kaihara S, Benvenuto MS, Choi RS, Kim BS, Mooney DJ, et al. Effects of anastomosis of tissue-engineered neointestine to native small bowel. J Surg Res 1999 Nov;87(1):6-13.

(83) Chen MK, Badylak SF. Small bowel tissue engineering using small intestinal submucosa as a scaffold. J Surg Res 2001 Aug;99(2):352-8.

(84) Choi RS, Vacanti JP. Preliminary studies of tissue-engineered intestine using isolated epithelial organoid units on tubular synthetic biodegradable scaffolds. Transplant Proc 1997 Feb;29(1-2):848-51.

(85) Stelzner M, Chen DC. To make a new intestinal mucosa. Rejuvenation Res 2006;9(1):20-5.

(86) Choi RS, Riegler M, Pothoulakis C, Kim BS, Mooney D, Vacanti M, et al. Studies of brush border enzymes, basement membrane components, and electrophysiology of tissue-engineered neointestine. J Pediatr Surg 1998 Jul;33(7):991-6.

(87) Perez A, Grikscheit TC, Blumberg RS, Ashley SW, Vacanti JP, Whang EE. Tissue-engineered small intestine: ontogeny of the immune system. Transplantation 2002 Sep 15;74(5):619-23.

(88) Kaihara S, Kim SS, Kim BS, Mooney D, Tanaka K, Vacanti JP. Long-term follow-up of tissue-engineered intestine after anastomosis to native small bowel. Transplantation 2000 May 15;69(9):1927-32.

(89) De FW, Tryphonopoulos P, Kleiner G, Santiago S, Gandia C, Ruiz P, et al. Study of the development and evolution of neointestine in a rat model. Transplant Proc 2004 Mar;36(2):375-6.

(90) Grikscheit TC, Siddique A, Ochoa ER, Srinivasan A, Alsberg E, Hodin RA, et al. Tissue-engineered small intestine improves recovery after massive small bowel resection. Ann Surg 2004 Nov;240(5):748-54.

(91) Kim SS, Kaihara S, Benvenuto M, Choi RS, Kim BS, Mooney DJ, et al. Regenerative signals for tissue-engineered small intestine. Transplant Proc 1999 Feb;31(1-2):657-60.

(92) Tavakkolizadeh A, Berger UV, Stephen AE, Kim BS, Mooney D, Hediger MA, et al. Tissue-engineered neomucosa: morphology, enterocyte dynamics, and SGLT1 expression topography. Transplantation 2003 Jan 27;75(2):181-5.

(93) Ramsanahie A, Duxbury MS, Grikscheit TC, Perez A, Rhoads DB, Gardner-Thorpe J, et al. Effect of GLP-2 on mucosal morphology and SGLT1 expression in tissue-engineered neointestine. Am J Physiol Gastrointest Liver Physiol 2003 Dec;285(6):G1345-G1352.

(94) Lloyd DA, Ansari TI, Gundabolu P, Shurey S, Maquet V, Sibbons PD, et al. A pilot study investigating a novel subcutaneously implanted pre-cellularised scaffold for tissue engineering of intestinal mucosa. Eur Cell Mater 2006;11:27-33.

(95) Lloyd DA, Ansari T, Shurey S, Maquet V, Sibbons PD, Boccaccini AR, et al. Prolonged maintenance of neointestine using subcutaneously implanted tubular scaffolds in a rat model. Transplant Proc 2006 Nov;38(9):3097-9.

(96) Kim SS, Penkala R, Abrahimi P. A perfusion bioreactor for intestinal tissue engineering. J Surg Res 2007 Oct;142(2):327-31.

(97) Chen MK, Badylak SF. Small bowel tissue engineering using small intestinal submucosa as a scaffold. J Surg Res 2001 Aug;99(2):352-8.

(98) Wang ZQ, Watanabe Y, Toki A. Experimental assessment of small intestinal submucosa as a small bowel graft in a rat model. J Pediatr Surg 2003 Nov;38(11):1596-601.

(99) Wang ZQ, Watanabe Y, Noda T, Yoshida A, Oyama T, Toki A. Morphologic evaluation of regenerated small bowel by small intestinal submucosa. J Pediatr Surg 2005 Dec;40(12):1898-902.

(100) Ansaloni L, Bonasoni P, Cambrini P, Catena F, De CA, Gagliardi S, et al. Experimental evaluation of Surgisis as scaffold for neointestine regeneration in a rat model. Transplant Proc 2006 Jul;38(6):1844-8.

(101) Lee M, Chang PC, Dunn JC. Evaluation of small intestinal submucosa as scaffolds for intestinal tissue engineering. J Surg Res 2008 Jun 15;147(2):168-71.

(102) De Ugarte DA, Choi E, Weitzbuch H, Wulur I, Caulkins C, Wu B, et al. Mucosal regeneration of a duodenal defect using small intestine submucosa. Am Surg 2004 Jan;70(1):49-51.

(103) Demirbilek S, Kanmaz T, Ozardali I, Edali MN, Yucesan S. Using porcine small intestinal submucosa in intestinal regeneration. Pediatr Surg Int 2003 Oct;19(8):588-92.

(104) Xu HM, Wang ZJ, Han JG, Ma HC, Zhao B, Zhao BC. Application of acellular dermal matrix for intestinal elongation in animal models. World J Gastroenterol 2010 Apr 28;16(16):2023-7.

(105) Pahari MP, Raman A, Bloomenthal A, Costa MA, Bradley SP, Banner B, et al. A novel approach for intestinal elongation using acellular dermal matrix: an experimental study in rats. Transplant Proc 2006 Jul;38(6):1849-50.

(106) Parnigotto PP, Marzaro M, Artusi T, Perrino G, Conconi MT. Short bowel syndrome: experimental approach to increase intestinal surface in rats by gastric homologous acellular matrix. J Pediatr Surg 2000 Sep;35(9):1304-8.

(107) Hori Y, Nakamura T, Matsumoto K, Kurokawa Y, Satomi S, Shimizu Y. Tissue engineering of the small intestine by acellular collagen sponge scaffold grafting. Int J Artif Organs 2001 Jan;24(1):50-4.

(108) Hori Y, Nakamura T, Matsumoto K, Kurokawa Y, Satomi S, Shimizu Y. Experimental study on in situ tissue engineering of the stomach by an acellular collagen sponge scaffold graft. ASAIO J 2001 May;47(3):206-10.

(109) Nakase Y, Nakamura T, Kin S, Nakashima S, Yoshikawa T, Kuriu Y, et al. Endocrine cell and nerve regeneration in autologous in situ tissue-engineered small intestine. J Surg Res 2007 Jan;137(1):61-8.

(110) Warner BW. Tissue engineered small intestine: a viable clinical option? Ann Surg 2004 Nov;240(5):755-6.

(111) Choi RS, Riegler M, Pothoulakis C, Kim BS, Mooney D, Vacanti M, et al. Studies of brush border enzymes, basement membrane components, and electrophysiology of tissue-engineered neointestine. J Pediatr Surg 1998 Jul;33(7):991-6.

(112) Grabow N, Schmohl K, Khosravi A, Philipp M, Scharfschwerdt M, Graf B, et al. Mechanical and structural properties of a novel hybrid heart valve scaffold for tissue engineering. Artif Organs 2004 Nov;28(11):971-9.

(113) Vedina LA, Sennikov SV, Trufakin VA, Kozlov VA. Stem cells of small intestinal epithelium. Bull Exp Biol Med 2008 Apr;145(4):495-8.

(114) Avansino JR, Chen DC, Woolman JD, Hoagland VD, Stelzner M. Engraftment of mucosal stem cells into murine jejunum is dependent on optimal dose of cells. J Surg Res 2006 May;132(1):74-9.

(115) Song Wu, Ying-Long Liu, Bin Cui, Xiang-Hua Qu, Guo-Qiang Chen. Study on Decellularized Porcine Aortic Valve/Poly (3-hydroxybutyrate-co-3-hydroxyhexanoate) Hybrid Heart Valve in Sheep Model. Artif.Organs 31[9], 689-697. 2008.
Ref Type: Generic

(116) Booth C, O'Shea JA, Potten CS. Maintenance of functional stem cells in isolated and cultured adult intestinal epithelium. Exp Cell Res 1999 Jun 15;249(2):359-66.

(117) Lalan S, Pomerantseva I, Vacanti JP. Tissue engineering and its potential impact on surgery. World J Surg 2001 Nov;25(11):1458-66.

(118) Nomi M, Atala A, Coppi PD, Soker S. Principals of neovascularization for tissue engineering. Mol Aspects Med 2002 Dec;23(6):463-83.

(119) Shatnawei A, Parekh NR, Rhoda KM, Speerhas R, Stafford J, Dasari V, et al. Intestinal failure management at the Cleveland Clinic. Arch Surg 2010 Jun;145(6):521-7.

(120) Folkman J, Hochberg M. Self-regulation of growth in three dimensions. J Exp Med 1973 Oct 1;138(4):745-53.

(121) Griffith CK, Miller C, Sainson RC, Calvert JW, Jeon NL, Hughes CC, et al. Diffusion limits of an in vitro thick prevascularized tissue. Tissue Eng 2005 Jan;11(1-2):257-66.

(122) De CP, Delo D, Farrugia L, Udompanyanan K, Yoo JJ, Nomi M, et al. Angiogenic gene-modified muscle cells for enhancement of tissue formation. Tissue Eng 2005 Jul;11(7-8):1034-44.

(123) Atala A, Bauer SB, Soker S, Yoo JJ, Retik AB. Tissue-engineered autologous bladders for patients needing cystoplasty. Lancet 2006 Apr 15;367(9518):1241-6.

(124) Klepetko W, Marta GM, Wisser W, Melis E, Kocher A, Seebacher G, et al. Heterotopic tracheal transplantation with omentum wrapping in the abdominal position preserves functional and structural integrity of a human tracheal allograft. J Thorac Cardiovasc Surg 2004 Mar;127(3):862-7.

(125) Rouwkema J, Rivron NC, Van Blitterswijk CA. Vascularization in tissue engineering. Trends Biotechnol 2008 Aug;26(8):434-41.

(126) Grounds MD. Muscling in on tissue engineering. Today's Life Science , 36-40. 2000.
Ref Type: Generic

(127) Sano MB, Neal RE, Garcia PA, Gerber D, Robertson J, Davalos RV. Towards the creation of decellularized organ constructs using irreversible electroporation and active mechanical perfusion. Biomed Eng Online 2010;9:83.

(128) Baptista PM, Orlando G, Mirmalek-Sani SH, Siddiqui M, Atala A, Soker S. Whole organ decellularization - a tool for bioscaffold fabrication and organ bioengineering. Conf Proc IEEE Eng Med Biol Soc 2009;2009:6526-9.

(129) Price AP, England KA, Matson AM, Blazar BR, Panoskaltsis-Mortari A. Development of a decellularized lung bioreactor system for bioengineering the lung: the matrix reloaded. Tissue Eng Part A 2010 Aug;16(8):2581-91.

(130) Flynn L, Semple JL, Woodhouse KA. Decellularized placental matrices for adipose tissue engineering. J Biomed Mater Res A 2006 Nov;79(2):359-69.

(131) Weymann A, Loganathan S, Takahashi H, Schies C, Claus B, Hirschberg K, et al. Development and Evaluation of a Perfusion Decellularization Porcine Heart Model. Circ J 2011 Feb 2.

(132) Schaner PJ, Martin ND, Tulenko TN, Shapiro IM, Tarola NA, Leichter RF, et al. Decellularized vein as a potential scaffold for vascular tissue engineering. J Vasc Surg 2004 Jul;40(1):146-53.

(133) Ott HC, Matthiesen TS, Goh SK, Black LD, Kren SM, Netoff TI, et al. Perfusion-decellularized matrix: using nature's platform to engineer a bioartificial heart. Nat Med 2008 Feb;14(2):213-21.

(134) Kasimir MT, Rieder E, Seebacher G, Silberhumer G, Wolner E, Weigel G, et al. Comparison of different decellularization procedures of porcine heart valves. Int J Artif Organs 2003 May;26(5):421-7.

(135) Bodnar E, Olsen EG, Florio R, Dobrin J. Damage of porcine aortic valve tissue caused by the surfactant sodiumdodecylsulphate. Thorac Cardiovasc Surg 1986 Apr;34(2):82-5.

(136) Kitaoka H, Kubo T, Okawa M, Hayato K, Yamasaki N, Matsumura Y, et al. Impact of metalloproteinases on left ventricular remodeling and heart failure events in patients with hypertrophic cardiomyopathy. Circ J 2010 Jun;74(6):1191-6.

(137) Waldrop FS, Puchtler H, Meloan SN, Younker TD. Histochemical investigations of different types of collagen. Acta Histochem Suppl 1980;21:23-31.

(138) Klebe RJ. Isolation of a collagen-dependent cell attachment factor. Nature 1974 Jul 19;250(463):248-51.

(139) Gailit J, Ruoslahti E. Regulation of the fibronectin receptor affinity by divalent cations. J Biol Chem 1988 Sep 15;263(26):12927-32.

(140) Hopkinson A, Shanmuganathan VA, Gray T, Yeung AM, Lowe J, James DK, et al. Optimization of amniotic membrane (AM) denuding for tissue engineering. Tissue Eng Part C Methods 2008 Dec;14(4):371-81.

(141) Elder BD, Kim DH, Athanasiou KA. Developing an articular cartilage decellularization process toward facet joint cartilage replacement. Neurosurgery 2010 Apr;66(4):722-7.

(142) Akhyari P, Kamiya H, Gwanmesia P, Aubin H, Tschierschke R, Hoffmann S, et al. In vivo functional performance and structural maturation of decellularised allogenic aortic valves in the subcoronary position. Eur J Cardiothorac Surg 2010 Nov;38(5):539-46.

(143) Gilbert TW, Freund JM, Badylak SF. Quantification of DNA in biologic scaffold materials. J Surg Res 2009 Mar;152(1):135-9.

(144) Wilshaw S, Kearney JN, Fisher J, Ingham E. Production of an Acellular Amniotic Membrane Matrix for Use in Tissue Engineering. Tissue Eng 12[8], 2117-2127. 2006.
Ref Type: Generic

(145) Crapo PM, Gilbert TW, Badylak SF. An overview of tissue and whole organ decellularization processes. Biomaterials 2011 Apr;32(12):3233-43.

(146) Patel A, Fine B, Sandig M, Mequanint K. Elastin biosynthesis: The missing link in tissue-engineered blood vessels. Cardiovasc Res 2006 Jul 1;71(1):40-9.

(147) Mavrilas D, Sinouris EA, Vynios DH, Papageorgakopoulou N. Dynamic mechanical characteristics of intact and structurally modified bovine pericardial tissues. J Biomech 2005 Apr;38(4):761-8.

(148) Mendoza-Novelo B, Avila EE, Cauich-Rodriguez JV, Jorge-Herrero E, Rojo FJ, Guinea GV, et al. Decellularization of pericardial tissue and its impact on tensile viscoelasticity and glycosaminoglycan content. Acta Biomater 2011 Mar;7(3):1241-8.

(149) Wainwright JM, Czajka CA, Patel UB, Freytes DO, Tobita K, Gilbert TW, et al. Preparation of cardiac extracellular matrix from an intact porcine heart. Tissue Eng Part C Methods 2010 Jun;16(3):525-32.

(150) Hodde JP, Record RD, Tullius RS, Badylak SF. Retention of endothelial cell adherence to porcine-derived extracellular matrix after disinfection and sterilization. Tissue Eng 2002 Apr;8(2):225-34.

(151) Mertsching H, Walles T, Hofmann M, Schanz J, Knapp WH. Engineering of a vascularized scaffold for artificial tissue and organ generation. Biomaterials 2005 Nov;26(33):6610-7.

(152) Badylak SF. Xenogeneic extracellular matrix as a scaffold for tissue reconstruction. Transpl Immunol 2004 Apr;12(3-4):367-77.

(153) Hodde J. Naturally occurring scaffolds for soft tissue repair and regeneration. Tissue Eng 2002 Apr;8(2):295-308.

(154) Yang B, Zhang Y, Zhou L, Sun Z, Zheng J, Chen Y, et al. Development of a porcine bladder acellular matrix with well-preserved extracellular bioactive factors for tissue engineering. Tissue Eng Part C Methods 2010 Oct;16(5):1201-11.

(155) Luttikhuizen DT, Harmsen MC, van Luyn MJ. Cellular and molecular dynamics in the foreign body reaction. Tissue Eng 2006 Jul;12(7):1955-70.

(156) Davis ME, Hsieh PC, Grodzinsky AJ, Lee RT. Custom design of the cardiac microenvironment with biomaterials. Circ Res 2005 Jul 8;97(1):8-15.

(157) Weibel ER. Fractal geometry: a design principle for living organisms. Am J Physiol 1991 Dec;261(6 Pt 1):L361-L369.

(158) Slomianka L, West MJ. Estimators of the precision of stereological estimates: an example based on the CA1 pyramidal cell layer of rats. Neuroscience 2005;136(3):757-67.

(159) Tinsley CJ, Bennett GW, Mayhew TM, Parker TL. Stereological analysis of regional brain volumes and neuron numbers in rats displaying a spontaneous hydrocephalic condition. Exp Neurol 2001 Mar;168(1):88-95.

(160) Howard CV, Reed MG. Unbiased Stereology, Three-Dimensional Measurment in Microscopy. 1998.

(161) Mayhew TM. The new stereological methods for interpreting functional morphology from slices of cells and organs. Exp Physiol 1991 Sep;76(5):639-65.

(162) Mandarim-de-Lacerda CA. Stereological tools in biomedical research. An Acad Bras Cienc 2003 Dec;75(4):469-86.

(163) Cruz-Orive LM, Weibel ER. Recent stereological methods for cell biology: a brief survey. Am J Physiol 1990 Apr;258(4 Pt 1):L148-L156.

(164) Garcia Y, Breen A, Burugapalli K, Dockery P, Pandit A. Stereological methods to assess tissue response for tissue-engineered scaffolds. Biomaterials 2007 Jan;28(2):175-86.

(165) Kou PM, Babensee JE. Macrophage and dendritic cell phenotypic diversity in the context of biomaterials. J Biomed Mater Res A 2011 Jan;96(1):239-60.

(166) Badylak SF, Valentin JE, Ravindra AK, McCabe GP, Stewart-Akers AM. Macrophage phenotype as a determinant of biologic scaffold remodeling. Tissue Eng Part A 2008 Nov;14(11):1835-42.

(167) Jones KS. Assays on the influence of biomaterials on allogeneic rejection in tissue engineering. Tissue Eng Part B Rev 2008 Dec;14(4):407-17.

(168) Stout RD, Jiang C, Matta B, Tietzel I, Watkins SK, Suttles J. Macrophages sequentially change their functional phenotype in response to changes in microenvironmental influences. J Immunol 2005 Jul 1;175(1):342-9.

(169) Brown BN, Valentin JE, Stewart-Akers AM, McCabe GP, Badylak SF. Macrophage phenotype and remodeling outcomes in response to biologic scaffolds with and without a cellular component. Biomaterials 2009 Mar;30(8):1482-91.

(170) Valentin JE, Badylak JS, McCabe GP, Badylak SF. Extracellular matrix bioscaffolds for orthopaedic applications. A comparative histologic study. J Bone Joint Surg Am 2006 Dec;88(12):2673-86.

(171) Liang HC, Chang Y, Hsu CK, Lee MH, Sung HW. Effects of crosslinking degree of an acellular biological tissue on its tissue regeneration pattern. Biomaterials 2004 Aug;25(17):3541-52.

(172) Langsjo TK, Hyttinen M, Pelttari A, Kiraly K, Arokoski J, Helminen HJ. Electron microscopic stereological study of collagen fibrils in bovine articular cartilage: volume and surface densities are best obtained indirectly (from length densities and diameters) using isotropic uniform random sampling. J Anat 1999 Aug;195 ( Pt 2):281-93.

(173) Atala A, Vacanti JP, Peters CA, Mandell J, Retik AB, Freeman MR. Formation of urothelial structures in vivo from dissociated cells attached to biodegradable polymer scaffolds in vitro. J Urol 1992 Aug;148(2 Pt 2):658-62.

(174) Baptista PM, Siddiqui MM, Lozier G, Rodriguez SR, Atala A, Soker S. The use of whole organ decellularization for the generation of a vascularized liver organoid. Hepatology 2011 Feb;53(2):604-17.

(175) Stamm C, Khosravi A, Grabow N, Schmohl K, Treckmann N, Drechsel A, et al. Biomatrix/polymer composite material for heart valve tissue engineering. Ann Thorac Surg 2004 Dec;78(6):2084-92.

(176) Mason RG, Read MS. Some species differences in fibrinolysis and blood coagulation. J Biomed Mater Res 1971 Jan;5(1):121-8.

(177) Wilson GJ, Courtman DW, Klement P, Lee JM, Yeger H. Acellular matrix: a biomaterials approach for coronary artery bypass and heart valve replacement. Ann Thorac Surg 1995 Aug;60(2 Suppl):S353-S358.

(178) Schultheiss D, Gabouev AI, Cebotari S, Tudorache I, Walles T, Schlote N, et al. Biological vascularized matrix for bladder tissue engineering: matrix preparation, reseeding technique and short-term implantation in a porcine model. J Urol 2005 Jan;173(1):276-80.

(179) Robotin-Johnson MC, Swanson PE, Johnson DC, Schuessler RB, Cox JL. An experimental model of small intestinal submucosa as a growing vascular graft. J Thorac Cardiovasc Surg 1998 Nov;116(5):805-11.

(180) Petersen TH, Calle EA, Zhao L, Lee EJ, Gui L, Raredon MB, et al. Tissue-engineered lungs for in vivo implantation. Science 2010 Jul 30;329(5991):538-41.

(181) Takagi K, Fukunaga S, Nishi A, Shojima T, Yoshikawa K, Hori H, et al. In vivo recellularization of plain decellularized xenografts with specific cell characterization in the systemic circulation: histological and immunohistochemical study. Artif Organs 2006 Apr;30(4):233-41.

(182) Tucker OP, Syburra T, Augstburger M, van MG, Gebhard S, Bosman F, et al. Small intestine without mucosa as a growing vascular conduit: a porcine experimental study. J Thorac Cardiovasc Surg 2002 Dec;124(6):1165-75.

(183) Derham C, Yow H, Ingram J, Fisher J, Ingham E, Korrosis SA, et al. Tissue engineering small-diameter vascular grafts: preparation of a biocompatible porcine ureteric scaffold. Tissue Eng Part A 2008 Nov;14(11):1871-82.

(184) Anghelina M, Krishnan P, Moldovan L, Moldovan NI. Monocytes/macrophages cooperate with progenitor cells during neovascularization and tissue repair: conversion of cell columns into fibrovascular bundles. Am J Pathol 2006 Feb;168(2):529-41.

(185) Hristov M, Weber C. Endothelial progenitor cells in vascular repair and remodeling. Pharmacol Res 2008 Aug;58(2):148-51.

(186) Gui L, Muto A, Chan SA, Breuer CK, Niklason LE. Development of decellularized human umbilical arteries as small-diameter vascular grafts. Tissue Eng Part A 2009 Sep;15(9):2665-76.

(187) Garrison AP, Helmrath MA, Dekaney CM. Intestinal stem cells. J Pediatr Gastroenterol Nutr 2009 Jul;49(1):2-7.

(188) van de WM, Sancho E, Verweij C, de LW, Oving I, Hurlstone A, et al. The beta-catenin/TCF-4 complex imposes a crypt progenitor phenotype on colorectal cancer cells. Cell 2002 Oct 18;111(2):241-50.

(189) May R, Riehl TE, Hunt C, Sureban SM, Anant S, Houchen CW. Identification of a novel putative gastrointestinal stem cell and adenoma stem cell marker, doublecortin and CaM kinase-like-1, following radiation injury and in adenomatous polyposis coli/multiple intestinal neoplasia mice. Stem Cells 2008 Mar;26(3):630-7.

(190) Avansino JR, Chen DC, Hoagland VD, Woolman JD, Stelzner M. Orthotopic transplantation of intestinal mucosal organoids in rodents. Surgery 2006 Sep;140(3):423-34.

(191) Andoh A, Bamba S, Brittan M, Fujiyama Y, Wright NA. Role of intestinal subepithelial myofibroblasts in inflammation and regenerative response in the gut. Pharmacol Ther 2007 Apr;114(1):94-106.

(192) Powell DW, Mifflin RC, Valentich JD, Crowe SE, Saada JI, West AB. Myofibroblasts. II. Intestinal subepithelial myofibroblasts. Am J Physiol 1999 Aug;277(2 Pt 1):C183-C201.

(193) Ootani A, Li X, Sangiorgi E, Ho QT, Ueno H, Toda S, et al. Sustained in vitro intestinal epithelial culture within a Wnt-dependent stem cell niche. Nat Med 2009 Jun;15(6):701-6.

(194) Yoshida A, Noda T, Tani M, Oyama T, Watanabe Y, Kiyomoto H, et al. The role of basic fibroblast growth factor to enhance fetal intestinal mucosal cell regeneration in vivo. Pediatr Surg Int 2009 Aug;25(8):691-5.

(195) Nakamura M, Okano H, Blendy JA, Montell C. Musashi, a neural RNA-binding protein required for Drosophila adult external sensory organ development. Neuron 1994 Jul;13(1):67-81.

(196) Potten CS, Booth C, Tudor GL, Booth D, Brady G, Hurley P, et al. Identification of a putative intestinal stem cell and early lineage marker; musashi-1. Differentiation 2003 Jan;71(1):28-41.

(197) Vedina LA, Sennikov SV, Trufakin VA, Kozlov VA. Stem cells of small intestinal epithelium. Bull Exp Biol Med 2008 Apr;145(4):495-8.

(198) May R, Riehl TE, Hunt C, Sureban SM, Anant S, Houchen CW. Identification of a novel putative gastrointestinal stem cell and adenoma stem cell marker, doublecortin and CaM kinase-like-1, following radiation injury and in adenomatous polyposis coli/multiple intestinal neoplasia mice. Stem Cells 2008 Mar;26(3):630-7.

(199) Slorach EM, Campbell FC, Dorin JR. A mouse model of intestinal stem cell function and regeneration. J Cell Sci 1999 Sep;112 Pt 18:3029-38.

(200) Mall JW, Philipp AW, Rademacher A, Paulitschke M, Buttemeyer R. Re-endothelialization of punctured ePTFE graft: an in vitro study under pulsed perfusion conditions. Nephrol Dial Transplant 2004 Jan;19(1):61-7.

(201) Day RM. Epithelial Stem Cell and Tinssue Engineered Intestine. Current Stem Cell Research & Therapy 1, 113-120. 2006.
Ref Type: Generic

(202) Rocha FG, Whang EE. Intestinal tissue engineering: from regenerative medicine to model systems. J Surg Res 2004 Aug;120(2):320-5.

(203) Jumarie C, Malo C. Caco-2 cells cultured in serum-free medium as a model for the study of enterocytic differentiation in vitro. J Cell Physiol 1991 Oct;149(1):24-33.

(204) Ray EC, Avissar NE, Sax HC. Methods used to study intestinal nutrient transport: past and present. J Surg Res 2002 Nov;108(1):180-90.

(205) Goldstein SA. Tissue engineering: functional assessment and clinical outcome. Ann N Y Acad Sci 2002 Jun;961:183-92.

(206) Hodde J. Extracellular matrix as a bioactive material for soft tissue reconstruction. ANZ J Surg 2006 Dec;76(12):1096-100.

(207) Bell E. Strategy for the selection of scaffolds for tissue engineering. Tissue Eng 1995;1(2):163-79.

(208) Place ES, Evans ND, Stevens MM. Complexity in biomaterials for tissue engineering. Nat Mater 2009 Jun;8(6):457-70.

(209) Wallis K, Walters JR, Gabe S. Short bowel syndrome: the role of GLP-2 on improving outcome. Curr Opin Clin Nutr Metab Care 2009 Sep;12(5):526-32.

(210) Atala A. Tissue engineering of human bladder. Br Med Bull 2011;97:81-104.

(211) Baiguera S, Jungebluth P, Burns A, Mavilia C, Haag J, De CP, et al. Tissue engineered human tracheas for in vivo implantation. Biomaterials 2010 Dec;31(34):8931-8.

(212) Junqueira L, Montes G, Sanchez E. The influence of tissue section thickness on the study of collagen by the Picrosirius-Polarization Method. Histochemistry 1982 74:153-6.

(213) Haley P. Species differences in the structure and function of the immune system. Toxicology 2003 Jun;188(1):49-71.